AUTOIMMUNITY AND CHRONIC INFLAMMATION IN EARLY LIFE

EDITED BY: Ravi Misra, Sarah Rowland-Jones, Michael Zemlin and Jennifer Konopa Mulligan

PUBLISHED IN: Frontiers in Immunology and Frontiers in Pediatrics

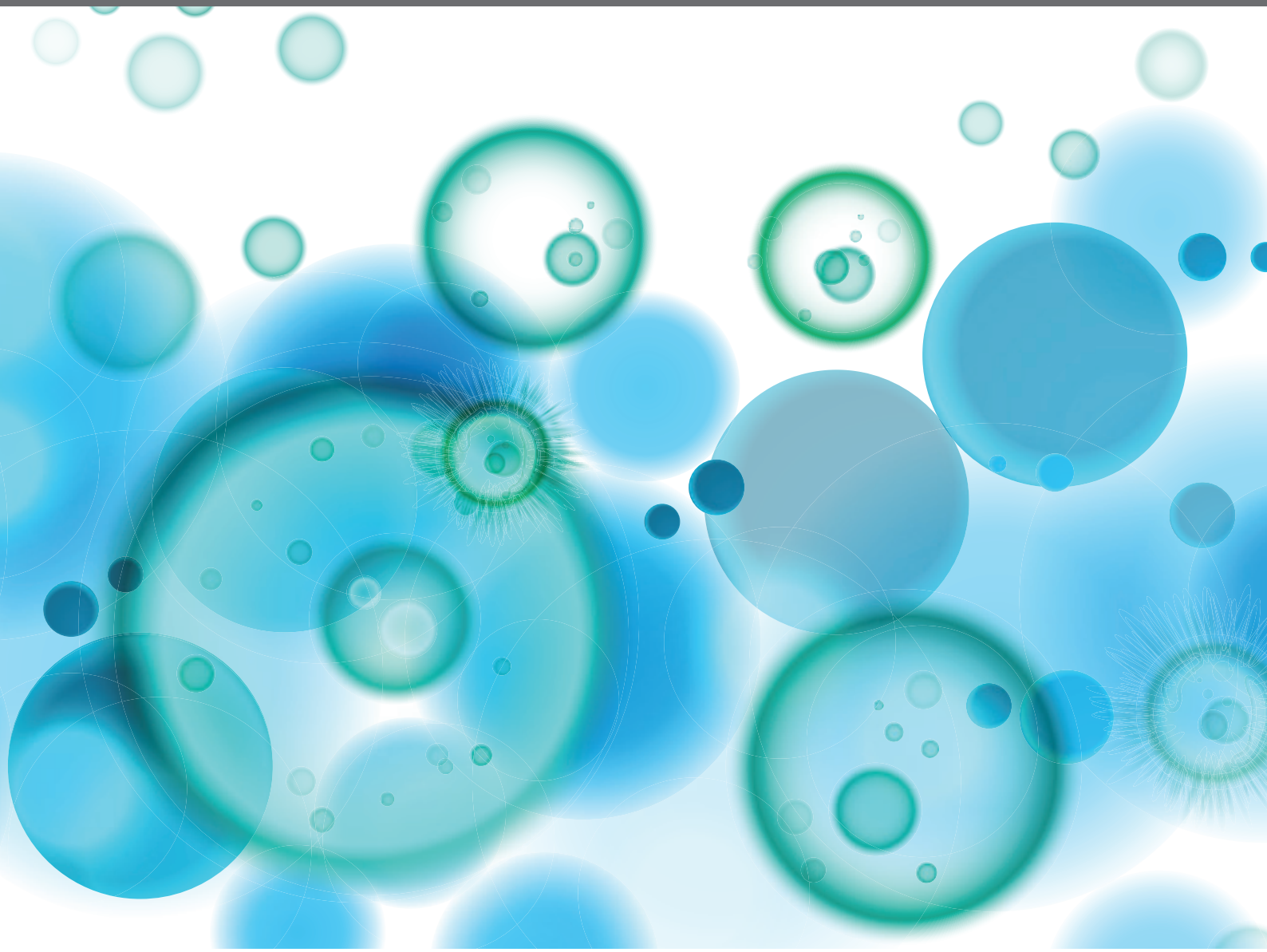

frontiers Research Topics

frontiers

ISSN 1664-8714
ISBN 978-2-88971-559-6
DOI 10.3389/978-2-88971-559-6

About Frontiers

Frontiers is more than just an open-access publisher of scholarly articles: it is a pioneering approach to the world of academia, radically improving the way scholarly research is managed. The grand vision of Frontiers is a world where all people have an equal opportunity to seek, share and generate knowledge. Frontiers provides immediate and permanent online open access to all its publications, but this alone is not enough to realize our grand goals.

Frontiers Journal Series

The Frontiers Journal Series is a multi-tier and interdisciplinary set of open-access, online journals, promising a paradigm shift from the current review, selection and dissemination processes in academic publishing. All Frontiers journals are driven by researchers for researchers; therefore, they constitute a service to the scholarly community. At the same time, the Frontiers Journal Series operates on a revolutionary invention, the tiered publishing system, initially addressing specific communities of scholars, and gradually climbing up to broader public understanding, thus serving the interests of the lay society, too.

Dedication to Quality

Each Frontiers article is a landmark of the highest quality, thanks to genuinely collaborative interactions between authors and review editors, who include some of the world's best academicians. Research must be certified by peers before entering a stream of knowledge that may eventually reach the public - and shape society; therefore, Frontiers only applies the most rigorous and unbiased reviews.
Frontiers revolutionizes research publishing by freely delivering the most outstanding research, evaluated with no bias from both the academic and social point of view. By applying the most advanced information technologies, Frontiers is catapulting scholarly publishing into a new generation.

What are Frontiers Research Topics?

Frontiers Research Topics are very popular trademarks of the Frontiers Journals Series: they are collections of at least ten articles, all centered on a particular subject. With their unique mix of varied contributions from Original Research to Review Articles, Frontiers Research Topics unify the most influential researchers, the latest key findings and historical advances in a hot research area! Find out more on how to host your own Frontiers Research Topic or contribute to one as an author by contacting the Frontiers Editorial Office: frontiersin.org/about/contact

AUTOIMMUNITY AND CHRONIC INFLAMMATION IN EARLY LIFE

Topic Editors:
Ravi Misra, University of Rochester, United States
Sarah Rowland-Jones, University of Oxford, United Kingdom
Michael Zemlin, Saarland University Hospital, Germany
Jennifer Konopa Mulligan, University of Florida, United States

Citation: Misra, R., Rowland-Jones, S., Zemlin, M., Mulligan, J. K., eds. (2021). Autoimmunity and Chronic Inflammation in Early Life. Lausanne: Frontiers Media SA. doi: 10.3389/978-2-88971-559-6

Table of Contents

frontiers in Immunology

EDITORIAL
published: 09 September 2021
doi: 10.3389/fimmu.2021.761160

Editorial: Autoimmunity and Chronic Inflammation in Early Life

Ravi Misra[1], *Jennifer Konopa Mulligan*[2], *Sarah Rowland-Jones*[3] *and Michael Zemlin*[4]*

[1] Department of Pediatrics, The University of Rochester Medical Center, Rochester, NY, United States, [2] Division of Pulmonary, Critical Care & Sleep Medicine, University of Florida, Gainesville, FL, United States, [3] Viral Immunology Unit, Nuffield Department of Medicine, Oxford, United Kingdom, [4] Department for General Pediatrics and Neonatology, Saarland University, Homburg, Germany

Keywords: autoimmunity, pediatrics - children, immune development and maturation, early life origin of disease, chronic inflammation

Editorial on the Research Topic

Autoimmunity and Chronic Inflammation in Early Life

INTRODUCTION

Non-communicable diseases such as cardiovascular diseases, metabolic disease and chronic inflammatory diseases are often attributed to an interplay between genetic predispositions and imprinting mechanisms early in life. In a simplified concept, the fetal development is characterized by the acquisition of immuno-tolerance towards maternal and self-antigens, whereas the neonatal period reflects the acquisition of immune-defense against potentially harmful environmental antigen. Immune development involves a complex cross talk of immune cells in various organs that is influenced by environmental antigen (1–3). During infancy and childhood, autoimmune diseases and chronic inflammation coincide with an exponential diversification of the adaptive immune system, causing potentially life-long consequences. Interestingly, the earlier hypothesis of an "immunodeficiency of immaturity" had to be partially revised since it has become clear that inflammatory states in the neonate, e.g. in the context of sepsis, represent a lack of controlling inflammation rather than a failure to mount inflammation. Thus, hyperinflammatory states can occur even in the very immature organism and can lay the ground for autoimmunity or various conditions of chronic inflammation. This knowledge may affect therapeutic approaches.

In this Research Topic, we have called for publications that relate to clinical or molecular aspects of aberrant immune responses in pediatric patients. Here we briefly present the 12 contributions that comprise six Original Research articles, three (mini) reviews and three case reports. The contributions can be grouped into three sections:

1. Clinical manifestations of early autoimmune and chronic inflammatory diseases
2. From molecular mechanisms to autoimmune phenotypes
3. The role of B- and T cells for autoimmune diseases and chronic inflammation in early life

CLINICAL MANIFESTATIONS OF EARLY AUTOIMMUNE AND CHRONIC INFLAMMATORY DISEASES

In a single center overview, Wang et al. present the genetic and clinical characteristics of 79 pediatric patients with monogenetic autoimmune diseases. The patients were affected with 18 different

OPEN ACCESS

Edited and reviewed by:
Betty Diamond, Feinstein Institute for Medical Research, United States

***Correspondence:**
Michael Zemlin
michael.zemlin@uks.eu

Specialty section:
This article was submitted to Autoimmune and Autoinflammatory Disorders, a section of the journal Frontiers in Immunology

Received: *19 August 2021*
Accepted: *23 August 2021*
Published: *09 September 2021*

Citation:
Misra R, Mulligan JK, Rowland-Jones S and Zemlin M (2021) Editorial: Autoimmunity and Chronic Inflammation in Early Life. Front. Immunol. 12:761160. doi: 10.3389/fimmu.2021.761160

diagnoses that can be grouped into inflammasomopathies (42%), non-inflammasome related conditions (48%) and type 1 interferonopathies (10%). 76% of the patients presented with skin disorders, making this the most common clinical clue to autoimmune diseases. In contrast, Chinello et al. address a new complication in a rare autoimmune disease by presenting a pediatric patient with lipopolysaccharide-responsive-beige-linked-anchor-protein (LRBA) deficiency that developed acute cervical longitudinally transverse myelitis. Chen et al. report a patient with symptoms of intestinal Behcet's disease that was associated with novel heterozygous mutation in the TNFAIP gene, potentially linking intestinal Behcet's disease with Haploinsufficiency A20.

FROM MOLECULAR MECHANISMS TO AUTOIMMUNE PHENOTYPES

Haploinsufficiency A20 (HA20) has recently been identified as one potential molecular mechanism of autoimmunity. In an analysis of 89 patients with this rare condition, Chen et al. present the typical clinical manifestations associated with HA20: Recurrent oral ulcers and fever episodes, gastrointestinal and genital ulcers as well as skin lesions are the hallmarks that can help clinicians to initiate targeted diagnostics in patients that often suffer a long odyssey prior to a correct diagnosis and therapy. Another diagnostic "chameleon", systemic lupus erythematosus has been addressed by Motwani et al.: In an elegant series of experiments, the authors could rule out a contribution of the cGAS-STING pathway to the clinical symptoms in a murine model of chronic SLE, thus questioning the potential of novel cGAS-STING directed therapeutic approaches. As shown by Wang et al. in this Research Topic, inflammasomopathies represent a major percentage of autoimmune diseases, including type 1 diabetes. In extension of these observations, Sun et al. review the literature on the assembly and function of the NLRP3 inflammasome and its role in type 1 diabetes.

THE ROLE OF B- AND T CELLS FOR AUTOIMMUNE DISEASES AND CHRONIC INFLAMMATION IN EARLY LIFE

While Sun et al. address the role of the NLRP3 inflammasome in diabetes, Shapiro et al. address T cell mediated mechanisms in the same disease: The severity of type 1 diabetes was reduced in CD226 deficient non-obese diabetic (NOD) mice. Using adoptive transfer experiments and other techniques, the authors could attribute this phenomenon to the impaired activation of peripheral T cells, which is mediated by CD226. Foth et al. contribute a review on the T cell repertoire during ontogeny and characteristic aberrations in inflammatory disorders. Ultimately, this relates to the unanswered question of whether the T cell is rather a bystander or a culprit during the development of autoimmunity and chronic inflammatory diseases. The small but still enigmatic subset of IL-17 expressing TH cells plays a key role in the pathogenesis of chronic mucocutaneous candidiasis in children and are diminished in other autoimmune diseases such as hyper IgE syndrome. Shamriz et al. give an overview on the immune mechanisms, current management and novel targeted therapies for monogenic mucocutaneous candidiasis with a focus on TH 17 cells. Two articles of this Research Topic focus on the immunologic and inflammatory aspects of lung disease: Bhattacharya et al. present transcriptomic profiles of purified CD8 + T cells from preterm neonates at the time of discharge. By identifying signaling pathways that differ between infants with and without bronchopulmonary dysplasia this study sheds new light into the patho-mechanisms of this condition, which remains a major cause of long-term morbidity in preterm neonates. Hwang et al. report that inducible Bronchus-Associated Lymphoid Tissue (iBALT) attenuates the allergic airway inflammation in a mouse model by sequestration of effector T cells. On the other hand, Breville et al. present a case report suggesting a role of IgG4 in severe complement-mediated thrombotic microangiopathy in a patient with IgG4 related disease. Interestingly, a genetic predisposition might enhance the susceptibility to form inhibitory anti-Factor H IgG4 antibodies.

CONCLUDING REMARKS

The article collection of the Research Topic gives an up-to-date overview on the clinical manifestations and molecular mechanisms of autoimmunity and chronic inflammation in early life. Thus, in the jungle of "diagnostic chameleons", clinicians may find important hints for linking characteristic symptoms with autoimmune diseases. On the other hand, basic researchers find a thorough overview of the current knowledge on disease mechanism that should inspire research projects in the field of diagnostics and novel therapeutic concepts.

AUTHOR CONTRIBUTIONS

MZ wrote the first draft of the manuscript. All authors contributed to the article and approved the submitted version.

FUNDING

This study was supported by BMBF PRIMAL study (01GL1746D) to MZ.

REFERENCES

1. Ubags NDJ, Alejandre Alcazar MA, Kallapur SG, Knapp S, Lanone S, Lloyd CM, et al. Early Origins of Lung Disease: Towards an Interdisciplinary Approach. *Eur Respir Rev* (2020) 29(157):200191. doi: 10.1183/16000617.0191-20202
2. Sarkar A, Yoo JY, Valeria Ozorio Dutra S, Morgan KH, Groer M. The Association Between Early-Life Gut Microbiota and Long-Term Health and Diseases. *J Clin Med* (2021) 10(3):459. doi: 10.3390/jcm100304593
3. Jian C, Carpén N, Helve O, de Vos WM, Korpela K, Salonen A. Early-Life Gut Microbiota and Its Connection to Metabolic Health in Children: Perspective on

Ecological Drivers and Need for Quantitative Approach. *EBioMedicine* (2021) 69:103475. doi 10.1016/j.ebiom.2021.103475

Conflict of Interest: The authors declare that the research was conducted in the absence of any commercial or financial relationships that could be construed as a potential conflict of interest.

Publisher's Note: All claims expressed in this article are solely those of the authors and do not necessarily represent those of their affiliated organizations, or those of the publisher, the editors and the reviewers. Any product that may be evaluated in this article, or claim that may be made by its manufacturer, is not guaranteed or endorsed by the publisher.

frontiers in Immunology

CASE REPORT
published: 03 July 2020
doi: 10.3389/fimmu.2020.01414

A20 Haploinsufficiency in a Chinese Patient With Intestinal Behcet's Disease-Like Symptoms: A Case Report

*Yu Chen[1], Huanjun Huang[1], Yao He[2], Minhu Chen[2], Ursula Seidler[3], De'an Tian[1] and Fang Xiao[1]**

[1] Department of Gastroenterology, Tongji Hospital of Tongji Medical College, Huazhong University of Science and Technology, Wuhan, China, [2] Department of Gastroenterology, First Affiliated Hospital of Sun Yat-sen University, Guangzhou, China, [3] Department of Gastroenterology of Hannover Medical School, Hanover, Germany

OPEN ACCESS

Edited by:
Sarah Rowland-Jones, University of Oxford, United Kingdom

Reviewed by:
Deepika Sharma, University of Chicago, United States
Bryce Binstadt, University of Minnesota Medical School, United States

***Correspondence:**
Fang Xiao
xiaofang@tjh.tjmu.edu.cn

Specialty section:
This article was submitted to Autoimmune and Autoinflammatory Disorders, a section of the journal Frontiers in Immunology

Received: 31 March 2020
Accepted: 02 June 2020
Published: 03 July 2020

Citation:
Chen Y, Huang H, He Y, Chen M, Seidler U, Tian D and Xiao F (2020) A20 Haploinsufficiency in a Chinese Patient With Intestinal Behcet's Disease-Like Symptoms: A Case Report. Front. Immunol. 11:1414. doi: 10.3389/fimmu.2020.01414

Objective: Intestinal Behcet's disease (iBD) is an autoimmune disorder diagnosed by typical intestinal ulcers and systemic Behcet's disease (BD) manifestations. Haploinsufficiency of A20 (HA20) is a recently described autoinflammatory disease with a phenotype resembling BD, caused by heterozygous loss-of-function mutations in *TNFAIP3* gene (encoding A20).

Methods: We described a 29-year-old female with iBD-like symptoms including relapsing ulceration of intestinal anastomosis, recurrent oral ulcers and vasculitis in extremities. Due to the atypical intestinal ulcers with long segmental involvement and intestinal obstruction, whole exome sequencing (WES) was performed to screen for the underlying genetic defect and the identified gene was confirmed by Sanger sequencing. The expression levels of A20 was evaluated by Western blot. Sanger sequencing and Western blot were also performed in the patient's family members.

Results: A heterozygous mutation of *TNFAIP3* (c.305A>G, p. Asn 102 Ser) was identified in the patient. The identical *TNFAIP3* mutation was also found in her father and brother who had suffered from recurrent oral ulcers since childhood. Functional experiments revealed that the expression of A20 was decreased in the peripheral blood mononuclear cells of the patient and her family members who carried the TNFAIP3 mutation.

Conclusion: We described a Chinese patient with a novel heterozygous mutation in *TNFAIP3* who developed iBD-like symptoms. We proposed that the *TNFAIP3* heterozygous mutation (c.305A>G, p. Asn 102 Ser) with an insufficient expression of A20 may be associated with the iBD phenotype in patients.

Keywords: haploinsufficiency of A20, intestinal Behçet's disease, autoimmune disorder, TNFAIP3, gene mutation, whole exome sequencing, autosomal-dominant-inherited disease, expressivity

INTRODUCTION

Behcet's disease (BD) is an autoimmune disease with a polygenic background and is mainly identified by recurrent oral aphthous ulcers, genital ulcers, and ocular, vascular, and gastrointestinal lesions (1). BD patients with predominantly gastrointestinal symptoms and intestinal ulceration may be diagnosed with intestinal Behcet's disease (iBD) (2). The diagnosis of iBD is dependent on the presence of typical intestinal ulcers and clinical manifestations (2). The typical intestinal ulcer of iBD is defined as less than five ulcers that are oval in shape, deep with discrete borders, and located in the ileocecal area (2). Haploinsufficiency of A20 (HA20) is a newly described autoimmune disorder with one of the various phenotypes resembling BD (3). HA20 is caused by heterozygous loss-of-function mutations of the *TNF Alpha Induced Protein 3 (TNFAIP3)* gene encoding A20 and the diagnosis of HA20 mainly depends on genetic analysis (4). Here, we reported a HA20 patient with intestinal Behcet's disease-like symptoms, including relapsing ulceration of intestinal anastomosis, recurrent oral ulcers and vasculitis in extremities.

CASE REPORT

The patient was a 29-year-old female who had suffered from recurrent oral ulcers, abdominal pain and diarrhea since the age of 15 years. Recurrent ascending colonic ulcers and anastomotic ulcers along with intestinal obstruction were observed prior to and for 8 years after right hemicolectomy surgery (**Figures 1A–C**), accompanied by vasculitis in extremities (**Figure 1D**). Laboratory data showed elevated C-reactive protein (19.6 mg/L; normal range (NR) <5 mg/L) and erythrocyte sedimentation rate (25 mm/h; NR<20 mm/h), along with a low titer of the antinuclear antibody (1:100). Serum IgG and IgM were within the normal range but IgA levels were low (IgG 19.3–25.8g/L, IgM 0.73–0.92 g/L, IgA <0.07g/L). The patient responded to a glucocorticoid and thalidomide in 3 months with reduced frequency of diarrhea and less severe abdominal pain. The patient's IgA increased but did not reach normal levels after treatment. Subsequent inquiries into the patient's family history revealed that her father suffered from recurrent oral ulcers when he was young, and her brother had suffered from recurrent fever, oral ulcers and erythema nodosum-like lesions in the skin since he was 4 years old. The level of serum immunoglobulins in the father and brother were in the normal ranges. Because of the mild and non-specific symptoms, they accepted treatment of only antimicrobial mouthwash and dental ulcer paste instead of immunomodulators.

GENETIC ANALYSIS

Whole exome sequencing (WES) was performed on the patient. In our study, single nucleotide variants (SNVs) with

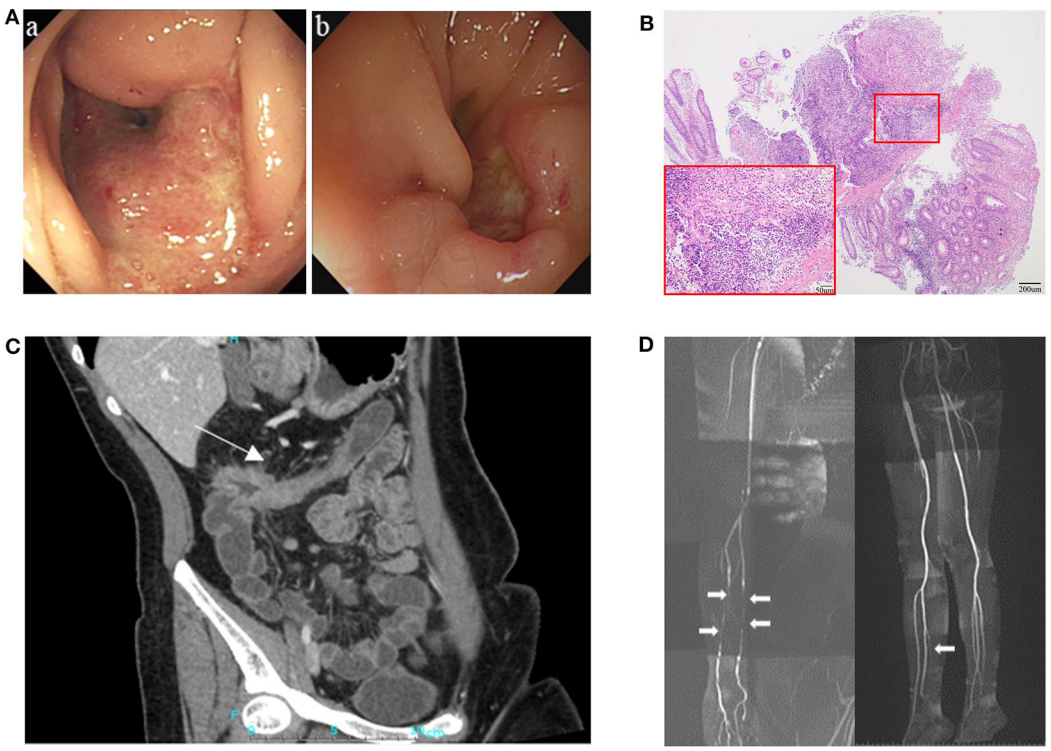

FIGURE 1 | Clinical presentation of the patient. **(A)** Endoscopy showed ulcers and stricture in the ascending colon in August 2010 (a), and relapsing ulceration of intestinal anastomosis and stricture in transverse colon 8 years after right hemicolectomy (b). **(B)** Pathological examination showed intestinal transmural inflammation with an increased number of inflammatory cells infiltration, loss of crypt and hyperplasia of fibrous tissue. **(C)** CT enterographic (CTE) image demonstrated thickening of the wall and stricture in the colon-hepatic curvature and the proximal transverse colon (arrow). **(D)** Magnetic resonance angiography (MRA) showed multiple arteritis stenosis in upper and lower limbs (white arrows).

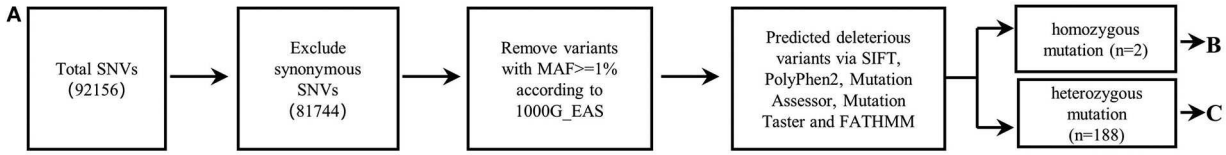

B

Gene	dbSNP ID	Coding change	Protein change	Functional effect	1000G_EAS	*SIFT/PolyPhen2/Mutation Assessor/Mutation Taster/FATHMM	Type
STRA8	rs372540894	c.730G>C	p. Glu244Gln	missense	0.0069	D/D/M/-/-	Homozygous
UEVLD	rs201635931	c.1362A>T	p. Lys454Asn	missense	0.001597	D/P/M/-/T	Homozygous

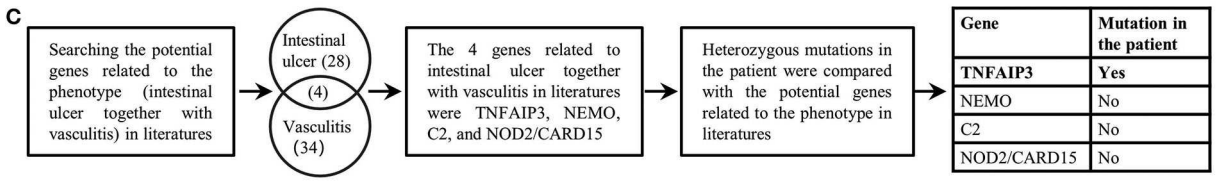

Gene	Mutation in the patient
TNFAIP3	Yes
NEMO	No
C2	No
NOD2/CARD15	No

D

Gene	dbSNP ID	Coding change	Protein change	Functional effect	1000G_EAS	*SIFT/PolyPhen2/Mutation Assessor/Mutation Taster/FATHMM	Type
TNFAIP3	rs146534657	c.305A>G	p.Asn102Ser	Structural interaction variant	0.0079	D/D/M/D/T	Heterozygous

Abbreviation: SNV: single nucleotide variants, MAF: minor allele frequency, db SNP: Database of single nucleotide polymorphism, 1000G_EAS : Asian population from the 1000 Geneomes Project control database.
*SIFT (T, tolerated; D, deleterious), PolyPhen2 (D, probably damaging; P, possibly damaging; B, benign), MutationAssessor (H, high; M, medium; L, low; N, neutral), MutationTaster (D, diseasing-causing; N, polymorphism) or FATHMM(T, tolerated; D, deleterious).

FIGURE 2 | Filtering strategies for candidate disease-causing SNVs in the patient. **(A)** Screening for predicted deleterious variants in the patient, including homozygous mutations and heterozygous mutations. **(B)** The genetic information of homozygous mutations identified in the patient. STRA8 and UEVLD mutations were not reported to be associated with intestinal ulcers or vasculitis. **(C)** The procedure of screening candidate variants based on the phenotype of the patient. Genes likely related to intestinal ulcer together with vasculitis were screened out by searching in literatures. And four genes including TNFAIP3, NEMO, C2, NOD2/CARD15 were reported to be related to intestinal ulcer together with vasculitis. By comparing the heterozygous gene mutations in the patient with the above four genes, the TNFAIP3 heterozygous mutation was identified as the candidate disease-causing mutation in the proband. **(D)** The genetic information of the TNFAIP3 gene mutation in the patient.

minor allele frequency (MAF)<0.01 in the Asian population of the 1,000 Genomes Project (1000G_EAS) were supposed to be potential disease-causing mutations; the distribution of BD shows a racial difference with a higher incidence in eastern Asian populations along the "Silk Road" (5). The 1,000 Genomes Project (1000G) facilitates genetic variation analysis within and between races by providing a detailed view of variation across several races which includes a Chinese group (6). The MAF of screened SNVs were also investigated in other common genome sequencing databases. Candidate disease-causing variants of the patient were screened based on the reported gene mutations associated with intestinal ulcer and vasculitis. The screening of a causal variant followed a standard procedure (7). The WES revealed two homozygous deleterious mutations of *stimulated by retinoic acid gene 8 (STRA8)* and *UEV and lactate/malate dehyrogenase domains (UEVLD)*, but these were not associated with the phenotype of intestinal ulcer and vasculitis according to the literature. A heterozygous deleterious mutation of TNFAIP3 related to intestinal ulcer and vasculitis was identified by the WES (c.305A>G, p. Asn 102 Ser) (MAF=0.0079 in 1000G_EAS, MAF=0.0130 in 1000G_ALL, MAF=0.0030 in GnomAD, MAF=0.0135 in GnomAD_EAS, MAF=0.01734 in ExAC). The details of the WES results and variant filtering procedure are given in **Figures 2A–D**. Sanger sequencing was performed for the patient's whole genealogy and the identical mutation of *TNFAIP3* was found in her father and younger brother (**Figure 3A**).

EXPRESSION OF A20 IN THE PATIENT AND HER FAMILY

Protein was extracted from the peripheral blood mononuclear cells (PBMCs) of the patient and her family members and the expression of A20 was evaluated by Western blot. The levels of A20 were decreased in the PBMCs of the patient and her family members who carried the identified mutation

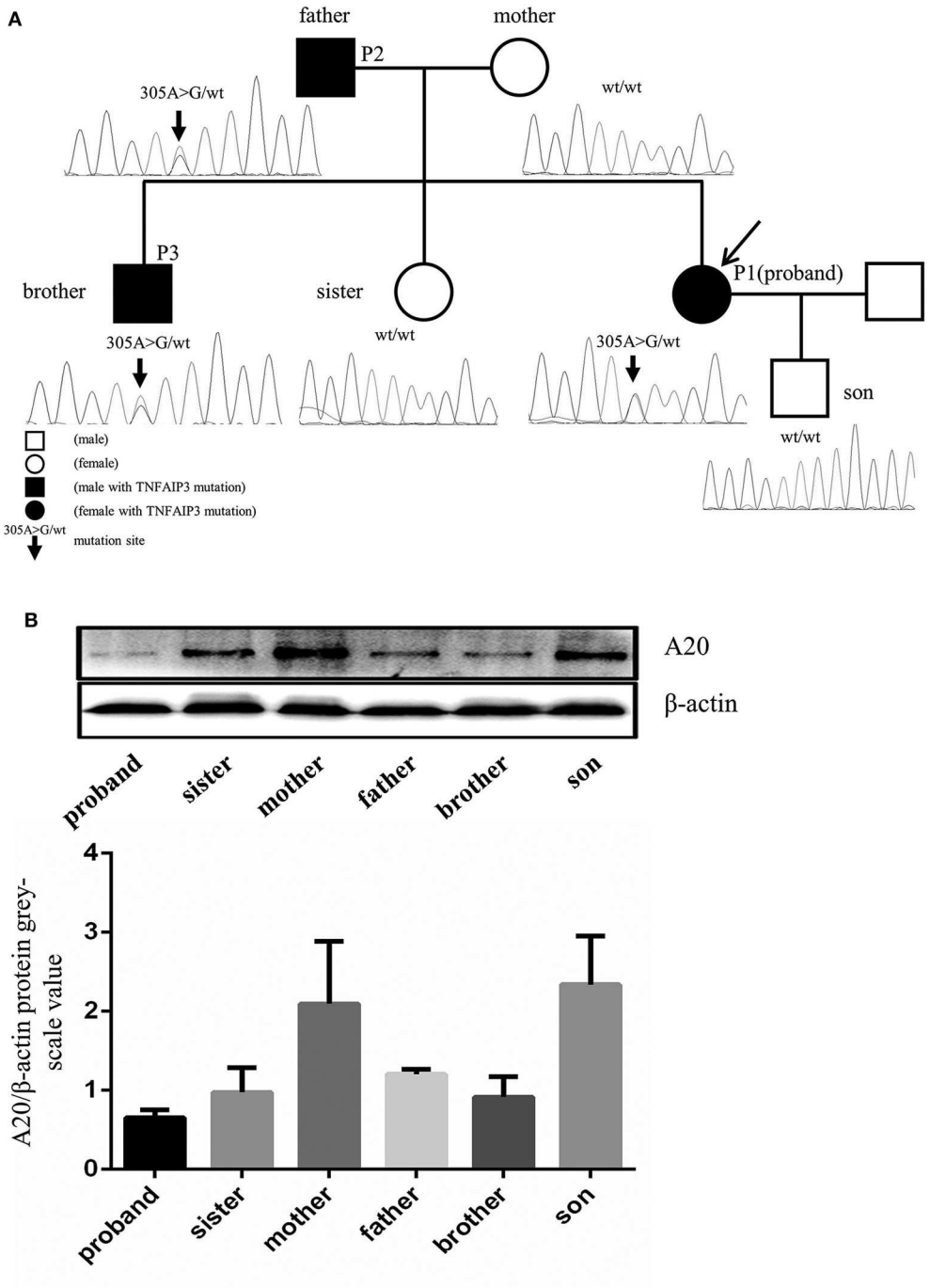

FIGURE 3 | TNFAIP3 mutation and the A20 expression in PBMC of the proband and her family members. **(A)** Sequencing analysis of the TNFAIP3 gene among the proband and her family members revealed a heterozygous mutation (c.305A>G, p. Asn 102 Ser) in the proband, her father and her brother. **(B)** Western blot analysis showed that TNFAIP3 expression in PBMC from the patient, her father, brother and sister were decreased as compared to other family members without TNFAIP3 mutation. The bar graph represented semi-quantification of Western blot analysis from 3 independent experiments.

(**Figure 3B**). To our surprise, her pregnant sister who lacked the *TNFAIP3* mutation also showed a lower level of A20 expression compared to other family members without the *TNFAIP3* mutation.

DISCUSSION

A20 plays an important role in regulating immunity by inhibiting NF-κB signaling, activation of NLRP3 inflammasome, and

apoptosis (8, 9). Haploinsufficiency of A20 is characterized by an upregulated inflammatory reaction and manifests symptoms that resemble many autoimmune diseases, including BD, rheumatoid arthritis (RA) and systemic lupus erythematosus (SLE) (3). The patient in our report presented with iBD-like symptoms, including relapsing ulceration of intestinal anastomosis, recurrent oral ulcers and vasculitis in extremities; although, the patient's intestinal ulcer was atypical due to the long segment involvement in the intestine and incomplete intestinal obstruction. WES and Sanger sequencing identified a novel *TNFAIP3* mutation in the patient that has not been previously reported in HA20. *TNFAIP3* mutations may lead to a reduced transcription and instability of mutant proteins (4, 7, 9). This mutation causes decreased A20 expression and results in immune dysregulation with increased NF-κB activity in response to TNF-α (10); it is also proposed as a risk factor for autoimmune disorders (11, 12). Additionally, *TNFAIP3* is reported to be linked with susceptibility to BD (4, 13, 14). Intestinal Behcet's disease is considered a polygenic disease with a strong genetic background, but its diagnosis is still based on typical intestinal ulcers and manifestations of systemic BD (2). The homozygous mutations of STRA8 and UEVLD revealed through WES were not considered the disease-causing genes because they were likely non-contributory to the disease phenotype of intestinal ulcer and vasculitis previously documented in the literature. Our case reported that the *TNFAIP3* gene is also associated with iBD-like symptoms, suggesting that for patients with iBD-like symptoms that lack typical intestinal ulcers, genetic screening for TNFAIP3 could be considered.

HA20 is an autosomal-dominant-inherited disease that has been described with considerable variation in its expressivity (15). Consistent with the features of an autosomal-dominant-inherited disease, the three members in the reported family that carried the identical *TNFAIP3* mutation showed varying degrees of symptoms. When an autosomal-dominant-inherited disease occurs in a pedigree without apparent familial hereditary traits, it is an option to identify the genetic mutation by initially screening for a causal mutation in the proband by WES and then further identifying the mutation in pedigrees by Sanger sequencing. When we analyze a genetic disease with a specific difference, deleterious variants should be screened for in an appropriate genome sequencing database in accordance with the relevant population.

A reproducible decrease in TNFAIP3 expression was also found in the patient's pregnant sister who lacked the *TNFAIP3* mutation. This can be explained by the fact that some factors other than TNFAIP3 mutation can influence the expression of A20, such as hyperglycemia, oxidative stress, and high levels of 17β-estradiol (16–18). The decreased level of A20 in the patient's sister may have resulted from these other factors rather than a *TNFAIP3* mutation.

In conclusion, we presented a HA20 patient with iBD-like symptoms and identified a novel *TNFAIP3* heterozygous mutation locus (c.305A>G, p. Asn 102 Ser) in HA20. Looking forward, genetic screening for TNFAIP3 could be considered for patients with iBD-like symptoms.

DATA AVAILABILITY STATEMENT

The original contributions presented in the study are included in the article/supplementary material, further inquiries can be directed to the corresponding author/s.

ETHICS STATEMENT

Informed consent and blood sample collection were obtained from the patient for the publication of this case report. Approval for the study was obtained from the Ethical Committee of Tongji Hospital, Tongji Medical College, Huazhong University of Science and Technology. Informed consent was provided according to the Declaration of Helsinki.

AUTHOR CONTRIBUTIONS

FX and YC: study concept and design, acquisition, analysis and interpretation of data, and drafting of the manuscript. HH, FX, YH, and DT: collection, analysis, and interpretation of clinical data. US and MC: a critical review of the manuscript. All the authors approved the final draft of the manuscript submitted for publication.

FUNDING

This work was supported by grants from the National Natural Science Foundation of China (81470807 to FX, 81873556 to FX) and Wu Jieping Medical Foundation (320.6750.17397 to FX).

ACKNOWLEDGMENTS

The authors thank the patient and her family for their cooperation and understanding of our research.

REFERENCES

1. International Team for the Revision of the International Criteria for Behcet's Disease. The International Criteria for Behcet's Disease (ICBD): a collaborative study of 27 countries on the sensitivity and specificity of the new criteria. *J Eur Acad Dermatol Venereol.* (2014) 28:338–47. doi: 10.1111/jdv.12107
2. Lee HJ, Cheon JH. Optimal diagnosis and disease activity monitoring of intestinal Behcet's disease. *Intest Res.* (2017) 15:311–7. doi: 10.5217/ir.2017.15.3.311
3. Yu MP, Xu XS, Zhou Q, Deuitch N, Lu MP. Haploinsufficiency of A20 (HA20): updates on the genetics, phenotype, pathogenesis and treatment. *World J Pediatr.* (2019) doi: 10.1007/s12519-019-00288-6. [Epub ahead of print].
4. Zhou Q, Wang H, Schwartz DM, Stoffels M, Park YH, Zhang Y, et al. Loss-of-function mutations in TNFAIP3 leading to A20 haploinsufficiency cause an early-onset autoinflammatory disease. *Nat Genet.* (2016) 48:67–73. doi: 10.1038/ng.3459
5. Yazici H, Seyahi E, Hatemi G, Yazici Y. Behcet syndrome: a contemporary view. *Nat Rev Rheumatol.* (2018) 14:107–19. doi: 10.1038/nrrheum.2017.208

6. Genomes Project Consortium, Abecasis GR, Auton A, Brooks LD, dePristo MA, Durbin RM, et al. An integrated map of genetic variation from 1,092 human genomes. *Nature.* (2012) 491:56–65. doi: 10.1038/nature11632
7. Tsuchida N, Kirino Y, Soejima Y, Onodera M, Arai K, Tamura E, et al. Haploinsufficiency of A20 caused by a novel nonsense variant or entire deletion of TNFAIP3 is clinically distinct from Behcet's disease. *Arthritis Res Ther.* (2019) 21:137. doi: 10.1186/s13075-019-1928-5
8. Catrysse L, Vereecke L, Beyaert R, van Loo G. A20 in inflammation and autoimmunity. *Trends Immunol.* (2014) 35:22–31. doi: 10.1016/j.it.2013.10.005
9. Rajamäki K, Keskitalo S, Seppänen M, Kuismin O, Vähäsalo P, Trotta L, et al. Haploinsufficiency of A20 impairs protein-protein interactome and leads into caspase-8-dependent enhancement of NLRP3 inflammasome activation. *RMD Open.* (2018) 4:e000740. doi: 10.1136/rmdopen-2018-000740
10. Zhang B, Naomi Nakamura B, Perlman A, Alipour O, Abbasi SQ, Sohn P, et al. Identification of functional missense single-nucleotide polymorphisms in TNFAIP3 in a predominantly Hispanic population. *J Clin Transl Sci.* (2018) 2:350–5. doi: 10.1017/cts.2019.3
11. Higuchi T, Oka S, Furukawa H, Nakamura M, Komori A, Abiru S, et al. Role of deleterious single nucleotide variants in the coding regions of TNFAIP3 for Japanese autoimmune hepatitis with cirrhosis. *Sci Rep.* (2019) 9:7925. doi: 10.1038/s41598-019-44524-5
12. Zhu L, Wang L, Wang X, Zhou L, Liao Z, Xu L, et al. Characteristics of A20 gene polymorphisms and clinical significance in patients with rheumatoid arthritis. *J Transl Med.* (2015) 13:215. doi: 10.1186/s12967-015-0566-1
13. Shigemura T, Kaneko N, Kobayashi N, Kobayashi K, Takeuchi Y, Nakano N, et al. Novel heterozygous C243Y A20/TNFAIP3 gene mutation is responsible for chronic inflammation in autosomal-dominant Behcet's disease. *RMD Open.* (2016) 2:e000223. doi: 10.1136/rmdopen-2015-000223
14. Oguz AK, Yilmaz ST, Oygur CS, Çandar T, Sayin I, Kiliçoglu SS, et al. Behcet's: a disease or a syndrome? Answer from an expression profiling study. *PLoS ONE.* (2016) 11:e0149052. doi: 10.1371/journal.pone.0149052
15. Kadowaki T, Ohnishi H, Kawamoto N, Hori T, Nishimura K, Kobayashi C, et al. Haploinsufficiency of A20 causes autoinflammatory and autoimmune disorders. *J Allergy Clin Immunol.* (2018) 141:1485–8.e11. doi: 10.1016/j.jaci.2017.10.039
16. Shrikhande GV, Scali ST, da Silva CG, Damrauer SM, Csizmadia E, Putheti P, et al. O-glycosylation regulates ubiquitination and degradation of the anti-inflammatory protein A20 to accelerate atherosclerosis in diabetic ApoE-null mice. *PLoS ONE.* (2010) 5:e14240. doi: 10.1371/journal.pone.0014240
17. Kulathu Y, Garcia FJ, Mevissen TE, Busch M, Arnaudo N, Carroll KS, et al. Regulation of A20 and other OTU deubiquitinases by reversible oxidation. *Nat Commun.* (2013) 4:1569. doi: 10.1038/ncomms2567
18. Vendrell JA, Ghayad S, Ben-Larbi S, Dumontet C, Mechti N, Cohen PA., et al. A20/TNFAIP3, a new estrogen-regulated gene that confers tamoxifen resistance in breast cancer cells. *Oncogene.* (2007) 26:4656–67. doi: 10.1038/sj.onc.1210269

Conflict of Interest: The authors declare that the research was conducted in the absence of any commercial or financial relationships that could be construed as a potential conflict of interest.

frontiers in Immunology

REVIEW
published: 27 August 2020
doi: 10.3389/fimmu.2020.01595

The NLRP3 Inflammasome and Its Role in T1DM

Xiaoxiao Sun[1,2†], Haipeng Pang[1,2†], Jiaqi Li[1,2], Shuoming Luo[1,2], Gan Huang[1,2], Xia Li[1,2], Zhiguo Xie[1,2] and Zhiguang Zhou[1,2*]*

[1] Department of Metabolism and Endocrinology, The Second Xiangya Hospital, Central South University, Changsha, China, [2] Key Laboratory of Diabetes Immunology (Central South University), Ministry of Education, National Clinical Research Center for Metabolic Diseases, Changsha, China

The NLRP3 (nucleotide-binding and oligomerization domain-like receptor family pyrin domain-containing 3) inflammasome is a protein complex expressed in cells. It detects danger signals and induces the production of active caspase-1 and the maturation and release of IL (interleukin)-33, IL-18, IL-1β and other cytokines. T1DM (type 1 diabetes mellitus) is defined as a chronic autoimmune disorder characterized by the autoreactive T cell-mediated elimination of insulin-positive pancreatic beta-cells. Although the exact underlying mechanisms are obscure, researchers have proposed that both environmental and genetic factors are involved in the pathogenesis of T1DM. Furthermore, immune responses, including innate and adaptive immunity, play an important role in this process. Recently, the NLRP3 inflammasome, a critical component of innate immunity, was reported to be associated with T1DM. Here, we review the assembly and function of the NLRP3 inflammasome. In addition, the activation and regulatory mechanisms that enhance or attenuate NLRP3 inflammasome activation are discussed. Finally, we focus on the relationship between the NLRP3 inflammasome and T1DM, as well as its potential value for clinical use.

Keywords: T1DM, NLRP3 inflammasome, IL-1β, innate immunity, autoimmune disorder

OPEN ACCESS

Edited by:
Michael Zemlin, Saarland University Hospital, Germany

Reviewed by:
Helen Thomas, The University of Melbourne, Australia
Tao Li, National Center of Biomedical Analysis (NCBA), China

***Correspondence:**
Zhiguo Xie
xiezhiguo@csu.edu.cn
Zhiguang Zhou
zhouzhiguang@csu.edu.cn

[†]These authors have contributed equally to this work

Specialty section:
This article was submitted to Autoimmune and Autoinflammatory Disorders, a section of the journal Frontiers in Immunology

Received: *15 March 2020*
Accepted: *16 June 2020*
Published: *27 August 2020*

Citation:
Sun X, Pang H, Li J, Luo S, Huang G, Li X, Xie Z and Zhou Z (2020) The NLRP3 Inflammasome and Its Role in T1DM. Front. Immunol. 11:1595. doi: 10.3389/fimmu.2020.01595

INTRODUCTION

The inflammatory response is a common mechanism of many diseases. However, the clinical manifestations caused by the combination of a certain microenvironment and a variety of stimuli from common or specific pathways are different. Currently, many chronic diseases, particularly diabetes, are serious threats to human health. Many researchers have recognized that inflammatory immune factors induce many chronic diseases. Innate immune cells induce a series of inflammatory responses by detecting various PAMPs (pathogen-associated molecular patterns) or DAMPs (damage-associated molecular patterns) through innate sensors (1). With a relative molecular mass of approximately 700,000 Da, the NLRP3 inflammasome is a polyprotein complex that plays a critical role in the course of inflammatory responses (2). The NLRP3 inflammasome is comprised of NLRP3, ASC (apoptosis-associated speck-like protein containing a caspase recruitment domain), and procaspase-1 (3, 4). It is the most well-studied inflammasome and functions as a site for the activation of caspase-1 (3, 5). Based on emerging evidence, activated caspase-1 causes the maturation of IL-1 (6, 7). Because the NLRP3 inflammasome may trigger the release of IL-1β after

stimulation with various danger signals, it represents a potentially effective target to regulate the onset and development of various autoimmune diseases, such as T1DM.

T1DM is defined as an organ-specific autoimmune disorder characterized by the autoreactive T cell-mediated elimination of insulin-producing pancreatic beta-cells (8). Although the exact underlying mechanisms are still unknown, a combination of environmental and genetic elements are involved in the pathophysiological process of T1DM (9–11). Both innate immunity and adaptive immunity are involved in the progression of T1DM (12–14). Innate immunity, which serves as the first line of defense against an exogenous attack by bacteria, viruses, and fungi, is a relatively conserved immune response compared with adaptive immunity (15, 16). Previous studies have confirmed that the innate immune system exerts its effect *via* highly conserved PRRs (pattern-recognition receptors) to initiate innate inflammatory responses to both exogenous and endogenous trigger factors and further activate adaptive immunity (16–18). Upon the recognition of DAMPs and PAMPs, which are associated with cellular stress and microbial pathogens, PRRs promote the secretion of proinflammatory cytokines by inducing either non-transcriptional or transcriptional innate immune responses (19, 20). NLRP3 is a PRR, and the NLRP3 inflammasome is a component of the innate immune system that plays a key role in the inflammatory response. In this review, we discuss the components and functions of the NLRP3 inflammasome and the activation mechanisms and regulatory mechanisms that potentiate or limit NLRP3 inflammasome activation. In addition, we describe the function of the NLRP3 inflammasome in T1DM to provide a potential treatment target for the prevention and improvement of this disorder.

COMPONENTS AND FUNCTION OF THE NLRP3 INFLAMMASOME

The NLRP3 inflammasome is a protein complex that includes procaspase-1, ASC and NLRP3 (21). NLRP3 is a member of the NLR (Nod like-receptor) protein family, which is widely expressed in macrophages, monocytes, and dendritic cells and has the function of recognizing pathogens. NLRP3 has a characteristic NLR protein family LRR (leucine-rich repeat) domain at the C-terminus (22). The middle region of NLRP3 is called the NBD (nucleotide-binding domain), also known as NOD or NACHT. The NBD belongs to the NTPase superfamily and hydrolyzes ATP into GTP. The N-terminus contains a PYD (pyrin domain), which is also called the CARD (caspase recruitment domain) or BIR (baculovirus IAP repeat) domain; this domain participates in multiple inflammatory responses by binding molecules with the same domain. For example, ASC is bound *via* the PYD-PYD interaction. ASC is the adapter protein of the NLRP3 inflammasome. The N-terminus of ASC contains a PYD domain that is the same as the PYD domain in NLRP3, whereas the C-terminus contains a CARD recruitment domain that is the same as the CARD domain in procaspase-1. Therefore, ACS functions as a dual adapter protein molecule that binds to both NLRP3 and procaspase-1 through PYD-PYD and CARD-CARD domain interactions. Caspase-1, also called IL-1β-converting enzyme, is an effector protein of the inflammasome that cleaves inactive proinflammatory cytokines, including pro-IL-1β and pro-IL-18, to produce activated IL-1β and IL-18 (**Figure 1**) (23, 24).

NLRP3 activation results in the oligomerization and recruitment of ASC and procaspase-1, which increase the autocleavage and maturation of procaspase-1. Active caspase-1 cleaves pro-IL-1β to produce mature IL-1β, which, when released, recruits other inflammatory cells and exerts direct cytotoxic effects. In addition, the NLRP3 inflammasome mediates a special type of programmed cell death named pyroptosis, which is inherently inflammatory and is triggered by pathological stimuli through the activation of caspase-1 (25, 26). The process of pyroptosis is mediated by Gasdermin (GSDMD), consisting of an amino-terminal cell death region, a carboxy-terminal autoinhibitory region, and a central linker domain (27). GSDMD is activated by caspase-1 through the removal of its carboxyl inhibitory terminus, and activated GSDMD induces cell death characterized by plasma membrane rupture, DNA cleavage and cell lysis by binding to the inner leaflet of the cell membrane, oligomerizing and forming a pore containing 16 symmetrical promoters (28). Based on the results of *in vitro* studies, activated GSDMD possesses a bactericidal property, but the exact mechanisms remain obscure (29). In addition, GSDMD-dependent pyroptosis promotes IL-1β and IL-18 release *via* a non-conventional pathway (30, 31). In conclusion, caspase-1 activation will result in the production of activated proinflammatory cytokines and lead to rapid cell death (32, 33).

NLRP3 is activated by a number of pathogens, as well as many PAMPs and DAMPs, which are structurally diverse, and environmental irritants. NLRP3 oligomerizes *via* homotypic interactions between NACHT domains to form a high-molecular-weight complex that triggers procaspase-1 activation when it is stimulated (22). The pathogenic agents that activate the NLRP3 inflammasome include (1) the fungi *Saccharomyces cerevisiae* and *Candida albicans* that function *via* the Syk signaling pathway (34); (2) a pore-forming toxin-producing bacteria (35); and (3) viruses, including the influenza virus, adenovirus, and the Sendai virus (36, 37).

MECHANISMS UNDERLYING THE ACTIVATION AND REGULATION OF THE NLRP3 INFLAMMASOME

Mechanisms Underlying the Activation of the NLRP3 Inflammasome

The NLRP3 inflammasome is activated by a wide range of stimuli. For example, the NLRP3 inflammasome detects signals produced by metabolism, such as increased extracellular glucose levels, which is an essential manifestation of diabetes (38). However, given their structural and chemical dissimilarity, NLRP3 is not likely to be activated through a direct interaction with its

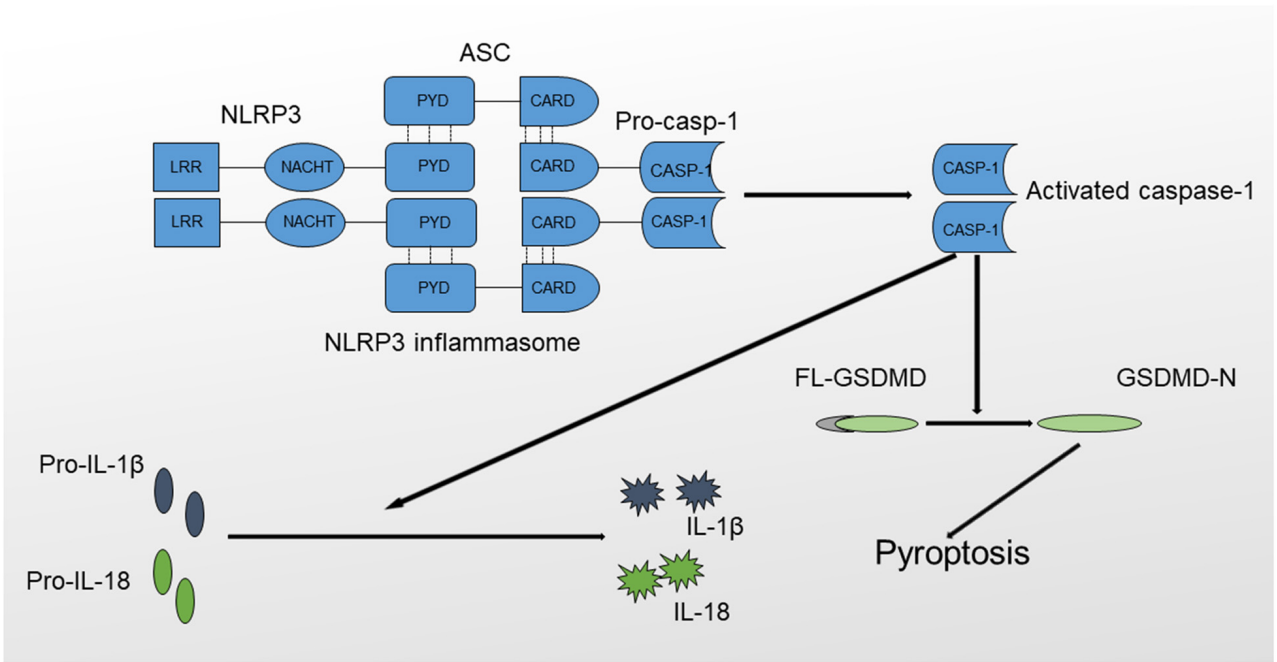

FIGURE 1 | Structure and function of the NLRP3 inflammasome. The NLRP3 inflammasome comprises NLRP3, ASC and procaspase-1. The formation of the NLRP3 inflammasome results in the activation of caspase-1 through the self-cleavage of procaspase-1. Activated caspase-1 causes the maturation of IL-1β and IL-18 and triggers inflammatory cell death mediated by GSDMD, also termed pyroptosis.

stimuli (39). Researchers have speculated that different agonists will lead to a common cellular event that ultimately activates the NLRP3 inflammasome.

When NLRP3 is not activated, the LRR domain interacts with HSP90 (heat-shock protein 90) and the ubiquitin ligase-associated protein SGT1HSP90, which are likely to maintain NLRP3 in an inactive but signaling-competent state (40). Two types of signals are needed to activate the NLRP3 inflammasome (41). First, a ligand binds to TLR4 on the membrane to provide the first signal that induces the expression of NLRP3, IL-1β, and IL-18 by triggering the NF-kB signaling pathway (42). In addition, TLR4 may provide the first signal *via* an unknown mechanism through the proteins myD88 and IRAK1. A low level of TLR4 stimulation is sufficient for the ATP activation pathway, and this pathway does not require the synthesis of new proteins (43–45). Because the expression of endogenous NLRP3 in immune cells is not sufficient to activate the NLRP3 inflammasome, the activation of NF-kB is necessary for the sufficient production of NLPR3. The second signal is the appearance of the activator of the NLRP3 inflammasome. The NLRP3 inflammasome begins to assemble when it is stimulated (46).

The mechanisms underlying the activation of the NLRP3 inflammasome are still not completely understood and may be associated with ROS (reactive oxygen species) production, lysosomal damage, P2X7R (purinergic ligand-gated ion channel 7 receptor) activation, and K^+ efflux. To date, three models explaining the activation of the NLRP3 inflammasome have been acknowledged by most researchers.

K^+ Efflux

The first model concerns the efflux of K^+, which is the most common mechanism of NLRP3 inflammasome activation. A decreasing cytosolic level of K^+ induced by NLRP3 stimuli, ATP, or nigericin mediates IL-1β activation and release in mouse macrophages and human monocytes (47, 48). Moreover, the efflux of K^+ alone results in the activation of NLRP3, and a high extracellular K^+ concentration inhibits NLRP3 activation (49). Therefore, the intracellular hypokalemia that induces mitochondrial damage and the subsequent release of ROS and mtDNA (mitochondrial DNA) is sufficient to activate the NLRP3 inflammasome (49, 50). In addition, K^+ efflux is necessary to activate NLRP3 in caspase-11-mediated non-canonical inflammasome signaling (6, 51).

Three explanations for K^+ efflux have been proposed. First, bacterial toxins destroy the integrity of the cell membrane, and thus K^+ flows out along the ion concentration gradient (52). Second, the combination of extracellular ATP and the pyrogenic P2X7 ATP-gated ion channel (53) triggers K^+ efflux. Another type of channel, pannexin-1, also participates in the activation of NLRP3 *via* other ATP-dependent pathways (54–56). Third, microbial molecules are delivered to the cytosol in a pannexin 1-independent manner (54). The generation of pores disrupts the intracellular K^+ concentration gradient and transports bacterial molecules to the cytosol, which may help clarify how bacteria that do not exist in the cytosol activate cytosolic sensors.

Although K^+ efflux has been considered the most common mechanism to activate the NLRP3 inflammasome, recent reports have indicated that some small molecules, including

CL097 and GB111-NH_2, activate NLRP3 independently of K^+ efflux (57). Moreover, an *NLRP3* mutant leads to inflammasome activation induced by lipopolysaccharides in the absence of K^+ efflux in mouse macrophages (58). In conclusion, K^+ efflux is sufficient, but not unique, in activating this inflammasome. Further investigations are needed to elucidate the underlying mechanisms by which NLRP3 senses alterations in the intracellular K^+ concentration.

Lysosomal Damage

The second model concerns lysosomal damage. Particulate matter, such as MSU, and adjuvants including alum (59, 60) activate the NLRP3 inflammasome in macrophages. The phagocytosis of specific particulate structures and crystalline structures results in lysosomal membrane disintegration and damage and the cytosolic release of lysosomal contents, which are sensed by the NLRP3 inflammasome to some extent.

Lysosomal disruption triggered by Leu-Leu-OMe activates the NLRP3 inflammasome (61). However, the exact mechanisms by which lysosomal damage contributes to the activation of NLRP3 remain obscure. Currently, two factors, lysosomal acidification and cathepsins, have been identified to be associated with the activation mechanisms. An H^+ ATPase inhibitor blocks NLRP3 inflammasome activation induced by particulate matter in macrophages (61). Additionally, both *in vitro* and *in vivo* experiments suggest that inhibitors of lysosomal acidification suppress IL-1β production (62). In fact, the acidic conditions tend to cause Na^+ release and increase cellular osmolarity and subsequent water influx, resulting in intracellular hypokalemia (62). Moreover, lysosomal rupture leads to enzyme release and the activation of the NLRP3 inflammasome. These proteases suppress the activation of negative regulators and increase the activation of NLRP3 through proteolytic reactions, which lead to inflammasome assembly (63). Lysosomal protease CTSB (cathepsin B) plays an important role in the model. CTSB inhibitors attenuate NLRP3 activation in macrophages treated with particulate matter (6). Furthermore, lysosomal CTSB release is required for IL-1β secretion, indicating the participation of CTSH in NLRP3 activation (64). Therefore, the cytosolic release of lysosomal contents is another mechanism of NLRP3 inflammasome activation. However, CTSB-deficient mouse macrophages show normal caspase-1 activation and IL-1β maturation induced by particulate NLRP3 agonists, suggesting that some undefined mechanisms exist (65). Further research is required to solve the existing conflicts and clarify the actual role of lysosomal damage in NLRP3 inflammasome activation.

Reactive Oxygen Species and Mitochondrial Dysfunction

The third model concerns the generation of ROS. In this model, all agonists of NLRP3 induce ROS production, and this collective pathway involves the NLRP3 inflammasome (66–68). All NLRP3 agonists that have been confirmed, including particulate activators and ATP, induce ROS production, and chemical scavengers that block ROS generation inhibit inflammasome activation (34, 66–69). Consistent with the role of ROS production, the activation of caspase-1 by asbestos is suppressed in NAC (*N*-acetyl cysteine)-treated cells, in which NAC inhibits ROS generation (67). The source of ROS is currently unknown, but NADPH oxidases may be associated with their production, as *in vitro* studies indicate that inhibition of the common p22 subunit, which plays a critical role in ROS formation, suppresses inflammasome activation (67). However, the genetic or pharmacological blockade of NADPH oxidase does not affect NLRP3 activation in both mouse and human cells. The tissue-specific role of ROS may explain the differences in the activation of NLRP3 inflammasome. NOX2 (NADPH oxidase 2) knockout mice were recently shown to display decreased production, assembly and activation of the NLRP3 inflammasome in the injured cerebral cortex, but not in the umbilical vein endothelium.

The mechanisms underlying ROS-dependent NLRP3 inflammasome activation remain to be revealed in more detail. Recently, a ROS-sensitive NLRP3 ligand, TXNIP/VDUP1 (thioredoxin-interacting protein), was shown to be involved in NLRP3 activation (38, 70). When cellular phagocytosis is dysfunctional, activators such as uric acid crystals increase ROS production and simultaneously trigger the dissociation of TXNIP from TRX (thioredoxin). TXNIP has been identified as a common binding partner of TRX (71). TXNIP decreases the reductase activity of TRX by directly interacting with the redox-active part of TRX. A yeast two-hybrid screen using the LRRs of NLRP3 as bait revealed that TXNIP is also a potential binding partner of NLRP3 (72, 73). Overexpressed TXNIP and endogenous TXNIP interact with the LRR region of NLRP3, and the nucleotide-binding NACHT domain of NLRP3 also interacts with TXNIP. NLRP3 detects the presence of ROS, the production of which in cells is directly or indirectly induced by activators of the NLRP3 inflammasome. The complex formed by TXNIP and TRX senses increasing amounts of ROS and causes the dissociation of the complex. Subsequently, the interaction of TXNIP and NLRP3 activates NLRP3, recruits ASC and procaspase-1, and leads to the assembly of the active NLRP3 inflammasome. Intriguingly, accumulating evidence indicates that TXNIP is associated with glucose metabolism and diabetes (74). In pancreatic beta-cells, the expression of TXNIP is downregulated by insulin and is consistently increased in patients diagnosed with T2DM (type 2 diabetes mellitus) (74). Additionally, mutations in TXNIP are associated with reduced plasma glucose levels and hypertriglyceridemia (75). Published data that have been confirmed suggest that the expression of TXNIP is substantially upregulated by exposure to high glucose concentrations in pancreatic islet cells (76, 77). Although the ROS model is supported by many studies, many questions still remain and need to be resolved. For example, researchers have not clarified whether the mechanism by which superoxide directly inhibits caspase-1 activity by regulating redox-sensitive cysteines (78) provides dose- or temporal-dependent negative feedback to limit the function of caspase-1 triggered by a ROS-dependent NLRP3 pathway.

In recent years, mitochondria have been shown to play an essential role in the activation of the NLRP3 inflammasome (79, 80). Mitochondria are an ideal platform to assemble the NLRP3 inflammasome. On the other hand, NLRP3 is directly affected

by molecules from mitochondria, such as mitochondrial ROS (mtROS), mtDNA, and cardiolipin.

Negative Regulatory Mechanisms of the NLRP3 Inflammasome

NLRP3 promotes the secretion of IL-33, IL-18, and IL-1β, which are very important molecules that control pathological infections. However, the excessive production of cytokines exerts a deleterious effect on the body. For instance, the excessive activation of proinflammatory cytokines, including TNF-α, IL-1β, and IFNs, is associated with autoimmune diseases, such as T1DM. Therefore, the activation of the NLRP3 inflammasome must be strictly regulated to maintain the balance of the internal environment and homeostasis. Four negative regulatory mechanisms of the NLRP3 inflammasome have been identified.

Negative Regulatory Molecules

The first mechanism is associated with negative regulatory molecules. A group of small proteins that consist of either a PYD or a CARD domain have emerged as key regulators of the inflammasome. As two types of endogenous dominant-negative proteins, both COPs (CARD-only proteins) and POPs (PYD-only proteins) decrease the activity of the NLRP3 inflammasome in response to tissue injury and pathogen infection (81).

POPs, such as POP1 and POP2, which display 64 and 37% homology with the PYD subunit of ASC, respectively, prevent ASC recruitment to NLRP3 by interacting with ASC in a PYD-dependent manner and replacing other proteins that interact with ASC (82). *In vitro* overexpression models confirm that POP1 and POP2 bind to ASC and block the interaction between NLRP3 and ASC (83). Moreover, *in vivo* studies using transgenic mice expressing POP2 have revealed decreased inflammatory cytokine levels in response to LPS, and the animals tend to resist bacterial infections compared with wild-type mice (84). To date, five proteins belonging to the COP family have been identified, including Iceberg, Nod2-S, caspase-12s, COP1/pseudo-ICE and INCA (27). COPs, which are extremely similar to the CARD subunit of procaspase-1, function as decoy proteins by isolating caspase-1 through CARD domain interactions and preventing its binding to activating adaptors (83). Because the expression of Iceberg is increased in the inflammatory environment, this protein appears to function as a negative feedback regulator that inhibits systemic inflammation. Notably, our understanding of the regulatory effects of POPs and COPs on NLRP3 activation is limited because these molecules are not expressed in mice. However, the development of transgenic mice provides a great opportunity to further analyze these proteins.

Cells and Cytokines

The second mechanism involves certain cells and cytokines. Various immunocytes and proinflammatory cytokines participate in the downregulation of inflammasome activation. For example, human-derived activated memory T cells negatively regulate the P2X7R signaling pathway, leading to the inhibition of the NLRP3 inflammasome (85). C5aR2 (C5a receptor 2), which is expressed on the T cell surface, inhibit NLRP3 inflammasome assembly by inversely modulating C5 activation and stimulating C5aR1 (C5a receptor 1) (85, 86). IL-1β signaling promotes the recruitment of neutrophils; in turn, increased neutrophil apoptosis results in the resolution of the inflammatory response (87). The type I interferon signaling pathway represses the activity of the NLRP3 inflammasome and inhibits the maturation of IL-1β through the STAT1 transcription factor (88).

Autophagy

The third mechanism is associated with autophagy. Autophagy, also referred to as macroautophagy, is a conserved process involving the transport of the cytoplasmic content to lysosomes *via* autophagosomes, and the substrates degraded by this process mainly include long-lived proteins, intracellular pathogens and organelles. Autophagy is involved in the pathogenesis of many inflammatory disorders and modulates many aspects of the immune response, including inflammation (89, 90).

Autophagy inhibits the formation of the NLRP3 inflammasome by degrading impaired mitochondria, decreasing mtROS production and disaggregating the ASC complex (91). *In vitro* experiments using macrophages from mouse models indicate that the depletion of beclin 1 and LC3B, proteins that are associated with autophagy, increases the activation of caspase-1 and release of IL-18 and IL-1β by impairing mitochondrial homeostasis (50, 92, 93). Additionally, autophagy dysfunction, whether it is caused by autophagy deficiency or mitochondrial inhibitors, increases the activation of the NLRP3 inflammasome via the production of mtROS (92). Consistent with the result obtained from cell-based experiments, *in vivo* studies suggest that LC3B-dificient mice produce caspase-1-depedent cytokines at higher levels and exhibit a greater susceptibility to LPS (92). Therefore, autophagy is closely associated with the well-being of mitochondria, and autophagy and the mitochondria modulate the NLRP3-dependent inflammatory response together.

NO and CO

Finally, the other mechanisms, including the production of NO (nitric oxide) and CO (carbon monoxide), negatively regulate the NLRP3 inflammasome. NO regulates multiple physiological responses and defends against pathogens. Endogenous NO downregulates NLRP3 inflammasome activation and stabilizes mitochondria. According to the results of *in vitro* experiments, NO blocks NLRP3-mediated caspase-1 and IL-1β activation in mice and human myeloid cells (94). Additionally, decreased production of NO caused by iNOS (inducible NO synthase) elimination or pharmacological blockade leads to increased cytokine production induced by the activated NLRP3 inflammasome and the accumulation of dysfunctional mitochondria *in vivo* (94). CO is toxic and damages the respiratory system. However, endogenous CO possesses anti-inflammatory properties. CO inhibits the production of IL-1β induced by inflammasomes and suppresses the activation of the NLRP3 inflammasome in bone marrow-derived macrophages; furthermore, CO inhibits mtROS generation, preserves the integrity of mitochondrial membrane, and prevents mtDNA translocation into cytosol (95, 96). Therefore, we conclude that NO and CO negatively modulate the activation of the NLRP3 inflammasome mainly by stabilizing mitochondria.

THE NLPR3 INFLAMMASOME AND T1DM

The NLRP3 inflammasome has consistently been shown to participate in the pathogenesis of many autoimmune disorders, including MS (multiple sclerosis), EAE (experimental autoimmune encephalomyelitis), IBD (inflammatory bowel disease) and T1DM (97–100). T1DM is a metabolic disease characterized by an absolute deficiency in insulin and subsequent hyperglycemia resulting from an autoimmune assault. Autoreactive T cells infiltrate pancreatic islets and induce insulitis, causing beta-cell death (101). In addition to adaptive immunity, innate immunity plays an important role in the pathogenesis of T1DM. Based on accumulating evidence, among all components of the innate immune system, the NLRP3 inflammasome and its downstream cytokines, particularly IL-1β, are involved in the development of T1DM (**Figure 2**) (102, 103).

IL-1β induces the migration of proinflammatory cells into pancreatic islets, mediates cytokine-induced beta-cell apoptosis, exerts direct cytotoxic effects on beta-cells, and may function as inflammatory signal in the early stage of T1DM (102, 104, 105). IL-1β levels are increased in both patients with a new T1DM diagnosis and patients with chronic T1DM compared with healthy controls, and after treatment, IL-1β levels are decreased in patients who have been newly diagnosed with T1DM (106–108). Furthermore, the levels of IL-1 receptor antagonist (IL-1RA), which inhibits the interaction between IL-1β and its receptor and blocks downstream signaling, are decreased in islets from non-diabetic donors exposed to sera from patients with T1DM, and decreased expression of IL-1RA not only results in insulin-producing beta-cell dysfunction and death but also IL-1β production, thus further affecting beta-cells (109). Additionally, NOD mice pretreated with IL-1RA exhibit reduced chemical-induced hyperglycemia, but not islet inflammation (110). Based on these findings, some new treatment strategies aiming to suppress IL-1β activity, such as synthetic IL-1RA and IL-1β traps, have been developed to reverse or ameliorate autoimmune diseases. Indeed, patients with T1DM have decreased requirements for insulin and similar HbA1c (hemoglobin A1c) levels after IL-1RA treatment (102, 111). However, some discrepancies remain to be solved. Animal experiments with NOD caspase-$1^{(-/-)}$ mice revealed reduced IL-1 levels, but an unchanged incidence of diabetes and sensitivity to streptozotocin compared with wild type NOD

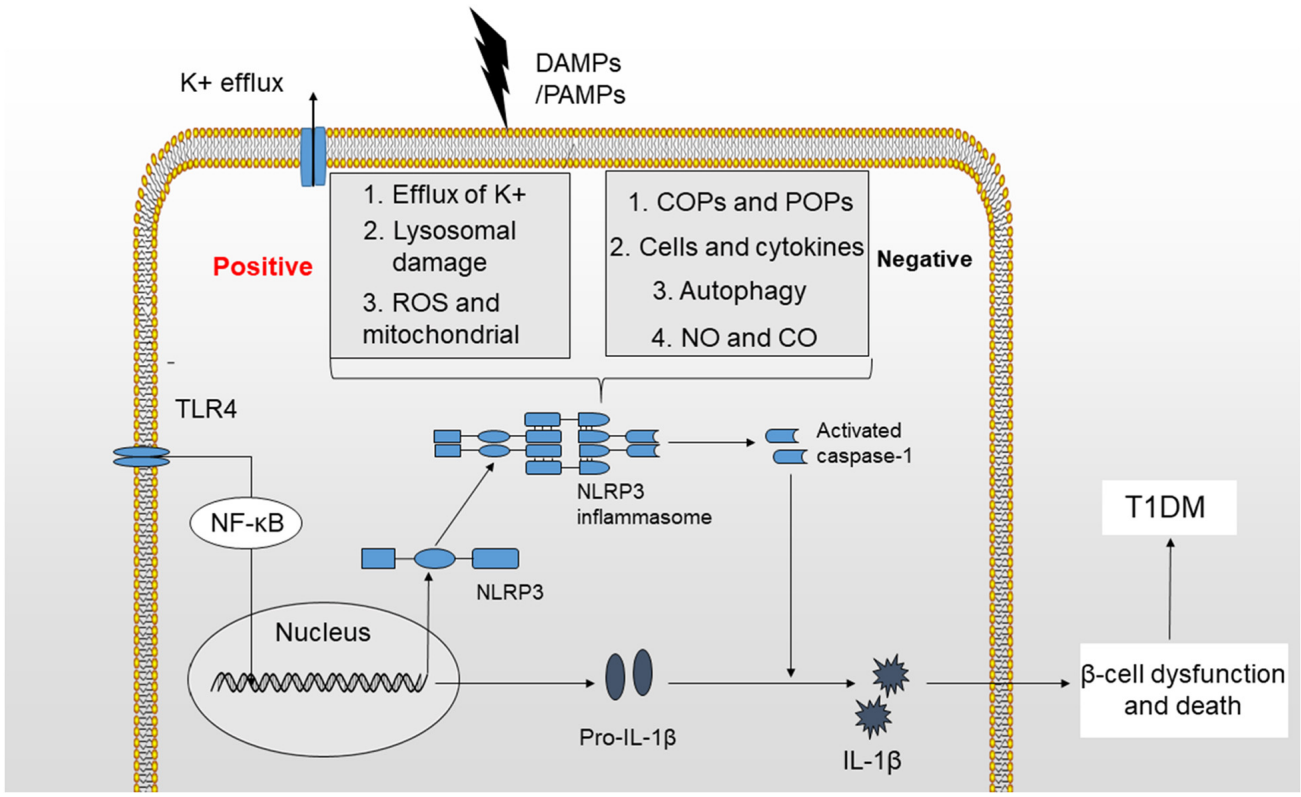

FIGURE 2 | Mechanisms of NLRP3 inflammasome activation. The activation of the NLRP3 inflammasome requires two signals. (1) TLR4 stimulation increases the production of NLRP3 and pro-IL-1β by activating the NF-κB signaling pathway. (2) K^+ efflux, cathepsin release by ruptured lysosomes and ROS generation provide a second signal that may activate the NLRP3 inflammasome and produce activated caspase-1, leading to the maturation of IL-1β. The activation of NLRP3 inflammasome is potentially negatively regulated by small molecules, such as COPs and POPs, cells and cytokines, autophagy, NO, and CO. Finally, IL-1β induces beta-cell dysfunction and death, which will ultimately lead to the development of T1DM.

mouse models (112). At a minimum, caspase-1-mediated IL-1β production is not indispensable for diabetes development in NOD mice. Another *in vivo* experiment also indicates that CD4 + T cell-induced beta-cell death and diabetes is independent of IL-1 and IL-18 in NOD mice (113). Moreover, the larger, multicenter preclinical studies did not observe synergistic effects of IL-1 blockade and anti-CD3 therapy on new-onset autoimmune diabetes in NOD mouse models (114). In conclusion, the role of IL-1β in T1DM pathogenesis is not completely understood and further research is required before its clinical application.

Because IL-1β exerts a systemic effect on immunological intolerance and plays a potential role in T1DM development, its upstream activator, the NLRP3 inflammasome, is a functionally plausible complex contributing to the pathogenesis of T1DM. that the expression of the NLRP3 inflammasome in human pancreatic islets is regulated by LPS (115). Interestingly, recent genetic association studies have indicated a potential association between polymorphisms in inflammasome genes and an increased risk of developing T1DM. As shown in our previous study, SNPs (single-nucleotide polymorphisms) in the NLRP1 gene are associated with T1DM, as well as the age of onset in Chinese Han patients with T1DM (100). More importantly, two SNPs within NLRP3 were found to be associated with an increased risk of T1DM and celiac disease in a separate study. An association between T1DM and a risk SNP (rs10754558) within NLRP3 in the northeastern Brazilian population was identified in a human study (116). However, the contribution of this mutation to the genetic predisposition should be further confirmed in other populations and its resulting function requires further study. In addition, the diabetogenic role of NLRP3 has been observed in animal experiments. NLRP3 was recently shown to play an important role in the immune development of T1DM in NOD mice (103). NLRP3 deficiency affects the activation and maturation of T cells, and more importantly, the elimination of NLRP3 alters the migration of T cells to pancreatic islets, which is a critical pathogenic process that causes beta-cell damage. Furthermore, NLRP3 knockout downregulates the expression of the chemokines CCL5 (C-C motif ligand 5) and CXCL10 (C-X-C motif ligand 10) in pancreatic islet cells in an IRF-1-dependent manner, suggesting that it regulates chemotaxis (103). Moreover, mtDNA-mediated NLRP3 activation induces caspase-1-dependent IL-1β production and contributes to STZ (streptozotocin)-induced T1DM in a murine model, directly indicating a diabetogenic effect of NLRP3-caspase-1-IL-1β signaling (117). Recently, mtDNA was also shown to be involved in the vascular dysfunction in individuals with T1DM, highlighting the association of the NLRP3 inflammasome with diabetic complications (118). Other studies have confirmed that glibenclamide and metformin, both of which are typical treatments for diabetes, have the potential to inhibit the activation of the NLRP3 inflammasome, indirectly indicating that the NLRP3 inflammasome is associated with T1DM. In summary, all of the evidence mentioned above indicates a close relationship between T1DM and the NLRP3 inflammasome.

However, some questions regarding the NLRP3 inflammasome remain to be explored and resolved. The inflammasome exerts a protective effect on maintaining immune homeostasis (119–121). More importantly, the expression of the NLRP3 inflammasome is downregulated in patients with SLE compared with healthy controls and is negatively correlated with disease activity, indicating a protective effect of the inflammasome on SLE (122). Consistent with these findings, another study examining T1DM also indicated that downregulated NLRP3 inflammasome signaling participates in the early stage of autoimmune diabetes (123). Further studies are required to investigate whether the downregulation of the NLRP3 inflammasome is an outcome or cause of the progression of autoimmune disorders. Moreover, some inflammasome-independent pathways activate IL-1β and are potentially involved in development of T1DM (124, 125), indicating that the onset of T1DM is caused by complex networks rather than a single pathway. In summary, a better understanding of the NLRP3 inflammasome is still needed to completely ascertain its effect on the pathogenesis of T1DM and develop new treatment strategies.

CONCLUSION AND PERSPECTIVES

Researchers have improved their knowledge of the NLRP3 inflammasome. We have identified many different activators and a close relationship with inflammatory diseases, including T1DM. However, the regulatory mechanisms and their function in the development of the disease must be further clarified. The discovery of the NLRP3 inflammasome has provided a new opportunity to explore the pathogenesis of inflammation-related diseases. In-depth research into the NLRP3 inflammasome, which is a regulator of IL-18 and IL-1β, will provide a new strategy for the treatment and prevention of inflammatory diseases.

Currently, the pathogenesis of T1DM is not completely understood. However, both environmental and genetic factors are involved in the onset and development of T1DM. The overactivation of the immune system, including innate immune responses, resulting from predisposing genetic mutations is the main cause of the loss and dysfunction of beta-cells. The NLRP3 inflammasome is much more likely to predispose an individual to the onset of T1DM. However, the mechanisms of NLRP3 inflammasome activation and regulation remain obscure, and the exact role of this inflammasome in the pathogenesis of T1DM requires further investigation. We propose that immunotherapy targeting the NLRP3 inflammasome is a promising approach to fight T1DM.

AUTHOR CONTRIBUTIONS

XS performed the literature search and wrote the first draft of the manuscript. HP generated the figures and revised the text. JL, SL, GH, and XL critically revised the text and provided substantial scientific contributions. ZZ and ZX proposed the project and revised the manuscript. All authors approved the final version of the manuscript.

FUNDING

This review was supported by grants from the National Natural Science Foundation of China (81873634 and 81400783), the National Key R&D Program of China (2016YFC1305000, 2016YFC1305001, and 2018YFC1315603), the Science and Technology Major Project of Hunan Province (2017SK1020), and Hunan Province Natural Science Foundation of China (2018JJ2573 and 2020JJ2053).

REFERENCES

1. Daskalaki MG, Tsatsanis C, Kampranis SC. Histone methylation and acetylation in macrophages as a mechanism for regulation of inflammatory responses. *J Cell Physiol*. (2018). 233:6495–507. doi: 10.1002/jcp.26497
2. Zhang C, Boini KM, Xia M, Abais JM, Li X, Liu Q, et al. Activation of Nod-like receptor protein 3 inflammasomes turns on podocyte injury and glomerular sclerosis in hyperhomocysteinemia. *Hypertension*. (2012) 60:154–62. doi: 10.1161/HYPERTENSIONAHA.111.189688
3. Song N, Li T. Regulation of NLRP3 inflammasome by phosphorylation. *Front Immunol*. (2018) 9:2305. doi: 10.3389/fimmu.2018.02305
4. Moossavi M, Parsamanesh N, Bahrami A, Atkin SL, Sahebkar A. Role of the NLRP3 inflammasome in cancer. *Mol Cancer*. (2018) 17:158. doi: 10.1186/s12943-018-0900-3
5. Stutz A, Golenbock DT, Latz E. Inflammasomes: too big to miss. *J Clin Invest*. (2009) 119:3502–11. doi: 10.1172/JCI40599
6. Kelley N, Jeltema D, Duan Y, He Y. The NLRP3 inflammasome: an overview of mechanisms of activation and regulation. *Int J Mol Sci*. (2019) 20:3328. doi: 10.3390/ijms20133328
7. Yu JW, Lee MS. Mitochondria and the NLRP3 inflammasome: physiological and pathological relevance. *Arch Pharm Res*. (2016) 39:1503–18. doi: 10.1007/s12272-016-0827-4
8. DiMeglio LA, Evans-Molina C, Oram RA. Type 1 diabetes. *Lancet*. (2018) 391:2449–62. doi: 10.1016/S0140-6736(18)31320-5
9. Esposito S, Toni G, Tascini G, Santi E, Berioli MG, Principi N. Environmental factors associated with type 1 diabetes. *Front Endocrinol*. (2019) 10:592. doi: 10.3389/fendo.2019.00592
10. Wang Z, Xie Z, Lu Q, Chang C, Zhou Z. Beyond genetics: what causes type 1 diabetes. *Clin Rev Allergy Immunol*. (2017) 52:273–86. doi: 10.1007/s12016-016-8592-1
11. Xia Y, Xie Z, Huang G, Zhou Z. Incidence and trend of type 1 diabetes and the underlying environmental determinants. *Diabetes Metab Res Rev*. (2019) 35:e3075. doi: 10.1002/dmrr.3075
12. Gao S, Wolanyk N, Chen Y, Jia S, Hessner MJ, Wang X. Investigation of coordination and order in transcription regulation of innate and adaptive immunity genes in type 1 diabetes. *BMC Med Genomics*. (2017) 10:7. doi: 10.1186/s12920-017-0243-8
13. Cabrera SM, Henschel AM, Hessner MJ. Innate inflammation in type 1 diabetes. *Transl Res*. (2016) 167:214–27. doi: 10.1016/j.trsl.2015.04.011
14. Huang J, Xiao Y, Xu A, Zhou Z. Neutrophils in type 1 diabetes. *J Diabetes Investig*. (2016) 7:652–63. doi: 10.1111/jdi.12469
15. Medzhitov R, Janeway C Jr. Innate immunity. *N Engl J Med*. (2000) 343:338–44. doi: 10.1056/NEJM200008033430506
16. Kubelkova K, Macela A. Innate immune recognition: an issue more complex than expected. *Front Cell Infect Microbiol*. (2019) 9:241. doi: 10.3389/fcimb.2019.00241
17. Chu H, Mazmanian SK. Innate immune recognition of the microbiota promotes host-microbial symbiosis. *Nat Immunol*. (2013) 14:668–75. doi: 10.1038/ni.2635
18. Medzhitov R. Recognition of microorganisms and activation of the immune response. *Nature*. (2007) 449:819–26. doi: 10.1038/nature06246
19. Brubaker SW, Bonham KS, Zanoni I, Kagan JC. Innate immune pattern recognition: a cell biological perspective. *Annu Rev Immunol*. (2015) 33:257–90. doi: 10.1146/annurev-immunol-032414-112240
20. Patin EC, Thompson A, Orr SJ. Pattern recognition receptors in fungal immunity. *Semin Cell Dev Biol*. (2019) 89:24–33. doi: 10.1016/j.semcdb.2018.03.003
21. Hamilton C, Anand PK. Right place, right time: localisation and assembly of the NLRP3 inflammasome. *F1000Res*. (2019) 8:F1000 Faculty Rev-676. doi: 10.12688/f1000research.18557.1
22. Schroder K, Tschopp J. The inflammasomes. *Cell*. (2010) 140:821–32. doi: 10.1016/j.cell.2010.01.040
23. Eisenbarth SC, Colegio OR, O'Connor W, Sutterwala FS, Flavell RA. Crucial role for the Nalp3 inflammasome in the immunostimulatory properties of aluminium adjuvants. *Nature*. (2008) 453:1122–6. doi: 10.1038/nature06939
24. Qiu Z, Lei S, Zhao B, Wu Y, Su W, Liu M, et al. NLRP3 inflammasome activation-mediated pyroptosis aggravates myocardial ischemia/reperfusion injury in diabetic rats. *Oxid Med Cell Longev*. (2017) 2017:9743280. doi: 10.1155/2017/9743280
25. Wang S, Yuan YH, Chen NH, Wang HB. The mechanisms of NLRP3 inflammasome/pyroptosis activation and their role in Parkinson's disease. *Int Immunopharmacol*. (2019) 67:458–64. doi: 10.1016/j.intimp.2018.12.019
26. Yu ZW, Zhang J, Li X, Wang Y, Fu YH, Gao XY. A new research hot spot: the role of NLRP3 inflammasome activation, a key step in pyroptosis, in diabetes and diabetic complications. *Life Sci*. (2020) 240:117138. doi: 10.1016/j.lfs.2019.117138
27. Swanson KV, Deng M, Ting JP. The NLRP3 inflammasome: molecular activation and regulation to therapeutics. *Nat Rev Immunol*. (2019) 19:477–89. doi: 10.1038/s41577-019-0165-0
28. Shi J, Zhao Y, Wang K, Shi X, Wang Y, Huang H, et al. Cleavage of GSDMD by inflammatory caspases determines pyroptotic cell death. *Nature*. (2015) 526:660–5. doi: 10.1038/nature15514
29. Liu X, Zhang Z, Ruan J, Pan Y, Magupalli VG, Wu H, et al. Inflammasome-activated gasdermin D causes pyroptosis by forming membrane pores. *Nature*. (2016) 535:153–8. doi: 10.1038/nature18629
30. Evavold CL, Ruan J, Tan Y, Xia S, Wu H, Kagan JC. The pore-forming protein gasdermin D regulates interleukin-1 secretion from living macrophages. *Immunity*. (2018) 48:35–44.e6. doi: 10.1016/j.immuni.2017.11.013
31. Monteleone M, Stanley AC, Chen KW, Brown DL, Bezbradica JS, von Pein JB, et al. Interleukin-1beta maturation triggers its relocation to the plasma membrane for gasdermin-D-dependent and -independent secretion. *Cell Rep*. (2018) 24:1425–33. doi: 10.1016/j.celrep.2018.07.027
32. Brennan MA, Cookson BT. *Salmonella* induces macrophage death by caspase-1-dependent necrosis. *Mol Microbiol*. (2000) 38:31–40. doi: 10.1046/j.1365-2958.2000.02103.x
33. Fink SL, Cookson BT. Pillars article: caspase-1-dependent pore formation during pyroptosis leads to osmotic lysis of infected host macrophages. Cell Microbiol. 2006. 8: 1812-1825. *J Immunol*. (2019) 202:1913–26. doi: 10.1111/j.1462-5822.2006.00751.x
34. Gross O, Poeck H, Bscheider M, Dostert C, Hannesschlager N, Endres S, et al. Syk kinase signalling couples to the Nlrp3 inflammasome for anti-fungal host defence. *Nature*. (2009) 459:433–6. doi: 10.1038/nature07965
35. Mariathasan S, Weiss DS, Newton K, McBride J, O'Rourke K, Roose-Girma M, et al. Cryopyrin activates the inflammasome in response to toxins and ATP. *Nature*. (2006) 440:228–32. doi: 10.1038/nature04515
36. Kanneganti TD, Body-Malapel M, Amer A, Park JH, Whitfield J, Franchi L, et al. Critical role for Cryopyrin/Nalp3 in activation of caspase-1 in response to viral infection and double-stranded RNA. *J Biol Chem*. (2006) 281:36560–8. doi: 10.1074/jbc.M607594200
37. Muruve DA, Petrilli V, Zaiss AK, White LR, Clark SA, Ross PJ, et al. The inflammasome recognizes cytosolic microbial and host DNA and triggers an innate immune response. *Nature*. (2008) 452:103–7. doi: 10.1038/nature06664
38. Zhou R, Tardivel A, Thorens B, Choi I, Tschopp J. Thioredoxin-interacting protein links oxidative stress to inflammasome activation. *Nat Immunol*. (2010) 11:136–40. doi: 10.1038/ni.1831
39. Lamkanfi M, Kanneganti TD. Nlrp3: an immune sensor of cellular stress and infection. *Int J Biochem Cell Biol*. (2010) 42:792–5. doi: 10.1016/j.biocel.2010.01.008
40. Mayor A, Martinon F, De Smedt T, Petrilli V, Tschopp J. A crucial function of SGT1 and HSP90 in inflammasome activity links mammalian and plant

innate immune responses. *Nat Immunol*. (2007) 8:497–503. doi: 10.1038/ni1459
41. Ding S, Xu S, Ma Y, Liu G, Jang H, Fang J. Modulatory mechanisms of the nlrp3 inflammasomes in diabetes. *Biomolecules*. (2019) 9:850. doi: 10.3390/biom9120850
42. Kesavardhana S, Kanneganti TD. Mechanisms governing inflammasome activation, assembly and pyroptosis induction. *Int Immunol*. (2017) 29:201–10. doi: 10.1093/intimm/dxx018
43. Fernandes-Alnemri T, Kang S, Anderson C, Sagara J, Fitzgerald KA, Alnemri ES. Cutting edge: TLR signaling licenses IRAK1 for rapid activation of the NLRP3 inflammasome. *J Immunol*. (2013) 191:3995–9. doi: 10.4049/jimmunol.1301681
44. Juliana C, Fernandes-Alnemri T, Kang S, Farias A, Qin F, Alnemri ES. Non-transcriptional priming and deubiquitination regulate NLRP3 inflammasome activation. *J Biol Chem*. (2012) 287:36617–22. doi: 10.1074/jbc.M112.407130
45. Schroder K, Sagulenko V, Zamoshnikova A, Richards AA, Cridland JA, Irvine KM, et al. Acute lipopolysaccharide priming boosts inflammasome activation independently of inflammasome sensor induction. *Immunobiology*. (2012) 217:1325–9. doi: 10.1016/j.imbio.2012.07.020
46. Jo EK, Kim JK, Shin DM, Sasakawa C. Molecular mechanisms regulating NLRP3 inflammasome activation. *Cell Mol Immunol*. (2016) 13:148–59. doi: 10.1038/cmi.2015.95
47. Perregaux D, Gabel CA. Interleukin-1 beta maturation and release in response to ATP and nigericin. Evidence that potassium depletion mediated by these agents is a necessary and common feature of their activity. *J Biol Chem*. (1994) 269:15195–203.
48. Walev I, Reske K, Palmer M, Valeva A, Bhakdi S. Potassium-inhibited processing of IL-1 beta in human monocytes. *EMBO J*. (1995) 14:1607–14. doi: 10.1002/j.1460-2075.1995.tb07149.x
49. Munoz-Planillo R, Kuffa P, Martinez-Colon G, Smith BL, Rajendiran TM, Nunez G. K(+) efflux is the common trigger of NLRP3 inflammasome activation by bacterial toxins and particulate matter. *Immunity*. (2013) 38:1142–53. doi: 10.1016/j.immuni.2013.05.016
50. Zhou R, Yazdi AS, Menu P, Tschopp J. A role for mitochondria in NLRP3 inflammasome activation. *Nature*. (2011) 469:221–5. doi: 10.1038/nature09663
51. Ruhl S, Broz P. Caspase-11 activates a canonical NLRP3 inflammasome by promoting K(+) efflux. *Eur J Immunol*. (2015) 45:2927–36. doi: 10.1002/eji.201545772
52. Sutterwala FS, Ogura Y, Zamboni DS, Roy CR, Flavell RA. NALP3: a key player in caspase-1 activation. *J Endotoxin Res*. (2006) 12:251–6. doi: 10.1179/096805106X118771
53. Kahlenberg JM, Dubyak GR. Mechanisms of caspase-1 activation by P2X7 receptor-mediated K+ release. *Am J Physiol Cell Physiol*. (2004) 286:C1100–8. doi: 10.1152/ajpcell.00494.2003
54. Kanneganti TD, Lamkanfi M, Kim YG, Chen G, Park JH, Franchi L, et al. Pannexin-1-mediated recognition of bacterial molecules activates the cryopyrin inflammasome independent of Toll-like receptor signaling. *Immunity*. (2007) 26:433–43. doi: 10.1016/j.immuni.2007.03.008
55. Pelegrin P, Barroso-Gutierrez C, Surprenant A. P2X7 receptor differentially couples to distinct release pathways for IL-1beta in mouse macrophage. *J Immunol*. (2008) 180:7147–57. doi: 10.4049/jimmunol.180.11.7147
56. Pelegrin P, Surprenant A. Pannexin-1 mediates large pore formation and interleukin-1beta release by the ATP-gated P2X7 receptor. *EMBO J*. (2006) 25:5071–82. doi: 10.1038/sj.emboj.7601378
57. Gross CJ, Mishra R, Schneider KS, Medard G, Wettmarshausen J, Dittlein DC, et al. K(+) efflux-independent NLRP3 inflammasome activation by small molecules targeting mitochondria. *Immunity*. (2016) 45:761–73. doi: 10.1016/j.immuni.2016.08.010
58. Meng G, Zhang F, Fuss I, Kitani A, Strober W. A mutation in the Nlrp3 gene causing inflammasome hyperactivation potentiates Th17 cell-dominant immune responses. *Immunity*. (2009) 30:860–74. doi: 10.1016/j.immuni.2009.04.012
59. Sharp FA, Ruane D, Claass B, Creagh E, Harris J, Malyala P, et al. Uptake of particulate vaccine adjuvants by dendritic cells activates the NALP3 inflammasome. *Proc Natl Acad Sci USA*. (2009) 106:870–5. doi: 10.1073/pnas.0804897106
60. Franchi L, Nunez G. The Nlrp3 inflammasome is critical for aluminium hydroxide-mediated IL-1beta secretion but dispensable for adjuvant activity. *Eur J Immunol*. (2008) 38:2085–9. doi: 10.1002/eji.200838549
61. Hornung V, Bauernfeind F, Halle A, Samstad EO, Kono H, Rock KL, et al. Silica crystals and aluminum salts activate the NALP3 inflammasome through phagosomal destabilization. *Nat Immunol*. (2008) 9:847–56. doi: 10.1038/ni.1631
62. Schorn C, Frey B, Lauber K, Janko C, Strysio M, Keppeler H, et al. Sodium overload and water influx activate the NALP3 inflammasome. *J Biol Chem*. (2011) 286:35–41. doi: 10.1074/jbc.M110.139048
63. Bruchard M, Mignot G, Derangere V, Chalmin F, Chevriaux A, Vegran F, et al. Chemotherapy-triggered cathepsin B release in myeloid-derived suppressor cells activates the Nlrp3 inflammasome and promotes tumor growth. *Nat Med*. (2013) 19:57–64. doi: 10.1038/nm.2999
64. Weber K, Schilling JD. Lysosomes integrate metabolic-inflammatory cross-talk in primary macrophage inflammasome activation. *J Biol Chem*. (2014) 289:9158–71. doi: 10.1074/jbc.M113.531202
65. Dostert C, Guarda G, Romero JF, Menu P, Gross O, Tardivel A, et al. Malarial hemozoin is a Nalp3 inflammasome activating danger signal. *PLoS One*. (2009) 4:e6510. doi: 10.1371/journal.pone.0006510
66. Cassel SL, Eisenbarth SC, Iyer SS, Sadler JJ, Colegio OR, Tephly LA, et al. The Nalp3 inflammasome is essential for the development of silicosis. *Proc Natl Acad Sci USA*. (2008) 105:9035–40. doi: 10.1073/pnas.0803933105
67. Dostert C, Petrilli V, Van Bruggen R, Steele C, Mossman BT, Tschopp J. Innate immune activation through Nalp3 inflammasome sensing of asbestos and silica. *Science*. (2008) 320:674–7. doi: 10.1126/science.1156995
68. Cruz CM, Rinna A, Forman HJ, Ventura AL, Persechini PM, Ojcius DM. ATP activates a reactive oxygen species-dependent oxidative stress response and secretion of proinflammatory cytokines in macrophages. *J Biol Chem*. (2007) 282:2871–9. doi: 10.1074/jbc.M608083200
69. Petrilli V, Papin S, Dostert C, Mayor A, Martinon F, Tschopp J. Activation of the NALP3 inflammasome is triggered by low intracellular potassium concentration. *Cell Death Differ*. (2007) 14:1583–9. doi: 10.1038/sj.cdd.4402195
70. Martinon F. Signaling by ROS drives inflammasome activation. *Eur J Immunol*. (2010) 40:616–9. doi: 10.1002/eji.200940168
71. Nishiyama A, Matsui M, Iwata S, Hirota K, Masutani H, Nakamura H, et al. Identification of thioredoxin-binding protein-2/vitamin D(3) up-regulated protein 1 as a negative regulator of thioredoxin function and expression. *J Biol Chem*. (1999) 274:21645–50. doi: 10.1074/jbc.274.31.21645
72. Kim SY, Suh HW, Chung JW, Yoon SR, Choi I. Diverse functions of VDUP1 in cell proliferation, differentiation, and diseases. *Cell Mol Immunol*. (2007) 4:345–51.
73. Kaimul AM, Nakamura H, Masutani H, Yodoi J. Thioredoxin and thioredoxin-binding protein-2 in cancer and metabolic syndrome. *Free Radic Biol Med*. (2007) 43:861–8. doi: 10.1016/j.freeradbiomed.2007.05.032
74. Chen J, Saxena G, Mungrue IN, Lusis AJ, Shalev A. Thioredoxin-interacting protein: a critical link between glucose toxicity and beta-cell apoptosis. *Diabetes*. (2008) 57:938–44. doi: 10.2337/db07-0715
75. van Greevenbroek MM, Vermeulen VM, Feskens EJ, Evelo CT, Kruijshoop M, Hoebee B, et al. Genetic variation in thioredoxin interacting protein (TXNIP) is associated with hypertriglyceridaemia and blood pressure in diabetes mellitus. *Diabet Med*. (2007) 24:498–504. doi: 10.1111/j.1464-5491.2007.02109.x
76. Minn AH, Hafele C, Shalev A. Thioredoxin-interacting protein is stimulated by glucose through a carbohydrate response element and induces beta-cell apoptosis. *Endocrinology*. (2005) 146:2397–405. doi: 10.1210/en.2004-1378
77. Turturro F, Friday E, Welbourne T. Hyperglycemia regulates thioredoxin-ROS activity through induction of thioredoxin-interacting protein (TXNIP) in metastatic breast cancer-derived cells MDA-MB-231. *BMC Cancer*. (2007) 7:96. doi: 10.1186/1471-2407-7-96
78. Meissner F, Molawi K, Zychlinsky A. Superoxide dismutase 1 regulates caspase-1 and endotoxic shock. *Nat Immunol*. (2008) 9:866–72. doi: 10.1038/ni.1633
79. Liu Q, Zhang D, Hu D, Zhou X, Zhou Y. The role of mitochondria in NLRP3 inflammasome activation. *Mol Immunol*. (2018) 103:115–24. doi: 10.1016/j.molimm.2018.09.010

80. Piantadosi CA. Mitochondrial DNA, oxidants, and innate immunity. *Free Radic Biol Med*. (2020) 152:455–61. doi: 10.1016/j.freeradbiomed.2020.01.013
81. Stehlik C, Dorfleutner A. COPs and POPs: modulators of inflammasome activity. *J Immunol*. (2007) 179:7993–8. doi: 10.4049/jimmunol.179.12.7993
82. Stehlik C, Krajewska M, Welsh K, Krajewski S, Godzik A, Reed JC. The PAAD/PYRIN-only protein POP1/ASC2 is a modulator of ASC-mediated nuclear-factor-kappa B and pro-caspase-1 regulation. *Biochem J*. (2003) 373(Pt 1):101–13. doi: 10.1042/bj20030304
83. Indramohan M, Stehlik C, Dorfleutner A. COPs and POPs patrol inflammasome activation. *J Mol Biol*. (2018) 430:153–73. doi: 10.1016/j.jmb.2017.10.004
84. Periasamy S, Porter KA, Atianand MK, T Le H, Earley S, Duffy EB, et al. Pyrin-only protein 2 limits inflammation but improves protection against bacteria. *Nat Commun*. (2017) 8:15564. doi: 10.1038/ncomms15564
85. Beynon V, Quintana FJ, Weiner HL. Activated human CD4+CD45RO+ memory T-cells indirectly inhibit NLRP3 inflammasome activation through downregulation of P2X7R signalling. *PLoS One*. (2012) 7:e39576. doi: 10.1371/journal.pone.0039576
86. Arbore G, West EE, Spolski R, Robertson AAB, Klos A, Rheinheimer C, et al. T helper 1 immunity requires complement-driven NLRP3 inflammasome activity in CD4(+) T cells. *Science*. (2016) 352:aad1210. doi: 10.1126/science.aad1210
87. Mitroulis I, Kambas K, Ritis K. Neutrophils, IL-1beta, and gout: is there a link? *Semin Immunopathol*. (2013) 35:501–12. doi: 10.1007/s00281-013-0361-0
88. Guarda G, Braun M, Staehli F, Tardivel A, Mattmann C, Forster I, et al. Type I interferon inhibits interleukin-1 production and inflammasome activation. *Immunity*. (2011) 34:213–23. doi: 10.1016/j.immuni.2011.02.006
89. Saitoh T, Fujita N, Jang MH, Uematsu S, Yang BG, Satoh T, et al. Loss of the autophagy protein Atg16L1 enhances endotoxin-induced IL-1beta production. *Nature*. (2008) 456:264–8. doi: 10.1038/nature07383
90. Matsuzawa-Ishimoto Y, Hwang S, Cadwell K. Autophagy and inflammation. *Annu Rev Immunol*. (2018) 36:73–101. doi: 10.1146/annurev-immunol-042617-053253
91. Sharma D, Kanneganti TD. The cell biology of inflammasomes: mechanisms of inflammasome activation and regulation. *J Cell Biol*. (2016) 213:617–29. doi: 10.1083/jcb.201602089
92. Nakahira K, Haspel JA, Rathinam VA, Lee SJ, Dolinay T, Lam HC, et al. Autophagy proteins regulate innate immune responses by inhibiting the release of mitochondrial DNA mediated by the NALP3 inflammasome. *Nat Immunol*. (2011) 12:222–30. doi: 10.1038/ni.1980
93. Shimada K, Crother TR, Karlin J, Dagvadorj J, Chiba N, Chen S, et al. Oxidized mitochondrial DNA activates the NLRP3 inflammasome during apoptosis. *Immunity*. (2012) 36:401–14. doi: 10.1016/j.immuni.2012.01.009
94. Mao K, Chen S, Chen M, Ma Y, Wang Y, Huang B, et al. Nitric oxide suppresses NLRP3 inflammasome activation and protects against LPS-induced septic shock. *Cell Res*. (2013) 23:201–12. doi: 10.1038/cr.2013.6
95. Jung SS, Moon JS, Xu JF, Ifedigbo E, Ryter SW, Choi AM, et al. Carbon monoxide negatively regulates NLRP3 inflammasome activation in macrophages. *Am J Physiol Lung Cell Mol Physiol*. (2015) 308:L1058–67. doi: 10.1152/ajplung.00400.2014
96. Wegiel B, Larsen R, Gallo D, Chin BY, Harris C, Mannam P, et al. Macrophages sense and kill bacteria through carbon monoxide-dependent inflammasome activation. *J Clin Invest*. (2014) 124:4926–40. doi: 10.1172/JCI72853
97. Barclay W, Shinohara ML. Inflammasome activation in multiple sclerosis and experimental autoimmune encephalomyelitis (EAE). *Brain Pathol*. (2017) 27:213–9. doi: 10.1111/bpa.12477
98. Tourkochristou E, Aggeletopoulou I, Konstantakis C, Triantos C. Role of NLRP3 inflammasome in inflammatory bowel diseases. *World J Gastroenterol*. (2019) 25:4796–804. doi: 10.3748/wjg.v25.i33.4796
99. Soares JL, Oliveira EM, Pontillo A. Variants in NLRP3 and NLRC4 inflammasome associate with susceptibility and severity of multiple sclerosis. *Mult Scler Relat Disord*. (2019) 29:26–34. doi: 10.1016/j.msard.2019.01.023
100. Sun X, Xia Y, Liu Y, Wang Y, Luo S, Lin J, et al. Polymorphisms in NLRP1 gene are associated with Type 1 diabetes. *J Diabetes Res*. (2019) 2019:7405120. doi: 10.1155/2019/7405120
101. Zheng Y, Wang Z, Zhou Z. miRNAs: novel regulators of autoimmunity-mediated pancreatic beta-cell destruction in type 1 diabetes. *Cell Mol Immunol*. (2017) 14:488–96. doi: 10.1038/cmi.2017.7
102. Grishman EK, White PC, Savani RC. Toll-like receptors, the NLRP3 inflammasome, and interleukin-1beta in the development and progression of type 1 diabetes. *Pediatr Res*. (2012) 71:626–32. doi: 10.1038/pr.2012.24
103. Hu C, Ding H, Li Y, Pearson JA, Zhang X, Flavell RA, et al. NLRP3 deficiency protects from type 1 diabetes through the regulation of chemotaxis into the pancreatic islets. *Proc Natl Acad Sci USA*. (2015) 112:11318–23. doi: 10.1073/pnas.1513509112
104. Vives-Pi M, Rodriguez-Fernandez S, Pujol-Autonell I. How apoptotic beta-cells direct immune response to tolerance or to autoimmune diabetes: a review. *Apoptosis*. (2015) 20:263–72. doi: 10.1007/s10495-015-1090-8
105. Pang H, Luo S, Huang G, Xia Y, Xie Z, Zhou Z. Advances in knowledge of candidate genes acting at the beta-cell level in the pathogenesis of T1DM. *Front Endocrinol*. (2020) 11:119. doi: 10.3389/fendo.2020.00119
106. Bradshaw EM, Raddassi K, Elyaman W, Orban T, Gottlieb PA, Kent SC, et al. Monocytes from patients with type 1 diabetes spontaneously secrete proinflammatory cytokines inducing Th17 cells. *J Immunol*. (2009) 183:4432–9. doi: 10.4049/jimmunol.0900576
107. Dogan Y, Akarsu S, Ustundag B, Yilmaz E, Gurgoze MK. Serum IL-1beta, IL-2, and IL-6 in insulin-dependent diabetic children. *Mediators Inflamm*. (2006) 2006:59206. doi: 10.1155/MI/2006/59206
108. Kaizer EC, Glaser CL, Chaussabel D, Banchereau J, Pascual V, White PC. Gene expression in peripheral blood mononuclear cells from children with diabetes. *J Clin Endocrinol Metab*. (2007) 92:3705–11. doi: 10.1210/jc.2007-0979
109. Maedler K, Sergeev P, Ehses JA, Mathe Z, Bosco D, Berney T, et al. Leptin modulates beta cell expression of IL-1 receptor antagonist and release of IL-1beta in human islets. *Proc Natl Acad Sci USA*. (2004) 101:8138–43. doi: 10.1073/pnas.0305683101
110. Schwarznau A, Hanson MS, Sperger JM, Schram BR, Danobeitia JS, Greenwood KK, et al. IL-1beta receptor blockade protects islets against pro-inflammatory cytokine induced necrosis and apoptosis. *J Cell Physiol*. (2009) 220:341–7. doi: 10.1002/jcp.21770
111. Sumpter KM, Adhikari S, Grishman EK, White PC. Preliminary studies related to anti-interleukin-1beta therapy in children with newly diagnosed type 1 diabetes. *Pediatr Diabetes*. (2011) 12:656–67. doi: 10.1111/j.1399-5448.2011.00761.x
112. Schott WH, Haskell BD, Tse HM, Milton MJ, Piganelli JD, Choisy-Rossi CM, et al. Caspase-1 is not required for type 1 diabetes in the NOD mouse. *Diabetes*. (2004) 53:99–104. doi: 10.2337/diabetes.53.1.99
113. Wen L, Green EA, Stratmann T, Panosa A, Gomis R, Eynon EE, et al. In vivo diabetogenic action of CD4+ T lymphocytes requires Fas expression and is independent of IL-1 and IL-18. *Eur J Immunol*. (2011) 41:1344–51. doi: 10.1002/eji.201041216
114. Gill RG, Pagni PP, Kupfer T, Wasserfall CH, Deng S, Posgai A, et al. A preclinical consortium approach for assessing the efficacy of combined anti-CD3 plus IL-1 blockade in reversing new-onset autoimmune diabetes in NOD mice. *Diabetes*. (2016) 65:1310–6. doi: 10.2337/db15-0492
115. Lebreton F, Berishvili E, Parnaud G, Rouget C, Bosco D, Berney T, et al. NLRP3 inflammasome is expressed and regulated in human islets. *Cell Death Dis*. (2018) 9:726. doi: 10.1038/s41419-018-0764-x
116. Pontillo A, Brandao L, Guimaraes R, Segat L, Araujo J, Crovella S. Two SNPs in NLRP3 gene are involved in the predisposition to type-1 diabetes and celiac disease in a pediatric population from northeast Brazil. *Autoimmunity*. (2010) 43:583–9. doi: 10.3109/08916930903540432
117. Carlos D, Costa FR, Pereira CA, Rocha FA, Yaochite JN, Oliveira GG, et al. Mitochondrial DNA activates the NLRP3 inflammasome and predisposes to type 1 diabetes in murine model. *Front Immunol*. (2017) 8:164. doi: 10.3389/fimmu.2017.00164
118. Pereira CA, Carlos D, Ferreira NS, Silva JF, Zanotto CZ, Zamboni DS, et al. Mitochondrial DNA promotes NLRP3 inflammasome activation and contributes to endothelial dysfunction and inflammation in type 1 diabetes. *Front Physiol*. (2019) 10:1557. doi: 10.3389/fphys.2019.01557

119. Zaki MH, Lamkanfi M, Kanneganti TD. The Nlrp3 inflammasome: contributions to intestinal homeostasis. *Trends Immunol*. (2011) 32:171–9. doi: 10.1016/j.it.2011.02.002
120. Zaki MH, Boyd KL, Vogel P, Kastan MB, Lamkanfi M, Kanneganti TD. The NLRP3 inflammasome protects against loss of epithelial integrity and mortality during experimental colitis. *Immunity*. (2010) 32:379–91. doi: 10.1016/j.immuni.2010.03.003
121. Hirota SA, Ng J, Lueng A, Khajah M, Parhar K, Li Y, et al. NLRP3 inflammasome plays a key role in the regulation of intestinal homeostasis. *Inflamm Bowel Dis*. (2011) 17:1359–72. doi: 10.1002/ibd.21478
122. Yang Q, Yu C, Yang Z, Wei Q, Mu K, Zhang Y, et al. Deregulated NLRP3 and NLRP1 inflammasomes and their correlations with disease activity in systemic lupus erythematosus. *J Rheumatol*. (2014) 41:444–52. doi: 10.3899/jrheum.130310
123. Liu H, Xu R, Kong Q, Liu J, Yu Z, Zhao C. Downregulated NLRP3 and NLRP1 inflammasomes signaling pathways in the development and progression of type 1 diabetes mellitus. *Biomed Pharmacother*. (2017) 94:619–26. doi: 10.1016/j.biopha.2017.07.102
124. Netea MG, Simon A, van de Veerdonk F, Kullberg BJ, Van der Meer JW, Joosten LA. IL-1beta processing in host defense: beyond the inflammasomes. *PLoS Pathog*. (2010) 6:e1000661. doi: 10.1371/journal.ppat.1000661
125. Wittmann M, Kingsbury SR, McDermott MF. Is caspase 1 central to activation of interleukin-1? *Joint Bone Spine*. (2011) 78:327–30. doi: 10.1016/j.jbspin.2011.02.004

Conflict of Interest: The authors declare that the research was conducted in the absence of any commercial or financial relationships that could be construed as a potential conflict of interest.

frontiers in Immunology

ORIGINAL RESEARCH
published: 04 September 2020
doi: 10.3389/fimmu.2020.02180

CD226 Deletion Reduces Type 1 Diabetes in the NOD Mouse by Impairing Thymocyte Development and Peripheral T Cell Activation

*Melanie R. Shapiro[1†], Wen-I Yeh[1†‡], Joshua R. Longfield[1], John Gallagher[1], Caridad M. Infante[1], Sarah Wellford[1], Amanda L. Posgai[1], Mark A. Atkinson[1,2], Martha Campbell-Thompson[1], Scott M. Lieberman[3], David V. Serreze[4], Aron M. Geurts[5], Yi-Guang Chen[6] and Todd M. Brusko[1,2]**

[1] Department of Pathology, Immunology and Laboratory Medicine, University of Florida Diabetes Institute, Gainesville, FL, United States, [2] Department of Pediatrics, University of Florida, Gainesville, FL, United States, [3] Stead Family Department of Pediatrics, University of Iowa Carver College of Medicine, Iowa City, IA, United States, [4] The Jackson Laboratory, Bar Harbor, ME, United States, [5] Department of Physiology, Medical College of Wisconsin, Milwaukee, WI, United States, [6] Department of Pediatrics, Medical College of Wisconsin, Milwaukee, WI, United States

The costimulatory molecule CD226 is highly expressed on effector/memory T cells and natural killer cells. Costimulatory signals received by T cells can impact both central and peripheral tolerance mechanisms. Genetic polymorphisms in *CD226* have been associated with susceptibility to type 1 diabetes and other autoimmune diseases. We hypothesized that genetic deletion of *Cd226* in the non-obese diabetic (NOD) mouse would impact type 1 diabetes incidence by altering T cell activation. CD226 knockout (KO) NOD mice displayed decreased disease incidence and insulitis in comparison to wild-type (WT) controls. Although female CD226 KO mice had similar levels of sialoadenitis as WT controls, male CD226 KO mice showed protection from dacryoadenitis. Moreover, CD226 KO T cells were less capable of adoptively transferring disease compared to WT NOD T cells. Of note, CD226 KO mice demonstrated increased $CD8^+$ single positive (SP) thymocytes, leading to increased numbers of $CD8^+$ T cells in the spleen. Decreased percentages of memory $CD8^+CD44^+CD62L^-$ T cells were observed in the pancreatic lymph nodes of CD226 KO mice. Intriguingly, $CD8^+$ T cells in CD226 KO mice showed decreased islet-specific glucose-6-phosphatase catalytic subunit-related protein (IGRP)-tetramer and CD5 staining, suggesting reduced T cell receptor affinity for this immunodominant antigen. These data support an important role for CD226 in type 1 diabetes development by modulating thymic T cell selection as well as impacting peripheral memory/effector $CD8^+$ T cell activation and function.

Keywords: type 1 diabetes, Sjögren's disease, costimulatory receptors, $CD8^+$ T cells, CD226

OPEN ACCESS

Edited by:
Michael Zemlin, Saarland University Hospital, Germany

Reviewed by:
Gaurang Jhala, St. Vincent's Institute of Medical Research, The University of Melbourne, Australia
Esteban Gurzov, Université libre de Bruxelles, Belgium

****Correspondence:***
Todd M. Brusko
tbrusko@ufl.edu

† These authors have contributed equally to this work

‡ Present address:
Wen-I Yeh, Fate Therapeutics, San Diego, CA, United States

Specialty section:
This article was submitted to Autoimmune and Autoinflammatory Disorders, a section of the journal Frontiers in Immunology

Received: *16 June 2020*
Accepted: *10 August 2020*
Published: *04 September 2020*

Citation:
Shapiro MR, Yeh W-I, Longfield JR, Gallagher J, Infante CM, Wellford S, Posgai AL, Atkinson MA, Campbell-Thompson M, Lieberman SM, Serreze DV, Geurts AM, Chen Y-G and Brusko TM (2020) CD226 Deletion Reduces Type 1 Diabetes in the NOD Mouse by Impairing Thymocyte Development and Peripheral T Cell Activation. Front. Immunol. 11:2180. doi: 10.3389/fimmu.2020.02180

INTRODUCTION

MHC class I hyper-expression and autoreactive $CD8^+$ T cell infiltration in pancreatic islets constitute two prominent histological features of type 1 diabetes and are thought to be involved in the direct cytotoxic killing of β-cells (1, 2). Other immune cell subsets, including $CD4^+$ T cells, B cells, monocytes, and natural killer (NK) cells have also been reported to contribute to insulitis and β-cell destruction (3, 4). Genetic studies have identified 57 independent genetic loci beyond MHC class II that contribute to the development of type 1 diabetes (5). These variants are thought to contribute to defects in immune tolerance, with a number of additional loci also associated with β-cell fragility and susceptibility to immune surveillance and attack (5–13). While many of the candidate single nucleotide polymorphisms (SNPs) and causative variants are being identified with greater resolution (14), there remain a number of outstanding questions regarding how candidate loci impact gene expression and function within tissues and cell types, as well as over various developmental time points and activation states during disease pathogenesis.

A SNP in *CD226* (rs763361) has been associated with genetic susceptibility to multiple autoimmune diseases including type 1 diabetes, multiple sclerosis, and rheumatoid arthritis (15). The SNP results in a missense mutation leading to a glycine to serine substitution at position 307 and is located proximally to two intracellular phosphorylation sites (Tyr322 and Ser329) of CD226 (16, 17). Hence, it has previously been shown that the rs763361 risk allele increases phosphorylation status of downstream signaling mediators, such as Erk, augmenting CD226 activity in human $CD4^+$ T cells (18). Notably, the *Idd21.1* risk locus of the non-obese diabetic (NOD) mouse model of type 1 diabetes contains the *Cd226* gene and is orthologous to the 18q22.2 region containing the human *CD226* gene (19), thereby making the NOD mouse a superb *in vivo* model of CD226 activity in the context of autoimmunity.

CD226 functions as an activating costimulatory receptor in the immunoglobulin superfamily (20) that is expressed largely on effector and memory T cells and NK cells (21, 22). CD226 activity is antagonized by an inhibitory counterpart, T cell Immunoreceptor with Ig and ITIM domains (TIGIT), which functions as a negative regulator with expression enriched on regulatory T cells (Tregs) (22) and NK cells (23). CD226 and TIGIT function in an analogous manner to the more widely studied CD28:CTLA-4 costimulatory axis (24), to promote activation or inhibition via immunoreceptor tyrosine-based activation (ITAM) or inhibitory motifs (ITIM), respectively. CD226 activation is reported to be dependent on homodimerization and binding to cognate ligands, including CD155 (PVR) and CD112, on antigen-presenting cells (APCs) (23, 25, 26). CD226 has been demonstrated by fluorescence resonance energy transfer to be inhibited in *cis* through interactions with TIGIT (27).

Costimulatory molecules are known to influence central tolerance by fine-tuning T cell receptor (TCR)-mediated signaling that defines thresholds for thymocyte selection (28). CD226, in particular, has been implicated in supporting the survival of $CD4^+CD8^+$ double positive (DP) as well as $CD4^+$ single positive (SP) thymocytes (29). The interaction between CD226 and CD155 has also been shown to drive the thymic retention and negative selection of $CD8^+$ SP thymocytes, shaping the $CD8^+$ T cell repertoire (30, 31). Together, these studies suggest that the balance of CD226:TIGIT signaling may influence positive and negative selection of thymocytes; however, the impact of this signaling pathway on the autoreactive T cell repertoire remains poorly defined.

Similar to other costimulatory molecules, CD226 and TIGIT are also known to regulate peripheral tolerance by impacting T cell and NK cell activation and function. CD226 promotes, while TIGIT inhibits, $CD4^+$ T cell proliferation and differentiation into a Th1 phenotype (32), as well as $CD8^+$ T cell (20, 27) and NK cell cytotoxicity (33, 34). While the roles of CD226 and TIGIT in type 1 diabetes pathogenesis remain unclear, blockade of CD226 has been shown to protect from experimental autoimmune encephalitis (EAE), another autoimmune mouse model in which disease pathogenesis is thought to be primarily T cell-mediated (35).

Therefore, we sought to understand how CD226 and TIGIT impact central and peripheral tolerance mechanisms in the context of type 1 diabetes. We hypothesized the genetic deletion of *Cd226* would attenuate disease development, whereas disruption of *Tigit* would promote type 1 diabetes. Herein, we present the impact of genetic disruption of these costimulatory receptors on the incidence of type 1 diabetes in the NOD mouse model. We further demonstrate mechanisms by which the elimination of CD226 impacts both central and peripheral T cell activation.

MATERIALS AND METHODS

Mice

CRISPR-Cas9 technology was used to knockout (KO) *Cd226* and *Tigit*, as previously described (36), on the NOD/ShiLtJ (NOD, IMSR Cat# JAX:001976, RRID:IMSR_JAX:001976) background. The following guide sequences were used to target genes of interest: *Cd226*, AAGTCCTGAGTCAGCGGCCA; *Tigit*, CTGCTGCTTCCAGTCGACTT. Founders were backcrossed to NOD/ShiLtJ mice for two generations prior to intercrossing heterozygous (HET) mice, to prevent potential off-target deletions from inheritance in the experimental breeders. Animals were bred and housed in specific pathogen-free facilities at the University of Florida, with food and water available *ad libitum*. All studies were conducted in accordance with protocols approved by the University of Florida Institutional Animal Care and Use Committee (UF IACUC) and in accordance with the National Institutes of Health Guide for Care and Use of Animals.

Genotyping

Offspring from CD226 or TIGIT HET x HET mating pairs were genotyped using custom Taqman SNP assays according to manufacturer's protocol (Thermo Fisher Scientific). Reporter 1 was marked with VIC and reporter 2 with FAM dyes to

distinguish alleles and quantitative PCR performed on a Roche LightCycler 480.

Cd226 Forward primer sequence: GGGAGCATGAAGAGC ATCCT, *Cd226* Reverse primer sequence: GCGACATCTGTAA AGTCCTGAGT, *Cd226* Reporter 1 sequence (wild-type, WT): CAAATGCCATGGCCGCT, *Cd226* Reporter 2 sequence (KO): CAAATGCCATGCCGCT.

Tigit Forward primer sequence: ATCTTACAGTGTCACTT CTCCTCTGA, *Tigit* Reverse primer sequence: TCAACACTA TAAATGGCCAGAAGCT, *Tigit* Reporter 1 sequence (WT): AAGTGACCCAAGTCGACTG, *Tigit* Reporter 2 sequence (KO): AAGTGACCCATCGACTG.

Measurement of Diabetes Incidence

Littermate CD226 or TIGIT WT, HET, and KO animals were monitored weekly starting at 9 weeks of age for onset of diabetes. Blood glucose levels were measured with AlphaTrak2 glucometer, and animals with blood glucose over 250 mg/dL were re-checked the following day. Those with a second consecutive reading over 250 mg/dL were considered diabetic.

Histology, Insulitis, Sialoadenitis, and Dacryoadenitis Scoring

Pancreata, submandibular salivary glands, and extraorbital lacrimal glands were removed at necropsy and fixed in 10% neutral buffered formalin overnight. Samples were embedded in paraffin and a total of three sections (4 μm) at 250 μm steps of each pancreas, or one section (5 μm) of paired salivary and lacrimal glands, were stained with hematoxylin and eosin. For pancreata, whole digital slide scans were performed using an Aperio CS scanner (Leica Biosystems) and for salivary and lacrimal glands, images were obtained with a PathScan Enabler IV slide scanner (Meyer Instrument). Insulitis scoring was performed by a blinded observer. At least 45 islets per mouse were scored using previously published criteria (37). An islet was defined as at least 10 endocrine cells. Briefly, a score of 0 = no infiltration, 1 = peri-insulitis, 2 $\leq$50% of islet infiltrated, 3 $\geq$50% of islet infiltrated with immune cells. Salivary and lacrimal infiltration was quantified using standard focus scoring as previously described (38). Foci were defined as $\geq$50 mononuclear cells and total number of foci were normalized by surface area of the section.

Adoptive Transfer

Pooled spleen and non-draining lymph nodes of age-matched female pre-diabetic (8–12 weeks of age) CD226 WT and CD226 KO mice were processed to single cell suspensions, and $CD4^+$ and $CD8^+$ T cells were separated by magnetic bead isolation (Miltenyi Biotec). 2×10^6 $CD4^+$ T cells and 1×10^6 $CD8^+$ T cells suspended in 100 μL PBS were transferred by tail vein injection into 6–8 week-old female NOD.SCID recipients, and diabetes incidence was monitored weekly for up to 20 weeks post-transfer.

Flow Cytometry

Spleen, thymus, and lymph nodes were processed using frosted glass slides and passed through a 40 micron filter, for lymphocyte analysis, or a 70 micron filter, for APC analysis, to create a single cell suspension. Red blood cells were lysed with ammonium-chloride-potassium buffer prior to staining for flow cytometry analysis. Pancreas was minced and digested with 0.5 mg/mL Collagenase IV (Life Technologies) for 35 minutes at 37°C prior to passing through a 70 micron filter. Ficoll density gradient centrifugation was performed to enrich for immune infiltrates within the pancreatic digest. Samples were stained with Fixable Live/Dead Near IR (Invitrogen), and Fc receptors were blocked with anti-CD16/32 (Clone 2.4G2, BD Biosciences Cat# 553142, RRID:AB_394657). Antibodies used included CD3e-BV605 (145-2C11, BioLegend Cat# 100351, RRID:AB_2565842), CD4-PerCP/Cy5.5 (RM4-5, Thermo Fisher Scientific Cat# 45-0042-82, RRID:AB_1107001) or –Pacific Blue (RM4-4, BioLegend Cat# 116007, RRID:AB_11147758), CD8a-eFluor450 (53-6.7, Thermo Fisher Scientific Cat# 48-0081-82, RRID:AB_1272198) or –BV711 (53-6.7, BioLegend Cat# 100759, RRID:AB_2563510), NKp46-FITC (29A1.4, BioLegend Cat# 137606, RRID:AB_2298210), CD44-PE (IM7, BioLegend Cat# 103008, RRID:AB_312959), CD62L-APC (MEL-14, BioLegend Cat# 104412, RRID:AB_313099), CD226-AF647 (10E5, BioLegend Cat# 128808, RRID:AB_1227541), TIGIT-PerCP/eFluor710 (GIGD7, Thermo Fisher Scientific Cat# 46-9501-82, RRID:AB_11150967), CD96-PE (3.3, BioLegend Cat# 131705, RRID:AB_1279389), MHC Class II (I-Ad)-FITC (AMS-32.1, BD Biosciences Cat# 553547, RRID:AB_394914) or -APC (AMS-32.1, Thermo Fisher Scientific Cat# 17-5323-80, RRID:AB_10717083), CD11c-eFluor450 (N418, Thermo Fisher Scientific Cat# 48-0114-82, RRID:AB_1548654), CD155-PE (4.24.1, BioLegend Cat# 132205, RRID:AB_1279105), CD112-FITC (502-57, LifeSpan Cat# LS-C210245, RRID:AB_2857846), and CD5-AF488 (53-7.3, BioLegend Cat# 100612, RRID:AB_493165). Pancreas and pancreatic lymph node (pLN) cells were stained with MHC I (H-2Kd) IGRP (206-214) tetramer obtained from NIH Tetramer Facility for 30 minutes at 4°C. The same batch of tetramer was used throughout the study in order to avoid variability in fluorescence intensity due to batch-to-batch differences. Data were acquired on an LSRFortessa (BD Biosciences) and analyzed with FlowJo (v10.3, Tree Star, RRID:SCR_008520).

Statistical Analysis

Data were analyzed using GraphPad Prism software version 7.0 (RRID:SCR_002798). Data are presented as mean ± standard deviation (SD) unless otherwise specified. Survival curves of CD226 or TIGIT WT, HET, and KO littermates were compared using log-rank (Mantel–Cox) test. Insulitis scoring was compared between WT and KO mice via chi-square test. Sialoadenitis, dacryoadenitis, and flow cytometric data of WT and KO mice were compared via Mann–Whitney test. Flow cytometric data from WT, HET, and KO mice were analyzed using Kruskal–Wallis with Dunn's multiple comparisons test. Comparisons of CD226, CD112, and CD155 expression between cell subsets within the same mouse were performed using Friedman test with Dunn's multiple comparisons test. $p < 0.05$ was considered significant.

RESULTS

CD226 KO Protected NOD Mice From Type 1 Diabetes

A single base pair deletion in the immunoglobulin-like region of *Cd226* was induced via CRISPR/Cas9 targeting (**Figure 1A**), creating a frameshift which resulted in premature translation termination and lack of membrane CD226 protein expression in KO mice, as confirmed by flow cytometry of $CD4^+$ T cells, $CD8^+$ T cells and NK cells (**Figures 1B–D**). A two-base pair deletion in the immunoglobulin-like region of *Tigit* was induced (**Supplementary Figure S1A**), resulting in a loss of membrane TIGIT protein expression, which was most apparent in NK cells (**Supplementary Figures S1B–D**). Animals HET for CD226 or TIGIT showed an intermediate level of protein expression, suggestive of a gene dosage effect (**Figures 1B–D** and **Supplementary Figures S1B–D**).

To measure disease incidence, littermate CD226 and TIGIT WT, HET and KO blood glucose levels were monitored weekly from 9 to 40 weeks of age. In our colony, diabetes develops in approximately 80% of female (**Figure 2A**) and 60% of male (**Figure 2B**) WT NOD mice. Importantly, we observed that CD226 KO showed significantly reduced diabetes incidence, with 52% of KO females (**Figure 2A**, $N = 11/21$, $p = 0.021$) and 13% of KO males (**Figure 2B**, $N = 2/16$, $p = 0.004$) developing disease. Female and male CD226 HET mice showed similar kinetics of early disease development as compared to WT mice, suggesting that a single copy of the gene was sufficient to promote type 1 diabetes (**Figure 2**). TIGIT HET and KO females and males showed similar diabetes incidence to WT littermates (**Supplementary Figure S2**). These data suggest a role for CD226 in promoting type 1 diabetes development, and thus, we chose to focus on this strain for the remainder of our studies.

Pancreatic and Lacrimal Inflammation Are Reduced in CD226 KO NOD

NOD mice spontaneously develop inflammation of the pancreatic islets as well as the salivary and lacrimal glands, leading to the manifestation of both type 1 diabetes and Sjögren's associated pathologies (39). Salivary and lacrimal infiltration are primarily observed in female and male NOD mice, respectively (40). We observed significantly reduced infiltration of the islets in pre-diabetic 12-week old female (**Figures 3A,B**) and 16-week old male (**Figure 3C**) CD226 KO versus WT NOD mice, likely close to potential disease onset (**Figures 2A,B**). Lacrimal inflammation was significantly reduced in male CD226 KO as compared to WT mice (**Figures 3D,E**), though the extent of salivary gland inflammation was consistent between age-matched female CD226 WT and KO mice (**Figure 3F**). These findings suggest that CD226 may influence the pathogenesis of both type 1 diabetes and Sjögren's disease and provided impetus for understanding the immunological mechanisms of protection against autoimmunity in the CD226 KO NOD model.

T Cell Expression of CD226 Contributes to Type 1 Diabetes Pathogenesis

We sought to determine whether the protection from type 1 diabetes seen in the global CD226 KO mouse could be attributed to the altered function of $CD4^+$ or $CD8^+$ T cells. Here, we transferred combinations of CD226 WT or KO $CD4^+$ and $CD8^+$ T cells into female NOD.SCID immunodeficient recipients and monitored disease incidence for up to 20 weeks post-transfer. WT $CD4^+$ + WT $CD8^+$ T cell transfers induced significantly increased disease incidence ($N = 8/10$, solid gray line) as compared to CD226 KO $CD4^+$ + CD226 KO $CD8^+$ T cell transfers ($N = 3/11$, dashed gray line, $p = 0.009$, **Figure 4**). WT $CD4^+$ + CD226 KO $CD8^+$ T cell ($N = 7/10$, solid black line) and CD226 KO $CD4^+$ + WT $CD8^+$ T cell ($N = 5/12$, dashed black line) transfers showed intermediate disease incidence (**Figure 4**). However, there was a significant difference in type 1 diabetes development in recipients of CD226 KO $CD4^+$ + CD226 KO $CD8^+$ T cells versus those in which only $CD8^+$ T cells were CD226 KO, suggesting that while CD226 expression on both $CD4^+$ and $CD8^+$ T cells may contribute toward diabetogenesis in the NOD mouse, the CD226 KO effect is primarily manifest in $CD4^+$ T cells in this adoptive transfer setting with a fixed $CD4^+$:$CD8^+$ T cell ratio.

CD226 KO Increases Thymic Output of $CD8^+$ T Cells in NOD Mice

To elucidate the role of CD226 in central tolerance, we sought to understand how CD226 KO impacted thymocyte development. We assessed CD226 expression in WT NOD thymocyte subpopulations and confirmed that $CD8^+$ SP thymocytes showed higher CD226 expression in comparison to $CD4^-CD8^-$ double negative (DN), $CD4^+CD8^+$ DP, and $CD4^+$ SP subsets (**Figures 5A,B**), similar to a previous report (29). CD226 showed elevated expression levels on peripheral $CD8^+$ as compared to $CD4^+$ T cells in WT female NOD (**Figures 5C,D**), mirroring CD226 expression in thymocytes (**Figures 5A,B**) and suggesting preferential CD226 signaling in the $CD8^+$ T cell compartment. The ligands of CD226, CD155, and CD112, are reported to be highly expressed on monocyte-derived dendritic cells (DCs) (41), and interestingly, we found that thymic $CD11c^+$MHC II^+ DCs expressed significantly higher levels of both CD155 (**Figures 5E,F**) and CD112 (**Figures 5G,H**) as compared to DCs in other secondary lymphoid organs surveyed. These data suggest that the interaction of CD226 on $CD8^+$ SP thymocytes with CD155 and CD112 on thymic DCs may play a role in thymic selection.

Indeed, 12-week old, pre-diabetic CD226 KO mice showed significantly increased percentages of $CD8^+$ SP thymocytes as compared to CD226 WT mice, while DN, DP, and $CD4^+$ SP percentages remained similar (**Figures 6A–E**). We observed a consistent and significant decrease in the percentage of $CD4^+$ T cells and increase in the percentage of $CD8^+$ T cells in the spleen (**Figures 6F–H**), leading to a significantly decreased ratio of $CD4^+$:$CD8^+$ T cells in the spleens of CD226 KO animals (**Figure 6I**). These data collectively suggest that CD226

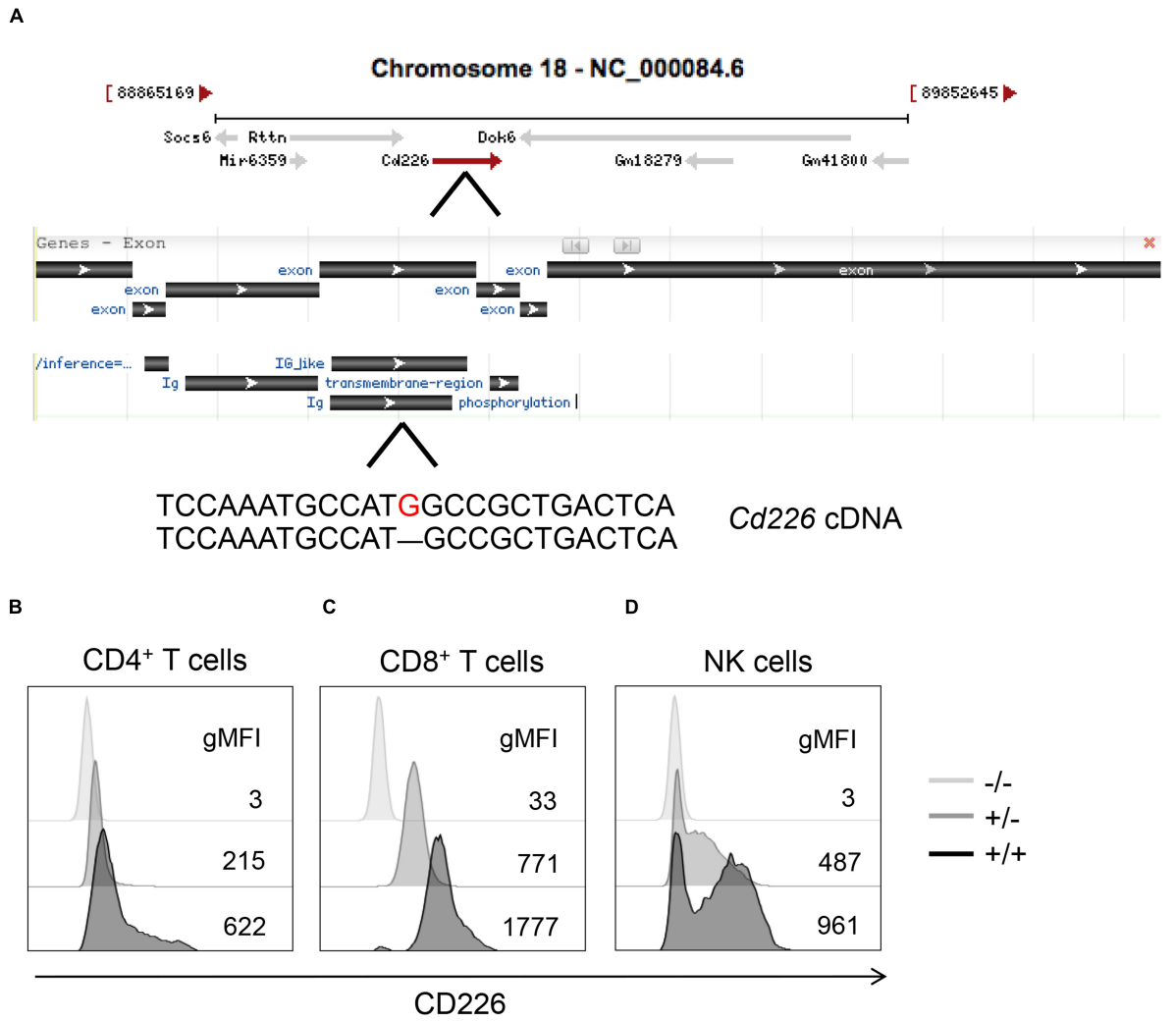

FIGURE 1 | CRISPR/Cas9 targeting methods for generation of CD226 KO strain. **(A)** A guide RNA was used to target the fourth exon of *Cd226*, inducing a single base pair deletion (red) that led to a frameshift and premature termination of CD226 protein translation. Modified image from Gene NCBI. Histograms showing CD226 expression in splenic **(B)** $CD4^+$ T cells, **(C)** $CD8^+$ T cells, and **(D)** NK cells of 12-week-old female, pre-diabetic WT (black), HET (gray), and KO (light gray) mice.

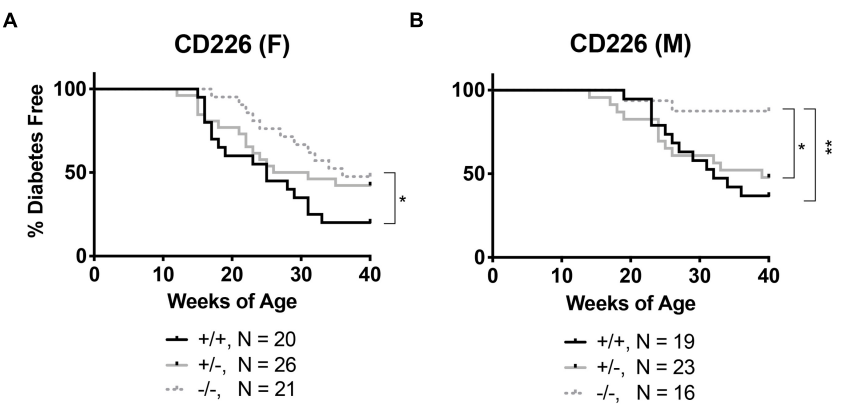

FIGURE 2 | CD226 KO NOD mice are protected from type 1 diabetes. Disease incidence was monitored weekly, with diabetes defined as two consecutive daily blood glucose readings >250 mg/dL. CD226 KO (dotted lines) significantly lowers disease incidence in **(A)** females and **(B)** males as compared to WT (solid black) or HET (solid gray) mice. Log-rank (Mantel–Cox) test; $^*p < 0.05$; $^{**}p < 0.01$. Female: +/+, $n = 20$; +/-, $n = 26$; –/–, $n = 21$; Male: +/+, $n = 19$; +/-, $n = 23$; –/–, $n = 16$.

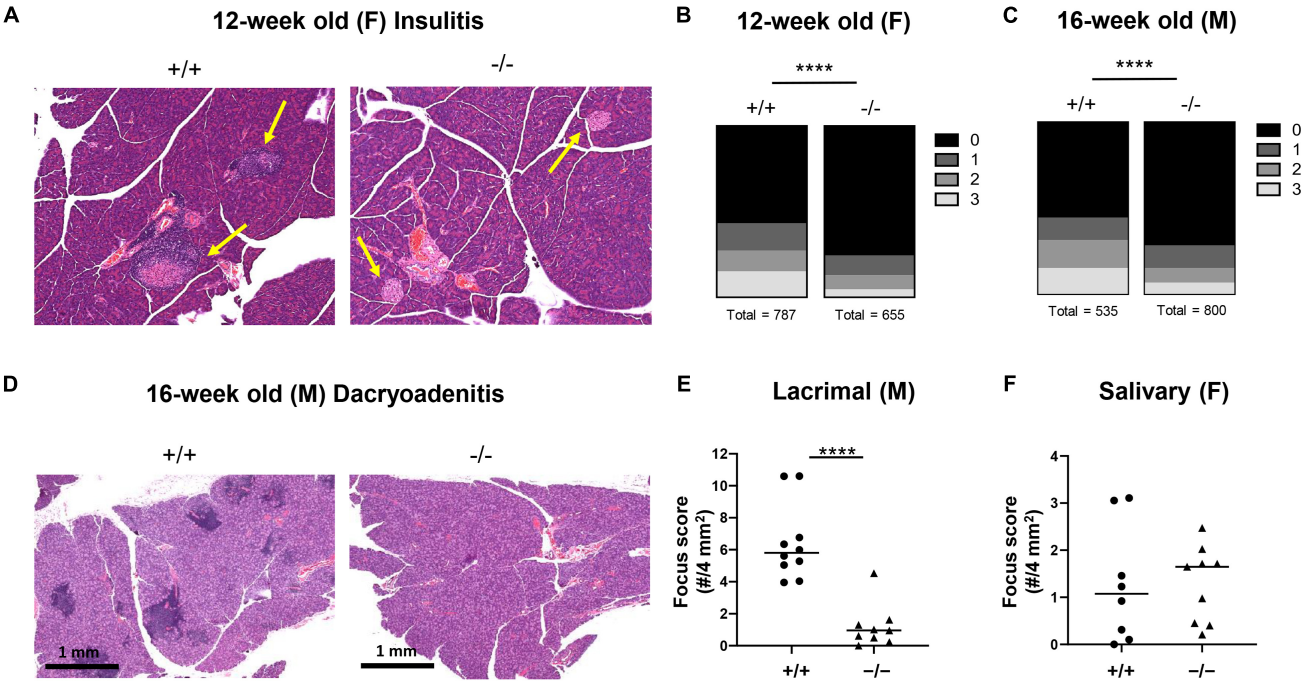

FIGURE 3 | CD226 KO mice have reduced insulitis and dacryoadenitis. At least 45 islets per mouse were analyzed from three sections 250 microns apart. **(A)** Representative images of hematoxylin and eosin-stained pancreata from 12-week old female CD226 WT and KO mice. Yellow arrows denote islets. **(B)** Total number of islets categorized by insulitis score for pre-diabetic 12-week old females or **(C)** pre-diabetic 16-week old males. Chi-square test; ****$p < 0.0001$. Female: N = +/+, 10; –/–, 10. Male: N = +/+, 7; N = –/–, 10. **(D)** Representative images of hematoxylin and eosin-stained lacrimal glands showing numerous inflammatory foci in CD226 WT, but not KO lacrimal glands. Bars are 1 mm. **(E)** Dacryoadenitis scoring from 10–16 week old male CD226 WT and KO mice. **(F)** Sialoadenitis scoring in 10–14 week old female CD226 WT and KO mice. Symbols represent individual mice. Lines are medians. Mann–Whitney test; ****$p < 0.0001$.

signaling may induce the negative selection of $CD8^+$ thymocytes, potentially shaping the peripheral $CD8^+$ T cell repertoire.

Decreased Peripheral Activation of $CD8^+$ T Cells in CD226 KO Mice

We next investigated how CD226 impacted peripheral tolerance by analyzing the naïve and memory $CD4^+$ and $CD8^+$ T cell compartments in various organs of 12-week old pre-diabetic mice. In the pLN, the percentages of naïve $CD44^-CD62L^+$ and memory $CD44^+CD62L^-$ $CD4^+$ T cells were not altered in CD226 KO mice (**Figures 7A–D**). However, CD226 KO mice showed a significantly decreased percentage of memory $CD44^+CD62L^-CD8^+$ T cells in the pLN as compared to WT mice (**Figures 7A,E**). The impact of CD226 KO on naïve and memory T cell proportions was not a global phenomenon, as these subsets were not significantly perturbed in the mesenteric lymph nodes (mLN, **Supplementary Figure S3**) or spleen (**Supplementary Figure S4**). Therefore, CD226 may augment peripheral $CD8^+$ T cell activation within the context of organ-specific autoimmunity.

Reduced Avidity of IGRP-Reactive $CD8^+$ T Cells in CD226 KO Mice

To understand the impact of CD226 KO on $CD8^+$ T cell autoreactivity, we characterized $CD8^+$ T cells recognizing an immunodominant type 1 diabetes epitope (42), islet-specific glucose-6-phosphatase catalytic subunit-related protein ($IGRP_{206-214}$) (43). Similar percentages of $CD8^+$IGRP-tetramer$^+$ T cells were observed within the spleen, pLN, mLN, and pancreas of the CD226 WT and KO mice (**Figures 8A,B**). However, the geometric mean fluorescence intensity (gMFI) of IGRP-tetramer staining within the IGRP-tetramer$^+$ population was significantly decreased in the pancreas of CD226 KO as compared to CD226 WT mice (**Figures 8A,C**). The magnitude of tetramer binding has previously been shown to correlate with TCR affinity for MHC I-antigen complex in $CD8^+$ T cells (44, 45). TCR affinity has also been correlated with CD5 expression levels on mature SP thymocytes and naïve T cells (46). Indeed, CD5 gMFI of naïve IGRP-tetramer$^+$ $CD8^+$ T cells in the spleen was significantly decreased in the CD226 KO as compared to WT mice (**Figures 8D,E**). These data suggest that autoreactive $CD8^+$ T cells of the CD226 KO mice may possess a decreased functional avidity for IGRP in the context of MHC I.

DISCUSSION

We show novel evidence that CD226 KO provided protection from type 1 diabetes in NOD mice. Similar proportions of type 1 diabetes seen in CD226 WT and HET mice suggested

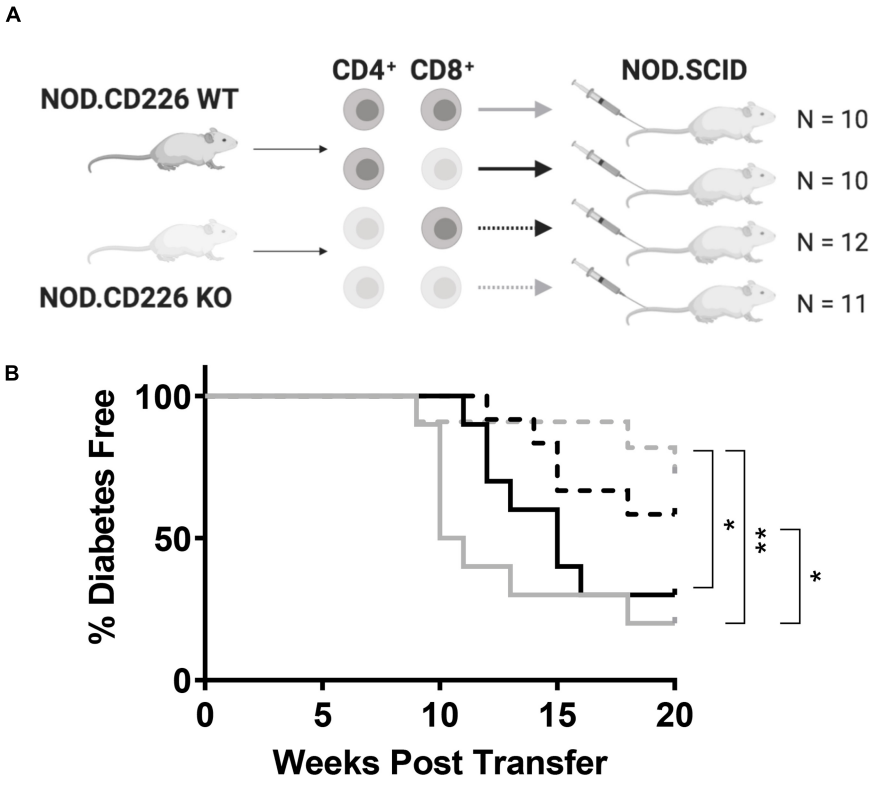

FIGURE 4 | CD226 expression in T cells exacerbates type 1 diabetes induction. **(A)** Schematic of $CD4^+$ and $CD8^+$ T cell transfer from pre-diabetic CD226 WT or KO mice to female NOD.SCID recipients. Created with BioRender. **(B)** Diabetes induction was monitored for up to 20 weeks post-transfer, with incidence significantly decreased in recipients of KO $CD4^+$ and KO $CD8^+$ (dashed gray) T cells as compared to WT $CD4^+$ and KO $CD8^+$ (solid black) or WT $CD4^+$ and WT $CD8^+$ (solid gray) T cell recipients. Mice receiving KO $CD4^+$ and WT $CD8^+$ (dashed black) also showed significantly decreased incidence as compared to WT $CD4^+$ and WT $CD8^+$ T cell recipients. Log-rank (Mantel–Cox) test; $^*p < 0.05$; $^{**}p < 0.01$. WT $CD4^+$ and WT $CD8^+$, $n = 10$; WT $CD4^+$ and KO $CD8^+$, $n = 10$; KO $CD4^+$ and WT $CD8^+$, $n = 12$; KO $CD4^+$ and KO $CD8^+$, $n = 11$.

that a single copy of *Cd226* was sufficient for maximal type 1 diabetes induction. However, TIGIT KO showed minimal impact on type 1 diabetes incidence. A potential explanation for the lack of phenotype observed in the TIGIT KO strain is that there is another inhibitory receptor in the immunoglobulin superfamily, CD96, which can bind to CD155 (47). Thereby, CD96 may compensate for the function of TIGIT in the TIGIT KO animals, allowing for relatively unperturbed T cell function. In support of this notion, combined TIGIT and CD96 blockade has shown increased efficacy at preventing tumor growth via a $CD8^+$ T cell-mediated mechanism in a mouse fibrosarcoma model in comparison to either antibody alone (48). Enhancement of $CD8^+$ T cell pathogenicity by dual TIGIT and CD96 blockade could therefore be expected to augment type 1 diabetes development in NOD mice.

CD226 KO animals also showed protection from Sjögren's-associated lacrimal gland inflammation, despite similar extent of salivary gland infiltration. Interestingly, transfer of $CD8^+$ T cells alone to NOD.SCID mice can induce lacrimal, but not salivary gland pathology (38). This suggests that the decreased lacrimal disease in the CD226 KO mice may be attributed to $CD8^+$ T cell alterations, in agreement with our findings regarding CD226 impacting $CD8^+$ T cell numbers, memory formation, and TCR avidity in the context of type 1 diabetes. Whether similar observations of decreased $CD8^+$ T cell activation or avidity are seen in the cervical-draining lymph nodes or lacrimal glands of the CD226 KO mice remain unknown.

While we observed that expression of CD226 on both $CD4^+$ and $CD8^+$ T cells increased the frequency of type 1 diabetes incidence, we did not detect any changes in the thymic development or peripheral activation of $CD4^+$ T cells in the absence of CD226. It is likely that CD226 drives pathogenicity in both cell types, and further interrogation of $CD4^+$ T cell phenotype in the CD226 KO mouse may uncover mechanisms by which CD226 expression on $CD4^+$ T cells contributes to type 1 diabetes. Importantly, the adoptive transfer experiments utilized a 2:1 ratio for $CD4^+$:$CD8^+$ T cell transfer, while the $CD4^+$:$CD8^+$ T cell ratio observed in the spleens of CD226 KO mice was closer to 3:2 due to an increase in $CD8^+$ T cell output by the thymus. It is plausible that adoptive transfer experiments with this modified ratio may show an enhanced role for CD226 expression on $CD8^+$ T cells driving disease, due to sheer increase in the number of autoreactive cells transferred. Regardless, these data suggest that $CD4^+$ and $CD8^+$ T cell interaction in the global CD226 KO mouse may synergize to drive disease. To further understand the role of CD226 in the immunological mechanisms leading to

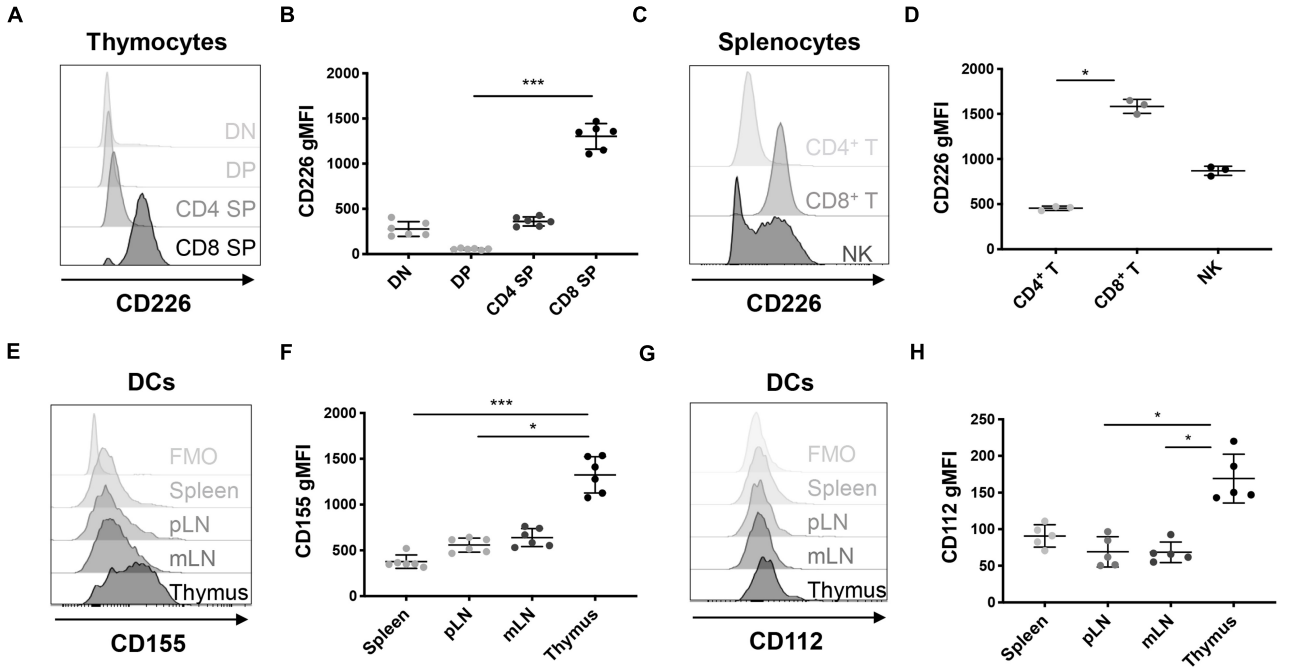

FIGURE 5 | CD226 and ligand expression are enriched on $CD8^+$ SP thymocytes and thymic dendritic cells (DCs), respectively. Cells were analyzed from 12-week old pre-diabetic female mice. **(A)** Representative histograms of CD226 geometric mean fluorescence intensity (gMFI) in thymocytes showing that **(B)** CD8 SP thymocytes have higher CD226 expression than DN, DP, and CD4 SP subsets. **(C)** Representative histogram of CD226 expression in spleen. **(D)** gMFI of CD226 elevated on $CD8^+$ as compared to $CD4^+$ T cells and NK cells. **(E)** Representative histograms of CD155 on $CD11c^+MHCII^+$ DCs from various organs. Fluorescence minus one (FMO) control shown. **(F)** CD155 gMFI is elevated on thymic DCs as compared to DCs from all other organs surveyed. **(G)** Representative histograms of CD112 reveal that **(H)** CD112 expression is highest on thymic DCs. Friedman test with Dunn's multiple comparisons test; $^*p < 0.05$; $^{**}p < 0.01$; $^{***}p < 0.001$. N = +/+, 6 for thymic CD226 and CD155, N = +/+, 5 for thymic CD112, N = +/+, 3 for splenic CD226 staining.

type 1 diabetes, generation of cell-specific CD226 KO strains are currently underway.

While assessing the impact of CD226 signaling on central tolerance mechanisms, we found increased thymic output of $CD8^+$ T cells in the CD226 KO NOD mouse. Others reported that CD226 KO led to decreased proportions of DP and $CD4^+$ SP thymocytes in the fetal thymus (29), however, these findings were not replicated in the adult thymus (30), in agreement with our observations in the adult CD226 KO mouse. In contrast to our findings, previous studies have observed that CD226 KO (30) or CD155 KO (31) on the non-autoimmune BALB/c background led to decreased percentages of $CD8^+$ SP thymocytes as a possible consequence of early thymic egress, although these studies did not observe differences in peripheral $CD8^+$ T cell numbers. These discrepancies may be explained by thymic alterations in NOD as compared to the BALB/c strain (30, 31). NOD mice are known to accumulate thymic medullary giant perivascular spaces (PVSs) with age, and mature $CD4^+$ and $CD8^+$ SP thymocytes have been found in these compartments (49). The retained SP thymocytes show defects in integrin-type fibronectin receptor expression, thought to impair migration (49–51). Therefore, disruption of CD226 interaction and stalling on Nectin family ligands might preferentially correct $CD8^+$ SP thymocyte migration and export to the periphery in NOD mice. Our findings warrant future studies of migration capabilities and numbers of $CD8^+$ SP thymocytes in the PVSs of the CD226 KO thymus. Additionally, treatment of NOD mice with CD226 blocking antibody (35, 52, 53) should be utilized to uncouple the effects of CD226 deletion on thymic selection versus peripheral tolerance, while validating our observation of CD226 disruption preventing type 1 diabetes onset.

Our findings suggest that CD226 KO also blunted the peripheral activation of $CD8^+$ T cells, particularly in the pLN. These data concur with the previously reported role of CD226 in promoting human $CD8^+$ T cell activation, leading to increased cytokine production and cytotoxicity against tumor cells (20). In response to viral infection, CD226 KO mice showed delayed lymphocytic choriomeningitis virus (LCMV) clearance, with reduced IFNγ and TNFα production by virus-specific $CD8^+$ T cells (54). Further characterization of the downstream effects of $CD8^+$ T cell activation in the CD226 KO NOD model via *ex vivo* analysis of cytokines, perforin, and granzymes (55) or *in vitro* analysis of antigen-specific proliferation and β cell killing (56) are currently underway to further understand the extent to which these mechanisms translate to human type 1 diabetes.

Further supporting the role of CD226 in promoting $CD8^+$ T cell pathogenicity in type 1 diabetes, CD226 KO mice showed evidence of reduced TCR avidity of IGRP-reactive $CD8^+$ T cells within the pancreas. In agreement with our findings, progression to type 1 diabetes in the NOD mouse has been suggested to

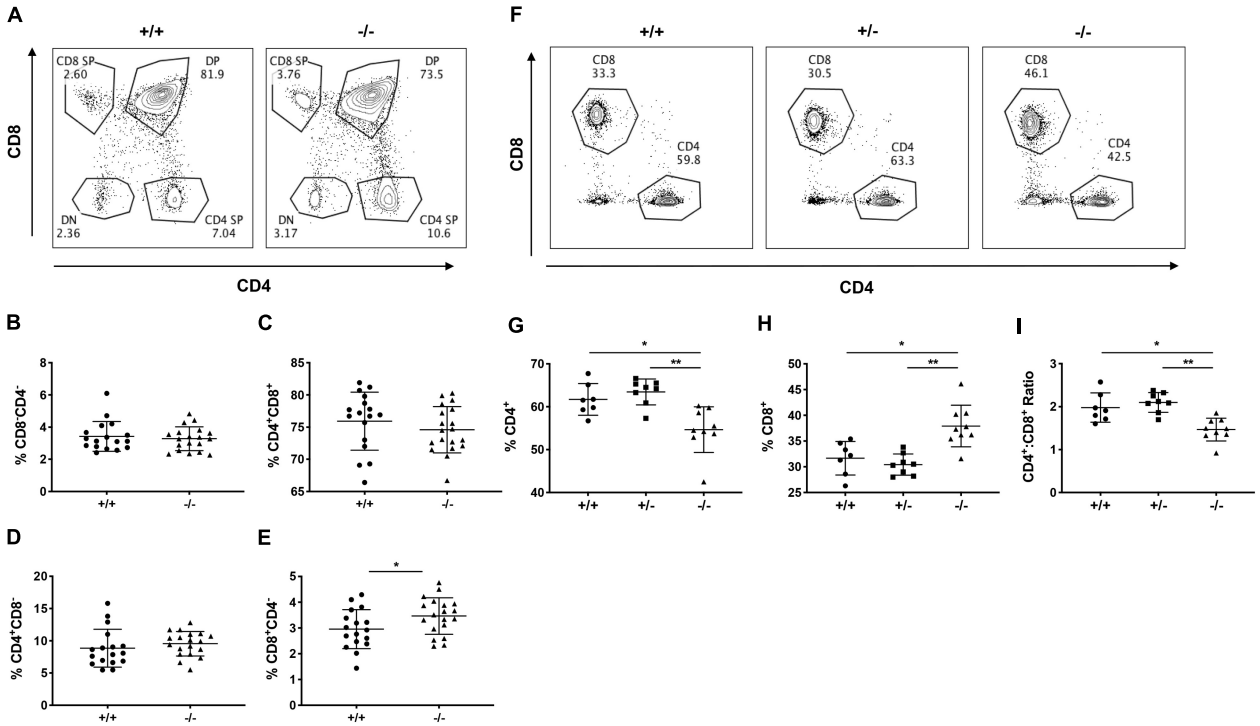

FIGURE 6 | CD226 KO mice have increased thymic output of CD8$^+$ T cells. Thymus and spleen were analyzed from 12-week old pre-diabetic female mice. **(A)** Representative flow cytometry plots showing percentage of **(B)** DN, **(C)** DP, and **(D)** CD4 SP thymocytes are similar between WT and KO mice. **(E)** Increased percentage of CD8 SP thymocytes in CD226 KO. Unpaired t test; *$p < 0.05$. N = +/+, 17; –/–, 19. **(F)** Representative flow cytometry plots from spleen, gated on live CD3$^+$ T cells. **(G)** Decreased percentage of CD4$^+$ and **(H)** increased percentage of CD8$^+$ T cells, resulting in **(I)** decreased CD4$^+$:CD8$^+$ ratio in CD226 KO mice. Kruskal–Wallis with Dunn's multiple comparisons test; *$p < 0.05$; **$p < 0.01$. N = +/+, 7; +/–, 8; –/–, 9.

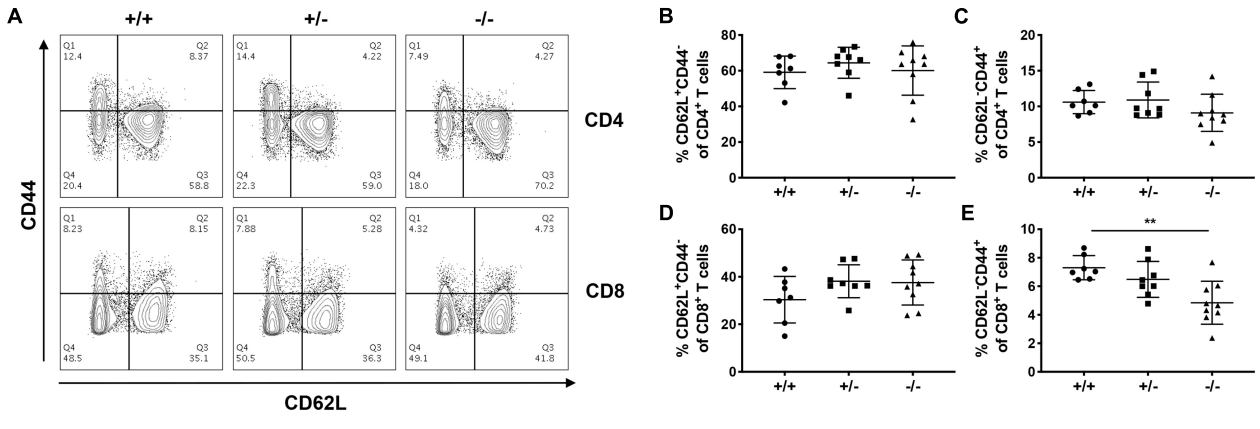

FIGURE 7 | Loss of memory CD8$^+$ T cells in the pancreatic-draining lymph nodes of CD226 KO mice. **(A)** Representative flow cytometry plots from 12-week old pre-diabetic females, gated on live CD3$^+$ T cells. While percentages of CD62L$^+$CD44$^-$ **(B)** naïve CD4$^+$, CD62L$^-$CD44$^+$ **(C)** memory CD4$^+$ T cells, and **(D)** naïve CD8$^+$ T cells remained unaltered in CD226 KO mice, the percentage of **(E)** memory CD8$^+$ T cells was reduced in the pancreatic lymph nodes of CD226 KO mice. Kruskal–Wallis with Dunn's multiple comparisons test; **$p < 0.01$. N = +/+, 7; +/–, 8; –/–, 9.

rely on avidity maturation of the IGRP-reactive T cell population in the pancreas via preferential expansion of high-avidity TCR clones (57). While costimulatory signaling, including that of CD226 (58), has been implicated in driving selective pressure toward high-avidity T cell clones (59), it is unclear whether our findings in the CD226 KO mouse are reflective of peripheral avidity maturation or, alternatively, a potential consequence of CD8$^+$ T cell repertoire modulation at the level of thymic selection. Future work to characterize the thymic output of IGRP-reactive T cells in CD226 KO NOD mice may help to address the mechanisms governing IGRP-specific CD8$^+$ T cell avidity. Additionally, the impact of CD226 on CD8$^+$ T cell avidity should

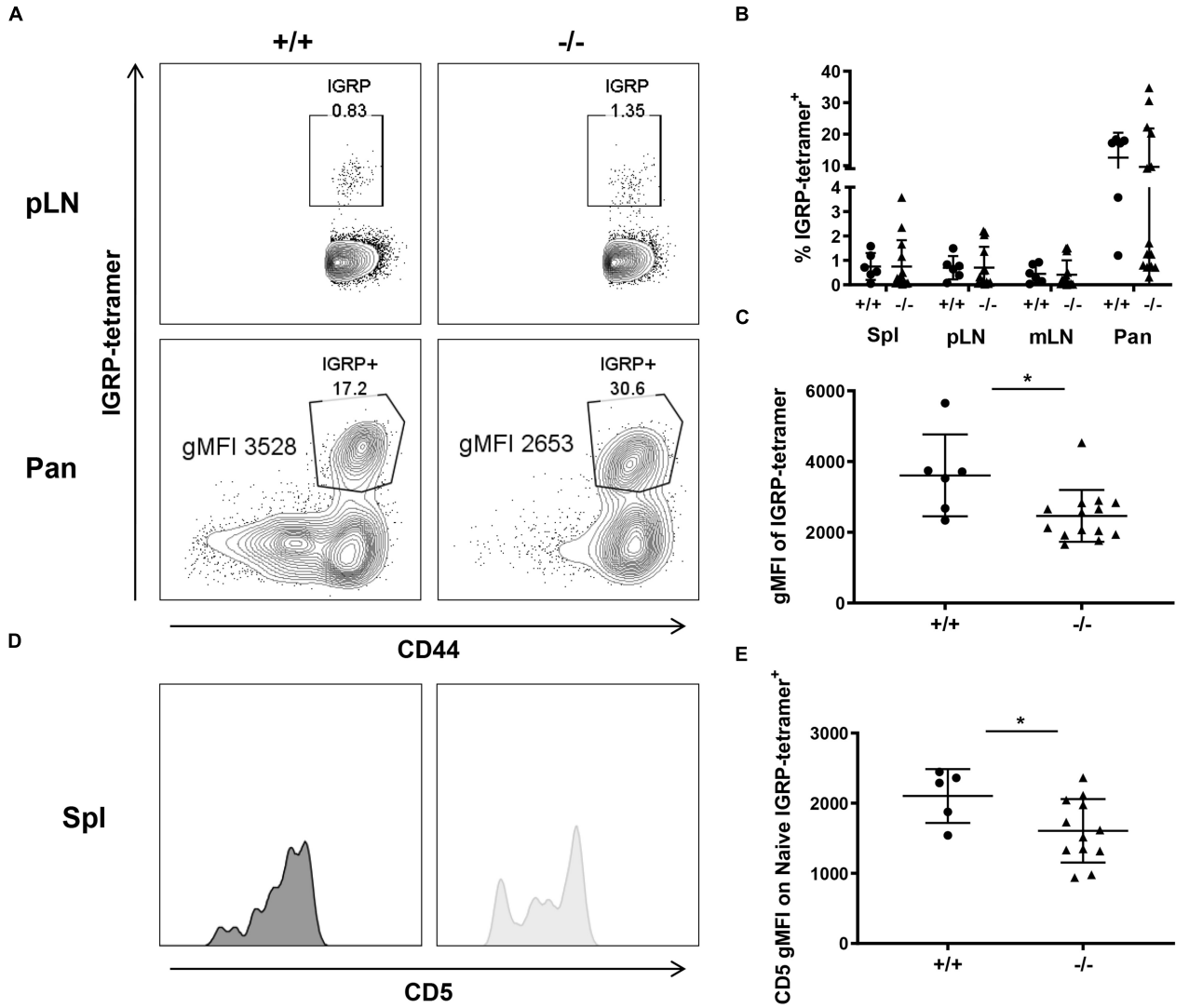

FIGURE 8 | Decreased IGRP avidity in CD226 KO mice. **(A)** Representative flow cytometry plots from 12-week old females, pancreatic-draining lymph node (pLN) gated on live $CD8^{+}CD44^{+}$ T cells and pancreas (Pan) gated on live $CD8^{+}$ T cells. **(B)** While percentages of IGRP-$tetramer^{+}$ cells are similar between WT and KO mice for all organs surveyed, **(C)** gMFI of the tetramer within the $tetramer^{+}$ gate is significantly reduced in CD226 KO mice. Mann–Whitney test; $^{*}p < 0.05$. N = +/+, 6; –/–, 12. **(D)** Representative histograms of CD5 expression on naïve IGRP-$tetramer^{+}$ $CD8^{+}$ T cells in the spleen. **(E)** CD5 gMFI on naïve IGRP-reactive cells is significantly decreased in CD226 KO mice. Unpaired t-test; $^{*}p < 0.05$. N = +/+, 5; –/–, 12.

be validated by measuring tetramer gMFI and CD5 expression on other islet-reactive specificities, such as the AI4-like $CD8^{+}$ T cell pool (60, 61).

We report that CD226 KO attenuates type 1 diabetes via altered thymocyte development in combination with impaired peripheral $CD8^{+}$ T cell activation and IGRP-specific TCR avidity. Our findings here elucidate the mechanisms by which CD226 contributes to type 1 diabetes and support future translational efforts to block CD226 signaling in individuals at-risk for type 1 diabetes and other autoimmune diseases with shared pathogenic mechanisms. Notably, CTLA-4 Ig has been demonstrated to block CD28-mediated costimulatory signaling, with success in recent onset type 1 diabetes at delaying loss of C-peptide (62, 63), endorsing the potential utility of therapeutics such as CD226 blockade in modulating T cell costimulation for the prevention or reversal of type 1 diabetes.

DATA AVAILABILITY STATEMENT

The raw data supporting the conclusions of this article will be made available by the authors, without undue reservation.

ETHICS STATEMENT

The animal study was reviewed and approved by the University of Florida Institutional Animal Care and Use Committee.

AUTHOR CONTRIBUTIONS

MS: writing – original draft, writing – review and editing, formal analysis, visualization, validation, investigation, project administration, and supervision. W-IY: conceptualization, writing – review and editing, formal analysis, visualization, validation, investigation, funding acquisition, project administration, and supervision. JL, JG, CI, and SW: investigation and writing – review and editing. AP and MA: writing – review and editing. MC-T: writing – review and editing, resources, and supervision. SL: writing – review and editing, investigation, formal analysis, validation, funding acquisition, and supervision. DS, AG, and Y-GC: writing – review and editing, resources, and funding acquisition. TB: conceptualization, writing – review and editing, funding acquisition, project administration, and supervision. All authors contributed to the article and approved the submitted version.

FUNDING

Project support was provided by grants from the National Institutes of Health (F31 DK117548 to MS, R01 EY027731 to SL, DP3 DK097605 to Y-GC and AG, PO1 AI42288 to MA, R01 DK107541 to Y-GC, R01 DK106191 to TB, and R01 DK46266 and DK95735 to DS). W-IY was supported by an American Diabetes Association fellowship (1-16-PDF-131).

ACKNOWLEDGMENTS

We thank Catherine Ramsey Grace (University of Florida) for technical assistance with blood glucose monitoring. We thank Paul Tenewitz and Juan Arnoletti (University of Florida) for assistance with insulitis scoring. We thank Heather Bonanno (University of Florida) for mouse breeding and husbandry. We also thank Xiaofang Wang (University of Iowa) for technical assistance with salivary and lacrimal gland slide preparation. Thanks to the UF Molecular Pathology Core for processing of pancreata, the NIH Tetramer Facility for production of IGRP tetramer, and the UF Center for Immunology and Transplantation (CIT) for flow cytometer access.

SUPPLEMENTARY MATERIAL

The Supplementary Material for this article can be found online at: https://www.frontiersin.org/articles/10.3389/fimmu.2020.02180/full#supplementary-material

REFERENCES

1. Coppieters KT, Dotta F, Amirian N, Campbell PD, Kay TW, Atkinson MA, et al. Demonstration of islet-autoreactive CD8 T cells in insulitic lesions from recent onset and long-term type 1 diabetes patients. *J Exp Med.* (2012) 209:51–60. doi: 10.1084/jem.20111187
2. Richardson SJ, Rodriguez-Calvo T, Gerling IC, Mathews CE, Kaddis JS, Russell MA, et al. Islet cell hyperexpression of HLA class I antigens: a defining feature in type 1 diabetes. *Diabetologia.* (2016) 59:2448–58. doi: 10.1007/s00125-016-4067-4
3. Dotta F, Fondelli C, Falorni A. Can NK cells be a therapeutic target in human type 1 diabetes? *Eur J Immunol.* (2008) 38:2961–3. doi: 10.1002/eji.200838851
4. Campbell-Thompson M, Fu A, Kaddis JS, Wasserfall C, Schatz DA, Pugliese A, et al. Insulitis and β-cell mass in the natural history of type 1 diabetes. *Diabetes.* (2016) 65:719–31. doi: 10.2337/db15-0779
5. Onengut-Gumuscu S, Chen WM, Burren O, Cooper NJ, Quinlan AR, Mychaleckyj JC, et al. Fine mapping of type 1 diabetes susceptibility loci and evidence for colocalization of causal variants with lymphoid gene enhancers. *Nat Genet.* (2015) 47:381–6. doi: 10.1038/ng.3245
6. Bradfield JP, Qu HQ, Wang K, Zhang H, Sleiman PM, Kim CE, et al. A genome-wide meta-analysis of six type 1 diabetes cohorts identifies multiple associated loci. *PLoS Genet.* (2011) 7:e1002293. doi: 10.1371/journal.pgen.1002293
7. Barrett JC, Clayton DG, Concannon P, Akolkar B, Cooper JD, Erlich HA, et al. Genome-wide association study and meta-analysis find that over 40 loci affect risk of type 1 diabetes. *Nat Genet.* (2009) 41:703–7. doi: 10.1038/ng.381
8. Consortium WTCC. Genome-wide association study of 14,000 cases of seven common diseases and 3,000 shared controls. *Nature.* (2007) 447:661–78. doi: 10.1038/nature05911
9. Cooper JD, Smyth DJ, Smiles AM, Plagnol V, Walker NM, Allen JE, et al. Meta-analysis of genome-wide association study data identifies additional type 1 diabetes risk loci. *Nat Genet.* (2008) 40:1399–401. doi: 10.1038/ng.249
10. Todd JA, Walker NM, Cooper JD, Smyth DJ, Downes K, Plagnol V, et al. Robust associations of four new chromosome regions from genome-wide analyses of type 1 diabetes. *Nat Genet.* (2007) 39:857–64. doi: 10.1038/ng2068
11. Fortune MD, Guo H, Burren O, Schofield E, Walker NM, Ban M, et al. Statistical colocalization of genetic risk variants for related autoimmune diseases in the context of common controls. *Nat Genet.* (2015) 47:839–46. doi: 10.1038/ng.3330
12. Evangelou M, Smyth DJ, Fortune MD, Burren OS, Walker NM, Guo H, et al. A method for gene-based pathway analysis using genomewide association study summary statistics reveals nine new type 1 diabetes associations. *Genet Epidemiol.* (2014) 38:661–70. doi: 10.1002/gepi.21853
13. Wallet MA, Santostefano KE, Terada N, Brusko TM. Isogenic cellular systems model the impact of genetic risk variants in the pathogenesis of type 1 diabetes. *Front Endocrinol (Lausanne).* (2017) 8:276.
14. Inshaw JRJ, Cutler AJ, Crouch DJM, Wicker LS, Todd JA. Genetic variants predisposing most strongly to type 1 diabetes diagnosed under age 7 years lie near candidate genes that function in the immune system and in pancreatic β-cells. *Diabetes Care.* (2019) 43:169–77. doi: 10.2337/dc19-0803
15. Qiu ZX, Zhang K, Qiu XS, Zhou M, Li WM. CD226 Gly307Ser association with multiple autoimmune diseases: a meta-analysis. *Hum Immunol.* (2013) 74:249–55. doi: 10.1016/j.humimm.2012.10.009
16. Shibuya K, Shirakawa J, Kameyama T, Honda S, Tahara-Hanaoka S, Miyamoto A, et al. CD226 (DNAM-1) is involved in lymphocyte function-associated antigen 1 costimulatory signal for naive T cell differentiation and proliferation. *J Exp Med.* (2003) 198:1829–39. doi: 10.1084/jem.20030958
17. Shirakawa J, Shibuya K, Shibuya A. Requirement of the serine at residue 329 for lipid raft recruitment of DNAM-1 (CD226). *Int Immunol.* (2005) 17:217–23. doi: 10.1093/intimm/dxh199
18. Gaud G, Roncagalli R, Chaoui K, Bernard I, Familiades J, Colacios C, et al. The costimulatory molecule CD226 signals through VAV1 to amplify TCR signals and promote IL-17 production by CD4. *Sci Signal.* (2018) 11:538.
19. Hollis-Moffatt JE, Hook SM, Merriman TR. Colocalization of mouse autoimmune diabetes loci Idd21.1 and Idd21.2 with IDDM6 (human) and Iddm3 (rat). *Diabetes.* (2005) 54:2820–5. doi: 10.2337/diabetes.54.9.2820
20. Shibuya A, Campbell D, Hannum C, Yssel H, Franz-Bacon K, McClanahan T, et al. DNAM-1, a novel adhesion molecule involved in the cytolytic function of T lymphocytes. *Immunity.* (1996) 4:573–81. doi: 10.1016/s1074-7613(00)70060-4
21. Ayano M, Tsukamoto H, Kohno K, Ueda N, Tanaka A, Mitoma H, et al. Increased CD226 expression on CD8+ T cells is associated with upregulated cytokine production and endothelial cell injury in patients with systemic sclerosis. *J Immunol.* (2015) 195:892–900. doi: 10.4049/jimmunol.1403046

22. Fuhrman CA, Yeh WI, Seay HR, Saikumar Lakshmi P, Chopra G, Zhang L, et al. Divergent phenotypes of human regulatory t cells expressing the receptors TIGIT and CD226. *J Immunol.* (2015) 195:145–55. doi: 10.4049/jimmunol.1402381
23. Yu X, Harden K, Gonzalez LC, Francesco M, Chiang E, Irving B, et al. The surface protein TIGIT suppresses T cell activation by promoting the generation of mature immunoregulatory dendritic cells. *Nat Immunol.* (2009) 10:48–57. doi: 10.1038/ni.1674
24. Salomon B, Bluestone JA. Complexities of CD28/B7: CTLA-4 costimulatory pathways in autoimmunity and transplantation. *Annu Rev Immunol.* (2001) 19:225–52. doi: 10.1146/annurev.immunol.19.1.225
25. Bottino C, Castriconi R, Pende D, Rivera P, Nanni M, Carnemolla B, et al. Identification of PVR (CD155) and Nectin-2 (CD112) as cell surface ligands for the human DNAM-1 (CD226) activating molecule. *J Exp Med.* (2003) 198:557–67. doi: 10.1084/jem.20030788
26. Tahara-Hanaoka S, Shibuya K, Onoda Y, Zhang H, Yamazaki S, Miyamoto A, et al. Functional characterization of DNAM-1 (CD226) interaction with its ligands PVR (CD155) and nectin-2 (PRR-2/CD112). *Int Immunol.* (2004) 16:533–8. doi: 10.1093/intimm/dxh059
27. Johnston RJ, Comps-Agrar L, Hackney J, Yu X, Huseni M, Yang Y, et al. The immunoreceptor TIGIT regulates antitumor and antiviral CD8(+) T cell effector function. *Cancer Cell.* (2014) 26:923–37. doi: 10.1016/j.ccell.2014.10.018
28. Xing Y, Hogquist KA. T-cell tolerance: central and peripheral. *Cold Spring Harb Perspect Biol.* (2012) 4:a006957.
29. Fang L, Zhang X, Miao J, Zhao F, Yang K, Zhuang R, et al. Expression of CD226 antagonizes apoptotic cell death in murine thymocytes. *J Immunol.* (2009) 182:5453–60. doi: 10.4049/jimmunol.0803090
30. Danisch S, Qiu Q, Seth S, Ravens I, Dorsch M, Shibuya A, et al. CD226 interaction with CD155 impacts on retention and negative selection of CD8 positive thymocytes as well as T cell differentiation to follicular helper cells in Peyer's Patches. *Immunobiology.* (2013) 218:152–8. doi: 10.1016/j.imbio.2012.02.010
31. Qiu Q, Ravens I, Seth S, Rathinasamy A, Maier MK, Davalos-Misslitz A, et al. CD155 is involved in negative selection and is required to retain terminally maturing CD8 T cells in thymus. *J Immunol.* (2010) 184:1681–9. doi: 10.4049/jimmunol.0900062
32. Lozano E, Joller N, Cao Y, Kuchroo VK, Hafler DA. The CD226/CD155 interaction regulates the proinflammatory (Th1/Th17)/anti-inflammatory (Th2) balance in humans. *J Immunol.* (2013) 191:3673–80. doi: 10.4049/jimmunol.1300945
33. Stanietsky N, Simic H, Arapovic J, Toporik A, Levy O, Novik A, et al. The interaction of TIGIT with PVR and PVRL2 inhibits human NK cell cytotoxicity. *Proc Natl Acad Sci USA.* (2009) 106:17858–63. doi: 10.1073/pnas.0903474106
34. Chan CJ, Andrews DM, McLaughlin NM, Yagita H, Gilfillan S, Colonna M, et al. DNAM-1/CD155 interactions promote cytokine and NK cell-mediated suppression of poorly immunogenic melanoma metastases. *J Immunol.* (2010) 184:902–11. doi: 10.4049/jimmunol.0903225
35. Dardalhon V, Schubart AS, Reddy J, Meyers JH, Monney L, Sabatos CA, et al. CD226 is specifically expressed on the surface of Th1 cells and regulates their expansion and effector functions. *J Immunol.* (2005) 175:1558–65. doi: 10.4049/jimmunol.175.3.1558
36. Qin W, Dion SL, Kutny PM, Zhang Y, Cheng AW, Jillette NL, et al. Efficient CRISPR/Cas9-mediated genome editing in mice by zygote electroporation of nuclease. *Genetics.* (2015) 200:423–30. doi: 10.1534/genetics.115.176594
37. Xue S, Posgai A, Wasserfall C, Myhr C, Campbell-Thompson M, Mathews CE, et al. Combination therapy reverses hyperglycemia in NOD mice with established type 1 diabetes. *Diabetes.* (2015) 64:3873–84. doi: 10.2337/db15-0164
38. Barr JY, Wang X, Meyerholz DK, Lieberman SM. CD8 T cells contribute to lacrimal gland pathology in the nonobese diabetic mouse model of Sjögren syndrome. *Immunol Cell Biol.* (2017) 95:684–94. doi: 10.1038/icb.2017.38
39. Humphreys-Beher MG, Peck AB. New concepts for the development of autoimmune exocrinopathy derived from studies with the NOD mouse model. *Arch Oral Biol.* (1999) 44(Suppl. 1):S21–5.
40. Toda I, Sullivan BD, Rocha EM, Da Silveira LA, Wickham LA, Sullivan DA. Impact of gender on exocrine gland inflammation in mouse models of Sjögren's syndrome. *Exp Eye Res.* (1999) 69:355–66. doi: 10.1006/exer.1999.0715
41. Pende D, Castriconi R, Romagnani P, Spaggiari GM, Marcenaro S, Dondero A, et al. Expression of the DNAM-1 ligands, Nectin-2 (CD112) and poliovirus receptor (CD155), on dendritic cells: relevance for natural killer-dendritic cell interaction. *Blood.* (2006) 107:2030–6. doi: 10.1182/blood-2005-07-2696
42. Santamaria P, Utsugi T, Park BJ, Averill N, Kawazu S, Yoon JW. Beta-cell-cytotoxic CD8+ T cells from nonobese diabetic mice use highly homologous T cell receptor alpha-chain CDR3 sequences. *J Immunol.* (1995) 154:2494–503.
43. Lieberman SM, Evans AM, Han B, Takaki T, Vinnitskaya Y, Caldwell JA, et al. Identification of the beta cell antigen targeted by a prevalent population of pathogenic CD8+ T cells in autoimmune diabetes. *Proc Natl Acad Sci USA.* (2003) 100:8384–8. doi: 10.1073/pnas.0932778100
44. Yee C, Savage PA, Lee PP, Davis MM, Greenberg PD. Isolation of high avidity melanoma-reactive CTL from heterogeneous populations using peptide-MHC tetramers. *J Immunol.* (1999) 162:2227–34.
45. Busch DH, Pamer EG. T cell affinity maturation by selective expansion during infection. *J Exp Med.* (1999) 189:701–10. doi: 10.1084/jem.189.4.701
46. Azzam HS, Grinberg A, Lui K, Shen H, Shores EW, Love PE. CD5 expression is developmentally regulated by T cell receptor (TCR) signals and TCR avidity. *J Exp Med.* (1998) 188:2301–11. doi: 10.1084/jem.188.12.2301
47. Chan CJ, Martinet L, Gilfillan S, Souza-Fonseca-Guimaraes F, Chow MT, Town L, et al. The receptors CD96 and CD226 oppose each other in the regulation of natural killer cell functions. *Nat Immunol.* (2014) 15:431–8. doi: 10.1038/ni.2850
48. Mittal D, Lepletier A, Madore J, Aguilera AR, Stannard K, Blake SJ, et al. CD96 is an immune checkpoint that regulates CD8. *Cancer Immunol Res.* (2019) 7:559–71. doi: 10.1158/2326-6066.cir-18-0637
49. Savino W, Boitard C, Bach JF, Dardenne M. Studies on the thymus in nonobese diabetic mouse. I. Changes in the microenvironmental compartments. *Lab Invest.* (1991) 64:405–17.
50. Mendes-da-Cruz DA, Smaniotto S, Keller AC, Dardenne M, Savino W. Multivectorial abnormal cell migration in the NOD mouse thymus. *J Immunol.* (2008) 180:4639–47. doi: 10.4049/jimmunol.180.7.4639
51. Cotta-de-Almeida V, Villa-Verde DM, Lepault F, Pléau JM, Dardenne M, Savino W. Impaired migration of NOD mouse thymocytes: a fibronectin receptor-related defect. *Eur J Immunol.* (2004) 34:1578–87. doi: 10.1002/eji.200324765
52. Avouac J, Elhai M, Tomcik M, Ruiz B, Friese M, Piedavent M, et al. Critical role of the adhesion receptor DNAX accessory molecule-1 (DNAM-1) in the development of inflammation-driven dermal fibrosis in a mouse model of systemic sclerosis. *Ann Rheum Dis.* (2013) 72:1089–98. doi: 10.1136/annrheumdis-2012-201759
53. Elhai M, Chiocchia G, Marchiol C, Lager F, Renault G, Colonna M, et al. Targeting CD226/DNAX accessory molecule-1 (DNAM-1) in collagen-induced arthritis mouse models. *J Inflamm (Lond).* (2015) 12:9. doi: 10.1186/s12950-015-0056-5
54. Welch MJ, Teijaro JR, Lewicki HA, Colonna M, Oldstone MB. CD8 T cell defect of TNF-α and IL-2 in DNAM-1 deficient mice delays clearance in vivo of a persistent virus infection. *Virology.* (2012) 429:163–70. doi: 10.1016/j.virol.2012.04.006
55. Trivedi P, Graham KL, Krishnamurthy B, Fynch S, Slattery RM, Kay TW, et al. Perforin facilitates beta cell killing and regulates autoreactive CD8+ T-cell responses to antigen in mouse models of type 1 diabetes. *Immunol Cell Biol.* (2016) 94:334–41. doi: 10.1038/icb.2015.89
56. Krishnamurthy B, Dudek NL, McKenzie MD, Purcell AW, Brooks AG, Gellert S, et al. Responses against islet antigens in NOD mice are prevented by tolerance to proinsulin but not IGRP. *J Clin Invest.* (2006) 116:3258–65. doi: 10.1172/jci29602
57. Amrani A, Verdaguer J, Serra P, Tafuro S, Tan R, Santamaria P. Progression of autoimmune diabetes driven by avidity maturation of a T-cell population. *Nature.* (2000) 406:739–42. doi: 10.1038/35021081
58. Braun M, Ress ML, Yoo YE, Scholz CJ, Eyrich M, Schlegel PG, et al. IL12-mediated sensitizing of T-cell receptor-dependent and -independent tumor cell killing. *Oncoimmunology.* (2016) 5:e1188245. doi: 10.1080/2162402x.2016.1188245

59. Viganò S, Utzschneider DT, Perreau M, Pantaleo G, Zehn D, Harari A. Functional avidity: a measure to predict the efficacy of effector T cells? *Clin Dev Immunol.* (2012) 2012:153863.
60. Graser RT, DiLorenzo TP, Wang F, Christianson GJ, Chapman HD, Roopenian DC, et al. Identification of a CD8 T cell that can independently mediate autoimmune diabetes development in the complete absence of CD4 T cell helper functions. *J Immunol.* (2000) 164:3913–8. doi: 10.4049/jimmunol.164.7.3913
61. Lieberman SM, Takaki T, Han B, Santamaria P, Serreze DV, DiLorenzo TP. Individual nonobese diabetic mice exhibit unique patterns of CD8+ T cell reactivity to three islet antigens, including the newly identified widely expressed dystrophia myotonica kinase. *J Immunol.* (2004) 173:6727–34. doi: 10.4049/jimmunol.173.11.6727
62. Orban T, Bundy B, Becker DJ, DiMeglio LA, Gitelman SE, Goland R, et al. Co-stimulation modulation with abatacept in patients with recent-onset type 1 diabetes: a randomised, double-blind, placebo-controlled trial. *Lancet.* (2011) 378:412–9. doi: 10.1016/s0140-6736(11)60886-6
63. Orban T, Bundy B, Becker DJ, Dimeglio LA, Gitelman SE, Goland R, et al. Costimulation modulation with abatacept in patients with recent-onset type 1 diabetes: follow-up 1 year after cessation of treatment. *Diabetes Care.* (2014) 37:1069–75. doi: 10.2337/dc13-0604

Conflict of Interest: The authors declare that the research was conducted in the absence of any commercial or financial relationships that could be construed as a potential conflict of interest.

frontiers in Immunology

ORIGINAL RESEARCH
published: 17 September 2020
doi: 10.3389/fimmu.2020.565099

Single-Center Overview of Pediatric Monogenic Autoinflammatory Diseases in the Past Decade: A Summary and Beyond

*Wei Wang†, Zhongxun Yu†, Lijuan Gou, Linqing Zhong, Ji Li, Mingsheng Ma, Changyan Wang, Yu Zhou, Ying Ru, Zhixing Sun, Qijiao Wei, Yanqing Dong and Hongmei Song**

Department of Pediatrics, Peking Union Medical College Hospital, Chinese Academy of Medical Sciences, Beijing, China

OPEN ACCESS

Edited by:
Jennifer Konopa Mulligan, Medical University of South Carolina, United States

Reviewed by:
Giuseppe Lopalco, University of Bari, Italy
Jurgen Sota, University of Siena, Italy

***Correspondence:**
Hongmei Song
songhm1021@hotmail.com

†These authors have contributed equally to this work

Specialty section:
This article was submitted to Autoimmune and Autoinflammatory Disorders, a section of the journal Frontiers in Immunology

Received: *23 May 2020*
Accepted: *13 August 2020*
Published: *17 September 2020*

Citation:
Wang W, Yu Z, Gou L, Zhong L, Li J, Ma M, Wang C, Zhou Y, Ru Y, Sun Z, Wei Q, Dong Y and Song H (2020) Single-Center Overview of Pediatric Monogenic Autoinflammatory Diseases in the Past Decade: A Summary and Beyond. Front. Immunol. 11:565099. doi: 10.3389/fimmu.2020.565099

Objective: Monogenic autoinflammatory diseases (AIDs) are inborn disorders caused by innate immunity dysregulation and characterized by robust autoinflammation. We aimed to present the phenotypes and genotypes of Chinese pediatric monogenic AID patients.

Methods: A total of 288 pediatric patients clinically suspected to have monogenic AIDs at the Department of Pediatrics of Peking Union Medical College Hospital between November 2008 and May 2019 were genotyped by Sanger sequencing, and/or gene panel sequencing and/or whole exome sequencing. Final definite diagnoses were made when the phenotypes and genotypes were mutually verified.

Results: Of the 288 patients, 79 (27.4%) were diagnosed with 18 kinds of monogenic AIDs, including 33 patients with inflammasomopathies, 38 patients with non-inflammasome related conditions, and eight patients with type 1 interferonopathies. Main clinical features were skin disorders (76%), musculoskeletal problems (66%), fever (62%), growth retardation (33%), gastrointestinal tract abnormalities (25%), central nervous system abnormalities (15%), eye disorders (16%), ear problems (9%), and cardiopulmonary disorders (8%). The causative genes were *ACP5*, *ADA2*, *ADAR1*, *IFIH1*, *LPIN2*, *MEFV*, *MVK*, *NLRC4*, *NLRP3*, *NLRP12*, *NOD2*, *PLCG2*, *PSMB8*, *PSTPIP1*, *TMEM173*, *TNFAIP3*, *TNFRSF1A*, and *TREX1*.

Conclusions: The present study summarized both clinical and genetic characteristics of 18 kinds of monogenic AIDs found in the largest pediatric AID center over the past decade, with fever, skin problems, and musculoskeletal system disorders being the most prevalent clinical features. Many of the mutations were newly discovered. This is by far the first and largest monogenic AID report in Chinese pediatric population and also a catalog of the phenotypic and genotypic features among these patients.

Keywords: autoinflammatory diseases, innate immunity, genetic sequencing, pediatric immunology, clinical rheumatology

INTRODUCTION

Autoinflammatory diseases (AIDs) are a group of disorders characterized by remarkable inflammation without high-titer autoantibodies or antigen-specific T cells (1). Most of AIDs harbor a single gene defect, hence called monogenic AIDs, while other disorders like PFAPA are polygenic AIDs (2). Since the identification of *MEFV*, a gene causing Familial Mediterranean Fever (FMF) once mutated (3), many monogenic AIDs have been identified over the past two decades assisted by the development of genetic sequencing technologies. According to the recent 2017 International Union of Immunological Societies (IUIS) classification, there are 36 monogenic AIDs across three branches, defects affecting the inflammasomes (inflammasomopathies), non-inflammasome related conditions, and type 1 interferonopathies (4).

An inflammasome is a multiprotein pro-inflammatory complex consisting of a sensor protein like NOD-like receptor (NLR) containing protein or pyrin, an adapter protein such as apoptosis-associated speck-like protein (ASC) and an effector protein such as caspase-1 (5). The sensors recognize pathogen associated molecular patterns (PAMPs) or danger associated molecular patterns (DAMPs) to initiate the assembly and activation of inflammasomes, thereby cleaving interleukin-1 (IL-1) and freeing IL-1β and IL-18 to cause further inflammation (6). The inflammasomopathies then denote a group of mechanistically similar diseases, resulting in inappropriate inflammasome activation (7). Non-inflammasome related conditions are a group of heterogeneous disorders such as Blau syndrome, pyogenic arthritis, pyoderma gangrenosum, and acne (PAPA) syndrome, and ADA2 deficiency (8). Each one arises from different genetic mutations. As for type 1 interferonopathies, they are uniquely characterized by an inappropriate overproduction of type 1 interferon (IFN-I) (9). Aicardi-Goutieres syndrome (AGS) and proteasome-associated autoinflammatory syndrome (PRAAS), such as chronic atypical neutrophilic dermatosis with lipodystrophy and elevated temperature (CANDLE), are two typical syndromes that belong to this category. However, this field is still rapidly advancing and newly discovered diseases, such as DNaseII deficiency (10), RIPK1 deficiency (11), are periodically added to the list.

Arriving at a final definite diagnosis of monogenic AID can be very difficult because of the multifaceted nature of the disease. A strong clinical clue plus solid genetic findings can help reach a correct diagnosis. In this report, we aim to provide an overview of monogenic AIDs diagnosed by a tertiary Chinese pediatric rheumatology disease center based in Beijing over the past decade.

METHODS

Patient Selection

A total of 288 pediatric patients (age 18 or less) suspected of having monogenic AIDs were included in this study at the Peking Union Medical Hospital between November 2008 and May 2019. They all had persistently or intermittently elevated inflammation indices with no evidence of malignancy or infection. In addition to unexplained elevated inflammation markers, AID diagnosis may be considered if a patient met one or more of the following three criteria as depicted in **Figure 1A**: (1) presenting with recurrent fever, rash and/or arthralgia and other systemic features; (2) diagnosed with autoimmune diseases previously but unresponsive to standard therapies; (3) had family history or had early onset symptoms. All these patients and legal guardians gave informed consent for genetic sequencing. The clinical information of all these patients was obtained from paper and electronic medical records. There was no consanguinity in these children. The Institutional Review Board of the Peking Union Medical College Hospital approved this study.

Genetic Analyses

We ordered genetic tests primarily based on the clinical pictures. For cases suspected of FMF, Blau syndrome, cryopyrin associated periodic syndrome (CAPS) or other very typical cases, the genomic DNA from peripheral blood samples of those suspected patients were genotyped for specific candidate genes such as *MEFV*, *NOD2*, *NLRP3*, or other specific AID genes using Sanger sequencing. For cases with overlapping clinical manifestations or previous negative Sanger sequencing, a gene panel including 347 primary immunodeficiency disease gene (PID panel) or Whole exome sequencing (WES) method would be recommended and utilized given patient family approval. Variants found in patients would be stringently analyzed with different information tools such as the Exome Aggregation Consortium, the ClinVar, the HGMD, the Infevers, and the 1000 Genomes Project. The prediction tools used for novel rare variants were SIFT, Polyphen 2, MutationTaster 2, CADD and UMD-Predictor. For each system, the most recent version would be used. Further, disease prevalence, expressivity, mode of inheritance and segregation would also be considered during data analyses. For all the disease-causing variants found by gene panel or WES, Sanger sequencing would be done for validation.

RESULTS

From 2008 to 2019, 288 patients suspected of having monogenic AID went through genetic sequencing. As shown in **Figures 1B**, **2**, we diagnosed 18 kinds of AID in 79 (27.4%) patients. Among them, 33 (42%) patients had inflammasomopathies, 38 (48%) had non-inflammasome related conditions, and 8 (10%) had type 1 interferonopathies. The genetic analysis methods used in each group of disorders are presented in **Figure 2A**. The clinical and genetic features of these three groups of patients are summarized below.

Inflammasomopathies

We diagnosed 33 cases of inflammasomopathies with mutations in 6 genes, *NLRP3*, *NLRP12*, *NLRC4*, *PLCG2*, *MEFV*, and *MVK*. The detailed clinical and genetic information is listed in **Table 1**. For the 12 NLRP3 related autoinflammatory disease (NLRP3-AID) cases, which were previously known as cryopyrin-associated periodic syndromes (CAPS), the median age of onset was 0.2 months with a range of 0.1

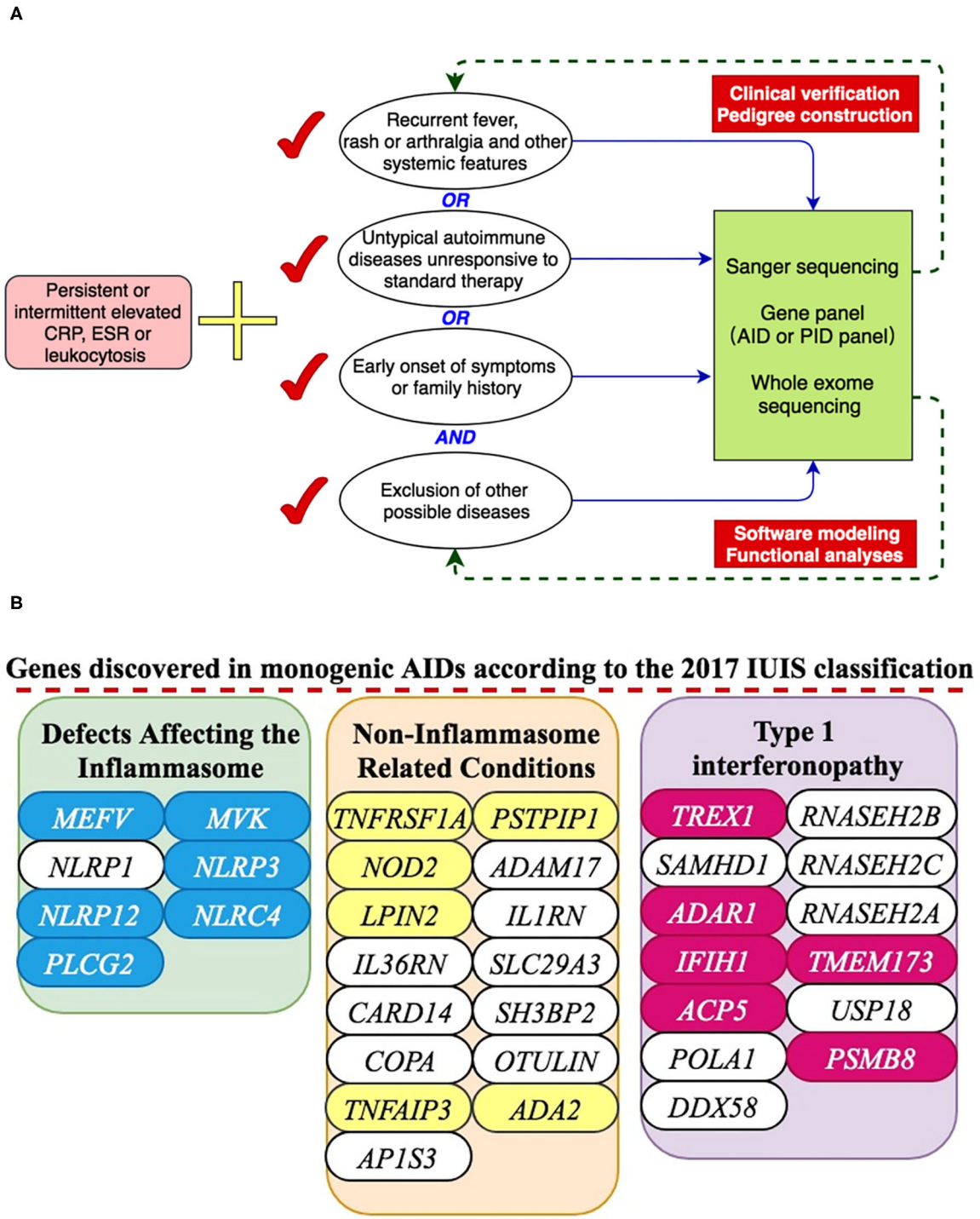

FIGURE 1 | A presentation of monogenic AID gene discovery. **(A)** Inclusion criteria for suspected AID patients and working flow of genetic analyses. **(B)** 18 genes were discovered in our center according to the 2017 IUIS classification.

months to 4.8 years, but the median age of diagnosis was 4.0 years with a range of 0.1 months to 20 years. The main clinical features were cutaneous rash, followed by fever, growth retardation, neurological abnormalities, lymphadenopathy, ocular manifestations, and arthralgia. All cases were autosomal dominant inherited and the variants were c.796C>T (p.L266F),

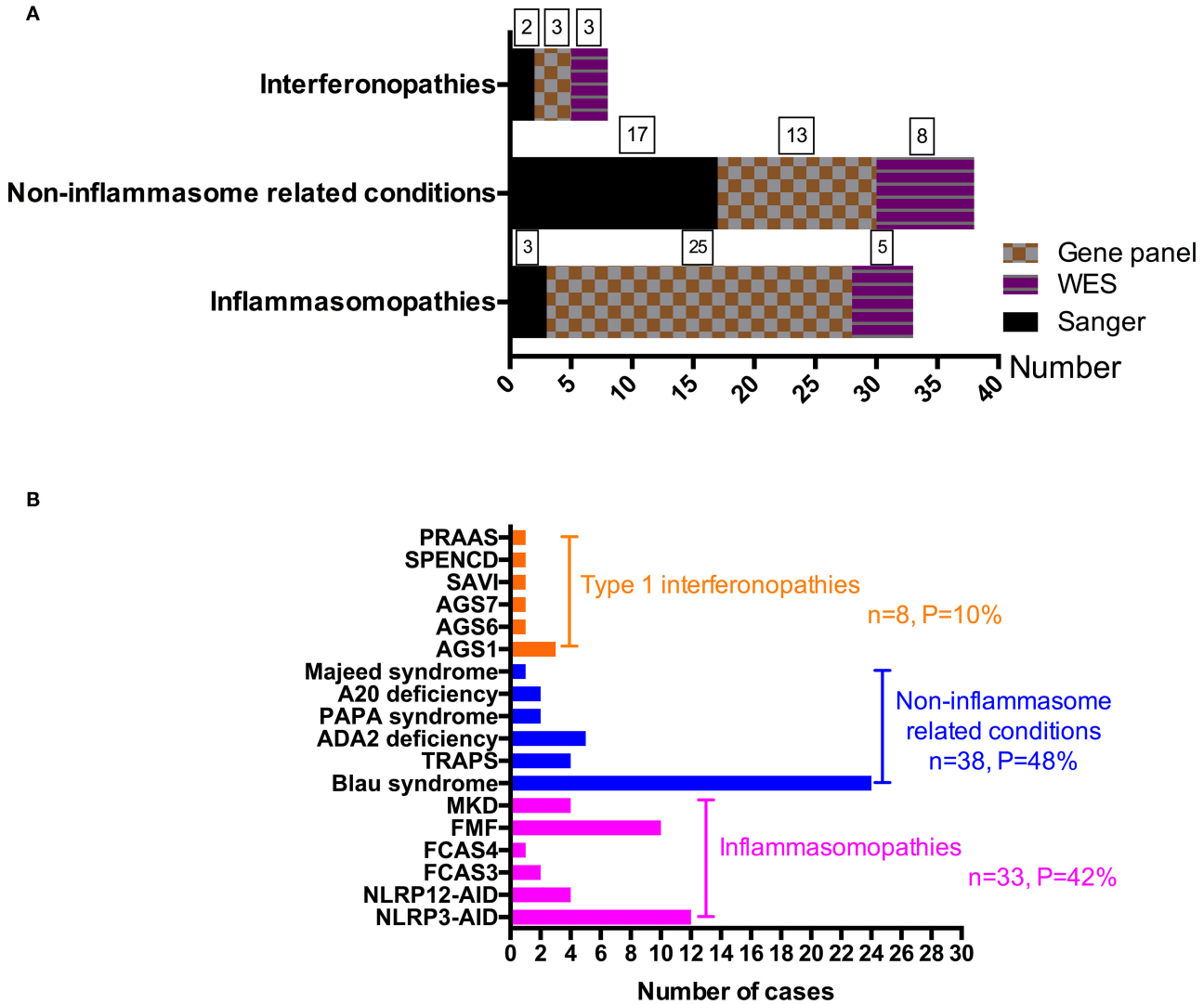

FIGURE 2 | A summary of monogenic AIDs by disease group and disease itself. **(A)** A summary of gene detection methods used in different disease groups. **(B)** A presentation of each monogenic disorder diagnosed in our center.

c.913G>A (p.D305N), c.918G>T (p.E306D), c.932T>C (p.F311S), c.1049C>T (p.T350M), c.1311G>T (p.K437N), c.1711G>C (p.G571R), c.1715A>G (p.Y572C), c.1991T>C (p.M664T) and c.2113C>A (p.Q705K).

For the 4 NLRP12-AID cases, the median age at disease onset was 4.0 years. Fever, skin rash, arthritis and ontological disorders were the most prevalent features. They each carried a heterozygous germline mutation including c.1673T>G (p.L558R), c.1742G>A (p.W581X), c.2188G>C (p.G730R) and c.2072+2dupT accordingly, which have been analyzed and reported previously (12).

We also diagnosed two familial cold autoinflammatory syndrome 3 (FCAS3) caused by *PLCG2* gain-of-function mutations. Both patients had fever, cold-induced urticarial rash and lymphadenopathy. One also developed facial edema and oral ulcer while the other one had hepatosplenomegaly. Both patients had family history with dominantly inherited traits. Though they had significantly elevated CRP and ESR, neither had antibody deficiency nor recurrent infections, which are characteristics of APLAID (*PLCG2*-associated antibody deficiency and immune dysregulation) syndrome (13). The two mutations were c.3244T>C (p.C1082R) and c.3524T>A (p.I1175K). These were two novel mutations.

NLRC4 inflammasomopathy has varied phenotypes including autoinflammation and infantile enterocolitis (AIFEC) and familial cold autoinflammatory syndrome 4 (FCAS4) (14). As for our patient, he carried a novel mutation, c.514G>A (p.G172S), in nucleotide binding domain (NBD) of NLRC4. He had urticarial-like skin rashes since 3 months of age. Later he had periodic fever once every 3–6 months. Like S171F, this mutation

TABLE 1 | Characteristics of Inflammasomopathies discovered in our center (Total $N = 33$).

Characteristics (*N*, %)	NLRP3-AID ($n = 12$)	NLRP12-AID ($n = 4$)	FCAS3 ($n = 2$)	FCAS4 ($n = 1$)	FMF ($n = 10$)	MKD ($n = 4$)
Male:Female	8:4	1:3	0:2	1:0	6:4	3:1
Age at onset (median, range)	0.2 m; (0.1 m−4.8 y)	4; (0–10)	12; (10–14)	1	7.5; (4–12)	0.6; (0.25–1)
Age at diagnosis (median, range)	4 (0.1 m−20 y)	11.5; (9–17)	15; (14–16)	2	10; (5–14)	2; (1–5)
Duration from onset to diagnosis (median, range)	4; (0–18)	7.5; (2–14)	3; (0–6)	1	1; (0–10)	1.5 (1–5)
Family history	0 (0)	0 (0)	2 (100)	0 (0)	0 (0)	1 (25)
Fever	11 (92)	4 (100)	2 (100)	1 (100)	10 (100)	4 (100)
Abdominal pain	0 (0)	1 (25)	0 (0)	0 (0)	5 (50)	1 (25)
Chest pain	0 (0)	0 (0)	0 (0)	0 (0)	0 (0)	0 (0)
Arthralgia/Arthritis	4 (33)	2 (50)	0 (0)	0 (0)	5 (50)	2 (50)
Myalgia	0 (0)	1 (25)	0 (0)	0 (0)	0 (0)	0 (0)
Cutaneous rash	12 (100)	3 (75)	2 (100)	1 (100)	5 (50)	3 (75)
Cold-induced urticarial	2 (17)	0 (0)	2 (100)	0 (0)	2 (20)	0 (0)
Facial edema	0 (0)	0 (0)	1 (50)	1 (100)	0 (0)	0 (0)
Neurological abnormalities	7 (58)	0 (0)	0 (0)	0 (0)	0 (0)	0 (0)
Oral ulcer	0 (0)	0 (0)	1 (50)	1 (100)	1 (10)	1 (25)
Ocular manifestations	5 (42)	1 (25)	0 (0)	0 (0)	0 (0)	0 (0)
Lymphadenopathy	6 (50)	1 (25)	2 (100)	0 (0)	1 (10)	2 (50)
Hepatosplenomegaly	2 (17)	1 (25)	1 (50)	0 (0)	1 (10)	1 (25)
Otological abnormalities	5 (42)	2 (50)	0 (0)	0 (0)	0 (0)	0 (0)
Vasculitis	0 (0)	0 (0)	0 (0)	0 (0)	1 (10)	0 (0)
Amyloidosis	0 (0)	0 (0)	0 (0)	0 (0)	0 (0)	0 (0)
Growth retardation	9 (75)	0 (0)	0 (0)	0 (0)	1 (10)	2 (50)
ANA positivity	2 (17)	1 (25)	1 (50)	0 (0)	1 (10)	0 (0)
Elevated ESR/CRP	12 (100)	4 (100)	2 (100)	1 (100)	10 (100)	4 (100)
Genes	*NLRP3*	*NLRP12*	*PLCG2*	*NLRC4*	*MEFV*	*MVK*
Inheritance	AD	AD	AD	AD	AR	AR
Gene mutations/variants	p.L266F p.D305N p.E306D p.F311S p.T350M p.K437N p.G571R p.Y572C p.M664T p.Q705K	p.L558R p.W581X p.G730R c.2072+2 dupT	p.C1082R p.I1175K	p.G172S	p.L110P p.P115R p.E148Q p.E230K p.G304R p.P369S p.P633L p.F636Y	p.V8M/p.G336S p.S118P/p.G211X p.G219R/p.P263L

AD, autosomal dominant; AR, autosomal recessive; FCAS, familial cold autoinflammatory syndrome; FMF, familial Mediterranean fever; MKD, mevalonate kinase deficiency; m, month; y, year.

would substitute a hydrophilic serine residue for a hydrophobic glycine residue at the adenosine diphosphate (ADP)-binding interface within the conserved NBD region, which disrupts the auto-inhibitory mechanism maintaining the inactive state of NLRC4 (15).

We also discovered 10 FMF patients over the past decade. The median age at disease onset was 7.5 (range, 4–12) years, while the median age at diagnosis was 10 (range, 5–14) years. Apparently, fever was the most common symptom, followed by abdominal pain, arthralgia and rash. Other less prevalent symptoms included oral ulcer, vasculitis, lymphadenopathy, hepatosplenomegaly and growth retardation. No amyloidosis was found in these patients. The *MEFV* variants of these patients were c.329T>C (p.L110P), c.344C>G (p.P115R), c.442G>C (p.E148Q), c.688G>A (p.E230K), c.910G>A (p.G304R), c.1105C>T (p.P369S), c.1898C>T (p.P633L), c.1907T>A (p.F636Y), and c.1759+8C>T. Each patient carried 2–5 variants, and E148Q was the most common one. Six patients responded well to colchicine treatment.

The last disease in this section is mevalonate kinase deficiency (MKD), which is an autosomal recessive disorder caused by mevalonate kinase gene (*MVK*) mutations. Defects in the mevalonate kinase pathway can promote pyrin inflammasome activation by dysregulating geranylgeranylation and function of small cellular GTPases (16). We discovered four patients in total and they all developed symptoms soon after birth. The median

age at diagnosis was 2.0 years (range, 1–5) and the median delay of diagnosis was 1.5 years (range, 1–5). All of them had typical periodic fever, while other symptoms were cutaneous rash, arthralgia/arthritis, growth retardation, gastrointestinal problems, and lymphadenopathy (25%). The genetic mutations were p.V8M, p.S118P, p.G211X, p.G219R, p.P263L, and p.G336S.

Non-inflammasome Related Conditions

We diagnosed 38 cases under this branch, and a brief summary is listed in **Table 2**.

Blau syndrome was initially described in 1985 with a triad of granulomatous arthropathy, uveitis, and dermatitis (17). Later in 2001, *NOD2* was discovered to be the causative gene, defects of which promote hyperactivation of NF-κB signaling and inflammation processes. A total of 24 patients were genetically diagnosed and all of them developed symptoms before 5 years old. Overall, 79% cases had granulomatous arthropathy, 54% cases had scaly rash/dermatitis, and 29% cases had bilateral uveitis. The uveitis was relatively severe because three cases turned out to be near blind regardless of treatment. Unfortunately, 13 patients were misdiagnosed as other diseases such as juvenile idiopathic arthritis (JIA) and atopic dermatitis before referral to our center. As for the *NOD2* mutations, all of them were located within or near the NOD/NACHT domain of the NOD2 protein, with p.R334Q (7/24, 29%) and p.R334W (7/24, 29%) being the most common ones. Other mutations were p.E383Q, p.G481D, p.M491L, p.E498G, p.D512Y, p.M513T, p.R587C (2/24, 8.3%), p.H603D, and p.H669R. Of these mutations, p.M491L, p.E498G, and p.H669R were novel variants.

Another classical non-inflammasome related condition is the TNF receptor-associated autoinflammatory syndrome (TRAPS), a dominantly inherited disorder caused by mutations in the TNF receptor (TNFR1) encoded by the TNF superfamily receptor 1A (*TNFRSF1A*) gene (18). Fever is often long lasting and can be accompanied by arthritis, a patchy migratory skin rash, serositis, and periorbital edema. All the four patients developed severe symptoms under 1 year of age. All of them had prolonged periodic fever, while both rash and arthritis occurred in three patients each. Two patients had abdominal pain, a sign of serositis, and two patients had overt reactive lymphadenopathy. The mutations of TNFRSF1A were p.C99S (2/4, 50%), p.T79M, and p.F141C, which were not reported elsewhere. Since TNFR1 is a transmembrane glycoprotein containing four tandem-repeat cysteine-rich domains (CRD1-4) (19), introducing (p.F141C) or removing (p.C99S) cysteine residues were believed to affect molecular structures and cause more severe phenotypes. The p.T79M mutation might disrupt hydrogen bonds between proteins.

Deficiency of adenosine deaminase type 2 (DADA2) is an autosomal recessive monogenic AID caused by *ADA2* (formerly known as *CECR1*) mutations and was first described in 2014 in patients with mild immune deficiency, systemic inflammation, and central nervous system vasculopathy (20). ADA2 deficiency leads to accumulation of adenosine, which then activates neutrophils and dysregulates macrophage differentiation to cause inflammation, damage and fibrosis of many tissues (21). We diagnosed five patients and the median age of onset was 3.2 years old. The main clinical features of these patients were fever (100%), rash (100%), livedo racemosa (40%), and early-onset recurrent stroke (20%). The genotypes for these patients were p.N85I/p.G284V, p.H293P/p.Y88C, p.G5R/p.V325Tfs*7 (exon 7 deletion), p.R169Q/p.R131Sfs*52, and p.Y411C/p. N328I accordingly. All these variants have not been reported other than p.V325Tfs*7, p.R169Q and p.N328I.

We also diagnosed two patients of *PSTPIP1*-associated inflammatory diseases (PAID), a dominantly inherited disease that can be subtyped into pyogenic arthritis, pyoderma gangrenosum, and acne (PAPA) syndrome, *PSTPIP1*-associated myeloid-related proteinemia inflammatory (PAMI) syndrome, and other PAPA-like syndromes (22). Both patients had skin rash, arthritis, persistent systemic inflammation, hepatosplenomegaly, pancytopenia, and growth retardation, which matched the typical phenotypes of PAMI. The genotypes were *de novo* mutations of p.E250K and p.N236K, resulting in charge changes of the F-BAR domain of PSTPIP1 and increased binding to pyrin (23).

We also diagnosed two cases of haploinsufficiency of A20 (HA20). A reduced expression of A20, encoded by *TNFAIP3*, leads to insufficient suppression of NF-κB activity and enhanced NLRP3 inflammasome activation, thereby generating large amounts of pro-inflammatory cytokines (24). The clinical phenotypes of the disorder are quite variable. For our patients, both suffered from recurrent oral ulcer. One patient was diagnosed as Behçet disease previously and the other one was diagnosed with undifferentiated connective tissue disease. Hashimoto′s thyroiditis was also found in one patient. The genetic sequencing yielded p.R271X of the *TNFAIP3* gene in one patient and p.R45X in the other one, which were known to be pathogenic variants (25, 26).

The last disease in this section is Majeed syndrome, which is an autosomal recessive disorder due to mutations in *LPIN2* that encodes the protein LIPIN2, a negative regulator of NLRP3 inflammasome (27). Early reports documented a classic triad of clinical findings including severe early onset chronic osteomyelitis, microcytic congenital dyserythropoietic anemia, and the neutrophilic dermatosis (28). Our case was a male patient who developed fever and bone pain soon after birth, and later presented with dermatosis. Diagnostic workup revealed highly elevated acute phase reactants, microcytic anemia and chronic osteomyelitis. Whole exome sequencing revealed c.2327+1G>C and c.1691_1694delGAGA of *LPIN2*. The c.2327+1G>C is a reported pathogenic mutation locating at a splice site of intron 17 and the c.1691_1694delGAGA is a frameshift mutation that has not been reported elsewhere.

Type 1 Interferonopathies

In total, we diagnosed five cases of AGS, one case of stimulator of interferon genes (STING)-associated vasculopathy with onset in infancy (SAVI), one case of spondyloenchondrodysplasia with immune dysregulation (SPENCD), and one case of PRAAS/CANDLE. The clinical characteristics and genotype information are summarized in **Table 3**. For AGS1 that caused

TABLE 2 | Characteristics of the non-inflammasome related conditions.

Disease	Age onset (median, range)	Gender (male: female)	Main clinical findings	Genetic defects	Inheritance
Blau syndrome ($n = 24$)	1 (0–4)	11:13	Arthropathy (19/24), rash (13/24), uveitis (7/24), growth retardation (7/24), camptodactyly (6/24)	*NOD2* p.R334Q, p.R334W, p.E383Q, p.G481D, p.M491L, p.E498G, p.D512Y, p.M513T, p.R587C, p.H603D, p.H669R	AD
TRAPS ($n = 4$)	0.5 (0–1)	4:0	Periodic ever (4/4), rash (3/4), arthritis (3/4), abdominal pain (2/4) lymphadenopathy, (2/4)	*TNFRSF1A* p.C99S p.T79M p.F141C	AD
ADA2 deficiency ($n = 5$)	3.2 (0–9)	3:2	Fever, rash, polyarteritis nodosa, early-onset recurrent stroke	*ADA2* p.N85I / p.G284V p.H293P / p.Y88C p.G5R / exon 7 deletion, p.R169Q / p.R131Sfs*52 p.Y411C / p. N328I	AR
PAID ($n = 2$)	2 (0–4)	1:1	Fever, hematological problems, arthritis, rash	*PSTPIP1* p.E250K, p.N236K	AD
A20 deficiency ($n = 2$)	4 (0–8)	0:2	Fever, rash, arthralgia, mucosal ulcers, bowel inflammation, CTD	*TNFAIP3* p.R45X, p.R271X	AD
Majeed syndrome ($n = 1$)	0.2	1:0	Fever, osteomyelitis, congenital anemia, skin disorders	*LPIN2* c.2327+1G>C c.1691_1694delGAGA	AR

AD, autosomal dominant; AR, autosomal recessive; CTD, connective tissue disease.

by *TREX1* mutations, rash, autoimmune features and intracranial calcifications were the main phenotypes. All of the variants were not reported previously. For AGS6, a patient with c.305_306del (p.Q102Rfs*22) of *ADAR1*, pulmonary artery hypertension (PAH) was noted in addition to chilblain rash, lupus phenotype and intracranial calcification. As for the case of AGS7, the age of disease onset was 0.5 years. He had prominent growth retardation, cutaneous rash and severe leukopenia. His interferon signature of the peripheral blood was high and the genetic analysis yielded p.A339D *de novo* mutation of *IFIH1*. He received Janus kinase (JAK) inhibitor treatment after diagnosis and remains stable till now. We also diagnosed 1 SAVI patient, who had severe PAH and interstitial lung disease at the time of first visit to our center. His lungs were already fibrotic but did not get worse after treatment with JAK inhibitors. As for the case of SPENCD, her initial chief of complaint was intermittent fever. During follow up period, she started to present features of systemic lupus erythematosus and short stature. Her spine X-ray revealed spondyloenchondrodysplasia. This is an autosomal recessive inherited disorder and the genetic variants of this patient were p.S267Lfs*20 and p.G239D of *ACP5*. For the PRAAS/CANDLE patient, the most prominent characteristic was lypodystrophy, other clinical features included fever, rash, PAH, arthritis, intracranial calcification, uveitis, loss of hearing, and growth retardation. He had compound heterozygous mutations of *PSMB8*, which were p.T75M and p.T74I.

DISCUSSION

Human innate immunity is first-line defense against the microbial world, and also serves as a guardian to limit danger molecules and prevent self-invasion. While an inadequate innate immune response can lead to severe infections, persistent excessive responses can generate systemic autoinflammatory disorders, most of which are monogenic inborn errors. Although just conceptualized around 20 years ago, the field of AIDs sitting within the domains of rheumatology and clinical immunology has expanded ever since. Here, we report the first and also the largest cohort of monogenic AIDs in Chinese pediatric population diagnosed over the past decade.

Overall, in our 79 monogenic AID patients, as depicted in **Figure 3**, skin disorders (76%), musculoskeletal problems (66%), and fever (62%) were the most common clinical features. Other features included central nervous system abnormalities (15%), eye disorders (16%), ear problems (9%), cardiopulmonary disorders (8%), and symptoms involving gastrointestinal tract system (25%). In addition to above presentations, one third of the sick kids would experience episodes of infections because of the dysregulated innate immunity. We also noticed that growth retardation was relatively common among these children (33%). Among those 26 patients with growth retardation, a total of 11 patients

TABLE 3 | Characteristics of the eight cases diagnosed as interferonopathies.

Case	Clinical presentation	Age onset	Genetics	Diagnosis	Inheritance	Intervention
1	Rash, growth retardation, intracranial calcification	1y	*TREX1*, c.505C>T, p.R169C; c.900delA, p.S301Lfs*31	AGS1	AR	Prednisone DMARD
2	Rash, glaucoma, intracranial calcification, lupus	3y	*TREX1*, c.139G>A, p.G47S c.458dupA p.C154Mfs*3	AGS1	AR	JAK inhibitor
3	Rash, mixed connective tissue disease, ILD	3y	*TREX1*, c.65C>T, p.T22M	AGS1	AD	JAK inhibitor
4	Lupus, rash, arthritis, PAH, intracranial calcification	3y	*ADAR1*, c.305_306del, p.Q102Rfs*22	AGS6	AD	Prednisone DMARD
5	Growth retardation, rash, intracranial calcification, leukopenia	6m	*IFIH1*, c.1016C>A, p.A339D	AGS7	AD	JAK inhibitor
6	Rash, growth retardation, PAH, ILD	1m	*TMEM173* c.463G>A, p.V155M	SAVI	AD	JAK inhibitor
7	Fever, bone dysplasia, nervous system problems, autoimmune disease	2y	*ACP5* c.798duC, p.S267Lfs*20; c.716G>A, p.G239D	SPENCD	AR	JAK inhibitor
8	Fever, rash, PAH, lipodystrophy, arthropathy, intracranial calcification, growth retardation	7m	*PSMB8* c.224C>T, p.T75M; c.221C>T, p.T74I	PRAAS	AR	Death prior to treatment

AD, autosomal dominant; AGS, Aicardi Goutieres syndrome; AR, autosomal recessive; ILD, interstitial lung disease; PAH, pulmonary artery hypertention; PRAAS, proteasome-associated autoinflammatory syndrome; SAVI, STING associated vasculopathy with onset in infancy; SPENCD, spondyloenchondrodysplasia with immune dysregulation.

had used glucocorticoids (GC). Only four of the 11 patients had received GC treatment for a long time and they were all Blau syndrome patients. Therefore, growth retardation is a kind of phenomenon worthy of attention in children with prolonged uncontrolled inflammation. We also need to address that there were 24 patients (30%) in total misdiagnosed as other diseases, with juvenile idiopathic arthritis being the most prevalent one (12/79), which prompts us pediatric rheumatologists to consider monogenic AIDs when making diagnosis of JIA.

Arriving at an accurate diagnosis of monogenic AID is quite difficult if only through reading clinical phenotypes. The genomic analysis has been integrated into the whole diagnosis process over the past 20 years and seen many breakthrough discoveries. Our center started screening AID genes in highly suspected AID patients such as patients with periodic fever in the year of 2008 with Sanger sequencing. Later we integrated primary immunodeficiency (PID) gene panel in 2012, which helped us diagnose more than half of these patients (46/79, 58%) and are still in current use. For untypical cases with prominent inflammatory phenotypes or typical cases with negative panel screening results, we used WES method, which dated back to the year of 2015. The WES method discovered 16 AID patients (16/79, 20%) in total and is playing a very important role in discovering and characterizing new disorders. Overall, the positive rate of genetic sequencing in our center was 27.4% (79/288). There might be several reasons for this. First, sequencing approach such as whole exome sequencing might miss deep intronic variants that can affect protein translation and expression. Second, disorders like periodic fever syndromes can be affected by environmental triggers through inducing epigenetic changes of specific genes, which cannot be detected by normal genetic sequencing methods (29). Third, a highly suspected AID with negative genetic test results could simply be due to misinterpretation of the genetic results or unknown genes to be identified. As such, the clinical diagnosis can't be excluded by the negative results of genetic sequencing and a further periodic re-evaluation and re-analysis of the genetic variants is highly recommended for undefined AID patients. We have to admit that in real-life clinical setting, there are indeed a small number of patients with typical phenotypes of periodic fever syndromes and negative genetic test results can be clinically diagnosed. However, these seemingly typical cases were not

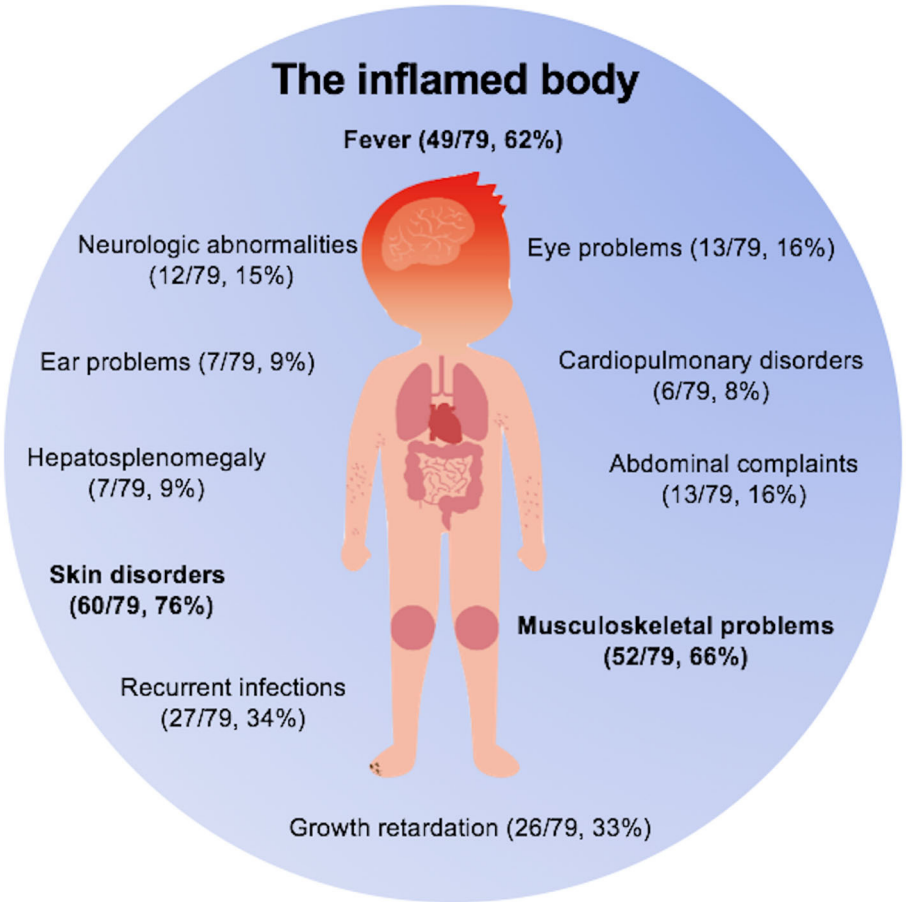

FIGURE 3 | The inflamed body cartoon. Fever, skin disorders, and musculoskeletal problems were three main clinical features of monogenic AIDs.

included in this study, because we observed the occurrence of malignancy in several cases during the long-term follow-up period. For suspected AID patients with unusual phenotypes, the interpretation of variant pathogenicity should be cautious and performed repeatedly under appropriate standardized protocol, especially for the genes that do not seem relevant to the phenotype of the patient.

The high-throughput sequencing technologies not only boost the pace of discovery of new monogenic AIDs, but also further expand our understanding of the innate immunity and help develop targeted therapies to treat autoinflammation. Since the autoinflammation largely depends on cytokines, cytokine directed therapies such as IL-1 inhibition, anti-TNF-α agents and JAK inhibitors have been used in monogenic AID patients (30). However, IL-1 inhibitors are not available in Mainland of China, most of our NLRP3-AID patients were treated by steroids or IL-6 inhibition with low to moderate efficacy. For Blau syndrome, DADA2 and HA20 patients, we initiated anti-TNF-α therapies and have observed some good responses. For type 1 interferonopathies, we tested JAK inhibitors including ruxolitinib and tofacitinib among these patients and the results were promising. All of these AID patients are under regular follow-up and the data pertaining to treatment plans and efficacy would be revealed in later reports.

This report is important because most of the monogenic AID studies were performed in Western countries and the data is scarce in Chinese pediatric population. The clinical characteristics and genetic information provided by our center can help increase the awareness of monogenic AIDs and further avoid misdiagnoses, unnecessary hospitalizations, and inappropriate therapeutic treatment. However, there are some limitations of this study. First, for undefined AID patients who initially received Sanger sequencing of the highly suspected genes, the sensitivity would be lower than in reality, even though we have tried to perform re-analysis in most of those patients. Second, the total number of patients of this report is still limited, and the information provided here is only a reflection of monogenic AIDs diagnosed in a tertiary pediatric center, although our center is already one of the biggest pediatric rheumatology centers in mainland of China. We aim to set up a national network and collaborate with other centers

in the near future to collect more solid data and perform more detailed analyses such as phenotype-genotype correlation in each disease in Chinese pediatric population. Third, for the newly discovered variants with unknown pathogenicity, we only used prediction software and did not validate them experimentally. However, we had rounds of discussions about those variants and correlating phenotypes, and had followed up those patients with undefined variants at a regular basis for better disease characterization.

CONCLUSIONS

In conclusion, the present study described the first cohort of monogenic AID patients in Chinese pediatric population. A total of 79 monogenic AID patients were diagnosed, with fever, skin problems, and musculoskeletal system disorders being the most prevalent clinical features. We totally found 18 kinds of monogenic AIDs with the help of genetic sequencing, and many of the variants in this cohort were newly discovered. By providing data from our center, we hope this report would reflect and also expand the phenotypic and genotypic profiles of Chinese pediatric patients with monogenic AIDs.

DATA AVAILABILITY STATEMENT

The original contributions presented in the study are included in the article/supplementary material, further inquiries can be directed to the corresponding author/s.

ETHICS STATEMENT

The studies involving human participants were reviewed and approved by Institutional Review Board of the Peking Union Medical College Hospital. Written informed consent to participate in this study was provided by the participants' legal guardian/next of kin.

AUTHOR CONTRIBUTIONS

WW and ZY contributed to the conceptualization, methodology, and writing of the original draft. WW performed genetic sequencing and genetic data analysis. ZY, LG, LZ, JL, MM, CW, YZ, YR, ZS, QW, YD, and HS managed patients and collected data. HS contributed to conceptualization, methodology, writing of the original draft, editing, funding acquisition, and supervision. All authors approved the final version of the manuscript.

FUNDING

This study was supported by funds from The Capital Health Research and Development of Special (2016-2-40114), Public Welfare Scientific Research Project of China (201402012), CAMS Innovation Fund for Medical Sciences (2016-I2M-1-008), National Key Research and Development Program of China (2016YFC0901500) to HS, and CAMS Central Public Welfare Scientific Research Institute Basal Research Expenses to WW (2016ZX310182-1).

REFERENCES

1. Georgin-Lavialle S, Fayand A, Rodrigues F, Bachmeyer C, Savey L, Grateau G. Autoinflammatory diseases: state of the art. *Presse Med.* (2019) 48:e25–48. doi: 10.1016/j.lpm.2018.12.003
2. Cattalini M, Soliani M, Rigante D, Lopalco G, Iannone F, Galeazzi M, et al. Basic characteristics of adults with periodic fever, aphthous stomatitis, pharyngitis, and adenopathy syndrome in comparison with the typical pediatric expression of disease. *Mediators Inflamm.* (2015) 2015:570418. doi: 10.1155/2015/570418
3. Consortium FF. A candidate gene for familial Mediterranean fever. *Nat Genet.* (1997) 17:25–31. doi: 10.1038/ng0997-25
4. Picard C, Bobby Gaspar H, Al-Herz W, Bousfiha A, Casanova JL, Chatila T, et al. International union of immunological societies: 2017 primary immunodeficiency diseases committee report on inborn errors of immunity. *J Clin Immunol.* (2018) 38:96–128. doi: 10.1007/s10875-017-0464-9
5. Harapas CR, Steiner A, Davidson S, Masters SL. An update on autoinflammatory diseases: inflammasomopathies. *Curr Rheumatol Rep.* (2018) 20:40. doi: 10.1007/s11926-018-0750-4
6. Hoffman HM, Broderick L. The role of the inflammasome in patients with autoinflammatory diseases. *J Allergy Clin Immunol.* (2016) 138:3–14. doi: 10.1016/j.jaci.2016.05.001
7. Rigante D, Lopalco G, Vitale A, Lucherini OM, Caso F, De Clemente C, et al. Untangling the web of systemic autoinflammatory diseases. *Mediators Inflamm.* (2014) 2014:948154. doi: 10.1155/2014/948154
8. Bousfiha A, Jeddane L, Picard C, Ailal F, Bobby Gaspar H, Al-Herz W, et al. The 2017 IUIS phenotypic classification for primary immunodeficiencies. *J Clin Immunol.* (2018) 38:129–43. doi: 10.1007/s10875-017-0465-8
9. Davidson S, Steiner A, Harapas CR, Masters SL. An update on autoinflammatory diseases: interferonopathies. *Curr Rheumatol Rep.* (2018) 20:38. doi: 10.1007/s11926-018-0748-y
10. Rodero MP, Tesser A, Bartok E, Rice GI, Della Mina E, Depp M, et al. Type I interferon-mediated autoinflammation due to DNase II deficiency. *Nat Commun.* (2017) 8:2176. doi: 10.1038/s41467-017-01932-3
11. Tao P, Sun J, Wu Z, Wang S, Wang J, Li W, et al. A dominant autoinflammatory disease caused by non-cleavable variants of RIPK1. *Nature.* (2020) 577:109–14. doi: 10.1038/s41586-019-1830-y
12. Wang W, Zhou Y, Zhong LQ, Li Z, Jian S, Tang XY, et al. The clinical phenotype and genotype of NLRP12-autoinflammatory disease: a Chinese case series with literature review. *World J Pediatr.* (2019). doi: 10.1007/s12519-019-00294-8. [Epub ahead of print].
13. Ombrello MJ, Remmers EF, Sun G, Freeman AF, Datta S, Torabi-Parizi P, et al. Cold urticaria, immunodeficiency, and autoimmunity related to PLCG2 deletions. *N Engl J Med.* (2012) 366:330–8. doi: 10.1056/NEJMoa1102140
14. Fusco WG, Duncan JA. Novel aspects of the assembly and activation of inflammasomes with focus on the NLRC4 inflammasome. *Int Immunol.* (2018) 30:183–93. doi: 10.1093/intimm/dxy009
15. Romberg N, Vogel TP, Canna SW. NLRC4 inflammasomopathies. *Curr Opin Allergy Clin Immunol.* (2017) 17:398–404. doi: 10.1097/ACI.0000000000000396
16. Munoz MA, Jurczyluk J, Simon A, Hissaria P, Arts RJW, Coman D, et al. Defective protein prenylation in a spectrum of patients with mevalonate kinase deficiency. *Front Immunol.* (2019) 10:1900. doi: 10.3389/fimmu.2019.01900
17. Rose CD, Pans S, Casteels I, Anton J, Bader-Meunier B, Brissaud P, et al. Blau syndrome: cross-sectional data from a multicentre study of clinical, radiological and functional outcomes. *Rheumatology.* (2015) 54:1008–16. doi: 10.1093/rheumatology/keu437
18. Mcdermott MF, Aksentijevich I, Galon J, Mcdermott EM, Ogunkolade BW, Centola M, et al. Germline mutations in the extracellular domains of the 55 kDa TNF receptor, TNFR1, define a family of

dominantly inherited autoinflammatory syndromes. *Cell.* (1999) 97:133–44. doi: 10.1016/S0092-8674(00)80721-7
19. Rigante D, Lopalco G, Vitale A, Lucherini OM, De Clemente C, Caso F, et al. Key facts and hot spots on tumor necrosis factor receptor-associated periodic syndrome. *Clin Rheumatol.* (2014) 33:1197–207. doi: 10.1007/s10067-014-2722-z
20. Zhou Q, Yang D, Ombrello AK, Zavialov AV, Toro C, Zavialov AV, et al. Early-onset stroke and vasculopathy associated with mutations in ADA2. *N Engl J Med.* (2014) 370:911–20. doi: 10.1056/NEJMoa1307361
21. Carmona-Rivera C, Khaznadar SS, Shwin KW, Irizarry-Caro JA, O'neil LJ, Liu Y, et al. Deficiency of adenosine deaminase 2 triggers adenosine-mediated NETosis and TNF production in patients with DADA2. *Blood.* (2019) 134:395–406. doi: 10.1182/blood.2018892752
22. Klötgen HW, Beltraminelli H, Yawalkar N, Van Gijn ME, Holzinger D, Borradori L. The expanding spectrum of clinical phenotypes associated with PSTPIP1 mutations: from PAPA to PAMI syndrome and beyond. *Br J Dermatol.* (2018) 178:982–3. doi: 10.1111/bjd.16136
23. Holzinger D, Roth J. PAPA syndrome and the spectrum of PSTPIP1-associated inflammatory diseases. In: P Efthimiou, editor. *Auto-Inflammatory Syndromes: Pathophysiology, Diagnosis, and Management.* Cham: Springer International Publishing (2019). p. 39–59. doi: 10.1007/978-3-319-96929-9_4
24. Aeschlimann FA, Batu ED, Canna SW, Go E, Gul A, Hoffmann P, et al. A20 haploinsufficiency (HA20): clinical phenotypes and disease course of patients with a newly recognised NF-kB-mediated autoinflammatory disease. *Ann Rheum Dis.* (2018) 77:728–35. doi: 10.1136/annrheumdis-2017-212403
25. Zhou Q, Wang H, Schwartz DM, Stoffels M, Park YH, Zhang Y, et al. Loss-of-function mutations in TNFAIP3 leading to A20 haploinsufficiency cause an early-onset autoinflammatory disease. *Nat Genet.* (2016) 48:67–73. doi: 10.1038/ng.3459
26. Kadowaki T, Ohnishi H, Kawamoto N, Hori T, Nishimura K, Kobayashi C, et al. Haploinsufficiency of A20 causes autoinflammatory and autoimmune disorders. *J Allergy Clin Immunol.* (2018) 141:1485–8.e1411. doi: 10.1016/j.jaci.2017.10.039
27. Lorden G, Sanjuan-Garcia I, De Pablo N, Meana C, Alvarez-Miguel I, Perez-Garcia MT, et al. Lipin-2 regulates NLRP3 inflammasome by affecting P2X7 receptor activation. *J Exp Med.* (2017) 214:511–28. doi: 10.1084/jem.20161452
28. Zhao Y, Ferguson PJ. Chronic nonbacterial osteomyelitis and chronic recurrent multifocal osteomyelitis in children. *Pediatr Clin North Am.* (2018) 65:783–800. doi: 10.1016/j.pcl.2018.04.003
29. Álvarez-Errico D, Vento-Tormo R, Ballestar E. Genetic and epigenetic determinants in autoinflammatory diseases. *Front Immunol.* (2017) 8:318. doi: 10.3389/fimmu.2017.00318
30. Pathak S, Mcdermott MF, Savic S. Autoinflammatory diseases: update on classification diagnosis and management. *J Clin Pathol.* (2017) 70:1–8. doi: 10.1136/jclinpath-2016-203810

Conflict of Interest: The authors declare that the research was conducted in the absence of any commercial or financial relationships that could be construed as a potential conflict of interest.

frontiers in Immunology

ORIGINAL RESEARCH
published: 23 September 2020
doi: 10.3389/fimmu.2020.574992

Association of Clinical Phenotypes in Haploinsufficiency A20 (HA20) With Disrupted Domains of A20

*Yu Chen[1], Zhenghao Ye[1], Liping Chen[1], Tingting Qin[2], Ursula Seidler[3], De'an Tian[1] and Fang Xiao[1]**

[1] Department of Gastroenterology, Tongji Hospital of Tongji Medical College, Huazhong University of Science and Technology, Wuhan, China, [2] Department of Biliary–Pancreatic Surgery, Tongji Hospital, Tongji Medical College, Huazhong University of Science and Technology, Wuhan, China, [3] Department of Gastroenterology of Hannover Medical School, Hanover, Germany

Background: Haploinsufficiency A20 (HA20) is a newly described monogenic disease characterized by a wide spectrum of manifestations and caused by heterozygous mutations in *TNFAIP3* which encodes A20 protein. *TNFAIP3* mutation leads to disruption of the A20 ovarian tumor (OTU) domain and/or the zinc finger (ZnF) domain. This study aims at exploring the association between the various manifestations of HA20 and different domains disruption of A20.

Methods: We reviewed the HA20 cases in previous literature and summarized the clinical features, *TNFAIP3* mutation loci and the disrupted domains caused by different sites and patterns of mutations. Patients were classified into three groups according to the A20 domains disruption.

Results: A total of 89 patients from 39 families with a genetic diagnosis of HA20 were included. Overall, the age at onset of HA20 was early (median:5.92, IQR:1-10). Patients in the ZnF group showed the earliest onset (median:2.5, IQR:0.6-5), followed by patients in the OTU+ZnF group (median:6, IQR:1-10) and patients in the OTU group (median:10, IQR:8-14). The main manifestations of HA20 patients were recurrent oral ulcers (70%), recurrent fever (42%), gastrointestinal ulcers (40%), skin lesion (38%), genital ulcers (36%), and musculoskeletal disorders (34%). The percentage of patients with musculoskeletal disorders was significantly different among the three groups ($p = 0.005$). Patients in the OTU+ZnF group and ZnF group were more likely to develop musculoskeletal disorders than patients in the OTU group ($p = 0.002$ and $p = 0.035$, respectively). Besides, forty-three percent of HA20 patients were initially diagnosed as Behcet's disease (BD). Compared to the ZnF group, the OTU+ZnF group and OTU group had a higher percentage of patients initially diagnosed as BD ($p = 0.006$ and $p < 0.001$, respectively).

Conclusion: HA20 is characterized by early-onset and the most common symptoms of HA20 are recurrent oral ulcers, fever and gastrointestinal ulcers. The onset of HA20 in patients with the ZnF domain disruption is earlier than patients with the OTU domain disruption. Compared to the OTU domain, the ZnF domain may be more closely related to musculoskeletal disorders.

Keywords: haploinsufficiency A20, autoinflammatory disorders, monogenic disease, TNFAIP3, OTU domain, ZnF domain, clinical manifestation

OPEN ACCESS

Edited by:
Sarah Rowland-Jones, University of Oxford, United Kingdom

Reviewed by:
Anna Shcherbina, Dmitry Rogachev National Research Center of Pediatric Hematology, Oncology and Immunology, Russia
Jillian M. Richmond, University of Massachusetts Medical School, United States

***Correspondence:**
Fang Xiao
xiaofang@tjh.tjmu.edu.cn

Specialty section:
This article was submitted to Autoimmune and Autoinflammatory Disorders, a section of the journal Frontiers in Immunology

Received: *22 June 2020*
Accepted: *24 August 2020*
Published: *23 September 2020*

Citation:
Chen Y, Ye Z, Chen L, Qin T, Seidler U, Tian D and Xiao F (2020) Association of Clinical Phenotypes in Haploinsufficiency A20 (HA20) With Disrupted Domains of A20. Front. Immunol. 11:574992. doi: 10.3389/fimmu.2020.574992

INTRODUCTION

A20, a protein encoded by the tumor necrosis factor alpha-induced protein 3 gene (*TNFAIP3*), is a crucial negative regulator of inflammation (1, 2). It is well- known to inhibit NF-κB signaling and has recently been shown to restrict the interferon regulatory factor (IRF) pathway and autophagy (3). A20 consists of two distinct domains: an amino-terminal ovarian tumor (OTU) domain and a carboxy-terminal zinc finger (ZnF) domain (4). The ZnF domain contains K63-linked E3 ubiquitin ligase and polyubiquitin-binding ability, while the OTU domain carries deubiquitinating activity (1). Different *TNFAIP3* mutations may result in distinct A20 domain disruption and symptomatic manifestation depending on their type and location.

Haploinsufficiency A20 (HA20) is a monogenic disease caused by heterozygous *TNFAIP3* mutations and is characterized by inflammation in multiple organs (5). Since the first case was reported in 2016 (5), more attention has been paid to HA20 and an increased number of cases has been reported. The manifestations of patients with HA20 are complicated and show individual variation (6, 7). It is assumed that the diverse clinical manifestations of HA20 may result from the variable expressivity in the autosomal-dominant inheritance pattern, the interaction with other genes and environments influences (8). Previous mouse models indicate that disruption of different A20 domains may result in different clinical manifestations of HA20. For example, HA20 symptoms in mice with the disrupted ZnF domain ($A20^{ZnF7/ZnF7}$ mice, $A20^{ZnF4ZnF7/ZnF4ZnF7}$ mice) presented differently than mice with the disrupted OTU domain ($A20^{OTU/OTU}$ mice) (2, 9). However, it remains uncertain whether different forms of A20 domain disruption directly affect the variable manifestations of HA20 patients. Here, we analyze the relationship between A20 domain disruption and corresponding clinical characteristics of HA20 patients.

METHODS

Literature Search Strategy

We searched literature up to March 2020 that reported HA20 patients. The search was conducted using PubMed, Google scholar, and the Chinese database CNKI. The keywords "haploinsufficiency A20" AND "autoinflammation," or "*TNFAIP3* mutation" AND "autoinflammation" were used for the search. No language or publication date restrictions were applied to the search.

Inclusion and Exclusion Criteria

The inclusion criteria for eligible cases were that the HA20 patients should be reported with the *TNFAIP3* gene mutation by genetic analysis. Patients with additional gene mutations were excluded.

Data Collection

The following information was extracted from each eligible HA20 case: age of HA20 onset, gender, details of *TNFAIP3* gene mutation, initial diagnosis, clinical manifestations, treatment, and response to treatment. We found a total of 33 *TNFAIP3* mutations at various loci (5, 8, 10–12). These mutations could result in OTU and/or ZnF domain disruption and were identified as missense, nonsense or frameshift mutations. Patients were divided into three groups according to the disrupted domain caused by *TNFAIP3* mutation: (1) nonsense and frameshift mutations in the OTU coding region that impaired the function of both OTU and ZnF domains (OTU+ZnF group), (2) missense mutations in OTU coding region that disrupted the OTU domain only (OTU group), and (3) mutations in the ZnF coding region that disrupted the ZnF domain function (ZnF group). The age of onset for HA20 patients was defined as the age when the initial disease symptoms were reported. The term "patients responded to treatment" in our study refers to the reported improvement of symptoms after treatment. To analyze the correlation between specific *TNFAIP3* mutations and the severity of symptoms in HA20, we classified H20 symptoms severity into three categories based on the number of organs involved: (1) mild: <4 organs involved, (2) moderate: 4 to 6 organs involved, (3) severe: more than 6 organs involved.

Statistical Analysis

All statistical analyses were performed with SPSS 19 (IBM, New York, USA) software. The age of HA20 onset was processed as median values with interquartile ranges (IQR). Group differences in the age of onset were compared by the Kruskal-Wallis test. Chi-square tests were used to evaluate differences between two or three groups and Fisher's exact test was used when the theoretical frequency was <5. A two-sided $p < 0.05$ indicated statistical significance.

RESULTS

Classification of A20 Disruption According to *TNFAIP3* Gene Mutations

We initially collected a total of 93 cases according to the inclusion criteria and 4 patients were excluded from the study due to the presence of additional mutations. The remaining 89 patients from 39 families were reported with heterozygous loss-of-function mutations in *TNFAIP3* (**Table S1**) which showed evident familial aggregation. We identified 33 disease-causing variants and 32 of which were indicated in **Figure 1A**. A large deletion mutation of exons 2–3 of *TNFAIP3* located in the OTU coding region was not shown on the schematic diagram because no exact mutation locus was identified in the case report (13). We found 7 frameshift mutations and 11 nonsense mutations in the OTU coding region (OTU+ZnF group), 2 missense mutations in the OTU coding region (OTU group), 11 frameshift mutations, 1 nonsense, and 1 missense mutation in the ZnF coding region (ZnF group) (**Figure 1B**). There were 50 patients (56%) from 23 families in the OTU+ZnF group, 13 patients (15%) from 3 families in the OTU group and 26 patients (29%) from 3 families in the ZnF group, respectively (**Figure 1C**, **Table S1**).

Clinical Characteristics of Patients With HA20

We observed diverse clinical manifestations in the 89 HA20 patients evaluated for this study. Overall, the most common

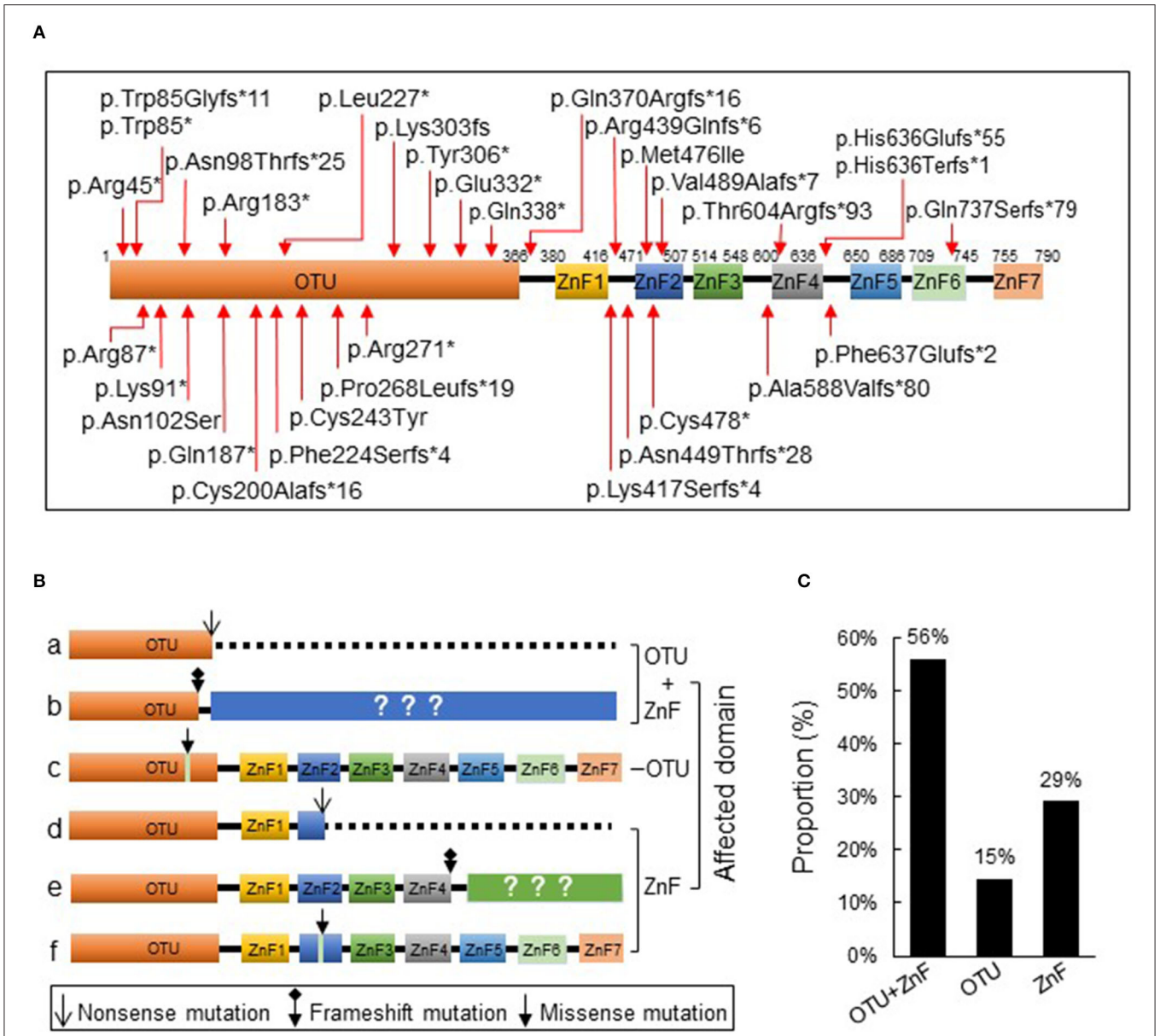

FIGURE 1 | Schematic diagram of A20 protein and its three types of disruption. **(A)** The protein A20 consists of an ovarian tumor (OTU) domain and seven zink-finger (ZnF) domains. The reported TNFAIP3 mutations from literature are indicated with arrow. **(B)** The reported TNAFIP3 mutations can result in three types of A20 disruption: disruption of both OTU and ZnF functional domains (a-b, OTU+ZnF), disruption of single functional domain OTU (c, OTU) or ZnF (d-f, ZnF). **(C)** The proportion of patients in each group. Patients were classified into the OTU+ZnF group, the OTU group and the ZnF group according to three types of A20 disruption.

symptom was oral ulcers (70%), followed by recurrent fever (42%), gastrointestinal ulcers (40%), skin lesions (38%), genital ulcers (36%), musculoskeletal disorders (34%), and autoimmune thyroid disorder (19%). Less than 10% of HA20 patients presented with ocular involvement (7%), vasculitis (6%), atrophic gastritis (3%), kidney injury (6%), liver injury (8%), recurrent respiratory tract infection (9%), interstitial lung disease (4%), or dental anomaly (4%) was. Additionally, while the majority of patients with interstitial lung disease were in the ZnF group, patients with specific symptoms were mainly distributed in the OTU+ZnF group (**Figure 2A**).

The initial diagnoses of HA20 patients in each of the three groups were shown in **Figure 2B**. Eighty percent (72/89) of patients were initially diagnosed with autoimmune diseases other than HA20. Forty-three percent of patients were initially diagnosed with Behcet's disease (BD), an autoimmune disease that cause vascular inflammation throughout the body, representing the largest proportion of initial diagnoses in HA20 patients. Twenty-six percent of HA20 patients met the diagnostic criteria of intestinal BD (iBD), with the hallmark features of BD and gastrointestinal ulcers (14). Other initial diagnoses of HA20 included juvenile idiopathic arthritis (JIA) (12%), periodic

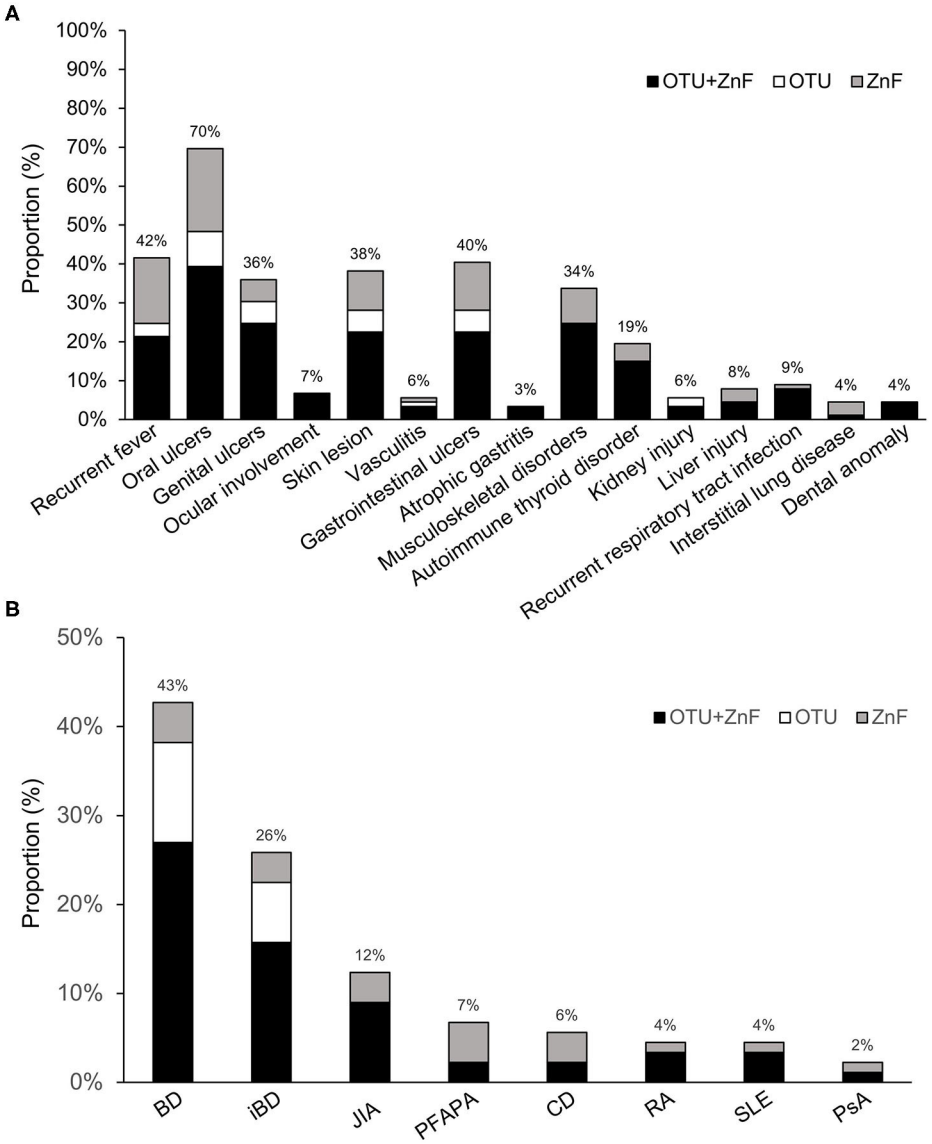

FIGURE 2 | Statistics of clinical manifestation in patients with HA20. **(A)** The percentage of various symptoms of HA20 in 89 patients. Patients were classified into the OTU+ZnF group, the OTU group and the ZnF group according to three types of A20 disruption. Except for interstitial lung disease, the patients with specific symptom of HA20 were mainly from OTU+ZnF group. **(B)** The proportion of initial diagnosis in HA20 and the distribution of each diagnosis in three groups.

fever with aphthous pharyngitis and adenitis (PFAPA) (7%), Crohn's disease (CD) (6%), rheumatoid arthritis (RA) (4%), systemic lupus erythematosus (SLE) (4%), and psoriatic arthritis (PsA) (2%). Patients who were initially diagnosed with BD, iBD, JIA, RA, or SLE were mainly a part of the OTU+ZnF group. No patients in the OTU group were initially diagnosed with JIA, PFAPA, CD, RA, SLE, PsA.

Comparison of Clinical Characteristics According to Types of A20 Disruption

Some symptoms of HA20 exhibited significantly different occurrences among the three groups. Patients with only the OTU domain or ZnF domain disruption did not present with ocular dysfunction, atrophic gastritis, or dental anomalies. Patients in the OTU group did not present with musculoskeletal disorders, autoimmune thyroid disorder, liver injury, recurrent respiratory tract infections, or interstitial lung disease. No patients in the ZnF group developed kidney injury.

The gender distributions were similar among patients in OTU+ZnF, OTU, and ZnF groups. The overall age of HA20 onset was early (median: 5.92, IQR:1–10), however there was a significant difference in age onset between the three groups ($p < 0.001$). Compared to patients in the OTU group (median onset age:10, IQR: 8–14), patients in the OTU+ZnF group (median onset age: 6, IQR: 1.165–7) and the ZnF group (median

TABLE 1 | Univariate analysis of clinical characteristics in patients with HA20 based on types of A20 disruption.

Clinical Feature	Total ($n = 89$)	OTU+ZnF ($n = 50$)	OTU ($n = 13$)	ZnF ($n = 26$)	χ2/ Fisher	*p* value
Age of onset(y) median (IQR)	5.92 (1–10)	6 (1.165-7)	10 (8–14)	2.5 (0.6-5)	18.269	<0.001
						<0.001[a]
						0.040[b]
						<0.001[c]
Gender					1.615	0.453
Male	40% (36/89)	38% (19/50)	31% (4/13)	50% (13/26)		
Female	60% (53/89)	62% (31/50)	69% (9/13)	50% (13/26)		
Manifestation						
Recurrent fever	42% (37/89)	38% (19/50)	23% (3/13)	58% (15/26)	4.707	0.096
Oral ulcers	70% (62/89)	70% (35/50)	62% (8/13)	73% (19/26)	0.552	0.759
Ocular involvement	7% (6/89)	12% (6/50)	0% (0/13)	0% (0/26)	3.810	0.109
Genital ulcers	36% (32/89)	44% (22/50)	38% (5/13)	19% (5/26)	4.600	0.100
Skin lesion	38% (34/89)	40% (20/50)	38% (5/13)	35% (9/26)	0.211	0.900
Gastrointestinal ulcers	40% (36/89)	40% (20/50)	38% (5/13)	42% (11/26)	0.063	0.969
Vasculitis	6% (5/89)	6% (3/50)	8% (1/13)	4% (1/26)	0.622	1
Atrophic gastritis	3% (3/89)	6% (3/50)	0% (0/13)	0% (0/26)	1.440	0.720
Musculoskeletal disorders	34% (30/89)	44% (22/50)	0% (0/13)	31% (8/26)	10.239	0.005
						0.002[a]
						0.327[b]
						0.035[c]
Autoimmune thyroid disorder	19% (17/89)	26% (13/50)	0% (0/13)	15% (4/26)	4.736	0.089
Kidney injury	6% (5/89)	6% (3/50)	15% (2/13)	0% (0/26)	3.555	0.118
Liver injury	8% (7/89)	8% (4/50)	0% (0/13)	12% (3/26)	1.213	0.559
Recurrent respiratory tract infection	9% (8/89)	14% (7/50)	0% (0/13)	4% (1/26)	2.691	0.233
Interstitial lung disease	4% (4/89)	2% (1/50)	0% (0/13)	12% (3/26)	3.240	0.173
Dental anomaly	4% (4/89)	8% (4/50)	0% (0/13)	0% (0/26)	2.097	0.354

[a]*Comparison of the clinical manifestations between OTU+ZnF and OTU groups.*
[b]*Comparison of the clinical manifestations between OTU+ZnF and ZnF groups.*
[c]*Comparison of the clinical manifestations between OTU and ZnF groups.*

onset age: 2.5, IQR: 0.6–5) showed earlier onset (all, $p < 0.001$). Patients in the ZnF group showed earlier onset of HA20 than patients in the OTU+ZnF group ($p = 0.040$) (**Table 1**). We further analyzed the specific loci of *TNFAIP3* mutations in these patients to identify which mutations may confer the earliest HA20 onset. We found that patients with the p.Leu227* mutation in the OTU+ZnF group appeared to confer the earliest onset of HA20 (median onset age:0.83, IQR: 0–1.25) (**Figure S1**).

The incidence of musculoskeletal disorders in HA20 patients was significantly different among the three patient groups ($p = 0.005$). No patients in the OTU group developed musculoskeletal disorders (0%). However, patients in the OTU+ZnF (44%) and ZnF groups (31%) were more likely to develop musculoskeletal disorders ($p = 0.002$ and $p = 0.035$, respectively), with no significant difference between the two groups ($p = 0.327$) (**Table 1**). Next, we explored which *TNFAIP3* mutation loci correlated with more severe symptoms (**Table S2**). We found that patients with the p.Phe224Serfs*4 mutation were more likely to show severe symptoms (**Table S2**). Patients with the p.Leu227* or p.Gln370Argfs*16 mutations were more likely to show moderate to severe symptoms (**Table S2**).

Most patients experienced improved symptoms after immunomodulatory treatment. Twenty-two patients were treated with biological agents, 19 of which responded well to the therapy (response rate: 86%). The response rates of glucocorticoid treatments, disease-modifying antirheumatic drugs, and colchicine were 71, 70, and 45%, respectively (**Table S2**). Two patients improved after autologous hematopoietic stem cell transplantation. However, treatment response in HA20 patients were variable. The response rate of colchicine was significantly different among the three patient groups ($p = 0.009$). Patients in the OTU+ZnF group were more likely to respond to colchicine treatment compared with patients in the OTU group ($p = 0.005$). The response rate of other treatments was comparable across the three groups (**Table 3**).

Comparison of Initial Diagnosis in HA20 Patients According to Types of A20 Disruption

The percentage of HA20 patients who were initially diagnosed with BD was significantly different among patients in the three

TABLE 2 | Univariate analysis of initial diagnosis in HA20 patients based on types of A20 disruption.

Initial diagnosis of HA20	Total ($n = 89$)	OTU+ZnF ($n = 50$)	OTU ($n = 13$)	ZnF ($n = 26$)	Fisher	*P*-value
BD	43% (38/89)	48% (24/50)	77% (10/13)	15% (4/26)	15.044	0.001
						0.116[a]
						0.006[b]
						<0.001[c]
iBD	26% (23/89)	28% (14/50)	46% (6/13)	12% (3/26)	5.654	0.068
JIA	12% (11/89)	16% (8/50)	0% (0/13)	12% (3/26)	2.052	0.362
PFAPA	7% (6/89)	4% (2/50)	0% (0/13)	15% (4/26)	3.526	0.172
CD	6% (5/89)	4% (2/50)	0% (0/13)	12% (3/26)	2.087	0.418
RA	4% (4/89)	6% (3/50)	0% (0/13)	4% (1/26)	0.508	1.000
SLE	4% (4/89)	6% (3/50)	0% (0/13)	4% (1/26)	0.508	1.000
PsA	2% (2/89)	2% (1/50)	0% (0/13)	4% (1/26)	0.920	1.000

[a]*Comparison of the initial diagnosis between OTU+ZnF and OTU groups;* [b]*Comparison of the initial diagnosis between OTU+ZnF and ZnF groups;* [c]*Comparison of the initial diagnosis between OTU and ZnF groups. BD, Behcet's disease; iBD, intestinal Behcet's disease; JIA, juvenile idiopathic arthritis; PFAPA, periodic fever with aphthous pharyngitis and adenitis; CD, Crohn's disease; RA, rheumatoid arthritis; SLE, systemic lupus erythematosus; PsA, psoriatic arthritis.*

TABLE 3 | Univariate analysis of treatment response of patients with HA20 based on types of A20 disruption.

Treatments	Total	OTU+ZnF	OTU	ZnF	$\chi 2$/ Fisher	*P* value
Biological agents	86%(19/22)	94%(15/16)	(0/0)	67%(4/6)	-	0.169
Glucocorticoid	71%(20/28)	69(11/16)	100%(4/4)	63%(5/8)	1.681	0.532
DMARDs	70%(14/20)	67%(10/15)	100%(1/1)	75%(3/4)	0.690	1.000
Immuno-suppressants	65%(11/17)	75%(9/12)	0%(0/1)	50%(2/4)	2.716	0.344
Colchicine	45%(13/29)	67%(10/15)	0%(0/7)	43%(3/7)	8.826	0.009
						0.005[a]
						0.376[b]
						0.192[c]

[a]*Comparison of the treatment response between OTU+ZnF and OTU groups;* [b]*Comparison of the treatment response between OTU+ZnF and ZnF groups;* [c]*Comparison of the treatment response between OTU and ZnF groups. DMARDs, disease-modifying antirheumatic drugs.*

groups ($p = 0.001$). The proportion of patients initially diagnosed with BD in the OTU+ZnF (48%) and OTU (77%) groups was significantly higher than the ZnF group (15%) ($p = 0.006$ and $p < 0.001$, respectively), with no significant difference between the OTU+ZnF and the OTU groups ($p = 0.116$). We observed no significant difference in initial diagnosis of iBD, JIA, PFAPA, CD, RA, SLE, or PsA between the three patient groups (**Table 2**).

DISCUSSION

HA20 is an autosomal-dominant-inherited disease characterized by systemic inflammation in multiple organs with a wide spectrum of manifestations (3). The specific mechanisms of this individual clinical variation in HA20 patients remain poorly understood. Here, we summarize the clinical characteristics of HA20 and highlight that distinct domain disruption of A20 influences the variation in HA20 symptoms and onset among patients.

Early HA20 recognition and diagnosis remain challenging due to its diverse clinical manifestations. The 89 cases of HA20 we evaluated featured a wide variety of symptoms including recurrent fever, oral ulcers, genital ulcers, ocular disorders, skin lesion, vasculitis, gastrointestinal ulcers, atrophic gastritis, musculoskeletal disorders, autoimmune thyroid disorder, kidney injury, liver injury, recurrent respiratory tract infection, interstitial lung disease, and dental anomalies. Based on these symptoms, some patients were initially diagnosed with autoimmune diseases other than HA20, such as BD or JIA. Consistent with previous reports (6, 7), we found that the hallmark features of BD, including oral ulcers, genital ulcers, gastrointestinal ulcers, and skin lesions were also frequent in HA20 patients. Therefore, patients with these symptoms were more likely to be initially diagnosed as BD (43%) than other autoimmune diseases (2–12%). Most HA20 patients exhibited early-onset of symptoms (median: 5.92, IQR: 1–10), which may aid proper diagnosis of HA20 over other autoimmune diseases and promote early HA20 diagnosis.

Our study suggests that mutations in different domains of the A20 protein might influence a variety of specific HA20-related manifestations in a domain-dependent manner. We divided the 89 HA20 patients into an OTU+ZnF group (50/89), an OTU group (13/89), and a ZnF group (26/89) according to the particular A20 domains that was disrupted. Notably, patients with the disrupted ZnF domain in either the OTU+ZnF or ZnF group presented symptoms earlier than patients with only the disrupted OTU domain. The early median overall onset of HA20 suggests that both the OTU and ZnF domains may impact the early onset of HA20. The earlier median age of onset in patients with the disrupted ZnF domain implies that the ZnF domain might play a more vital role in the early HA20 onset. Recent evidence suggests that the A20 protein restricts inflammation through E3 ligase activity and the ubiquitin-binding activity of the ZnF domain (9, 15). Prior studies found that $A20^{ZnF7/ZnF7}$ mice presented arthritis or physical retardation by 9 weeks in age, and $A20^{ZnF4ZnF7/ZnF4ZnF7}$ mice developed inflammation in multiple organs within 3 weeks of birth (2, 9, 15). Comparatively, $A20^{OTU/OTU}$ mice gradually developed splenomegaly at 6 months of age with increased myeloid cells (16, 17). These findings indicated that mice with the disrupted ZnF domain ($A20^{ZnF7/ZnF7}$ mice, $A20^{ZnF4ZnF7/ZnF4ZnF7}$ mice) developed severe pathological signs earlier than mice with the disrupted OTU domain ($A20^{OTU/OTU}$ mice). The earlier age of onset in mice with the disrupted ZnF domain supported the implication that the ZnF domain might be more relevant to the early onset of HA20.

Here, we show that patients with disrupted OTU plus ZnF domains or just the ZnF domain were more likely to develop musculoskeletal disorders than patients with only the disrupted OTU domain. Additionally, the incidence of musculoskeletal disorders was not significantly different between the OTU+ZnF group and the ZnF group. These results suggest that the ZnF domain may play an important role in the pathogenesis of musculoskeletal disorders in HA20 patients. Further, mice with the dysfunctional ZnF domain showed spontaneous arthritis with increased Th17 cells and higher production of proinflammatory cytokines than control mice (15). The ZnF domain was also reported to prevent inflammasome-dependent arthritis by inhibiting macrophage necroptosis through its ubiquitin-binding domain (2). We propose that the ZnF domain of A20 might influence musculoskeletal disorders more than the OTU domain in H20.

In our study, patients in the OTU+ZnF and OTU groups were more likely to be initially diagnosed with BD compared to patients in the ZnF group. One potential explanation for this is that they were more likely to present BD-like symptoms, including recurrent oral ulcers, genital ulcers, gastrointestinal ulcers, skin lesions, and ocular lesions (18).

There were several limitations in our study. Since HA20 is a newly identified rare monogenetic disease, the study was limited by the sample size. Additionally, patients with disruption of ZnF (1–7) domains should be further classified into subgroups to increase understanding of ZnF's mechanistic role in HA20. Finally, the recall bias of the patient's history may have influenced the analysis of HA20 patients' manifestations.

In conclusion, our findings suggest that inflammatory lesions of HA20 generally start in early childhood and the most common symptoms are recurrent oral ulcers, fever, and gastrointestinal ulcers. Compared to patients with disruption in the OTU domain, patients with the ZnF domain disruption tend to show earlier onset of HA20 with a higher risk of musculoskeletal disorders. Further work should explore the specific molecular mechanisms of these different A20 domains that affect the manifestations of HA20.

DATA AVAILABILITY STATEMENT

The raw data supporting the conclusions of this article will be made available by the authors, without undue reservation.

AUTHOR CONTRIBUTIONS

FX and YC: study concept and design, acquisition, analysis and interpretation of data, and drafting of the manuscript. ZY, LC, and TQ: collection, analysis and interpretation of data. US and DT: critical review of the manuscript. All authors contributed to the article and approved the submitted version.

FUNDING

This work was supported by grants from the National Natural Science Foundation of China (81470807 to FX, 81873556 to FX) and the Tongji Hospital Clinical Research Flagship Program (2019CR209 to DT).

SUPPLEMENTARY MATERIAL

The Supplementary Material for this article can be found online at: https://www.frontiersin.org/articles/10.3389/fimmu.2020.574992/full#supplementary-material

REFERENCES

1. Martens A, van Loo G. A20 at the crossroads of cell death, inflammation, and autoimmunity. *Cold Spring Harb Perspect Biol.* (2020) 12:a036418. doi: 10.1101/cshperspect.a036418
2. Polykratis A, Martens A, Eren RO, Shirasaki Y, Yamagishi M, Yamaguchi Y, et al. A20 prevents inflammasome-dependent arthritis by inhibiting macrophage necroptosis through its ZnF7 ubiquitin-binding domain. *Nat Cell Biol.* (2019) 21:731–42. doi: 10.1038/s41556-019-0324-3
3. Catrysse L, Vereecke L, Beyaert R, van Loo G. A20 in inflammation and autoimmunity. *Trends Immunol.* (2014) 35:22–31. doi: 10.1016/j.it.2013.10.005
4. Wertz IE, O'Rourke KM, Zhou H, Eby M, Aravind L, Seshagiri S, et al. De-ubiquitination and ubiquitin ligase domains of A20 downregulate NF-kappaB signalling. *Nature.* (2004) 430:694–9. doi: 10.1038/nature02794

5. Zhou Q, Wang H, Schwartz DM, Stoffels M, Park YH, Zhang Y, et al. Loss-of-function mutations in TNFAIP3 leading to A20 haploinsufficiency cause an early-onset autoinflammatory disease. *Nat Genet.* (2016) 48:67–73. doi: 10.1038/ng.3459
6. Berteau F, Rouviere B, Delluc A, Nau A, Le Berre R, Sarrabay G, et al. Autosomic dominant familial Behcet disease and haploinsufficiency A20: a review of the literature. *Autoimmun Rev.* (2018) 17:809–15. doi: 10.1016/j.autrev.2018.02.012
7. Aeschlimann FA, Batu ED, Canna SW, Go E, Gul A, Hoffmann P, et al. A20 haploinsufficiency (HA20): clinical phenotypes and disease course of patients with a newly recognised NF-kB-mediated autoinflammatory disease. *Ann Rheum Dis.* (2018) 77:728–35. doi: 10.1136/annrheumdis-2017-212403
8. Kadowaki T, Ohnishi H, Kawamoto N, Hori T, Nishimura K, Kobayashi C, et al. Haploinsufficiency of A20 causes autoinflammatory autoimmune disorders. *J Allergy Clin Immunol.* (2018) 141:1485–8 e11. doi: 10.1016/j.jaci.2017.10.039
9. Razani B, Whang MI, Kim FS, Nakamura MC, Sun X, Advincula R, et al. Non-catalytic ubiquitin binding by A20 prevents psoriatic arthritis-like disease and inflammation. *Nat Immunol.* (2020) 21:422–33. doi: 10.1038/s41590-020-0634-4
10. Shigemura T, Kaneko N, Kobayashi N, Kobayashi K, Takeuchi Y, Nakano N, et al. Novel heterozygous C243Y A20/TNFAIP3 gene mutation is responsible for chronic inflammation in autosomal-dominant Behcet's disease. *RMD Open.* (2016) 2:e000223. doi: 10.1136/rmdopen-2015-000223
11. Ohnishi H, Kawamoto N, Seishima M, Ohara O, Fukao T. A Japanese family case with juvenile onset Behcet's disease caused by TNFAIP3 mutation. *Allergol Int.* (2017) 66:146–8. doi: 10.1016/j.alit.2016.06.006
12. Chen Y, Huang H, He Y, Chen M, Seidler U, Tian D, et al. A20 haploinsufficiency in a chinese patient with intestinal behcet's disease-like symptoms: a case report. *Front Immunol.* (2020) 11:1414. doi: 10.3389/fimmu.2020.01414
13. Shimizu M, Matsubayashi T, Ohnishi H, Nakama M, Izawa K, Honda Y, et al. Haploinsufficiency of A20 with a novel mutation of deletion of exons 2-3 of TNFAIP3. *Mod. Rheumatol.* (2020) 2020:1–5. doi: 10.1080/14397595.2020.1719595
14. Lee HJ, Cheon JH. Optimal diagnosis and disease activity monitoring of intestinal Behcet's disease. *Intest Res.* (2017) 15:311–7. doi: 10.5217/ir.2017.15.3.311
15. Martens A, Priem D, Hoste E, Vetters J, Rennen S, Catrysse L, et al. Two distinct ubiquitin-binding motifs in A20 mediate its anti-inflammatory and cell-protective activities. *Nat. Immunol.* (2020) 21:381–7. doi: 10.1038/s41590-020-0621-9
16. Lu TT, Onizawa M, Hammer GE, Turer EE, Yin Q, Damko E, et al. Dimerization and ubiquitin mediated recruitment of A20, a complex deubiquitinating enzyme. *Immunity.* (2013) 38:896–905. doi: 10.1016/j.immuni.2013.03.008
17. Wertz IE, Newton K, Seshasayee D, Kusam S, Lam C, Zhang J, et al. Phosphorylation and linear ubiquitin direct A20 inhibition of inflammation. *Nature.* (2015) 528:370–5. doi: 10.1038/nature16165
18. International Team for the Revision of the International Criteria for Behcet's D. The International Criteria for Behcet's Disease (ICBD): a collaborative study of 27 countries on the sensitivity specificity of the new criteria. *J Eur Acad Dermatol Venereol.* (2014) 28:338–47. doi: 10.1111/jdv.12107

Conflict of Interest: The authors declare that the research was conducted in the absence of any commercial or financial relationships that could be construed as a potential conflict of interest.

frontiers in Immunology

ORIGINAL RESEARCH
published: 25 September 2020
doi: 10.3389/fimmu.2020.570661

Inducible Bronchus–Associated Lymphoid Tissue (iBALT) Attenuates Pulmonary Pathology in a Mouse Model of Allergic Airway Disease

*Ji Young Hwang[1,2], Aaron Silva-Sanchez[1], Damian M. Carragher[3], Maria de la Luz Garcia-Hernandez[4], Javier Rangel–Moreno[4] and Troy D. Randall[1]**

[1] Division of Clinical Immunology and Rheumatology, The Department of Medicine, University of Alabama at Birmingham, Birmingham, AL, United States, [2] Department of Microbiology and Immunology, University of Rochester, Rochester, NY, United States, [3] The Trudeau Institute, Saranac Lake, NY, United States, [4] Division of Allergy Immunology and Rheumatology, The Department of Medicine, University of Rochester, Rochester, NY, United States

Inducible Bronchus Associated Lymphoid Tissue (iBALT) is an ectopic lymphoid tissue associated with severe forms of chronic lung diseases, including chronic obstructive pulmonary disease, rheumatoid lung disease, hypersensitivity pneumonitis and asthma, suggesting that iBALT may exacerbate these clinical conditions. However, despite the link between pulmonary pathology and iBALT formation, the role of iBALT in pathogenesis remains unknown. Here we tested whether the presence of iBALT in the lung prior to sensitization and challenge with a pulmonary allergen altered the biological outcome of disease. We found that the presence of iBALT did not exacerbate Th2 responses to pulmonary sensitization with ovalbumin. Instead, we found that mice with iBALT exhibited delayed Th2 accumulation in the lung, reduced eosinophil recruitment, reduced goblet cell hyperplasia and reduced mucus production. The presence of iBALT did not alter Th2 priming, but instead delayed the accumulation of Th2 cells in the lung following challenge and altered the spatial distribution of T cells in the lung. These results suggest that the formation of iBALT and sequestration of effector T cells in the context of chronic pulmonary inflammation may be a mechanism by which the immune system attenuates pulmonary inflammation and prevents excessive pathology.

Keywords: inducible bronchus associated lymphoid tissue, asthma, pulmonary inflammation, ectopic lymphoid tissue, pulmonary allergy

OPEN ACCESS

Edited by:
Michael Zemlin, Saarland University Hospital, Germany

Reviewed by:
Deepika Sharma, University of Chicago, United States
Avery August, Cornell University, United States

***Correspondence:**
Troy D. Randall
randallt@uab.edu

Specialty section:
This article was submitted to Autoimmune and Autoinflammatory Disorders, a section of the journal Frontiers in Immunology

Received: *08 June 2020*
Accepted: *24 August 2020*
Published: *25 September 2020*

Citation:
Hwang JY, Silva-Sanchez A, Carragher DM, Garcia-Hernandez MdlL, Rangel–Moreno J and Randall TD (2020) Inducible Bronchus–Associated Lymphoid Tissue (iBALT) Attenuates Pulmonary Pathology in a Mouse Model of Allergic Airway Disease. Front. Immunol. 11:570661. doi: 10.3389/fimmu.2020.570661

INTRODUCTION

Inducible Bronchus Associated Lymphoid Tissue (iBALT) is an ectopic lymphoid tissue that forms in the lung following inflammation or infection (1, 2). Large B cell follicles that often contain germinal centers (GCs) and a dense network of follicular dendritic cells (FDCs) are the most prominent features of iBALT (3). Unlike conventional lymph nodes, iBALT is not encapsulated, but is instead embedded in the lung tissue, most often along large bronchi or filling the peri-vascular space of pulmonary artieries (4, 5). Despite being in a mucosal tissue, iBALT often lacks a well-defined M cell-containing dome epithelium (6) and its high endothelial venules (HEVs) express peripheral lymph node addressin (PNAd) (7) rather than mucosal addressin cell adhesion molecule

(MAdCAM). Thus, although iBALT clearly participates in pulmonary mucosal immune responses, it lacks some of the features often associated with classic mucosal lymphoid organs.

Unlike conventional lymphoid organs, which develop independently of antigen during embryogenesis (8, 9), iBALT forms following pulmonary infection or inflammation (10, 11). Although iBALT may develop at any time after birth given the proper pulmonary insult, it most easily forms in neonatal mice due to the relative paucity of Tregs and the relative abundance of IL-17-producing γδT cells (12–14). Similarly, infant humans also seem to develop (or maintain) iBALT more easily than adults, as the frequency of iBALT areas in the lungs of healthy subjects progressively declines with age (15, 16). Interestingly, the neonatal period is the same developmental window when microbial exposure, or lack thereof, imprints the immune system to be more or less susceptible to developing atopic responses to foreign antigens (17, 18) or developing autoreactive responses to self antgens—the so—called hygiene effect.

Given that it functions as a lymphoid tissue (19), it is not too surprising that iBALT plays an important role in immunity to pulmonary infections. For example, mice lacking conventional lymphoid organs develop iBALT following infection with influenza and are able to resist doses of virus that would normally be lethal to mice lacking iBALT (19). Conversely, mice lacking the chemokines that promote iBALT formation succumb to much lower doses of influenza virus (7). Those same chemokines are essential for the proper formation of pulmonary granulomas, the recruitment of antigen-specific T cells to the lung and the development of protective immunity to *Mycobacterium tuberculosis* (20, 21). Moreover, the pulmonary administration of inflammatory agents that trigger iBALT formation also leads to enhanced resistance to influenza, SARS corona virus, pneumovirus, *Francicella tulerensis* and *Coxiella burnetti* (12, 19, 22–24). Thus, the presence of iBALT is clearly beneficial in the context of pulmonary infections.

In contrast, iBALT is a feature of pulmonary pathology that is associated with a variety of chronic lung diseases, including chronic obstructive pulmonary disease (COPD) (25, 26), rheumatoid lung disease (3), hypersensitivity pneumonitis (27), and asthma (28, 29), suggesting that iBALT may exacerbate these clinical conditions. For example, COPD patients make autoantibodies that react with pulmonary antigens (30) and patients with advanced disease have reactive iBALT areas with well-developed GCs that show evidence of antigen-driven selection (31). Similarly, patients with rheumatoid lung disease develop large GC-containing areas of iBALT that are surrounded by plasma cells that produce autoantibodies (3). Thus, many investigators have concluded that the presence of iBALT contributes to pathology in the context of chronic inflammatory diseases. However, it is not clear whether iBALT is a cause or consequence of pulmonary inflammation or whether it contributes in any way to pulmonary pathology (32).

Given the link between iBALT and pulmonary pathology, we tested whether pre-existing iBALT would affect acute allergic responses to a pulmonary allergen. Surprisingly, we found that the presence of iBALT did not exacerbate allergic responses to repeated pulmonary sensitization with ovalbumin (OVA). Instead, mice with iBALT had reduced Th2-associated mRNA expression, less eosinophil recruitment to the lungs and airways, attenuated goblet cell hyperplasia and reduced mucus production following pulmonary sensitization and challenge with OVA. Interestingly, the presence of iBALT did not alter the initial priming of Th2 cells, but instead delayed their recruitment to the lung and altered their spatial distribution following challenge—Th2 cells were preferentially sequestered in iBALT, which reduced the numbers of Th2 cells in the lung parenchyma. These results suggest that the formation of iBALT and sequestration of effector T cells in the context of pulmonary inflammation may be a mechanism by which the immune system attenuates pulmonary inflammation and prevents excessive pathology.

RESULTS

The Presence of iBALT Prior to Sensitization Ameliorates Allergen–Induced Pathology

To test the role of iBALT in a mouse model of allergic lung inflammation, we intranasally administered 10 μg LPS 5 times over the course of 10 days starting on day 2 after birth and analyzed the lungs by histology on day 70 (**Figure 1A**). As expected (14), we observed iBALT structures with separated B and T cell zones and distinct FDC networks in the LPS-treated lungs, but not in the control lungs (**Figure 1B**). We also quantified the number of GC B cells by flow cytometry and found that GC B cells were present in LPS-treated lungs, but not in control lungs (**Figures 1C,D**). Given that GCs only form in organized lymphoid tissues, we conclude that pulmonary exposure of neonates to LPS promotes the formation of functional iBALT areas.

To test the effect of iBALT on the immune response to a pulmonary allergen, we administered LPS (or PBS) to neonatal mice as described above, allowed the mice to rest until they were 7 weeks old, then intranasally sensitized the iBALT and control groups with 100 μg OVA in combination with low dose (0.1 μg) LPS on days 49, 50, and 51 and challenged them on days 63, 64, 67, and 68 with 25 μg OVA (**Figure 1E**). We first examined the GC B cell response in the lungs of sensitized and challenged mice and found that GC B cells were abundant in the lungs of mice with iBALT, but were rare in control mice and almost undetectable in completely naïve mice (**Figures 1F,G**). We also examined the inflammatory response in the lung and airways by cytospin and found that the proportion (**Figures 1H,I**) and number (**Figures 1J,K**) of eosinophils were elevated in mice that had been sensitized and challenged with OVA compared to those in naïve mice, however, the proportion (**Figures 1H,I**) and number (**Figures 1J,K**) of eosinophils in mice with iBALT were reduced compared to those in control mice. Reductions in eosinophils were observed in both the lungs (**Figures 1H,J**) and the airways (**Figures 1I,K**) of mice with iBALT compared to those in control mice. The proportions of macrophage/monocytes, lymphocytes, and neutrophils are also shown in **Figure 1H** and the numbers of those cells are shown in **Supplementary Figure 1**. We also found that total

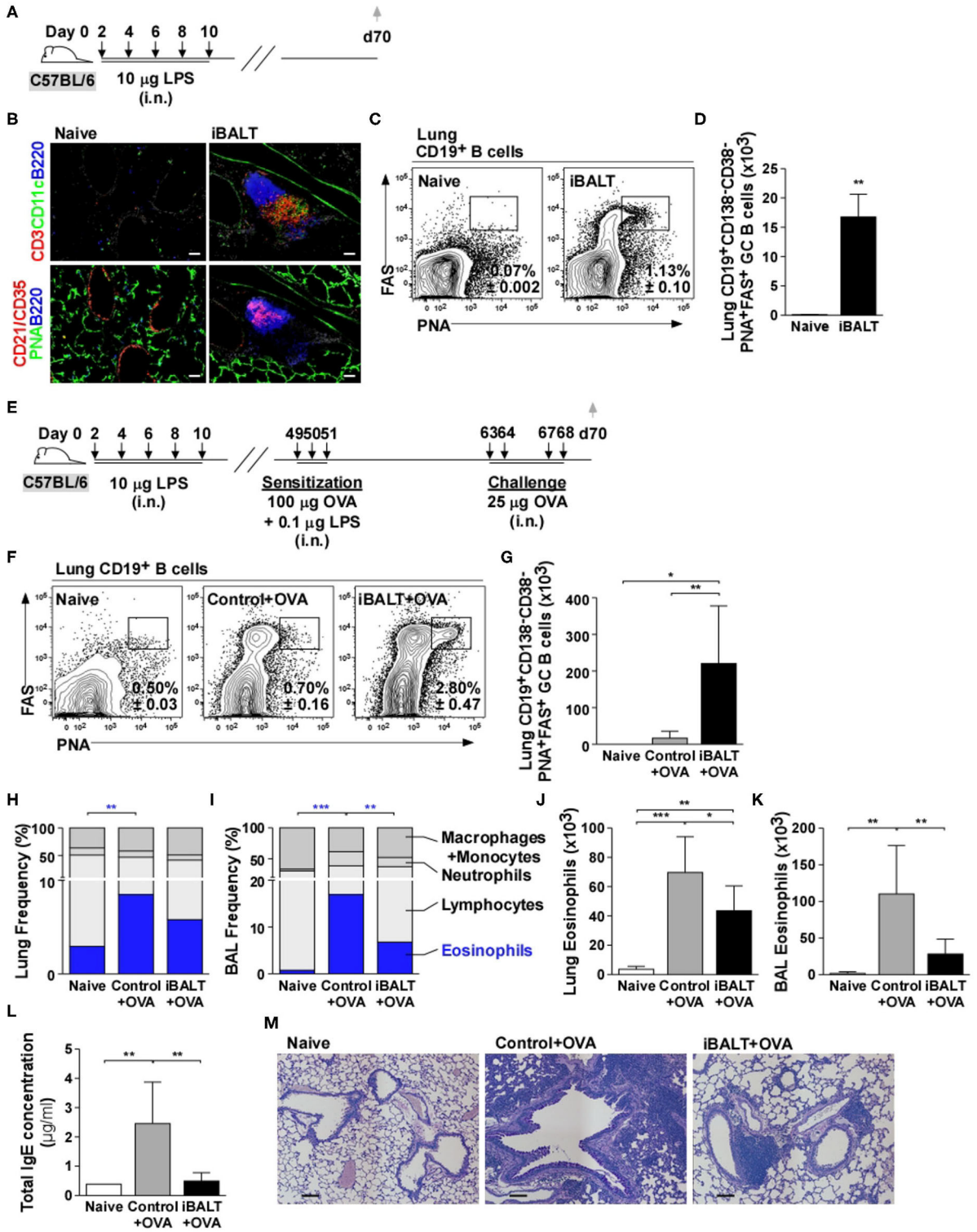

FIGURE 1 | The presence of iBALT reduces OVA–induced eosinophilia and pulmonary pathology. **(A)** Timing of iBALT induction and analysis. **(B)** We probed cryosections of lungs with antibodies against CD3, CD11c, B220, CD21/35 and PNA (scale bar = 100 μm). **(C,D)** The frequencies **(C)** and numbers **(D)** of $CD19^+CD138^-CD38^-PNA^+FAS^+$ GC B cells in the lung were determined by flow cytometry. **(E)** Timing of iBALT induction, allergic sensitization and antigen challenge and analysis. **(F,G)** The frequencies **(F)** and numbers **(G)** of $CD19^+CD138^-CD38^-PNA^+FAS^+$ GC B cells were determined by flow cytometry. **(H–K)** Differential cell counts were determined by cytospin and the proportion of eosinophils in the lung and BAL are shown as frequencies **(H,I)** and numbers **(J,K)**. **(L)** Total serum IgE concentration was measured by ELISA. **(M)** PAS staining of paraffin–embedded lung sections (scale bar = 100 μm). All data show mean ± SD of 4–5 mice per group; $^*P < 0.05$, $^{**}P < 0.01$, $^{***}P < 0.001$. Experiments were performed 5 times **(A–D)** or 4 times **(E–M)**.

serum IgE concentration was elevated in control mice, but less IgE was detected in mice with iBALT (**Figure 1L**). Upon a histological examination of lung sections, we found that OVA-exposed mice with pre-existing iBALT had densely-packed areas of lymphocytes to one side of the bronchi, but relatively clear airspaces, whereas OVA-exposed control mice had extensive areas of diffuse inflammation that surrounded the bronchi and extended into the alveolar airspaces (**Figure 1M**). Thus, contrary to our expectations, the presence of iBALT did not exacerbate OVA-induced pulmonary inflammation, but rather reduced the inflammatory response.

Th2 Cells Are Generated in Mice With and Without iBALT

The presence of iBALT could have altered T cell priming so that fewer Th2 cells were initially generated after antigen exposure. To test this possibility, we next used IL-4 reporter (4get) mice to enumerate Th2 cells. The 4get mice have the enhanced green fluorescent protein (EGFP) targeted into the IL-4 locus with an internal ribosome entry site (IRES) separating the IL-4 coding sequence from the EGFP coding sequence (33). Thus, any cells that express IL-4 mRNA will also express EGFP and can be easily identified using flow cytometry (34). Therefore, we treated neonatal 4get mice with LPS to initiate iBALT formation, waited until they were adults and then intranasally sensitized iBALT and control mice with 100 μg OVA and 0.1 μg LPS on days 49, 50, and 51 (**Figure 2A**). Two days after the last sensitization, we enumerated IL-4 reporter (EGFP)-expressing $CD4^+$ T cells. We found a significant expansion of $EGFP^+CD4^+$ T cells in both iBALT and control mice relative to naïve mice, but did not observe any difference in the frequencies (**Figure 2B**) or numbers (**Figure 2C**) of $EGFP^+CD4^+$ T cells between control and iBALT groups. These data suggested that iBALT did not dramatically affect Th2 priming in the lung.

Although the previous assay evaluated Th2 priming, we had no way of enumerating antigen-specific cells. Therefore, to test this possibility in another way, we transferred 1 x 10^6 naïve OVA-specific $CD4^+$ T cells (OT-II cells) into control and iBALT mice on day 48 after birth, sensitized the recipient mice with OVA on days 49, 50, and 51, challenged them on days 63, 64, 67, and 68 and enumerated the responding cells 2 days later in the lung (**Figure 2D**). We found that the frequency (**Figure 2E**) and number (**Figure 2F**) of OT-II cells that accumulated in the lungs of sensitized and challenged mice were the same in control and iBALT groups. These data suggest that the presence of iBALT does not affect OVA-specific T cell accumulation in the lung after sensitization and challenge.

Although Th2 priming and expansion appeared normal in mice with iBALT, it was not clear whether the final effector cells could actually make Th2 cytokines. Therefore, to determine whether CD4 T cells primed by OVA sensitization and challenge could actually produce Th2 cytokines, we sensitized and challenged mice with and without pre-existing iBALT and measured the mRNA expression of Th2 cytokines in the lungs 48 h after the last OVA challenge (**Figure 3A**). We found that mRNAs encoding IL-4, IL-5, and IL-13 were increased in OVA-exposed and challenged lungs relative to their expression in naïve lungs, but we did not observe a significant difference between the control and iBALT groups (**Figure 3B**).

We next tested whether $CD4^+$ T cells from OVA sensitized and challenged control and iBALT mice were equally capable of making Th2 cytokines. To test this possibility, we collected cells from the lung tissue, restimulated them with PMA and calcimycin for 4 h and assessed the production of IL-4, IL-5, and IL-13 by intracellular staining. We found that the total number of activated $CD44^{hi}CD4^+$ T cells was increased in control and iBALT mice relative to that in naïve mice (**Figures 3C,D**), but there was little difference between the control and iBALT groups. We also found that the numbers of $CD44^{hi}CD4^+$ T cells that made IL-4, IL-5, or IL-13 were increased in control and iBALT mice relative to those in naïve mice (**Figure 3E**), but there was little difference between the control and iBALT groups. These data suggest that the presence of iBALT does not significantly alter the number of T cells capable of producing Th2 cytokines following sensitization and challenge.

Th2 cytokines act on other cells in the lung, such as epithelial cells and macrophages, and promote their activation and differentiation, which changes gene expression. For example, genes like chitinase-3-like-4 (Chi3l4) and mucin 5ac (Muc5ac) are expressed in in the lung following IL-13 signaling (35). Thus, we next examined the expression of mRNAs encoding these genes in the lungs of iBALT and control mice after OVA sensitization and challenge as in **Figure 3A**. We found that mRNAs encoding Chi3l4 and Muc5ac were increased in OVA-exposed and challenged lungs relative to their expression in naïve lungs, but their expression in the iBALT group was significantly less than that in the control group (**Figure 3F**). Thus, the expression of genes that are responsive to Th2 cytokines were reduced in the lungs of iBALT mice relative to those in control mice. These data are more consistent with the reduced histopathology that we see in the lungs of iBALT mice compared to those in the lungs of control mice, suggesting that the difference between the groups is not in Th2 priming and expansion, but in the response to Th2 cytokines.

The Presence of iBALT Alters Pulmonary Pathology Independently of Th2 Priming

In the experiments above, we were unable to independently control the initial steps of T cell priming and expansion. To rigorously show that these steps were unaffected by the presence or absence of iBALT, we next generated OVA-specific Th2 effector T cells *in vitro* and showed that, upon restimulation, a high frequency of these cells made IL-13, whereas less than 1% made IFNγ and almost none of them made IL-17 (**Figure 4A**). We next adoptively transferred 1 x 10^6 of these Th2 cells into 48-day-old control or iBALT mice and challenged them with OVA on days 49, 50, 53, and 54 (**Figure 4B**). One day after the final challenge, we enumerated donor T cells in the lungs and found that a similar frequency (**Figure 4C**) and number (**Figure 4D**) of donor T cells had accumulated in the lungs of both groups. We also enumerated GC B cells in the lungs and found that a high frequency (**Figure 4E**) and

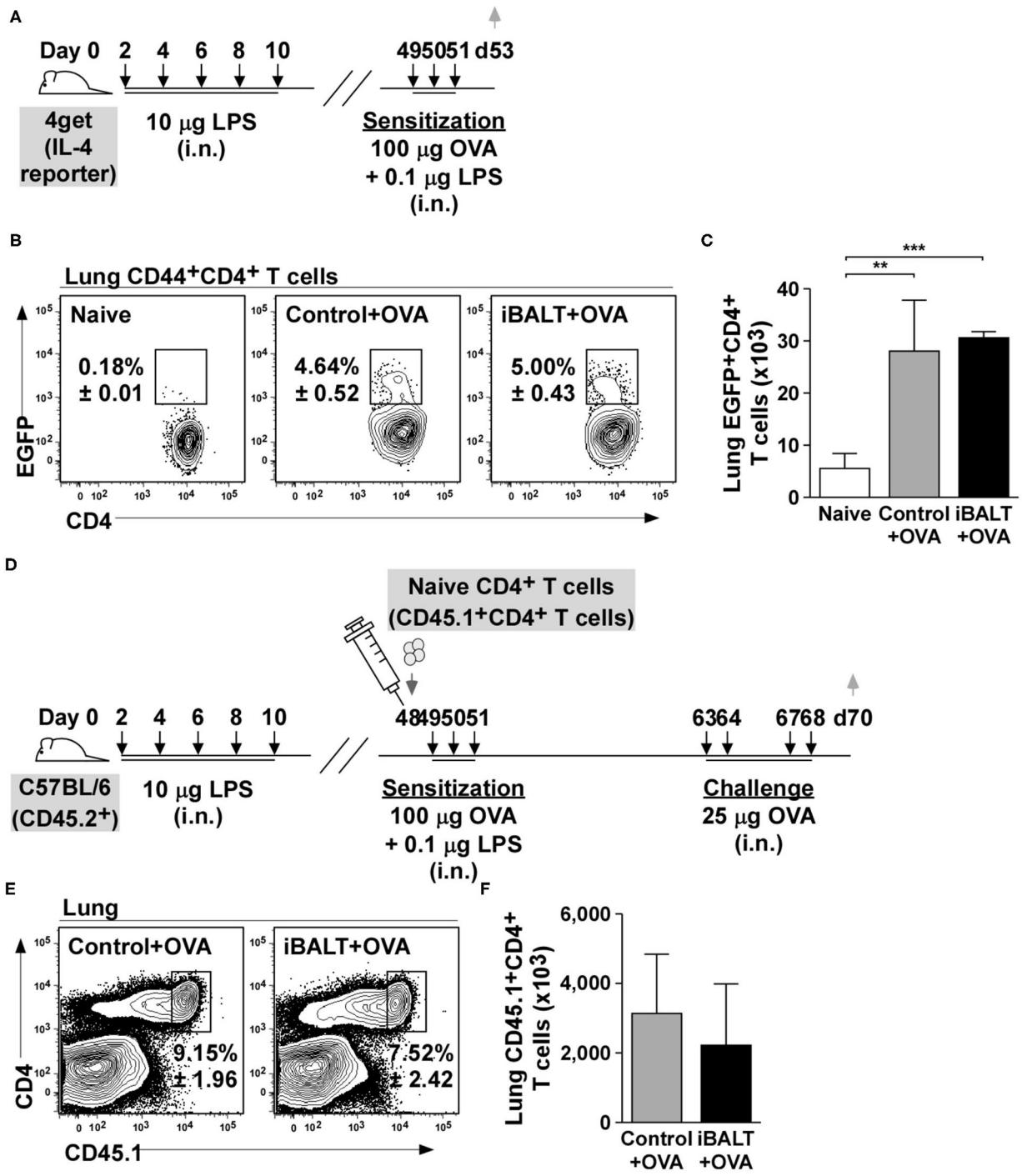

FIGURE 2 | The presence of iBALT does not affect Th2 priming or accumulation in the lung. **(A)** Timing of iBALT induction, allergic sensitization and analysis. **(B,C)** The frequencies **(B)** and numbers **(C)** of $EGFP^{+}CD4^{+}$ T cells were determined by flow cytometry. **(D)** Timing of iBALT induction, transfer of naïve OTII cells, allergic sensitization, antigen challenge and analysis. **(E,F)** The frequency **(E)** and number **(F)** of donor T cells in the lungs were determined by flow cytometry. All data show mean ± SD of 5 mice per group; $^{**}P < 0.01$, $^{***}P < 0.001$. Experiments were performed 2 times **(A–C)** or 3 times **(D–F)**.

number (**Figure 4F**) of GC B cells accumulated in the lungs of mice in the iBALT group, but not in the lungs of control or naïve mice.

Despite having similar numbers of donor Th2 cells in the lungs of each group, the histology of the lungs was dramatically different, with the control group exhibiting extensive goblet cell

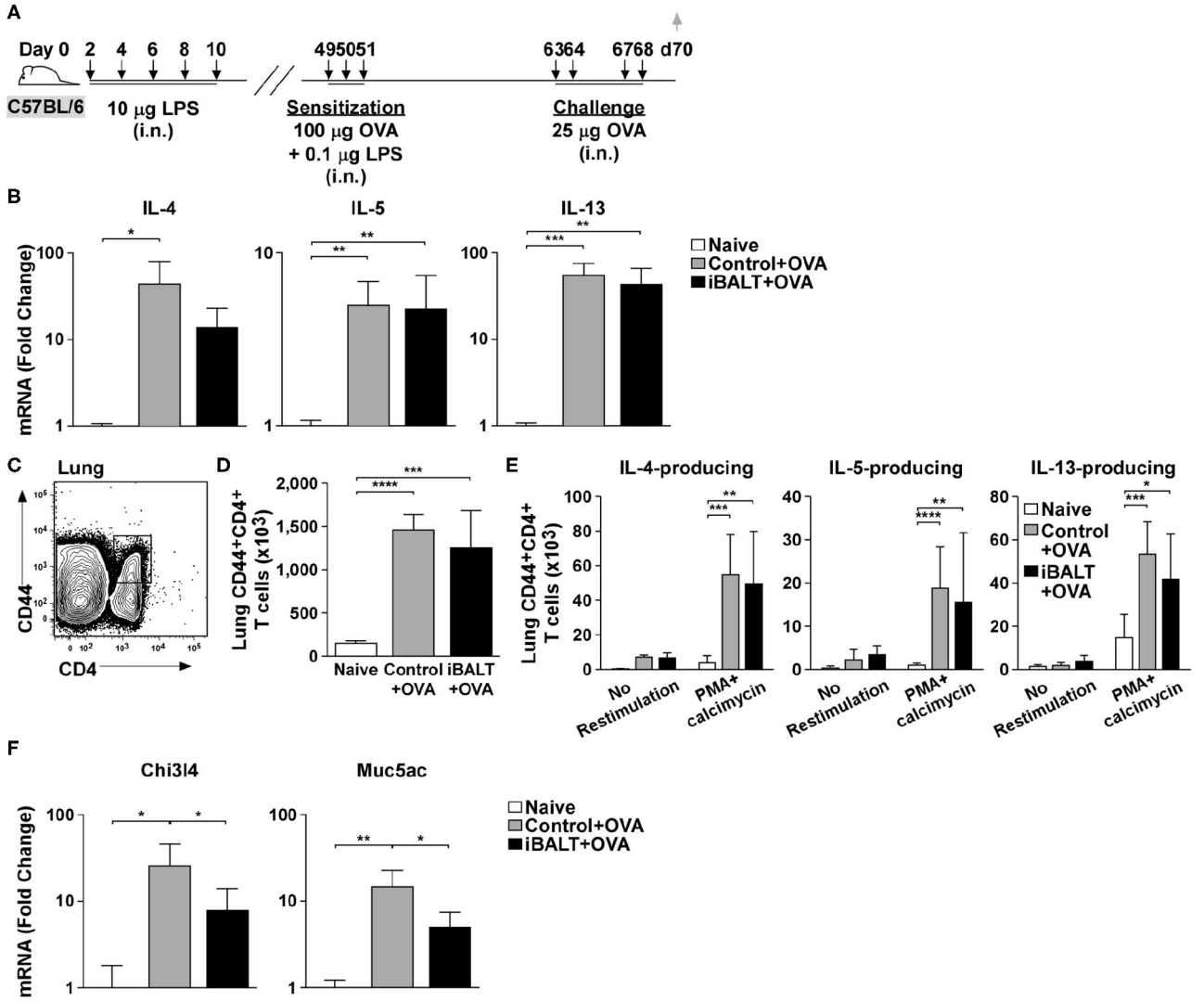

FIGURE 3 | The presence of iBALT impacts allergic airway disease downstream of Th2 cytokine expression. **(A)** Timing of iBALT induction, allergic sensitization, antigen challenge and tissue collection. **(B)** mRNA expression of IL−4, IL−5, and IL−13 was determined by quantitative PCR. Data is normalized to the expression in naïve lung. **(C–E)** Lung cells from OVA primed and challenged mice were restimulated with PMA/calcimycin for 4 h and we determined the frequencies **(C)** and numbers **(D)** of $CD4^+CD44^{hi}$ T cells as well as the numbers of cytokine–producing $CD4^+$ T cells **(E)** by intracellular staining and flow cytometry. **(F)** mRNA expression of Chi3l4 and Muc5ac was determined by quantitative PCR. Data is normalized to the expression in naïve lung. All data show mean ± SD of 5 mice per group; $^*P < 0.05$, $^{**}P < 0.01$, $^{***}P < 0.001$, $^{****}P < 0.0001$. Experiments were performed 3 times **(B,F)** or 4 times **(C–E)**.

hyperplasia and diffuse inflammatory infiltrate throughout the lungs, whereas the iBALT mice exhibited minimal goblet cell hyperplasia and dense lymphoid accumulations (iBALT) adjacent to, but not surrounding, the airways and in the perivascular space (**Figure 4G**). We also quantified the amount of Th2 cytokines in the BAL fluid 6 h after the last challenge and found that, although the amount of IL-4, IL-5, and IL-13 was slightly less than in the BAL fluid of iBALT mice than in control mice, the differences were not significant (**Figure 4H**). Together, these data demonstrate that, despite starting with the same number of Th2 cells in the lung, the biological outcome of inflammation was dramatically different in control and iBALT mice.

The Presence of iBALT Does Not Alter Treg Accumulation or Epithelial Cell Conditioning

Given that the biological outcome of disease was so different despite starting with similar numbers of fully differentiated Th2 cells, we reasoned that iBALT must engage some sort of regulatory mechanism. One important cell type that has the ability to powerfully attenuate inflammatory responses is the Treg population (36). Tregs are immunosuppressive $CD4^+$ T cells that have differentiated in a way that promotes the expression of the transcription factor, FoxP3 (37). $CD4^+FoxP3^+$ Tregs can reduce eosinophilia (38), impair humoral responses

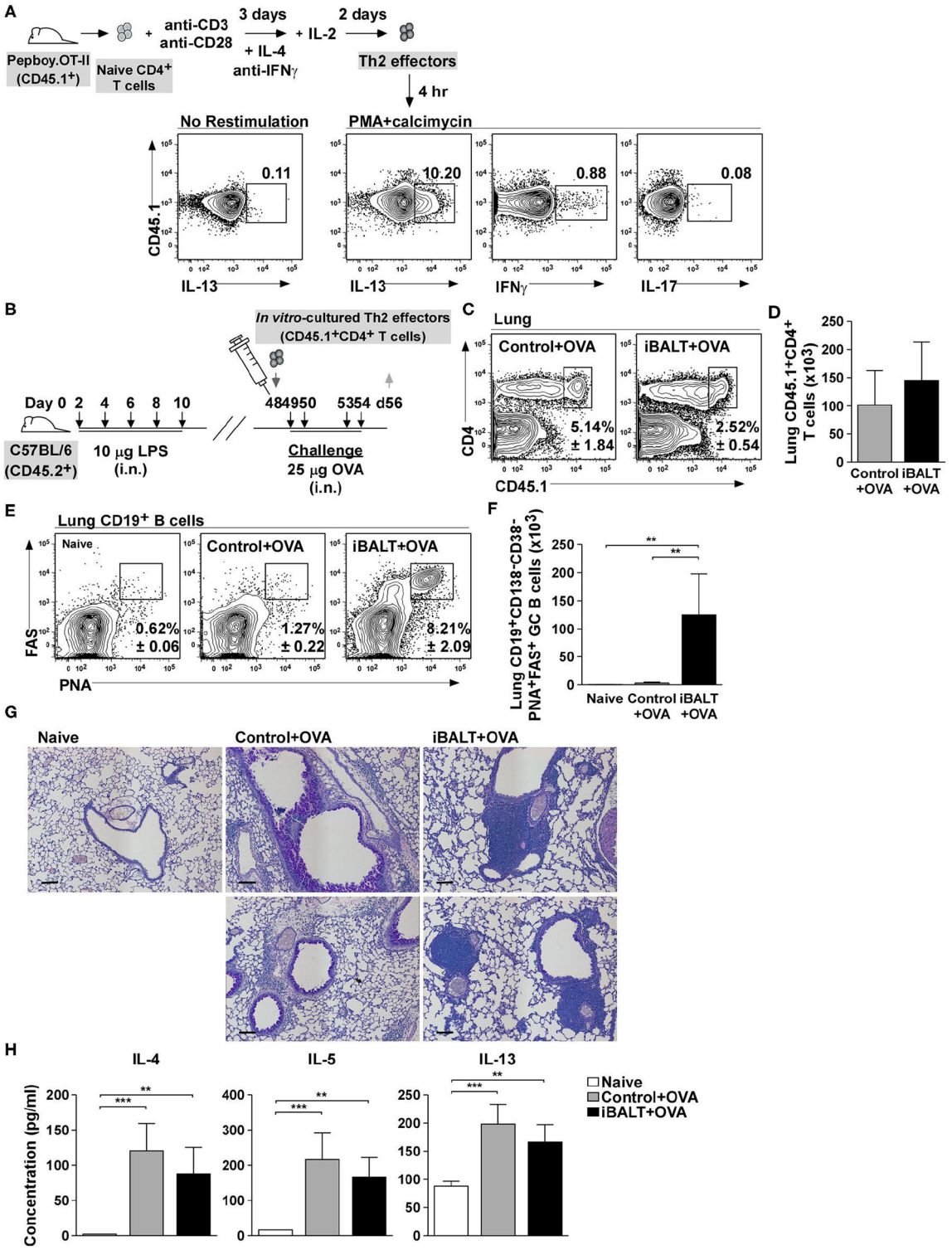

FIGURE 4 | iBALT alters pulmonary pathology independently of Th2 effector priming. **(A)** Purified CD4$^+$ OTII cells were expanded *in vitro* under Th2 conditions and their expression of IL−13, IFNγ, and IL−17 was determined by intracellular staining and flow cytometry after 4 h restimulation with PMA and calcimycin. **(B)** *In vitro*–activated Th2 cells were adoptively transferred into iBALT or control mice on day 48 and the recipients were intranasally challenged with OVA on days 49, 50, 53, and 54. **(C,D)** The frequencies **(C)** and numbers **(D)** CD45.1$^+$CD4$^+$ T cells in the lungs were determined by flow cytometry on day 56. **(E,F)** The frequencies **(E)** and numbers **(F)** of CD19$^+$CD138–CD38–PNA$^+$FAS$^+$ GC B cells in the lung were determined by flow cytometry. **(G)** Periodic–acid schiff (PAS) staining of paraffin–embedded lung sections on day 52 (scale bar = 100 μm). **(H)** The concentration of IL−4, IL−5, and IL−13 in the BAL fluid was determined by ELISA 6 h after the last OVA challenge. All data show mean ± SD of 4–5 mice per group; $^{**}P < 0.01$, $^{***}P < 0.001$. Experiments were performed 5 times **(A–G)** or 2 times **(H)**.

and secret an inhibitory cytokines, such as IL-10 and TGFβ (39), which suppress the effector functions of activated T cells and reduce inflammation. Thus, changes in Treg number or activity can have dramatic consequences on immune responses regardless of the number of antigen-specific effector T cells. Given the immunosuppressive capacity of Tregs, we enumerated $CD4^+FoxP3^+$ T cells in the lungs of iBALT and control mice following OVA sensitization and challenge. We found that although the frequency (**Figure 5A**) and number (**Figure 5B**) of Tregs increased in the lungs following OVA sensitization and challenge, there was no difference in Tregs between iBALT and control groups. Thus, alterations in Treg numbers do not explain why mice with iBALT exhibit attenuated allergic responses in their lungs.

Previous reports show that pulmonary administration of LPS to the lung conditions epithelial cells in a way that promotes the over-expression of A20 (40), an ubiquitin-modifying enzyme that blunts NF-kB signaling thereby reducing expression of pro-Th2 cytokines like IL-33 (41). Thus, we were concerned that the exposure of neonatal mice to LPS may permanently suppress pulmonary inflammatory responses. To test this possibility, we treated neonatal mice with LPS or PBS to trigger iBALT formation and, when the mice were 7-weeks old, transferred OVA-specific Th2 effector cells and

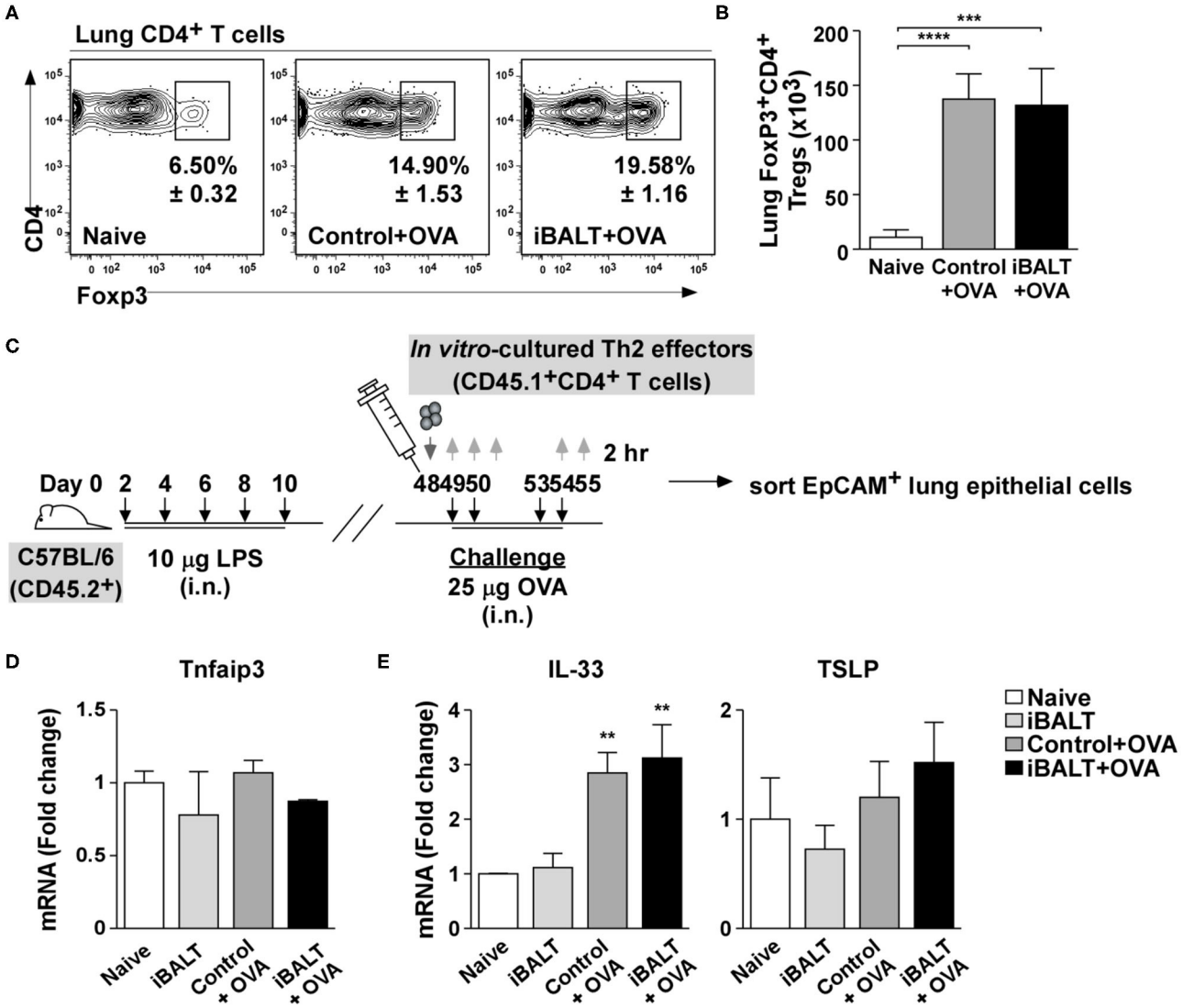

FIGURE 5 | The presence of iBALT does not influence Treg accumulation or epithelial cell conditioning. Mice with and without iBALT were sensitized and challenged with OVA according to the schedule in **Figure 1E** and the frequencies **(A)** and numbers **(B)** of $Foxp3^+CD4^+$ T cells were determined by flow cytometry (mean ± SD of 4–5 mice per group; $^{***}P < 0.001$, $^{****}P < 0.0001$). **(C)** Timing of iBALT induction, Th2 transfer, antigen challenge and tissue collection. **(D,E)** mRNA expression of **(D)** Tnfaip3 and **(E)** IL-33 and TSLP from sorted lung epithelial cells was determined by quantitative PCR 2 h after the last OVA challenge. Data is normalized to the expression in naïve lung (mean ± SD of 4–5 mice pooled per group; $^{**}P < 0.01$). Experiments were performed 4 times **(A,B)** or 3 times **(C–E)**.

challenged the recipients 4 times with either OVA or PBS (**Figure 5C**). We then enzymatically digested the lung tissue, sorted $EpCAM^{+}CD31^{-}Sca1^{-}CD45^{-}$ bronchial epithelial cells and performed qPCR for *Tnfaip3*, the gene encoding the A20 enzyme. We found that *Tnfaip3* expression was similar in all groups of bronchial epithelial cells (**Figure 5D**), regardless of whether they came from mice that received LPS as neonates or whether they came from mice that were challenged with OVA as adults. We also performed qPCR to quantify the expression of the inflammatory cytokines, IL-33 and TSLP. We found that although IL-33 expression was strongly increased following OVA challenge, it was not altered by previous exposure to LPS (**Figure 5E**). We also found that TSLP expression was not changed by either OVA challenge or previous exposure to LPS (**Figure 5E**). Thus, the pulmonary exposure of neonatal mice to LPS did not permanently alter the ability of bronchial epithelial cells to express inflammatory cytokines.

Altered Kinetics of Effector Th2 Responses in the Lungs of Mice With iBALT

Despite the overall reduction in Th2-driven pathology in the mice with iBALT, the number of Th2 effector cells seemed to be similar at the endpoint of the experiment. However, we didn't know whether they accumulated in the lung at the same rate. To determine whether the kinetics of T cell recruitment was the same in mice with and without iBALT, we generated Th2 effectors from naïve OTII cells *in vitro* and then adoptively transferred 1 x 10^6 Th2 effectors 24 h prior to a series of 4 OVA challenges (**Figure 6A**). We then enumerated the transferred Th2 cells and the recruited eosinophils in the lungs and BAL 24 h after each OVA challenge. Not surprisingly, the numbers of donor T cells and eosinophils increased over time following each challenge (**Figures 6B–E**). Unexpectedly however, we observed significant reductions in the numbers of Th2 effectors (**Figures 6B,D**) and eosinophils (**Figures 6C,E**) in both the lungs (**Figures 6B,C**) and airways (**Figures 6D,E**) of iBALT mice relative to controls after the first 3 challenges. However, by the fourth challenge, there was no difference in the numbers of T cells. These data suggest that the presence of iBALT slows the accumulation of Th2 effectors as well as eosinophils following pulmonary allergen exposure. These data may also explain why we saw little difference in T cell numbers at the endpoints of earlier experiments, even though we observed significant differences in lung pathology.

The Presence of iBALT Alters the Positioning of Th2 Cells in the Lung

The most unique attribute of iBALT is its dense accumulations of spatially ordered lymphocytes in a tissue (the lung) that normally has relatively few lymphocytes and rarely has them so densely organized. Therefore, we next asked whether the specialized environment of iBALT alters the spatial organization of T cells in the lung following Ag exposure. To test this possibility, we generated OVA-specific Th2 effector cells *in vitro* using OTII cells. These cells were subsequently transferred into iBALT and control mice and the recipients were challenged with OVA 4 times before we examined the lungs by histology (**Figure 7A**). We performed immunofluorescence looking for the donor T cell marker (CD45.1), B cells (B220), and FDCs (CD21). We found that the donor effector Th2 cells preferentially accumulated in the iBALT areas of iBALT mice and were relatively dilute in the rest of the lung (**Figure 7B**). In contrast, the donor Th2 effector cells were distributed more evenly in the control mice. These data were quantified in **Figure 7C**. Importantly, we found that the total number of donor Th2 effector cells in the lungs of mice with and without iBALT were indistinguishable at this time (**Figure 7D**). We also examined CD4+FOXP3+ Tregs in tissue sections from mice with and without iBALT. We found that Tregs were densely clustered in areas of iBALT, but were relatively dilute in the rest of the lung (**Figures 7E,F**), despite the similar numbers of Tregs in the lungs of mice with and without iBALT (**Figures 5A,B**). Together, these data suggest that the spatial distribution of effector Th2 cells and Tregs is affected by the presence of iBALT (they cluster together), which may explain how iBALT and control mice can have similar numbers of Th2 cells in their lungs, but have so profoundly different outcomes in terms of eosinophil accumulation and histopathology.

Pulmonary Exposure, but Not Systemic Exposure, to LPS Promotes iBALT and Reduces Allergen-Induced Inflammation

The above experiments used mice that had been administered LPS as neonates in order to form iBALT. However, one concern with these experiments is that neonatal exposure to LPS might have altered systemic immunity in some way that ameliorated subsequent inflammatory responses independently of iBALT formation. To rule out this possibility, we generated *in vitro*–differentiated OTII Th2 cells and transferred 1 x 10^6 Th2 effector cells into control mice, mice that received pulmonary LPS as neonates (iBALT mice) and mice that received peritoneal LPS as neonates (i.p. LPS mice). The following 2 days, we administered 25 μg OVA intranasally to all groups and measured germinal center B cells and eosinophils in the lungs 24 h later (**Figure 8A**).

When we enumerated Th2 effectors (**Figure 8B**) and eosinophils (**Figure 8C**) in the lung tissue, the numbers were reduced in the presence of iBALT compared to control mice, but in mice treated with LPS intraperitoneally, the number of effector T cells and eosinophils were the same as in the control mice (**Figures 8B,C**). Thus, the exposure of neonates to pulmonary LPS dramatically decreased the inflammatory response in adults, whereas the exposure of neonates to peritoneal LPS did not. We also observed that mice that receive pulmonary LPS as neonates (iBALT mice) had a significantly higher frequency (**Figure 8D**) and number (**Figure 8E**) of GC B cells in the lungs, whereas mice that received LPS intraperitoneally as neonates (i.p. LPS mice) did not accumulate GC B cells and were comparable to control mice (**Figures 8D,E**). These data indicate that systemic exposure to LPS does not lead to iBALT formation (as monitored by the germinal center response in the lungs). These data are consistent with the conclusion that LPS-mediated iBALT formation alleviates Th2-dependent inflammatory responses in the lung, independently of any systemic effect of LPS on immunity.

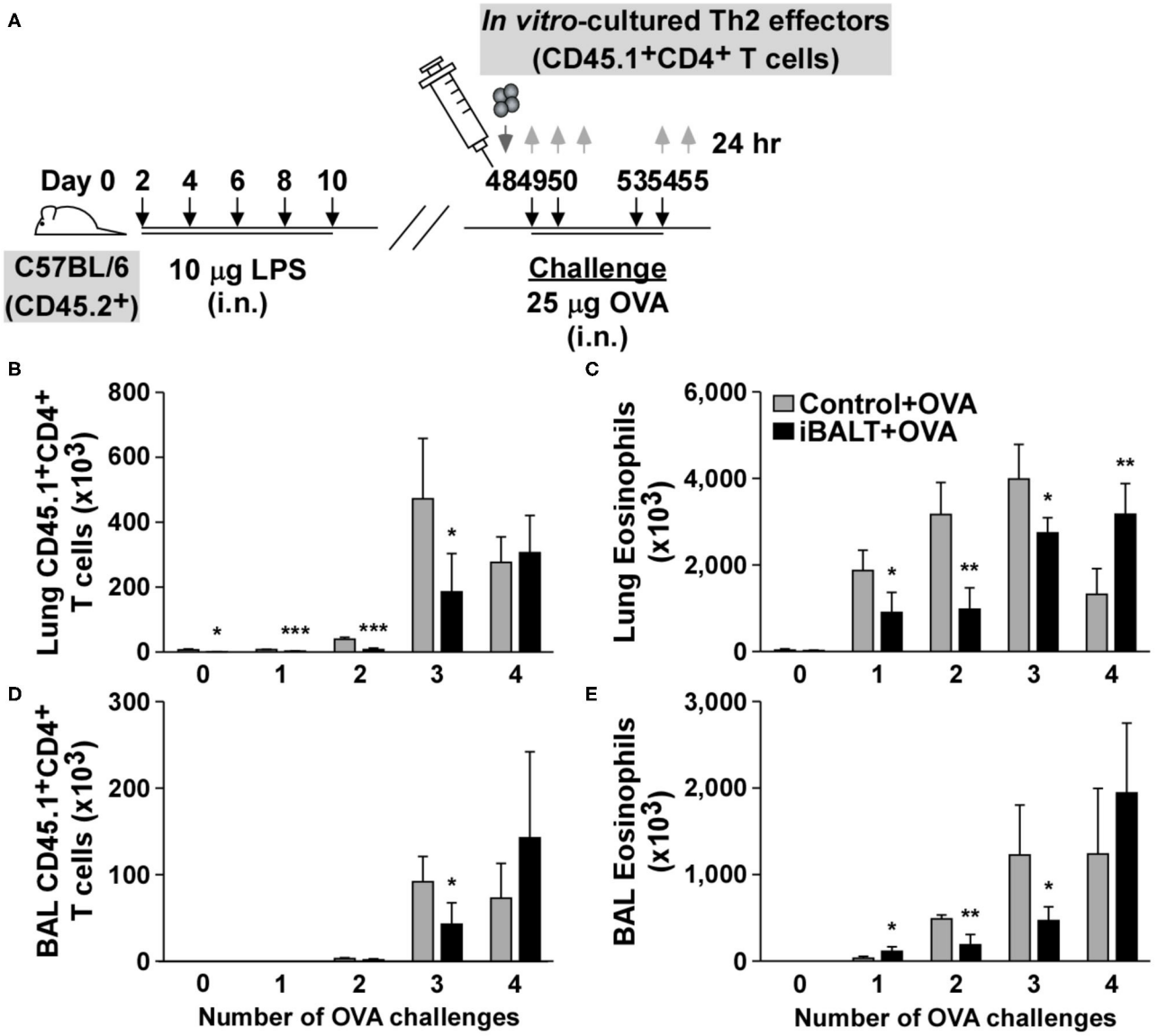

FIGURE 6 | The presence of iBALT alters the kinetics of Th2 accumulation in the lungs. **(A)** Timing of iBALT induction, Th2 effector cell transfer and antigen challenge. Tissues were collected 24 h after each challenge. The numbers of donor T cells **(B)** and eosinophils **(C)** in the lung were determined by flow cytometry. The numbers of donor T cells **(D)** and eosinophils **(E)** in the BAL fluid were determined by flow cytometry. All data show mean ± SD of 4–5 mice per group; $^{*}P < 0.05$, $^{**}P < 0.01$, $^{***}P < 0.001$. Experiments were performed 3 times **(A–E)**.

DISCUSSION

Our data show that the presence of iBALT in the lungs prior to pulmonary sensitization and challenge with OVA does not exacerbate Th2 responses, but rather attenuates Th2-driven pulmonary pathology. In fact, mice with iBALT exhibit delayed Th2 accumulation, reduced eosinophil recruitment, reduced goblet cell hyperplasia and reduced mucus production compared to their control counterparts. Although the initial priming of Th2 cells is not affected by the presence of iBALT, the accumulation of Th2 cells in the lung is delayed following pulmonary challenge. More importantly, the spatial distribution of effector T cells is altered by the presence of iBALT, such that effector CD4 T cells as well as Tregs become concentrated in iBALT areas and relatively diluted in the rest of the lung. These results suggest that iBALT functionally sequesters effector T cells, thereby limiting the exposure of the lung parenchyma to T cell-produced inflammatory cytokines, which attenuates pulmonary inflammation and prevents excessive pathology.

IBALT is associated with a wide variety of inflammatory lung diseases, including COPD (26), hypersensitivity pneumonitis (27) and rheumatoid lung disease (3), all of which are the result of chronic exposure to antigens or inflammatory agents. Although asthma is also a chronic lung disease, the mouse model of

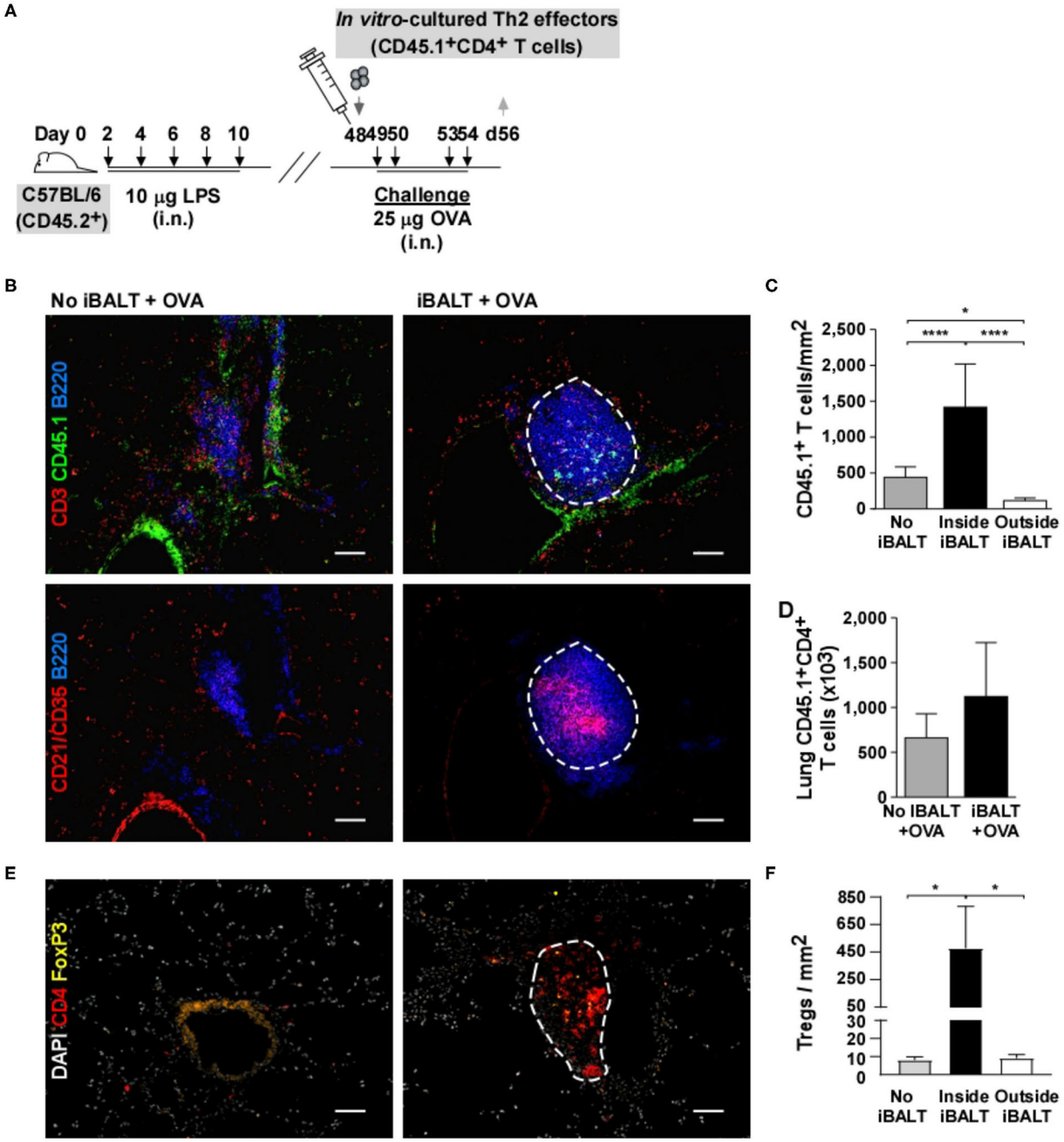

FIGURE 7 | The presence of iBALT alters the spatial distribution of T cells. **(A)** Timing of iBALT induction, effector Th2 transfer and antigen challenge. **(B)** Serial cryosections were probed with antibodies against CD3, CD45.1 and B220 or with antibodies against CD21/CD35 and B220 as indicated. Images were obtained with 20X objective (scale bar = 100 μm). **(C)** The frequency of CD45.1$^+$ T cells per μm^2 was determined in areas of iBALT (an example is outlined in white) or in non–iBALT areas using a mosaic of high–magnification images. **(D)** The numbers of lung CD45.1$^+$CD4$^+$ T cells were determined by flow cytometry. **(E)** Cryosections were probed with antibodies against CD4 and FOXP3. Images were obtained with 20X objective (scale bar = 100 μm). **(F)** The frequency of CD45.1$^+$ T cells per μm^2 was determined in areas of iBALT (an example is outlined in white) or in non–iBALT areas using a mosaic of high–magnification images. All data show mean ± SD of 4–5 mice per group; $^*P < 0.05$, $^{****}P < 0.0001$. Experiments were performed 3 times **(A–D)** or 1 time **(E,F)**.

repeated sensitization and challenge with OVA is more like an acute allergic response. However, our data demonstrate that the mere presence of iBALT does not necessarily lead to an increased inflammatory response or pulmonary pathology in the context of pulmonary allergen exposure as one might expect if iBALT was facilitating antigen presentation and T cell activation. Therefore, despite participating in local immune responses, iBALT may be beneficial in the context of inflammatory diseases by sequestering

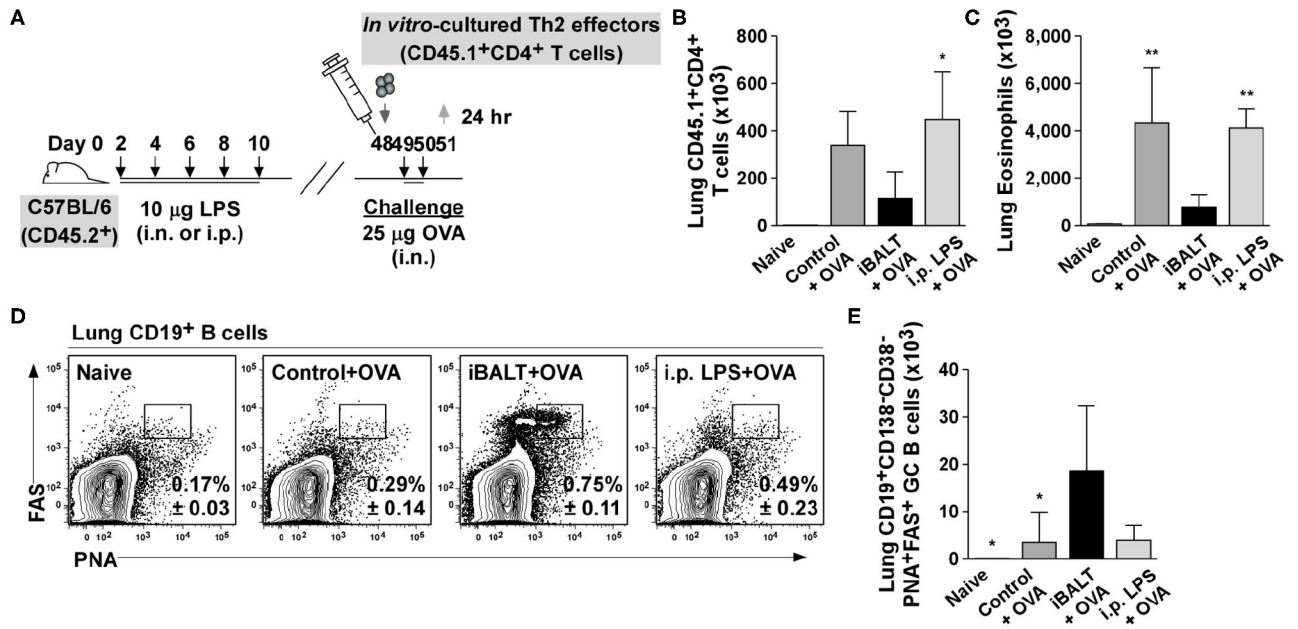

FIGURE 8 | Pulmonary, but not systemic LPS administration leads to iBALT formation and reduced inflammatory responses in the lung. **(A)** Timing of iBALT induction, transfer of effector Th2 cells and antigen challenge. The numbers of donor T cells **(B)** and eosinophils **(C)** in the lungs was demined by flow cytometry 24 h after the last OVA challenge. The frequency **(D)** and number **(E)** of GC B cells in the lungs was determined 24 h after the last OVA challenge by flow cytometry. All data show mean ± SD of 4–5 mice per group; $*P < 0.05$, $**P < 0.01$. Experiments were performed 3 times **(A–E)**.

activated lymphocytes. The idea of reducing inflammation by sequestering T cells in lymphoid tissue is consistent with the activities of the immunosuppressant drug, FTY720, which prevents T cells from exiting lymphoid organs—effectively sequestering them and preventing their recirculation through peripheral tissues (42, 43). In fact, treatment with FTY720 reduces airway remodeling and pulmonary inflammation in a rat model of OVA-induced asthma (44). Interestingly, iBALT areas are expanded in the lungs of FTY720-treated animals, suggesting that the FTY720-mediated sequestration of lymphocytes can occur in either conventional lymphoid organs or in areas of iBALT in the lung (13).

Another physical change that occurs in the lung concomitantly with the development of iBALT is the formation of additional lymphatic vessels surrounding the iBALT follicles (45). Live imaging of iBALT suggests that these lymphatic vessels may facilitate the collection of DCs from the airways (46). Static imaging also shows that iBALT areas collect inhaled antigens and particulates (47), suggesting that iBALT may sequester antigen as well as T cells. In this context, it is interesting to note that mice that spontaneously develop iBALT in the context of rheumatoid lung disease are highly resistant to developing fibrosis following pulmonary challenge with bleomycin (48). If iBALT areas efficiently collect and sequester intratracheally administered bleomycin or remove it from the lung via lymphatics, then one would expect to observe reduced fibrosis. Similarly, if iBALT areas collect and sequester pulmonary antigens like OVA and remove them from the lung parenchyma, one would expect reduced pulmonary inflammation. Thus, iBALT may protect the lung by collecting antigens and inflammatory substances as well as T cells.

Our data are also consistent with observations that iBALT attenuates inflammatory responses and improves clinical outcomes following infection with a variety of pulmonary pathogens. For example, the presence of iBALT promotes the survival of mice that are challenged with normally lethal doses of influenza virus, pneumovirus and SARS corona virus (24) and attenuates the pulmonary pathology associated with these infections. Much of the clinical pathology, such as weight loss, associated with pulmonary viral infections is linked to the production of inflammatory cytokines by T cells. Thus, if iBALT sequesters virus-specific effector T cells, it may limit the exposure of the rest of the lung to inflammatory cytokines and chemokines and reduce the recruitment of additional inflammatory cells—thereby attenuating pathology. However, iBALT-mediated resistance to pneumovirus is associated with impressive increases, rather than decreases, in the mRNA expression of IFNγ, CXCL10, and CCL3 in the lung (12). These responses were measured by PCR using mRNA extracted from whole lungs, so it is difficult to know whether the increases were predominantly confined to iBALT areas or not. In addition, it is not clear whether the reported increase is due to an overall increased magnitude of the response or altered kinetics, such that more T cells are responding earlier. This last possibility seems plausible, given that accelerated antibody responses are also observed in mice with iBALT (24). Interestingly, we also observe altered kinetics of effector T cell recruitment to the lungs following pulmonary challenge with allergen. However, we find

that fewer effector Th2 cells accumulate in the lungs at early times after allergen exposure. The differences between our results and those reported for pneumovirus may be due to the types of antigens (replicating virus vs. inert allergen) or to the types of T cells (virus–specific CD8 and Th1 cells vs. allergen-specific Th2 cells). In any case, the presence of iBALT clearly has an impact on the kinetics of pulmonary immune responses.

T cells are often imprinted with particular effector functions that differ depending on the secondary lymphoid organ in which they were primed (49, 50). Thus, one could envision that iBALT skews CD4 T cell differentiation away from a Th2 pathway and thereby attenuates the symptoms of allergic disease. However, we found equivalent numbers and frequencies of Th2 cells primed in mice with or without iBALT, suggesting that CD4 T cell differentiation is not deviated toward an alternative effector function. Moreover, we observed reduced pathology in mice with iBALT following the adoptive transfer of *in vitro* differentiated Th2 effector cells, demonstrating that even when T cell priming occurs *in vitro*, the functional outcome of the effector response is altered beneficially in mice with iBALT. Interestingly, naïve T cells primed in aorta–associated lymphoid tissues in $Apoe^{-/-}$ mice preferentially differentiate into Tregs that suppress atherosclerosis (51). Although the preferential formation of Tregs in iBALT areas would help to explain the reduced inflammation and pulmonary pathology in mice with iBALT following OVA sensitization and challenge, we did not observe changes in either the number and frequency of Tregs in the lung, regardless of whether iBALT was present. Nevertheless, we did find that Tregs were preferentially concentrated in iBALT areas and co-localized with effector T cells, suggesting that Tregs in iBALT may more effectively suppress the inflammatory functions of effector T cells in this location. Thus, in the context of pulmonary sensitization with allergens such as OVA, iBALT seems to alter the placement of T cells rather than changing their differentiation pathways.

Considering that many of the adoptively transferred Th2 cells are being sequestered in the iBALT areas and seem to be located in the B cell follicle, it is possible that they are converting to IL-4-expressing Tfh cells (52). This possibility would be consistent with the large GCs and high frequencies of GC B cells that we observe in the lungs following adoptive transfer of Th2 cells and sensitization with antigen. In addition, iBALT-induced resistence to influenza and SARS corona virus is associated with accelerated antibody responses (24), suggesting that local Tfh cells are promoting B cell differentiation. Although Th2-Tfh cells in B cell follicles are potent producers of IL-4 (53), they are directing cytokine secretion toward B cells rather than pulmonary epithelial cells, which would likely lead to accelerated antibody secretion, but reduced pulmonary pathology. Thus, iBALT may be sequestering T cells and directing cytokine secretion toward alternative cell types, both of which should attenuate pulmonary pathology.

In summary, our data show that the presence of iBALT does not exacerbate pulmonary pathology following sensitization and challenge with an allegen, but rather attenuates Th2-induced inflammatory responses. This same mechanism may also explain the ability of iBALT to ameliorate pulmonary pathology in the context of infection and may be a general mechanism by which ectopic follicles in a variety of tissues attempt to cope with chronic inflammatory responses. Thus, we may want to develop treatments that promote, rather than prevent, ectopic follicle formation in the context of chronic inflammatory conditions.

MATERIALS AND METHODS

Mice

C57BL/6, B6.SJL–$Ptprc^{a}Pepc^{b}$/BoyJ (CD45.1) and B6.Cg–Tg(TcraTcrb)425Cbn/J (OTII) mice were originally obtained from Jackson Laboratories. These strains were interbred to generate CD45.1–OTII mice. B6.129–$Il4^{tm1Lky}$/J (4get) mice were obtained from M. Mohrs. All mice were on a C57BL/6 background and were bred at the University of Rochester or University of Alabama at Birmingham animal facilities and all experimental procedures were approved by the University of Rochester University Committee on Animal Resources (UCAR) or University of Alabama at Birmingham Institutional Animal Care and Use Committee (IACUC) and were performed according to guidelines outlined by the National Research Council.

Induction of iBALT, Ova Sensitization, and Challenge

To induce iBALT, pups were intranasally administered 10 μg LPS from *Escherichia coli* (055:B5; Sigma) in 10 μl PBS every other day starting on day 2 after birth for a total of 5 times. In control experiments, pups were intraperitoneally injected with 10 μg LPS in 10 μl PBS every other day starting on day 2 after birth for a total of 5 times. Control mice received 10 μl PBS or nothing according to the same schedule. To induce allergic airway inflammation, adult mice were sensitized intranasally with 100 μg OVA (Sigma) plus 0.1 μg LPS in 100 μl PBS and subsequently challenged intranasally with 25 μg OVA in 100 μl PBS according to the schedule indicated in each experiment. In the DC labeling experiments, we intratracheally administered 25 μg OVA labeled with Alexa Flour® 647 (Invitrogen).

OTII Purification, Th2 Differentiation, and Adoptive Transfer

$CD4^+$ T cells were purified from the spleens of naive $CD45.1^+$ B6 congenics using LS columns and anti–CD4 MACS beads (Miltenyi Biotec) according to the manufacturer's instructions. Single T cell preparations were > 95% pure as determined by flow cytometry. Th2 effectors were generated by activating naïve T cells for 48–72 h with plate–bound anti–CD3 (2 μg/ml; 145–2C11; BioXcell) and anti–CD28 (0.5 μg/ml; 37.51; eBioscience) in the presence of IL−4 (50 U/ml; DNAX) and anti–IFNγ (10 μg/ml; XMG1.2; eBioscience) followed by feeding with IL−2 (20 U/ml; Peprotech) for additional 48 h. Naïve and effector $CD4^+$ ($CD45.1^+$) T cells (1 x 10^6/mouse) were injected intravenously into no iBALT and iBALT recipients that were subsequently immunized with OVA.

Cell Preparation and Flow Cytometry

Lungs were cut into small fragments and digested with 0.6 mg/ml collagenase A (Sigma) and 30 μg/ml DNase I (Sigma) in RPMI 1640 medium (Gibco) at 37°C for 45 min to obtain single–cell suspensions. Digested tissues were mechanically disrupted by passage through a metal strainer. Cell suspensions from lungs and mediastinal LNs were centrifuged and resuspended in 150 mM NH_4Cl, 10 mM $KHCO_3$, and 0.5 mM ethylenediaminetetraacetic acid (EDTA; Lonza) for 5 min to lyse red cells. Cell suspensions were then filtered through a 70 μm nylon cell strainer (BD Biosciences), washed, and resuspended in phosphate–buffered saline (PBS) with 5% donor calf serum and 10 μg/ml Fc Block (2.4G2; Trudeau Institute) on ice for 10 min before staining with fluorochrome–conjugated antibodies against the following antigens: CD4 (RM4–5), CD11b (M1/70), CD25 (PC61), CD45R (B220; RA3–6B2), CD95 (FAS; Jo2), CD138 (281–2), Siglec–F (E50–2440), and I–A^b (AF6–120.1; all from BD Biosciences); CD11c (N418), CD44 (IM7), CD45.1 (A20), CD103 (2E7), and Foxp3; (FJK−16s); all from eBioscience; CD19 (6D5); from BioLegend; CD38 (NIMR−5); from SouthernBiotech; and goat anti–rabbit–Alexa Flour® 647 (Invitrogen). For intracellular staining, single–cell suspensions from the lungs were stimulated on plates coated with anti–CD3 (2 μg/ml; 145–2C11; BioXcell) in the presence of Brefeldin A (12.5 μg/ml; Sigma) for 4 h. The restimulated cells were surface stained, then fixed in 4% paraformaldehyde, made permeable with 0.1% Triton™ X−100 (Sigma), and stained with anti–IL−4 (11B11), anti–IL−5 (TRFK4; all from BD Biosciences) or anti–IL−13 (13A; eBioscience). Cells were analyzed with a LSR II (BD Biosciences) or FACSCanto II (BD Biosciences) located at the University of Rochester and University of Alabama at Birmingham Flow Cytometry Core Facility.

To isolate lung epithelial cells, we perfused the lungs with PBS containing 0.05 mM EDTA (Lonza), instilled with 1 ml Dispase (160 μg/ml; Corning), and incubated them in a shaker at 37°C for 15 min. Using forceps, lungs were torn into small pieces, and put back in the shaker at 37°C for an additional 30 min in Dispase (160 μg/ml; Corning) and DNaseI (250 μg/ml; Worthington Biochemical). Digested tissues were red cell lysed, filtered through a 70 μm nylon cell strainer (BD Biosciences), resuspended in PBS with 5% donor calf serum, 10 μg/ml Fc Block (2.4G2; Trudeau Institute) and anti-CD45 MACS beads (Miltenyi Biotec) on ice for 10 min. Cell suspensions were depleted of CD45-expressing cells using LS columns (Miltenyi Biotec) according to the manufacturer's instructions. The flow through cells were stained with anti-CD31 (390; Invitrogen); anti-CD45.2 (104) and anti-CD326 (EpCAM; G8.8; all from Biolegend) and anti-Sca-1 (Ly6A/E; D7; Invitrogen). Lung epithelial cells were sorted with FACSAria II (BD Biosciences) located at University of Alabama at Birmingham Flow Cytometry Core Facility.

BAL Fluid Collection and Differential Cell Counts

Lungs were instilled with 3 ml Hank's balanced salt solution (HBSS; Corning) containing 0.05 mM EDTA (Lonza) and cell suspensions (≈10,000 cells in 100 μl) were centrifuged at 800 rpm for 5 min in a Shandon CytoSpin 3 cytocentrifuge (Cell Preparation System). The cytospin pellets were air dried on glass slides, stained with Shandon Kwik–Diff™ Stain kit (Thermo Scientific) and were mounted with Richard–Allan Scientific™ Cytoseal™ 60 (Thermo Scientific).

Enzyme–Linked Immunosorbent Assay (ELISA)

Total IgE levels were determined by coating plates with 1 μg/ml purified rat anti–mouse IgE (R35–72; BD Biosciences). Standard curve was prepared with purified mouse IgE κ (C38–2; BD Biosciences) and bound Abs in serum samples were detected with biotin rat anti–mouse IgE (R35–118; BD Biosciences) and streptavidin–alkaline phosphatase (Invitrogen). Alkaline phosphate substrate (Moss, Inc.) was added, and color development was detected with SpectraMax® M2 (Molecular Devices) at 405 nm.

Histology and Immunofluorescence

Paraffin–embedded sections (5 μm in thickness) were stained with hematoxylin and eosion (H&E) for standard histology and Periodic acid–Schiff (PAS) for airway mucus production. Frozen sections (8 μm in thickness) were prepared from lungs perfused with a mixture of optimum cutting temperature (OCT) compound (Sakura Finetek) in PBS at a 1:1 ratio. Sections were fixed in cold acetone for 10 min and blocked with Fc Block (10 μg/ml) and 5% (vol/vol) normal donkey serum in PBS at 25°C for 30 min. Sections were then stained with the following primary Abs in PBS at RT for 30 min: goat anti–CD3ε (M−20; Santa Cruz Biotechnology), anti–CD11c (HL3), and anti–CD45R (B220; RA3–6B2; all from BD Biosciences); anti–CD21/CD35 (7E9; BioLegend); and peanut agglutinin (PNA; Sigma). Primary Abs were detected with donkey anti–goat–Alexa Flour® 568, rabbit fluorescein–Alexa Fluor® 488, streptavidin–Alexa Fluor® 555, and streptavidin–Alex Flour® 488 (all from Invitrogen) at RT for 30 min. Slides were mounted with SlowFade® Gold Antifade Mountant with 4′,6–diamidino−2–phenylindole (DAPI; Invitrogen). Images were collected with a Zeiss Axiocam digital camera (Zeiss) or Nikon Andor Clara camera (Nikon). The images were obtained with a 20x objective for a final magnification of x200. T cells in immunofluorescent images were quantified by counting $CD45.1^+$ cells in iBALT areas (defined manually using the outline tool) and by counting $CD45.1^+$ cells in non–iBALT areas (excluding large empty airways). The mean number of T cells per μm^2 was determined using a mosaic of images obtained from control and iBALT–containing lungs that were sectioned at a similar depth and orientation. Data were obtained from multiple sections from each mouse and 5 mice per group.

RNA Isolation and Quantitative Real–Time PCR (qPCR)

Total RNA was extracted from lungs with TRIzol according to the manufacturer's specifications (Invitrogen) and was repurified with an RNeasy mini kit (Qiagen). Ribonucleic

acid (RNA; 2.2 μg) was reverse–transcribed with Superscript II and random primers (Invitrogen) and complementary deoxyribonucleic acid (cDNA; 25 ng) was amplified with following primers and probes: *glyceraldehyde−3–phosphate dehydrogenase* (*Gapdh*; Trudeau Institute), *Il4*, *Il5*, *Il13*, *Chi3l4*, *Muc5ac*. *Tnfaip3*, and *Tslp* (all from Applied Biosystems), with TaqMan® Gene Expression Master mix (Applied Biosystems) and all reactions were run on a Lightcycler 480 Real–time PCR System (Roche). The relative level of messenger RNA (mRNA) expression for each gene was first normalized to the expression of *Gapdh* and then compared to the average level of mRNA expression in lungs from naïve B6 mice. Data is expressed as logarithmic fold changes in mRNA expression.

Quantifying Cytokines in BAL Fluid

Lungs were instilled with 1 ml HBSS (Corning) containing 0.02 mM EDTA (Lonza) and SIGMA*FAST*™ Protease Inhibitor Cocktail Tablets (Sigma). Total protein levels of cytokines IL−4, IL−5, and IL−13 in lavage were quantified by mouse–specific Milliplex® multi–analyte kits (EMD Millipore) using a MagPix® instrument platform and related xPONENT® software (Luminex Corporation). The readouts were analyzed with the standard version of the Milliplex Analyst software (EMD Millipore).

Statistical Analysis

The difference in mean values between two groups was analyzed with a two–tailed Student's *t*–test. If three or more groups were compared, Tukey's multiple comparison test was used (GraphPad Prism Version 6.0). *P*-values of less than 0.05 were considered statistically significant.

DATA AVAILABILITY STATEMENT

The raw data supporting the conclusions of this article will be made available by the authors, without undue reservation.

ETHICS STATEMENT

The animal study was reviewed and approved by Institutional Animal Care and Use Committee, University of Alabama at Birmingham.

AUTHOR CONTRIBUTIONS

JH, AS-S, DC, MG-H, and JR-M designed and performed experiments. JH and TR wrote the manuscript. TR helped design experiments and obtained funding for the work. All authors contributed to the article and approved the submitted version.

ACKNOWLEDGMENTS

This work was supported by NIH grants HL−69409 and AI−100127, the Sandler Program for Asthma Research (now the American Asthma Foundation) and the Rheumatic Diseases Core Center AI−078907. The authors thank Scott Simpler and Uma Mudunuru for animal husbandry and Kristen Southworth for technical assistance.

SUPPLEMENTARY MATERIAL

The Supplementary Material for this article can be found online at: https://www.frontiersin.org/articles/10.3389/fimmu.2020.570661/full#supplementary-material

REFERENCES

1. Bienenstock J. Bronchus-associated lymphoid tissue. *Int Arch Allergy Appl Immunol.* (1985) 76(Suppl. 1):62–9. doi: 10.1159/000233736
2. Randall TD. Bronchus-associated lymphoid tissue (BALT) structure and function. *Adv Immunol.* (2010) 107:187–241. doi: 10.1016/B978-0-12-381300-8.00007-1
3. Rangel-Moreno J, Hartson L, Navarro C, Gaxiola M, Selman M, Randall TD. Inducible bronchus-associated lymphoid tissue (iBALT) in patients with pulmonary complications of rheumatoid arthritis. *J Clin Invest.* (2006) 116:3183–94. doi: 10.1172/JCI28756
4. Bienenstock J, Johnston N, Perey DY. Bronchial lymphoid tissue. I Morphologic characteristics. *Lab Invest.* (1973) 28:686–92.
5. Woodland DL, Randall TD. Anatomical features of anti-viral immunity in the respiratory tract. *Semin Immunol.* (2004) 16:163–70. doi: 10.1016/j.smim.2004.02.003
6. Gregson RL, Davey MJ, Prentice DE. The response of rat bronchus-associated lymphoid tissue to local antigenic challenge. *Br J Exp Pathol.* (1979) 60:471–82.
7. Rangel-Moreno J, Moyron-Quiroz JE, Hartson L, Kusser K, Randall TD. Pulmonary expression of CXC chemokine ligand 13, CC chemokine ligand 19, and CC chemokine ligand 21 is essential for local immunity to influenza. *Proc Natl Acad Sci USA*. (2007) 104:10577–82. doi: 10.1073/pnas.0700591104
8. Mebius RE. Organogenesis of lymphoid tissues. *Nat Rev Immunol.* (2003) 3:292–303. doi: 10.1038/nri1054
9. Randall TD, Carragher DM, Rangel-Moreno J. Development of secondary lymphoid organs. *Annu Rev Immunol.* (2008) 26:627–50. doi: 10.1146/annurev.immunol.26.021607.090257
10. Carragher DM, Rangel-Moreno J, Randall TD. Ectopic lymphoid tissues and local immunity. *Semin Immunol.* (2008) 20:26–42. doi: 10.1016/j.smim.2007.12.004
11. Delventhal S, Hensel A, Petzoldt K, Pabst R. Effects of microbial stimulation on the number, size and activity of bronchus-associated lymphoid tissue (BALT) structures in the pig. *Int J Exp Pathol.* (1992) 73:351–7.
12. Foo SY, Zhang V, Lalwani A, Lynch JP, Zhuang A, Lam CE, et al. Regulatory T cells prevent inducible BALT formation by dampening neutrophilic inflammation. *J Immunol.* (2015) 194:4567–76. doi: 10.4049/jimmunol.1400909
13. Kocks JR, Davalos-Misslitz AC, Hintzen G, Ohl L, Forster R. Regulatory T cells interfere with the development of bronchus-associated lymphoid tissue. *J Exp Med.* (2007) 204:723–34. doi: 10.1084/jem.20061424
14. Rangel-Moreno J, Carragher DM, de la Luz Garcia-Hernandez M, Hwang JY, Kusser K, Hartson L, et al. The development of inducible bronchus-associated lymphoid tissue depends on IL-17. *Nat Immunol.* (2011) 12:639–46. doi: 10.1038/ni.2053
15. Gould SJ, Isaacson PG. Bronchus-associated lymphoid tissue (BALT) in human fetal and infant lung. *J Pathol.* (1993) 169:229–34. doi: 10.1002/path.1711690209
16. Tschernig T, Kleemann WJ, Pabst R. Bronchus-associated lymphoid tissue (BALT) in the lungs of children who had died from sudden infant death syndrome and other causes. *Thorax.* (1995) 50:658–60. doi: 10.1136/thx.50.6.658
17. Ege MJ, Mayer M, Normand AC, Genuneit J, Cookson WO, Braun-Fahrlander C, et al. Exposure to environmental microorganisms and childhood asthma. *N Engl J Med.* (2011) 364:701–9. doi: 10.1056/NEJMoa1007302

18. von Mutius E, Vercelli D. Farm living: effects on childhood asthma and allergy. *Nat. Rev Immunol.* (2010) 10:861–8. doi: 10.1038/nri2871
19. Moyron-Quiroz JE, Rangel-Moreno J, Kusser K, Hartson L, Sprague F, Goodrich S, et al. Role of inducible bronchus associated lymphoid tissue (iBALT) in respiratory immunity. *Nat Med.* (2004) 10:927–34. doi: 10.1038/nm1091
20. Khader SA, Rangel-Moreno J, Fountain JJ, Martino CA, Reiley WW, Pearl JE, et al. In a murine tuberculosis model, the absence of homeostatic chemokines delays granuloma formation and protective immunity. *J.Immunol.* (2009) 183:8004–14. doi: 10.4049/jimmunol.0901937
21. Slight SR, Rangel-Moreno J, Gopal R, Lin Y, Fallert Junecko BA, Mehra S, et al. CXCR5(+) T helper cells mediate protective immunity against tuberculosis. *J Clin Invest.* (2013) 123:712–26. doi: 10.1172/JCI65728
22. Chiavolini D, Rangel-Moreno J, Berg G, Christian K, Oliveira-Nascimento L, Weir S, et al. Bronchus-associated lymphoid tissue (BALT) and survival in a vaccine mouse model of tularemia. *PLoS ONE.* (2010) 5:e11156. doi: 10.1371/journal.pone.0011156
23. Moyron-Quiroz JE, Rangel-Moreno J, Hartson L, Kusser K, Tighe MP, Klonowski KD, et al. Persistence and responsiveness of immunologic memory in the absence of secondary lymphoid organs. *Immunity.* (2006) 25:643–54. doi: 10.1016/j.immuni.2006.08.022
24. Wiley JA, Richert LE, Swain SD, Harmsen A, Barnard DL, Randall TD, et al. (2009). Inducible bronchus-associated lymphoid tissue elicited by a protein cage nanoparticle enhances protection in mice against diverse respiratory viruses. *PLoS ONE* 4:e7142. doi: 10.1371/journal.pone.0007142
25. Gosman MM, Willemse BW, Jansen DF, Lapperre TS, van Schadewijk A, Hiemstra PS, et al. Increased number of B-cells in bronchial biopsies in COPD. *Eur Respir J.* (2006) 27:60–64. doi: 10.1183/09031936.06.00007005
26. Hogg JC, Chu F, Utokaparch S, Woods R, Elliott WM, Buzatu L, et al. The nature of small-airway obstruction in chronic obstructive pulmonary disease. *N Engl J Med.* (2004) 350:2645–53. doi: 10.1056/NEJMoa032158
27. Suda T, Chida K, Hayakawa H, Imokawa S, Iwata M, Nakamura H, et al. Development of bronchus-associated lymphoid tissue in chronic hypersensitivity pneumonitis. *Chest.* (1999) 115:357–63. doi: 10.1378/chest.115.2.357
28. Elliot JG, Jensen CM, Mutavdzic S, Lamb JP, Carroll NG, James AL. Aggregations of lymphoid cells in the airways of nonsmokers, smokers, and subjects with asthma. *Am J Respir Crit Car. Med.* (2004) 169:712–8. doi: 10.1164/rccm.200308-1167OC
29. Lee JJ, McGarry MP, Farmer SC, Denzler KL, Larson KA, Carrigan PE, et al. Interleukin-5 expression in the lung epithelium of transgenic mice leads to pulmonary changes pathognomonic of asthma. *J Exp Med.* (1997) 185:2143–56. doi: 10.1084/jem.185.12.2143
30. Feghali-Bostwick CA, Gadgil AS, Otterbein LE, Pilewski JM, Stoner MW, Csizmadia E, et al. Autoantibodies in patients with chronic obstructive pulmonary disease. *Am J Respir Crit Care Med.* (2008) 177:156–63. doi: 10.1164/rccm.200701-014OC
31. Demoor T, Bracke KR, Maes T, Vandooren B, Elewaut D, Pilette C, et al. Role of lymphotoxin-alpha in cigarette smoke-induced inflammation and lymphoid neogenesis. *Eur Respir J.* (2009) 34:405–16. doi: 10.1183/09031936.00101408
32. Brusselle GG, Demoor T, Bracke KR, Brandsma CA, Timens W. Lymphoid follicles in (very) severe COPD: beneficial or harmful? *Eur Respir J.* (2009) 34:219–30. doi: 10.1183/09031936.00150208
33. Mohrs M, Shinkai K, Mohrs K, Locksley RM. Analysis of type 2 immunity *in vivo* with a bicistronic IL-4 reporter. *Immunity.* (2001) 15:303–11. doi: 10.1016/S1074-7613(01)00186-8
34. Mohrs K, Wakil AE, Killeen N, Locksley RM, Mohrs M. A two-step process for cytokine production revealed by IL-4 dual-reporter mice. *Immunity.* (2005) 23:419–29. doi: 10.1016/j.immuni.2005.09.006
35. Wills-Karp M, Luyimbazi J, Xu X, Schofield B, Neben TY, Karp CL, et al. Interleukin-13: central mediator of allergic asthma. *Science.* (1998) 282:2258–61. doi: 10.1126/science.282.5397.2258
36. Sakaguchi S, Yamaguchi T, Nomura T, Ono M. Regulatory T cells and immune tolerance. *Cell.* (2008) 133:775–87. doi: 10.1016/j.cell.2008.05.009
37. Sakaguchi S, Miyara M, Costantino CM, Hafler DA. FOXP3+ regulatory T cells in the human immune system. *Nat Rev Immunol.* (2010) 10:490–500. doi: 10.1038/nri2785
38. Jaffar Z, Sivakuru T, Roberts K. CD4+CD25+ T cells regulate airway eosinophilic inflammation by modulating the Th2 cell phenotype. *J.Immunol.* (2004) 172:3842–9. doi: 10.4049/jimmunol.172.6.3842
39. Akbari O, Freeman GJ, Meyer EH, Greenfield EA, Chang TT, Sharpe AH, et al. Antigen-specific regulatory T cells develop via the ICOS-ICOS-ligand pathway and inhibit allergen-induced airway hyperreactivity. *Nat Med.* (2002) 8:1024–32. doi: 10.1038/nm745
40. Schuijs MJ, Willart MA, Vergote K, Gras D, Deswarte K, Ege MJ, et al. Farm dust and endotoxin protect against allergy through A20 induction in lung epithelial cells. *Science.* (2015) 349:1106–10. doi: 10.1126/science.aac6623
41. Hammad H, Chieppa M, Perros F, Willart MA, Germain RN, Lambrecht BN. House dust mite allergen induces asthma via Toll-like receptor 4 triggering of airway structural cells. *Nat Med.* (2009) 15:410–6. doi: 10.1038/nm.1946
42. Brinkmann V, Cyster JG, Hla T. FTY720: sphingosine 1-phosphate receptor-1 in the control of lymphocyte egress and endothelial barrier function. *Am. J Transpl.* (2004) 4:1019–25. doi: 10.1111/j.1600-6143.2004.00476.x
43. Zhi L, Kim P, Thompson BD, Pitsillides C, Bankovich AJ, Yun SH, et al. FTY720 blocks egress of T cells in part by abrogation of their adhesion on the lymph node sinus. *J Immunol.* (2011) 187:2244–51. doi: 10.4049/jimmunol.1100670
44. Karmouty-Quintana H, Siddiqui S, Hassan M, Tsuchiya K, Risse PA, Xicota-Vila L, et al. Treatment with a sphingosine-1-phosphate analog inhibits airway remodeling following repeated allergen exposure. *Am J Physiol Lung Cell Mol Physiol.* (2012) 302:L736–45. doi: 10.1152/ajplung.00050.2011
45. Baluk P, Adams A, Phillips K, Feng J, Hong YK, Brown MB, et al. Preferential lymphatic growth in bronchus-associated lymphoid tissue in sustained lung inflammation. *Am J Pathol.* (2014) 184:1577–92. doi: 10.1016/j.ajpath.2014.01.021
46. Halle S, Dujardin HC, Bakocevic N, Fleige H, Danzer H, Willenzon S, et al. Induced bronchus-associated lymphoid tissue serves as a general priming site for T cells and is maintained by dendritic cells. *J Exp Med.* (2009) 206:2593–601. doi: 10.1084/jem.20091472
47. Hiramatsu K, Azuma A, Kudoh S, Desaki M, Takizawa H, Sugawara I. Inhalation of diesel exhaust for three months affects major cytokine expression and induces bronchus-associated lymphoid tissue formation in murine lungs. *Exp Lung Res.* (2003) 29:607–22. doi: 10.1080/01902140390240140
48. Shilling RA, Williams JW, Perera J, Berry E, Wu Q, Cummings OW, et al. Autoreactive T and B cells induce the development of bronchus-associated lymphoid tissue in the lung. *Am J Respir Cell Mol Biol.* (2013) 48:406–14. doi: 10.1165/rcmb.2012-0065OC
49. Coombes JL, Siddiqui KR, Arancibia-Carcamo CV, Hall J, Sun CM, Belkaid Y, et al. A functionally specialized population of mucosal CD103+ DCs induces Foxp3+ regulatory T cells via a TGF-beta and retinoic acid-dependent mechanism. *J Exp Med.* (2007) 204:1757–64. doi: 10.1084/jem.20070590
50. Mora JR, Bono MR, Manjunath N, Weninger W, Cavanagh LL, Rosemblatt M, et al. Selective imprinting of gut-homing T cells by Peyer's patch dendritic cells. *Nature.* (2003) 424:88–93. doi: 10.1038/nature01726
51. Hu D, Mohanta SK, Yin C, Peng L, Ma Z, Srikakulapu P, et al. Artery tertiary lymphoid organs control aorta immunity and protect against atherosclerosis via vascular smooth muscle cell lymphotoxin beta receptors. *Immunity.* (2015) 42:1100–15. doi: 10.1016/j.immuni.2015.05.015
52. Glatman Zaretsky A, Taylor JJ, King IL, Marshall FA, Mohrs M, Pearce EJ. T follicular helper cells differentiate from Th2 cells in response to helminth antigens. *J Exp Med.* (2009) 206:991–9. doi: 10.1084/jem.20090303
53. King IL, Mohrs M. IL-4-producing CD4+ T cells in reactive lymph nodes during helminth infection are T follicular helper cells. *J Exp Med.* (2009) 206:1001–7. doi: 10.1084/jem.20090313

Conflict of Interest: The authors declare that the research was conducted in the absence of any commercial or financial relationships that could be construed as a potential conflict of interest.

frontiers in Pediatrics

CASE REPORT
published: 16 October 2020
doi: 10.3389/fped.2020.580963

Acute Cervical Longitudinally Extensive Transverse Myelitis in a Child With Lipopolysaccharide-Responsive-Beige-Like-Anchor-Protein (LRBA) Deficiency: A New Complication of a Rare Disease

Matteo Chinello[1], Margherita Mauro[2], Gaetano Cantalupo[3], Giacomo Talenti[4], Sara Mariotto[5], Rita Balter[1], Massimiliano De Bortoli[1], Virginia Vitale[1], Ada Zaccaron[1], Elisa Bonetti[1], Daniela Di Carlo[6], Federica Barzaghi[7] and Simone Cesaro[1]*

[1] Pediatric Hematology Oncology, Azienda Ospedaliera Universitaria Integrata, Verona, Italy, [2] Pediatric Department, Santa Maria Degli Angeli Hospital, Pordenone, Italy, [3] Child Neuropsychiatry, University of Verona, Verona, Italy, [4] Department of Diagnostics and Pathology, Neuroradiology Unit, Verona University Hospital, Verona, Italy, [5] Neurology Unit, Department of Neurosciences, Biomedicine and Movement Sciences, University of Verona, Verona, Italy, [6] Pediatric Department, University of Verona, Verona, Italy, [7] Pediatric Immunohematology and Bone Marrow Transplantation Unit, San Raffaele Telethon Institute for Gene Therapy, Milan, Italy

OPEN ACCESS

Edited by:
Michael Zemlin,
Saarland University Hospital, Germany

Reviewed by:
Gholamreza Azizi,
Alborz University of Medical Sciences, Iran
Cinzia Milito,
Sapienza University of Rome, Italy

***Correspondence:**
Matteo Chinello
matteo.chinello@aovr.veneto.it

Specialty section:
This article was submitted to Pediatric Immunology, a section of the journal Frontiers in Pediatrics

Received: 07 July 2020
Accepted: 10 September 2020
Published: 16 October 2020

Citation:
Chinello M, Mauro M, Cantalupo G, Talenti G, Mariotto S, Balter R, De Bortoli M, Vitale V, Zaccaron A, Bonetti E, Di Carlo D, Barzaghi F and Cesaro S (2020) Acute Cervical Longitudinally Extensive Transverse Myelitis in a Child With Lipopolysaccharide-Responsive-Beige-Like-Anchor-Protein (LRBA) Deficiency: A New Complication of a Rare Disease. Front. Pediatr. 8:580963. doi: 10.3389/fped.2020.580963

Lipopolysaccharide responsive beige-like anchor protein (LRBA) deficiency is a primary immunodeficiency disorder (PID) that can cause a common variable immunodeficiency (CVID)-like disease. The typical features of the disease are autoimmunity, chronic diarrhea, and hypogammaglobulinemia. Neurological complications are also reported in patients affected by LRBA deficiency. We describe a 7-year old female with an acute cervical longitudinally extensive transverse myelitis (LETM) as a feature of LRBA deficiency. This is the first case of LETM associated with LRBA deficiency described in literature.

Keywords: lipopolysaccharide responsive beige-like anchor protein (LRBA), myelitis, acute cervical longitudinally extensive transverse myelitis, common variable immune deficiency (CVID), autommunity

INTRODUCTION

Lipopolysaccharide responsive beige-like anchor protein (LRBA) deficiency is a primary immunodeficiency disorder (PID) described as a cause of common variable immunodeficiency (CVID)-like disease (1). Several genes responsible of different subgroups of CVID have been identified (2), but the majority of patients with CVID have an unknown genetic etiology. CVID is a diagnosis of exclusion and so it is not surprising that CVID has heterogeneous clinical and laboratory presentations (3). This disease can be caused by LRBA gene defects (1). LRBA is a member of BEACH-WD40 protein family and it is expressed in several tissues (1, 4). The LRBA gene is located on 4q31.3, contains 57 exons and encodes a protein containing 2851 amino acid

residues (5). The LRBA protein is widely expressed in several cell types including hematopoietic, neural, gastrointestinal, and endocrine cells[1] with an high expression especially in lymphocytes (1, 6). This intracellular protein regulates the lysosomal degradation of cytotoxic T lymphocytes antigen-4 (CTLA-4), an inhibitory checkpoint receptor on T cells (6). For this reason patients with LRBA deficiency present an increase in CTLA4 degradation with clinical signs similar to CTLA4 haploinsufficient individuals (7, 8). An increase expression of LRBA is also described in many cancers, suggesting that the protein promotes cell survival by inhibiting apoptosis (9). The clinical features in patients affected by LRBA deficiency are heterogeneous with age of presentation ranging from 2 months to 12 years. There is not a genotype-phenotype correlation (10). LRBA deficiency can present with a wide spectrum of clinical manifestations such as inflammatory bowel disease (IBD)-like enteropathy, splenomegaly, pneumonia, autoimmune disease (AID) like immune thrombocytopenia purpura (ITP) and autoimmune hemolytic anemia (AIHA), hypogammaglobulinemia, B-cell deficiency, reduction in numbers of CD4+ T cells and regulatory T cells and autophagy (1, 6, 10–13). LRBA deficiency is suspected on the basis of heterogeneous clinical manifestations and immunological dysregulation that can be found through blood tests. The diagnosis currently relies on gene sequencing approaches or on the detection of LRBA protein by flow cytometry (14). The conventional treatment options for this disease have included various immunosuppressive agents such as corticosteroids, sirolimus, abatacept (soluble CTLA4- immunoglobulin fusion protein) (6, 13, 15) or Hematopoietic Stem Cell Transplantation (HSCT) (16). Neurological complications in patient affected by LRBA deficiency are described (6, 10, 17) even if they are not one of the typical features of the disease. We describe a 7-year old female with an acute cervical longitudinally extensive transverse myelitis (LETM) as a feature of LRBA deficiency. This is the first case of LETM associated with LRBA deficiency described in literature.

CASE REPORT

A 7-year-old female affected by LRBA deficiency was referred to our hospital for fever, stiff neck, and right cervical lymphadenopathy, that were unresponsive to anti-inflammatory drugs and oral antibiotic therapy.

The patient was born to unrelated parents after a full-term gestation. The birth weight was 2,420 g. The girl had normal psychomotor development. From 6 months of age she began to present recurrent severe infections during neutropenia associated with diffuse lymphadenomegaly (inguinal, abscellar, laterocervical, and mesenteric) and a diagnosis of autoimmune neutropenia was made. At 18 months she was hospitalized for cholelithiasis and hepatomegaly with autoimmune hepatitis and initial signs of cirrhosis. At 2 years she developed chronic diarrhea, hypertriglyceridemia, diffuse lipodystrophy, and splenomegaly. Double negative T cells resulted high (2.6% of total lymphocytes, normal value NV < 1.7%) and FAS-mediated apoptosis was abnormal. Genetic tests for autoimmune lymphoproliferative syndrome (ALPS) were negative (FAS, FAS ligand and caspase 10). In the suspicion of (ALPS)-like phenotype disease a therapy with mycophenolate mofetil was started. After one year, for the worsening of the lipodystrophy, anakinra, and then canakinumab were administered with initial but temporary clinical improvement. For persistent hypogammaglobulinemia the patient needed monthly administrations of immunoglobulins. At 4.5 years she underwent splenectomy for splenic abscess and started prophylaxis with amoxicillin/clavulanate and antiplatelet therapy with aspirin. At 5 years a mutation of Insulin Receptor Substrate 1 (IRS-1) which could lead to insulin resistance, leptin deficiency, and steatohepatitis, was detected. Therefore, leptin was administered with reduction of liver dimension, improvement of triglycerides level and no longer needing of insulin. The patient started empirical immunosuppressive therapy with prednisone (max 1 mg/kg/day) and sirolimus due to poor response to previous therapy. After few months the LRBA deficiency was identified by next generation sequencing (NGS) demonstrating double heterozygosity for two LRBA mutations; one inherited from the father (non sense c.7681 C>T: p.Q2561X) and one from the mother (splice disruption, c.1359 + 1G>A). Only sirolimus therapy was ongoing at the time of admission to our department.

On admission, she was conscious alert and oriented. Her heart rate, respiratory rate, blood pressure and body temperature were within normal range. She presented severe cervical pain associated with left deviation of the neck. The low-grade fever (37.6–37.8°C) and the stiff neck appeared 10 days earlier, but the pain was initially moderate and the patient was treated with anti-inflammatory drugs and oral antibiotic therapy. She received the last administrations of immunoglobulins 2 days before hospitalization. On examination, a right laterocervical lymphadenomegaly was observed. After few hours she developed right upper limb hyposthenia and fecal incontinence. Blood exams showed an increase of white blood cells (WBC) with low inflammatory markers (**Table 1**). Microbiological analysis were negative (blood cultures, urine culture, stool culture; Cytomegalovirus (CMV), Epstein Barr Virus (EBV), Adenovirus and Toxoplasma gondii serology; antistreptolysin antibodies, EBV, and CMV DNA copy number quantification by real-time polymerase chain reaction). Magnetic Resonance Imaging (MRI) was performed and showed extensive spinal cord T2- hyperintense lesion extending from the medulla oblongata to D3 level, with significant spinal cord

TABLE 1 | Blood exams.

	Value	Normal value
White blood cells (WBC)	20.840/mm^3	4,500–13,500
Neutrophils	13.970/mm^3	600–6,400
C-reactive protein (CRP)	6 mg/L	<5

[1]GeneCards. http://www.genecards.org/cgi-bin/carddisp.pl?gene=LRBA

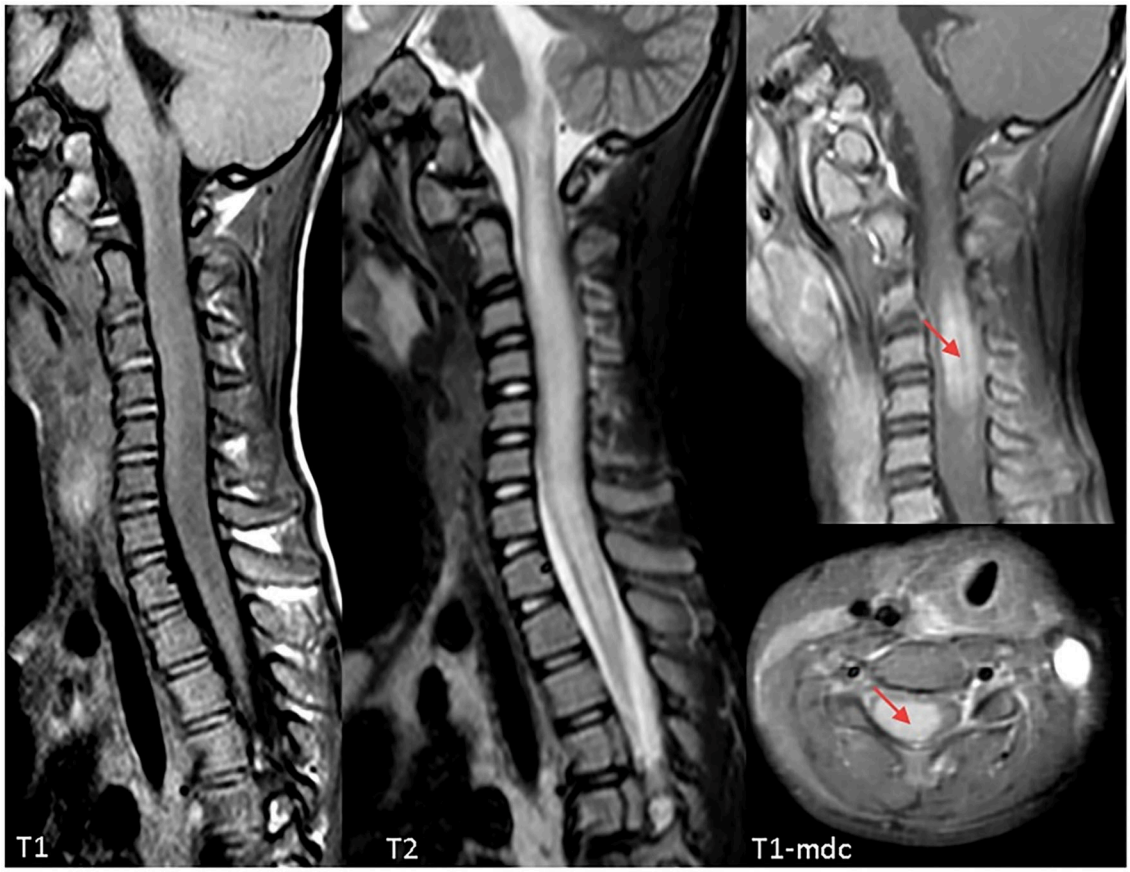

FIGURE 1 | Cervical Magnetic Resonance Imaging (MRI) at clinical onset demonstrating a longitudinally extensive signal abnormality involving the cervical spinal cord, extending from the obex to D3. The cord appears markedly swollen, both gray and white matter are involved, and post-contrast sequences demonstrate marked cord enhancement between C3 and C5 (red arrows). Findings are compatible with acute longitudinally extensive transverse myelitis (LETM).

TABLE 2 | Cerebrospinal fluid (CSF) analysis.

	Value	Normal value
Cellularity	70 cells/uL (100% lymphocytes)	<8
Glucose level	50 mg/dL	50–81
Protein content	1.35 g/L	0.15–0.45
IgG levels	82 mg/L	<34 mg/L
Albumin	874 mg/L	<320 mg/L
CSF/serum albumin quotient	23.75	<7
IgG-index	0.46	<0.70

swelling and marked contrast enhancement at C3–C5 level which was compatible with acute Longitudinally Extensive Transverse Myelitis (LETM) (**Figure 1**). Cerebrospinal fluid (CSF) analysis revealed an increase of white blood cells (100% lymphocytes), proteins and IgG levels with high CSF/serum albumin quotient and normal IgG-index (**Table 2**). CSF analysis for bacterial and viral infections yielded negative results (*Escherichia coli*, Haemophilus influenzae, Listeria monocytogenes, Neisseria meningitidis, Streptococcus agalatiae, Streptococcus pneumoniae, EBV, CMV, Herpes simplex Virus 1 (HSV1), Herpes simplex Virus 2 (HSV2), Human parechovirus, Varicella zoster virus (VZV), Enterovirus and Cryptococcus neoformans). Serum antibodies to myelin oligodendrocyte glycoprotein (MOG live cell-based assay) and aquaporin-4 (AQP4 fixed cell-based assay, Euroimmune commercial kit-4) were negative. Isoelectrofocusing revealed the presence of oligoclonal bands in both serum and CSF type 4 "mirror" pattern. An extensive autoimmune screening was negative [antinuclear antibodies (ANA), anti-double stranded DNA antibodies (anti-ds-DNA), anti-neutrophil cytoplasmic antibodies (ANCA, p-ANCA, c-ANCA, a-ANCA, anti PR3, anti myeloperoxidase antibodies MPO), anti-saccharomyces cerevisiae antibodies (ASCA), anti-smooth muscle antibody (ASMA), anti-liver-kidney microsome antibodies (LKM), anti-insulin antibody, TSH receptor antibodies (TRAb)]. The patient received intravenous dexamethasone at the dosage of 0.15 mg/kg for 27 days followed by a 9-week tapering dose of oral steroids which resulted in a rapid clinical improvement. Follow-up MRIs, performed after 20 and 55 days, respectively, (**Figure 2**),

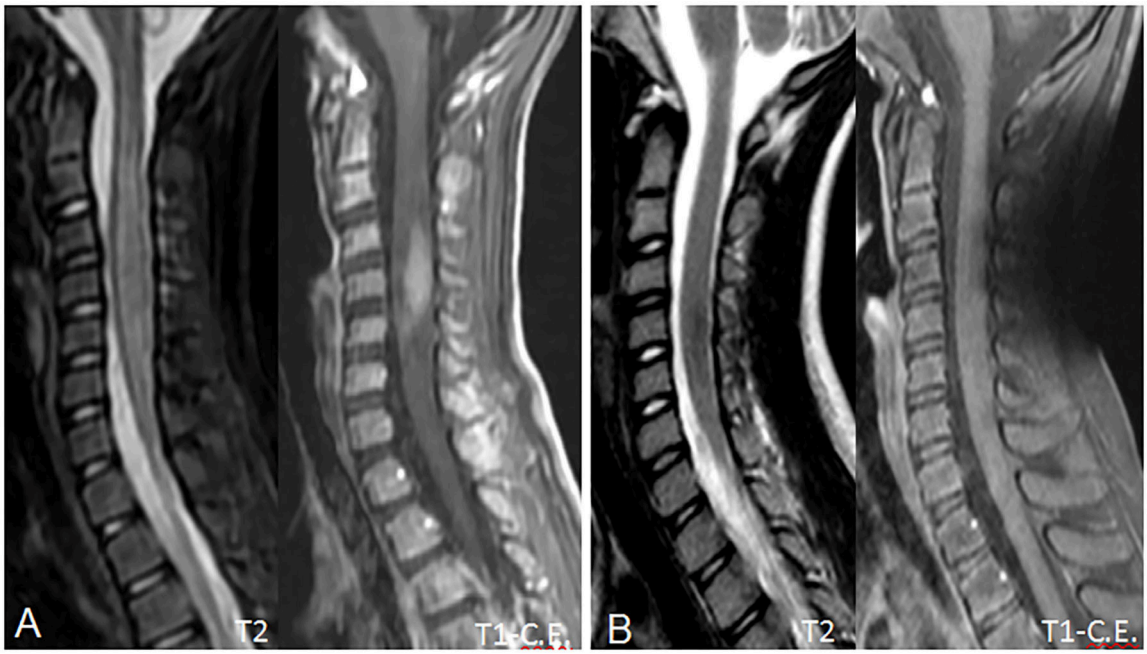

FIGURE 2 | Follow-up MRI scans at 20 **(A)** and 55 **(B)** days, showing progressive reduction of the spinal cord swelling and contrast enhancement. In **(B)**, contrast enhancement has completely regressed, due to blood-brain barrier restoration, and the spinal cord shows a near-normal appearance with no residual disease. No spinal cord atrophy is noted.

showed progressive improvement of spinal cord oedema and enhancement in parallel with a complete clinical recovery. The patient was then transferred to another institution for stem cell transplantation and the last follow-up MRI before transplant she was referred completely negative (image not available).

DISCUSSION

Patients with LRBA deficiency typically present immunodeficiency, inflammatory bowel disease (IBD)-like enteropathy, and autoimmune disease (AID) (1, 11–13). Some studies report an imbalance in Th subsets, in particular in Th1-like Th17 and Treg cells and their corresponding cytokines in LRBA deficiency. This condition might be important in the immunopathogenesis of autoimmunity and enteropathy (18). According to some publications a defect of LRBA can be associated with an IPEX-like (19) or ALPS-like (20) clinical presentation thus similar to our patient's phenotype. Neurological complications of the disease have been described (6, 10, 17). Alkhairy et al. (10) reported that neurological features occur in 23% of patients. The authors, with the exception of myasthenia gravis which has an autoimmune etiology, describe patients with cerebral lesions and nervous tissue atrophy. They report two patients with cerebral granulomas, one with granuloma-like lesion with demyelination resulting in unilateral optic nerve atrophy, one with unilateral optic nerve atrophy, one with cerebral and cerebellar atrophy and another with parietal lobe lesion complicated by seizures (10). Tesi et al. described a patient with LRBA deficiency complicated with an acute disseminated encephalomyelitis (ADEM) who underwent hematopoietic stem cell transplant (17). ADEM has also been described in one CTLA-4 haploinsufficient patient (7) and in patient with CVID (21). To the best of our knowledge this is the first ever reported patient with LETM associated with LRBA deficiency. We believe that the high value of white blood count is a consequence of inflammation. The exclusion of infectious and neoplastic nature of the lesion, together with the good response to steroid treatment, allow us to consider it an inflammatory seronegative LETM. This condition is observed in a group of inflammatory autoimmune disorders, often in the context of neuromyelitis optica spectrum disorders (NMOSD) (22–25). These disorders are mostly related to the presence of antibodies against aquaporin (AQP4) or against myelin oligodendrocyte glycoprotein (MOG) (24–26). However, in some patients AQP4-Antibodies and MOG-Antibodies are lacking, thus these patients are usually labeled "double seronegative LETM" or "seronegative LETM" (26, 27). We consider LETM as one of the possible immune-mediated manifestations that compose the clinical spectrum of LRBA deficiency.

DATA AVAILABILITY STATEMENT

The original contributions presented in the study are included in the article/supplementary material, further inquiries can be directed to the corresponding author/s.

AUTHOR CONTRIBUTIONS

MC: involvement in medical diagnosis and follow up of the patient, first writer of the manuscript. MM: involvement in medical diagnosis of the patient and she helped to write the manuscript. GC, GT, SM, RB, MD, VV, AZ, EB, and DD: involvement in diagnosis and management of the patient. FB involvement in genetic diagnosis. SC: involvement in diagnosis and management of the patient, supervision of the process of the manuscript. All authors read and approved the final manuscript.

REFERENCES

1. Lopez-Herrera G, Tampella G, Pan-Hammarström Q, Herholz P, Trujillo-Vargas CM, Phadwal K, et al. Deleterious mutations in LRBA are associated with a syndrome of immunodeficiency and autoimmunity. *Am J Hum Genet*. (2012) 90:986–1001. doi: 10.1016/j.ajhg.2012.04.015
2. Abolhassani H, Sagvand BT, Shokuhfar T, Mirminachi B, Rezaei N, Aghamohammadi A. A review on guidelines for management and treatment of common variable immunodeficiency. *Expert Rev Clin Immunol*. (2013) 9:561–75. doi: 10.1586/eci.13.30
3. Yong PF, Thaventhiran JE, Grimbacher B. "A rose is a rose is a rose," but CVID is Not CVID common variable immune deficiency (CVID), what do we know in 2011? *Adv Immunol*. (2011) 111:47–107. doi: 10.1016/B978-0-12-385991-4.00002-7
4. De Lozanne A. The role of BEACH proteins in Dictyostelium. *Traffic*. (2003) 4:6–12. doi: 10.1034/j.1600-0854.2003.40102.x
5. EnsemblGenomeBrowser. (2015). Available online at: http://www.ensembl.org/Homo_sapiens/Transcript/Sequence_Protein?db=core;g$=$ENSG00000198589;r$=$4:151185594--151936879;t$=$ENST00000510413 (accessed June 30, 2020).
6. Lo B, Zhang K, Lu W, Zheng L, Zhang Q, Kanellopoulou C, et al. Patients with LRBA deficiency show CTLA4 loss and immune dysregulation responsive to abatacept therapy. *Science*. (2015) 349:436–40. doi: 10.1126/science.aaa1663
7. Schubert D, Bode C, Kenefeck R, Hou TZ, Wing JB, Kennedy A, et al. Autosomal dominant immune dysregulation syndrome in humans with CTLA4 mutations. *Nat Med*. (2014) 20:1410–6. doi: 10.1038/nm.3746
8. Kuehn HS, OuyangW, Lo B, Deenick EK, Niemela JE, Avery DT, et al. Immune dysregulation in human subjects with heterozygous germline mutations in CTLA4. *Science*. (2014) 345:1623–7. doi: 10.1126/science.1255904
9. Wang JW, Gamsby JJ, Highfill SL, Mora LB, Bloom GC, Yeatman TJ, et al. Deregulated expression of LRBA facilitates cancer cell growth. *Oncogene*. (2004) 23:4089–97. doi: 10.1038/sj.onc.1207567
10. Alkhairy OK, Abolhassani H, Rezaei N, Fang M, Andersen KK, Chavoshzadeh Z, et al. Spectrum of phenotypes associated with mutations in LRBA. *J Clin Immunol*. (2016) 36:33–45. doi: 10.1007/s10875-015-0224-7
11. Burns SO, Zenner HL, Plagnol V, Curtis J, Mok K, Eisenhut M, et al. LRBA gene deletion in a patient presenting with autoimmunity without hypogammaglobulinemia. *J Allergy Clin Immunol*. (2012) 130:1428–32. doi: 10.1016/j.jaci.2012.07.035
12. Alangari A, Alsultan A, Adly N, Massaad MJ, Kiani IS, Aljebreen A, et al. LPS-responsive beige-like anchor (LRBA) gene mutation in a family with inflammatory bowel disease and combined immunodeficiency. *J Allergy Clin Immunol*. (2012) 130:481–8. doi: 10.1016/j.jaci.2012.05.043
13. Habibi S, Zaki-Dizaji M, Rafiemanesh H, Lo B, Jamee M, Gámez-Díaz L, et al. Clinical, immunologic, and molecular spectrum of patients with LPS-responsive beige-like anchor protein deficiency: a systematic review. *J Allergy Clin Immunol Pract*. (2019) 7:2379–86.e5. doi: 10.1016/j.jaip.2019.04.011
14. Gámez-Díaz L, Sigmund EC, Reiser V, Vach W, Jung S, Grimbacher B. Rapid flow cytometry-based test for the diagnosis of lipopolysaccharide responsive beige-like anchor (LRBA) deficiency. *Front Immunol*. (2018) 9:720. doi: 10.3389/fimmu.2018.00720
15. Azizi G, Abolhassani H, Mahdaviani, SA, Chavoshzadeh Z, Eshghi P, Yazdani R, et al. Clinical, immunologic, molecular analyses and outcomes of iranian patients with LRBA deficiency: a longitudinal study. *Pediatr Allergy Immunol*. (2017) 28:478–84. doi: 10.1111/pai.12735
16. Tesch VK, Abolhassani H, Shadur B, Zobel J, Mareika Y, Sharapova S, et al. Inborn errors, clinical, and registry working parties of the european society for blood and marrow transplantation and the European society for Immunodeficiencies. Long-term outcome of LRBA deficiency in 76 patients after various treatment modalities as evaluated by the immune deficiency and dysregulation activity (IDDA) score. *J Allergy Clin Immunol*. (2020) 145:1452–63. doi: 10.1016/j.jaci.2019.12.896
17. Tesi B, Priftakis P, Lindgren F, Chiang SC, Kartalis N, Löfstedt A, et al., Successful hematopoietic stem cell transplantation in a patient with LPS-responsive beige-like anchor (LRBA) gene mutation. *J Clin Immunol*. (2016) 36:480–9. doi: 10.1007/s10875-016-0289-y
18. Azizi G, Mirshafiey A, Abolhassani H, Yazdani R, Ghanavatinejad A, Noorbakhsh F, et al. The imbalance of circulating T helper subsets and regulatory T cells in patients with LRBA deficiency: correlation with disease severity. *J Cell Physiol*. (2018) 233:8767–777. doi: 10.1002/jcp.26772
19. Jamee M, Zaki-Dizaji M, Lo B, Abolhassani H, Aghamahdi F, Mosavian M, et al. Clinical, immunological, and genetic features in patients with immune dysregulation, polyendocrinopathy, enteropathy, X-linked (IPEX) and IPEX-like syndrome. *J Allergy Clin Immunol Pract*. (2020) 8:P2747–2760.E7. doi: 10.1016/j.jaip.2020.04.070
20. Revel-Vilk S, Fischer U, Keller B, Nabhani S, Gámez-Díaz L, Rensing-Ehl A, et al. Autoimmune lymphoproliferative syndrome-like disease in patients with LRBA mutation. *Clin Immunol*. (2015) 159:84–92. doi: 10.1016/j.clim.2015.04.007
21. Kondo M, Fukao T, Teramoto T, Kaneko H, Takahashi Y, OkamotoH, et al. A common variable immunodeficiency patient who developed acute disseminated encephalomyelitis followed by the lennox-gastaut syndrome. *Pediatr Allergy Immunol*. (2005) 16:357–60. doi: 10.1111/j.1399-3038.2005.00279.x
22. Hor JY, Asgari N, Nakashima I, Broadley SA, Isabel Leite M, Kissani N. et al. Epidemiology of neuromyelitis optica spectrum disorder and its prevalence and incidence worldwide. *Front Neurol*. (2020) 11:501. doi: 10.3389/fneur.2020.00501
23. Sepúlveda M, Armangué T, Sola-Valls N, Arrambide G, Meca-Lallana JE, Oreja-Guevara C, et al. Neuromyelitis optica spectrum disorders: comparison according to the phenotype and serostatus. *Neurol Neuroimmunol Neuroinflamm*. (2016) 3:e225. doi: 10.1212/nxi.0000000000000225
24. Lechner C, Baumann M, Hennes EM, Schanda K, Marquard K, Karenfort M, et al. Antibodies to MOG and AQP4 in children with neuromyelitis optica and limited forms of the disease. *J Neurol Neurosurg Psychiatry*. (2016) 87:897–905. doi: 10.1136/jnnp-2015-311743
25. Höftberger R, Sepulveda M, Armangue T, Blanco Y, Rostásy K, Cobo Calvo A, et al. Antibodies to MOG and AQP4 in adults with neuromyelitis optica and suspected limited forms of the disease. *Mult Scler*. (2015) 21:866–74. doi: 10.1177/1352458514555785
26. Maillart E, Durand-Dubief F, Louapre C, Audoin B, Bourre B, Derache N, et al. Outcome and risk of recurrence in a large cohort of idiopathic longitudinally extensive transverse myelitis without AQP4/MOG antibodies. *J Neuroinflammation*. (2020) 17:128. doi: 10.1186/s12974-020-01773-w
27. Álvaro C-C, María S, Raphael B-V, Anne R, David B, Sergio M-Y, et al. Antibodies to myelin oligodendrocyte glycoprotein in aquaporin 4 antibody seronegative longitudinally extensive transverse myelitis: clinical and prognostic implications. *Mult Scler J*. (2016) 22:312–9. doi: 10.1177/1352458515591071

Conflict of Interest: The authors declare that the research was conducted in the absence of any commercial or financial relationships that could be construed as a potential conflict of interest.

frontiers in Immunology

MINI REVIEW
published: 16 October 2020
doi: 10.3389/fimmu.2020.593289

Chronic Mucocutaneous Candidiasis in Early Life: Insights Into Immune Mechanisms and Novel Targeted Therapies

Oded Shamriz[1,2*†], *Yuval Tal*[1†], *Aviv Talmon*[1] *and Amit Nahum*[3]

[1] *Allergy and Clinical Immunology Unit, Hadassah-Hebrew University Medical Center, Jerusalem, Israel,* [2] *The Lautenberg Center for Immunology and Cancer Research, Institute of Medical Research Israel-Canada, Hebrew University-Hadassah Medical School, Jerusalem, Israel,* [3] *Pediatrics Department A, Soroka University Medical Center and Faculty of Health Sciences, Ben-Gurion University of the Negev, Beer Sheva, Israel*

Children with chronic mucocutaneous candidiasis (CMC) experience recurrent infections with *Candida spp*. Moreover, immune dysregulation in the early life of these patients induces various autoimmune diseases and affects normal growth and development. The adaptive and innate immune system components play a significant role in anti-fungal response. This response is mediated through IL-17 production by T helper cells. Inborn errors in IL-17-mediated pathways or *Candida spp.* sensing molecules are known to cause CMC. In this review, we describe underlying immune mechanisms of monogenic primary immune deficiency disorders known to cause CMC. We will explore insights into current management of these patients and novel available therapies.

Keywords: CMC, chronic mucocutaneous candidiasis, immune dysregulation, primary immune deficiency, autoimmunity

OPEN ACCESS

Edited by:
Ravi Misra,
University of Rochester, United States

Reviewed by:
Satoshi Okada,
Hiroshima University, Japan
Beáta Tóth,
University of Debrecen, Hungary

***Correspondence:**
Oded Shamriz
odeds@hadassah.org.il

† These authors have contributed equally to this work and share first authorship

Specialty section:
This article was submitted to Autoimmune and Autoinflammatory Disorders, a section of the journal Frontiers in Immunology

Received: *10 August 2020*
Accepted: *08 September 2020*
Published: *16 October 2020*

Citation:
Shamriz O, Tal Y, Talmon A and Nahum A (2020) Chronic Mucocutaneous Candidiasis in Early Life: Insights Into Immune Mechanisms and Novel Targeted Therapies. Front. Immunol. 11:593289. doi: 10.3389/fimmu.2020.593289

INTRODUCTION

Children with chronic mucocutaneous candidiasis (CMC) experience recurrent infections with *Candida spp*. Infections can be mucosal or invasive, and isolated or associated with other infections. CMC can involve the vagina, esophagus, skin, and other organs. Moreover, severe immune dysregulation in the early life of these patients induces various autoimmune diseases and affects normal growth and development. Medical care is complex and usually warrants a combination of systemic anti-fungal and immunosuppressive agents (1–3).

Advances in genetic tests in the recent decade have expanded our knowledge of underlying immune mechanisms in CMC, elucidating an increasing number of newly defined primary immune-deficiency disorders (4). An in-depth characterization of the impaired immune pathways associated with CMC is critical in order to offer treatment tailored to the individual patient.

In this review, we describe monogenic primary immune-deficiency disorders known to cause CMC. Based on insights into underlying immune mechanisms, we explore different targeted therapies currently available or under development for these patients.

IMMUNE MECHANISMS UNDERLYING MONOGENIC CHRONIC MUCOCUTANEOUS CANDIDIASIS

The discovery of monogenic causes for CMC has enabled us to expand our knowledge of fundamental immune mechanisms (**Figure 1**).

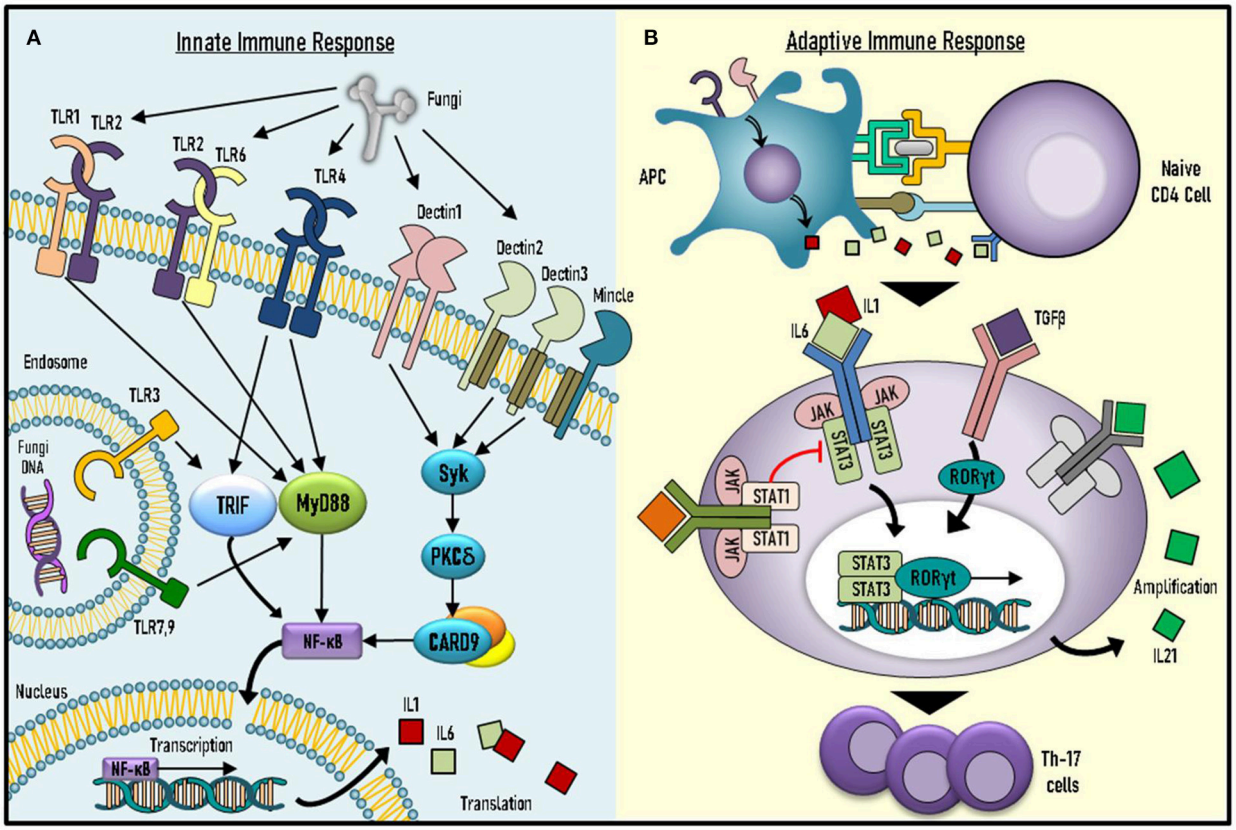

FIGURE 1 | Underlying mechanisms of immune responses against *Candida spp*. **(A)** *Candida spp.* recognition and initial immune response involve key molecules of the innate system. **(B)** Adaptive response against *Candida spp.* includes activation and differentiation of naïve $CD4^+$ T cells into effector T helper 17 (Th17) cells. TLR, toll-like receptor; PKC-δ, Protein kinase C-δ; MYD-88, Myeloid differentiation primary response 88; NFκB, Nuclear factor kappa-light-chain-enhancer of activated B cells; IL-Interleukin; APC, Antigen presenting cell; TGF-β, Transforming growth factor beta (TGF-β); JAK-Janus Kinase; STAT, Signal transducer and activator of transcription; RORγT, RAR-related orphan receptor gamma.

Immunity against *Candida* spp. consists of innate and adaptive responses. The innate response involves recognition of pathogen-associated molecular patterns (PAMPs) by pattern recognition receptors (PRRs) found in different cells of the innate immune system, such as monocytes and natural killer (NK) cells (5). Various PRRs are known to induce pro- and anti-inflammatory cytokine production in response to PAMP ligand binding. These PRRs include toll-like receptors (TLRs) 2, 3, 4, 6, and 9, as well as other receptors, such as dectin 1–3 (5). PAMP ligand binding to Dectin-1 leads to signal transduction via adaptor-molecule caspase activation and recruitment domain-containing 9 (CARD9) (5).

The adaptive immune system components also play a significant role in anti-fungal response. This includes pathways mediated by interleukin (IL)-17 and IL-22, which are produced by Th17 cells (6). Indeed, defective fungal sensing by the innate system, as well as abnormalities in IL-17-mediated pathways can induce CMC (**Table 1**). Impairments in the adaptive response can be further subdivided into decreased IL-17 cytokine production, impaired IL-17-mediated intracellular signaling or increased peripheral neutralization by anti-IL-17 autoantibodies.

Production of Neutralizing Autoantibodies Against IL-17 and IL-22

T cell development in the thymus includes clonal deletion of self-reactive T cells. This is achieved by the introduction of self-antigens to naive T cells by medullary thymic epithelial (mTEC) and dendritic cells. mTECs express autoimmune regulator (AIRE), an important facilitator of self-antigen gene expression (7).

AIRE deficiency is characterized by loss of self-tolerance and the presence of autoreactive T cells and multiple severe autoimmune diseases. *AIRE* loss-of-function (LOF) induces autoimmune polyendocrinopathy-candidiasis-ectodermal dystrophy (APECED). APECED is characterized by a classical triad of CMC, hypoparathyroidism, and Addison's disease (8), but other systems can be affected by autoimmunity in APECED, which can induce type 1 diabetes, hypothyroidism, hypogonadism, vitiligo, and various other autoimmune diseases (8). CMC in APECED patients is explained by decreased IL-17 and IL-22 cytokine serum levels, with corresponding increased titers of anti-IL-17 and anti-IL-22 neutralizing autoantibodies (9, 10). Thus, anti-IL-17/22 autoantibody production in

TABLE 1 | Reported genes associated with chronic mucocutaneous candidiasis.

Underlying immune mechanism	Syndrome	Involved gene	Inheritance	References
Anti-IL-17 neutralizing autoantibodies	APECED	*AIRE*	AR	(1–3)
IL-17 and IL-17 receptor decreased production	CMC	*IL17F* *IL17RC* *IL17RA*	AR	(4–7)
Defective Th17 differentiation or intracellular signaling	STAT1 gain of function	*STAT1*	AD	(2, 8–18)
	HIES	*STAT3*	AD	(19, 20)
		DOCK8	AR	(21)
		TYK2	AR	(22)
		ZNF341	AR	(23)
		PGM3	AR	(24)
		CARD11	AD	(25)
	RORγT deficiency	*RORC*	AR	(26)
	ACT1 deficiency	*ACT1*	AR	(27, 28)
	JNK1 deficiency	*MAPK8*	AD	(29)
	MSMD	*IL12*	AR	(30)
		IL12B		
		IL12RB1		
Decreased *Candida spp.* recognition	CARD9 deficiency	*CARD9*	AR	(31–33)
	Dectin 1 deficiency	*CLEC7A*	AR	(34)

IL, interleukin; APECED, Autoimmune polyendocrinopathy candidiasis ectodermal dystrophy; AIRE, autoimmune regulator; Th17, T helper 17; DOCK8, dedicator of cytokinesis 8; STAT, Signal transducer and activator of transcription; HIES, hyper IgE syndromes; RORγT, RAR-related orphan receptor gamma; CARD, Caspase recruitment domain-containing protein; PGM3, phosphoglucomutase 3; MSMD, Mendelian Susceptibility to Mycobacterial Diseases; TYK2, tyrosine-protein kinase 2; JNK1, c-Jun N-terminal kinase 1; AD, autosomal dominant; AR, autosomal recessive; CLEC7A, C-Type Lectin Domain Containing 7A.

APECED demonstrates the important association between immune dysregulation and CMC susceptibility.

Inborn Errors in IL-17 Production or IL-17 Receptor Surface Expression

IL-17R-mediated signaling has been shown in murine models to be essential in the immune response against *Candida spp.* (11, 12). In 2011, a single patient was reported to have a homozygous c.850C>T mutation in *IL-17RA* that caused reduced surface expression of IL-17RA on peripheral blood mononuclear cells (PBMC), reduced lymphocyte response to IL-17A/F stimuli, and increased susceptibility to *Candida spp.* infections (13). Two other patients with CMC had impaired IL-17F cytokine production due to *IL-17F* gene mutation (13, 14). Since then, several cohorts of CMC patients with IL-17R deficiencies have been reported, including 21 patients from 12 unrelated families with *IL-17RA* deficiency (15) and three patients with *IL-17RC* deficiency (16).

Defective Th17 Differentiation or Intracellular Signaling

Antigen-presenting cells produce IL-6, IL1-β, and IL-23, as well as activate transforming growth factor (TGF)-β in response to fungal infections. These cytokines bind to naïve $CD4^+$ T cells and trigger STAT3 followed by RAR-related orphan receptor (ROR)γT-mediated transcription. RORγT enhances production of IL-17A, IL-17F, and IL-21 by lymphocytes, through which they differentiate into Th17 cells. In turn, IL-21 further self-amplifies Th17-mediated immune responses (17, 18).

STAT1 Gain of Function

Inborn errors in any of the key players in Th17 differentiation can result in CMC. STAT1 is such a key component as was demonstrated from the study of autosomal dominant (AD) gain-of-function (GOF) mutations. *STAT1* mutations are probably the most common cause of monogenic CMC. These patients present with a wide clinical spectrum of immune dysregulation and increased susceptibility to bacterial, viral and fungal infections (19). Delayed dephosphorylation of STAT1 in these patients impairs the function of IL-6 and IL-21, thus decreasing STAT3-dependent differentiation of naïve $CD4^+$ T cells into Th17 cells (20). Of note, a recent report suggests that some *STAT1* GOF mutations may cause STAT1 levels to be high, although phosphorylation is normal (21). Disease severity appears to vary according to the mutation. For example, patients with the T385M mutation are somewhat phenotypically different from others. The T385M clinical spectrum consists of chronic candidiasis, recurrent severe invasive infections with bacterial pathogens, severe viral infections such as cytomegalovirus and John Cunningham virus and, last but not least, severe autoimmune phenomena reminiscent of a combined immunodeficiency disease. These patients show progressive loss of T and B cell function (22).

Hyper IgE Syndromes

Another striking example of impaired Th17 differentiation is *STAT3* LOF mutations known to cause autosomal dominant hyper immunoglobulin E syndrome (AD-HIES). These patients have severe eczema, skin abscesses, staphylococcal infections, and decreased or absent Th17 cells, resulting in increased susceptibility to *Candida* infections (23, 24). Markedly increased IgE levels and eosinophilia are indicative of immune dysregulation in these patients (25). *STAT3* LOF patients are distinctive by their non-immunologic features, which include dysmorphic facial features, retained primary teeth, vascular aneurysms, scoliosis, osteoporosis, and other musculoskeletal manifestations (26).

Autosomal recessive (AR) HIES is caused by mutations in *dedicator of cytokinesis* (*DOCK*) *8, ZNF341,* and *tyrosine kinase (TYK)2*. DOCK8 plays an important role in T cell activation and proliferation via its role in T cell cytoskeleton and actin reorganization. *DOCK8* mutation results in abnormal Th17 polarization and function (27). Clinical manifestations include an immune dysregulation phenotype consisting of allergic disorders, such as atopic dermatitis and food allergies, as well as increased susceptibility to staphylococcal, sino-pulmonary and viral infections (26).

Other gene mutations causing AR-HIES have been reported in *ZNF341*. This factor regulates the transcription

of *STAT3*, therefore patients with ZNF341 deficiencies are clinically similar to HIES with *STAT3* LOF. They are reported to have low levels of STAT3, reduced numbers of Th17 cells, and high risk for CMC (28). *TYK2*, a JAK family member, is critical for normal IL-12 and type I IFN expression. Mutation of *TYK2* can also cause AR-HIES. A patient with a homozygous TYK2 mutation was reported to have increased susceptibility to viral infections due to an impaired IFN-mediated response, and increased risk for fungal infections most probably due to defective IL-12/IL-23-mediated responses (29).

In addition, we should mention phosphoglucomutase (*PGM)3 and CARD11 deficiencies, both* reported in some studies to induce CMC and HIES. PGM3 deficiency is an AR-HIES disorder characterized by glycosylation defects that have multi-systemic manifestations including a neurodegenerative course. Sassi et al. reported occurrence of CMC in four out of nine patients (30), whereas Zhang et al. and Stray-Pederson et al. did not describe such findings (31, 32). LOF mutations in CARD11 were associated with severe atopy and immune dysregulation (33). In both disorders, it appears that Th17 cells are present, rather than absent. Therefore, the defect is probably functional and in the context of global T cell defects.

IL-12/IL-12 Receptor Pathway

Inborn errors in IL-12-mediated pathways are known to play a major cause for Mendelian susceptibility to mycobacterial disease (MSMD), increasing the risk for mycobacterial and viral infections. Interestingly, impaired defective IL-12 or IL-12R may underlie abnormal IL-23-mediated signaling, thus also exposing these patients to risk of developing CMC (13). Defective IL-23- and IL-12-mediated pathways were previously reported in patients with IL-23R and IL-12Rβ2 deficiencies, respectively. Impaired signaling in these patients induced MSMD; however no CMC was observed (34).

RORC, ACT1, and MAPK8 Mutations

STAT3 induces RORγT transcription, which leads to Th17 differentiation. AR mutations in RORγT have been demonstrated to decrease Th17 cell counts and result in CMC. Interestingly, these patients also presented with increased susceptibility to mycobacterial infections due to impaired interferon (IFN)-γ-mediated immunity, which also requires RORγT (35).

Regarding the IL-17-mediated pathway, one should also remember other proteins downstream. ACT1 is an intracellular adaptor protein in the IL-17-mediated signaling pathway. Several human mutations in *ACT1* are known to impair Th17 function and induce CMC (36, 37). *Staphylococcus aureus* blepharitis (37) and recurrent pneumonia (36) were also noted in these patients, who display characteristics of primary immune deficiency with dysregulation.

Finally, we should also mention mutations in *MAPK8*. AD *MAPK8* mutations resulting in c-Jun N-terminal kinase 1 (JNK1) deficiencies were previously reported to induce CMC. Impaired Th17 differentiation and decreased responses to IL-17A and IL-17F stimuli were shown. Interestingly, JNK1-deficient patients with CMC were also found to have a novel connective tissue disease, thus distinguishing mutant *MAPK8* from other monogenic inducers (38).

Decreased Recognition of Candida Infections

The innate response against *Candida spp*. is complex. Recognition of fungal PAMPs by PRR is critical for *Candida spp*. sensing, as is the Dectin-1–Syk–CARD9 signaling pathway. Biallelic mutations in CARD9 are reported to induce CMC and general increased susceptibility to fungal infections (39–45). In comparison with IL-17-associated inborn errors, CARD9 deficiency is thought to induce a more severe and invasive candidiasis, affecting various tissues including even the central nervous system (CNS) (46).

Dectin-1 deficiency has also been shown to induce reduced recognition of β-glucans with increased susceptibility to *Candida spp*. infections. However, an important feature of this disorder is the lack of susceptibility to other infections, which defines it as an isolated CMC (47). Impairment of the Dectin-1–Syk–CARD9 pathway also affects the differentiation of $CD4^+$ naïve T cells into Th17 cells, thereby interfering with the adaptive immune response to *Candida spp*. (6). Indeed, Tyr238X mutation in dectin-1 was previously described to cause CMC and onychomycosis phenotypes, as well as decreased IL-17 levels. However, phagocytosis and killing of *Candida spp*. in these patients were intact (47). Although dectin-1 deficiency is not included in International Union of Immunological Societies (IUIS) 2019 classification (4), the Tyr238X mutation can be found in gnomAD[1].

CURRENT MANAGEMENT OF MONOGENIC CHRONIC MUCOCUTANEOUS CANDIDIASIS

Current management of CMC consists mainly of prophylactic anti-fungal agents, such as fluconazole (1). However, other therapeutic modalities are currently available. Granulocyte-macrophage colony-stimulating factor (GM-CSF) production by PBMC is suggested to be reduced in CARD9-deficient patients. A patient with a hypomorphic CARD9 mutation presenting with CNS candidiasis was found to achieve clinical remission after GM-CSF administration (46), and GM-CSF has been found to be effective in other patients with CARD9 deficiency (48).

Histone deacetylase (HDAC) inhibitors were also examined in the management of CMC, especially in patients with STAT1 GOF mutations. Inhibition of histone acetylation is thought to affect the adaptive and innate immune systems. Indeed, HDAC inhibitors were found to rescue STAT3-mediated pathways in STAT1 GOF patients (49). Moreover, *in-vitro* treatment with HDAC inhibitors resulted in increased IL-22 production in response to *Candida spp*. (49).

[1]https://gnomad.broadinstitute.org/variant/12-10271087-A-C?dataset=gnomad_r2_1

Hematopoietic stem cell transplantations (HSCT) have some efficacy in CMC. For example, in two patients with CARD9 deficiency, HSCT from haploidentical and fully matched donors was successful, although a second HSCT was required in the first patient. Complete clinical resolution of fungal infections was noted in both patients (45). There are reports of successful HSCT in *STAT1* GOF patients as well, with complete resolution of immune dysregulation and rescue of Th17 differentiation and function (50). However, the results of HSCT in *STAT1* GOF are generally not favorable, with high rates of secondary graft failure (51).

Targeted immunotherapies for CMC-inducing inborn errors are therefore warranted. Ruxolitinib, a Janus kinase (JAK)1/2 inhibitor, is reportedly effective in *STAT1* GOF. Ruxolitinib treatment of a *STAT1* GOF child presenting with a clinical picture of CMC and autoimmune cytopenia was shown to directly intervene with the impaired immune pathways. It improved Th17 differentiation, decreased Th1-mediated responses, and attenuated CMC and immune dysregulation (52). Another study found that ruxolitinib in *STAT1* GOF patients can rescue NK cell maturation. Moreover, it was effective in restoring perforin expression on NK cells, thus rescuing NK cytotoxic function (53). Other reports of children with *STAT1* GOF mutations have confirmed the efficacy and safety of ruxolitinib in this disorder (54–56).

CONCLUSIONS

Current advances in next-generation sequencing have revealed various monogenic inducers of CMC. Understanding the impaired immune pathways involved in CMC is critical in the management of these patients. CMC is strongly associated with immune dysregulation and autoimmunity in early childhood. Therefore, a joint collaboration between immunologists, endocrinologists, and infectious disease and other specialists is needed in order to offer a personally tailored, effective, treatment to these patients.

AUTHOR CONTRIBUTIONS

OS study design, review of the literature, and manuscript writing. YT and AN study supervision and manuscript revisions. AT immune consultation and manuscript revision. All authors agree to be accountable for the content of the work.

REFERENCES

1. Pappas PG, Kauffman CA, Andes DR, Clancy CJ, Marr KA, Ostrosky-Zeichner L, et al. Clinical practice guideline for the management of candidiasis: 2016 update by the infectious diseases society of america. *Clin Infect Dis.* (2016) 62:e1–50. doi: 10.1093/cid/civ1194
2. Carey B, Lambourne J, Porter S, Hodgson T. Chronic mucocutaneous candidiasis due to gain-of-function mutation in STAT1. *Oral Dis.* (2019) 25:684–92. doi: 10.1111/odi.12881
3. Okada S. CMCD: chronic mucocutaneous candidiasis disease. *Nihon Rinsho Meneki Gakkai Kaishi*. (2017) 40:109–17. doi: 10.2177/jsci.40.109
4. Bousfiha A, Jeddane L, Picard C, Al-Herz W, Ailal F, Chatila T, et al. Human inborn errors of immunity: 2019 update of the iuis phenotypical classification. *J Clin Immunol.* (2020) 40:66–81. doi: 10.1007/s10875-020-00758-x
5. Netea MG, Leo Joosten JW. van der Meer JWM, Kullberg BJ, van de Veerdonk LF. Immune defence against Candida fungal infections. *Nat Rev Immunol.* (2015) 15:630–42. doi: 10.1038/nri3897
6. Okada S, Puel A, Casanova JL, Kobayashi M. Chronic mucocutaneous candidiasis disease associated with inborn errors of IL-17 immunity. *Clin Transl Immunol.* (2016) 5:e114. doi: 10.1038/cti.2016.71
7. Proekt I, Miller CN, Lionakis MS, Anderson MS. Insights into immune tolerance from AIRE deficiency. *Curr Opin Immunol.* (2017) 49:71–8. doi: 10.1016/j.coi.2017.10.003
8. Constantine GM, Lionakis MS. Lessons from primary immunodeficiencies: autoimmune regulator and autoimmune polyendocrinopathy-candidiasis-ectodermal dystrophy. *Immunol Rev.* (2019) 287:103–20. doi: 10.1111/imr.12714
9. Kisand K, Boe Wolff AS, Podkrajsek KT, Tserel L, Link M, Kisand KV, et al. Chronic mucocutaneous candidiasis in APECED or thymoma patients correlates with autoimmunity to Th17-associated cytokines. *J Exp Med.* (2010) 207:299–308. doi: 10.1084/jem.20091669
10. Puel A, Doffinger R, Natividad A, Chrabieh M, Barcenas-Morales G, Picard C, et al. Autoantibodies against IL-17A, IL-17F, and IL-22 in patients with chronic mucocutaneous candidiasis and autoimmune polyendocrine syndrome type I. *J Exp Med.* (2010) 207:291–7. doi: 10.1084/jem.20091983
11. Conti HR, Bruno VM, Childs EE, Daugherty S, Hunter JP, Mengesha BG, et al. IL-17 receptor signaling in oral epithelial cells is critical for protection against oropharyngeal candidiasis. *Cell Host Microbe.* (2016) 20:606–17. doi: 10.1016/j.chom.2016.10.001
12. Conti HR, Gaffen SL. IL-17-mediated immunity to the opportunistic fungal pathogen candida albicans. *J Immunol.* (2015) 195:780–8. doi: 10.4049/jimmunol.1500909
13. Puel A, Cypowyj S, Bustamante J, Wright JF, Liu L, Lim HK, et al. Chronic mucocutaneous candidiasis in humans with inborn errors of interleukin-17 immunity. *Science.* (2011) 332:65–8. doi: 10.1126/science.1200439
14. Bader O, Weig MS, Gross U, Schon MP, Mempel M, Buhl T. Photo quiz. A. 32-year-old man with ulcerative mucositis, skin lesions, nail dystrophy. Chronic mucocutaneous candidiasis by multidrug-resistant Candida albicans. *Clin Infect Dis.* (2012) 54:972. doi: 10.1093/cid/cir958
15. Levy R, Okada S, Beziat V, Moriya K, Liu C, Chai LY, et al. Genetic, immunological, and clinical features of patients with bacterial and fungal infections due to inherited IL-17RA deficiency. *Proc Natl Acad Sci USA.* (2016) 113:E8277–E285. doi: 10.1073/pnas.1618300114
16. Veverka KK, Feldman SR. Chronic mucocutaneous candidiasis: what can we conclude about IL-17 antagonism? *J Dermatolog Treat.* (2018) 29:475–80. doi: 10.1080/09546634.2017.1398396
17. Zhang S. The role of transforming growth factor beta in T helper 17 differentiation. *Immunology*, (2018) 155:24–35. doi: 10.1111/imm.12938
18. Puel A, Picard C, Cypowyj S, Lilic D, Abel L, Casanova JL. Inborn errors of mucocutaneous immunity to Candida albicans in humans: a role for IL-17 cytokines? *Curr Opin Immunol.* (2010) 22:467–74. doi: 10.1016/j.coi.2010.06.009
19. Toubiana J, Okada S, Hiller J, Oleastro M, Lagos Gomez M, Aldave Becerra JC, et al. Heterozygous STAT1 gain-of-function mutations underlie an unexpectedly broad clinical phenotype. *Blood.* (2016) 127:3154–64. doi: 10.1182/blood-2015-11-679902
20. Liu L, Okada S, Kong XF, Kreins AY, Cypowyj S, Abhyankar A, et al. Gain-of-function human STAT1 mutations impair IL-17 immunity and underlie chronic mucocutaneous candidiasis. *J Exp Med.* (2011) 208:1635–48. doi: 10.1084/jem.20110958

21. Zimmerman O, Olbrich P, Freeman AF, Rosen LB, Uzel G, Zerbe CS, et al. STAT1 gain-of-function mutations cause high total STAT1 levels with normal dephosphorylation. *Front Immunol.* (2019) 10:1433. doi: 10.3389/fimmu.2019.01433
22. Sharfe N, Nahum A, Newell A, Dadi H, Ngan B, Pereira SL, et al. Fatal combined immunodeficiency associated with heterozygous mutation in STAT1. *J Allergy Clin Immunol.* (2014) 133:807–17. doi: 10.1016/j.jaci.2013.09.032
23. Milner JD, Brenchley JM, Laurence A, Freeman AF, Hill BJ, Elias KM, et al. Impaired T(H)17 cell differentiation in subjects with autosomal dominant hyper-IgE syndrome. *Nature.* (2008) 452:773–6. doi: 10.1038/nature06764
24. de Beaucoudrey Puel AL, Filipe-Santos O, Cobat A, Ghandil P, Chrabieh M, et al. Mutations in STAT3 and IL12RB1 impair the development of human IL-17-producing T cells. *J Exp Med.* (2008) 205:1543–50. doi: 10.1084/jem.20080321
25. Gernez Y, Freeman AF, Holland SM, Garabedian E, Patel NC, Puck JM, et al. Autosomal dominant hyper-IgE syndrome in the USIDNET registry. *J Allergy Clin Immunol Pract.* (2018) 6:996–1001. doi: 10.1016/j.jaip.2017.06.041
26. Bergerson JRE, Freeman AF. An update on syndromes with a hyper-ige phenotype. *Immunol Allergy Clin North Am.* (2019) 39:49–61. doi: 10.1016/j.iac.2018.08.007
27. Engelhardt KR, McGhee S, Winkler S, Sassi A, Woellner C, Lopez-Herrera G, et al. Large deletions and point mutations involving the dedicator of cytokinesis 8 (DOCK8) in the autosomal-recessive form of hyper-IgE syndrome. *J Allergy Clin Immunol.* (2009) 124:1289–302.e4. doi: 10.1016/j.jaci.2009.10.038
28. Beziat V, Li J, Lin JX, Ma CS, Li P, Bousfiha A, et al. A recessive form of hyper-IgE syndrome by disruption of ZNF341-dependent STAT3 transcription and activity. *Sci Immunol.* (2018) 3:eaat4956. doi: 10.1126/sciimmunol.aat4956
29. Minegishi Y, Saito M, Morio T, Watanabe K, Agematsu K, Tsuchiya S, et al. Human tyrosine kinase 2 deficiency reveals its requisite roles in multiple cytokine signals involved in innate and acquired immunity. *Immunity.* (2006) 25:745–55. doi: 10.1016/j.immuni.2006.09.009
30. Sassi A, Lazaroski S, Wu G, Haslam SM, Fliegauf M, Mellouli F, et al. Hypomorphic homozygous mutations in phosphoglucomutase 3 (PGM3) impair immunity and increase serum IgE levels. *J Allergy Clin Immunol.* (2014) 133:1410–9. doi: 10.1016/j.jaci.2014.02.025
31. Zhang Y, Yu X, Ichikawa M, Lyons JJ, Datta S, Lamborn IT, et al. Autosomal recessive phosphoglucomutase 3 (PGM3) mutations link glycosylation defects to atopy, immune deficiency, autoimmunity, neurocognitive impairment. *J Allergy Clin Immunol.* (2014) 133:1400–9. doi: 10.1016/j.jaci.2014.02.013
32. Stray-Pedersen A, Backe PH, Sorte HS, Morkrid L, Chokshi NY, Erichsen HC, et al. PGM3 mutations cause a congenital disorder of glycosylation with severe immunodeficiency and skeletal dysplasia. *Am J Hum Genet.* (2014) 95:96–107. doi: 10.1016/j.ajhg.2014.05.007
33. Dorjbal B, Stinson JR, Ma CA, Weinreich MA, Miraghazadeh B, Hartberger JM, et al. Hypomorphic caspase activation and recruitment domain 11 (CARD11) mutations associated with diverse immunologic phenotypes with or without atopic disease. *J Allergy Clin Immunol.* (2019) 143:1482–95. doi: 10.1016/j.jaci.2018.08.013
34. Martinez-Barricarte R, Markle JG, Ma CS, Deenick EK, Ramirez-Alejo N, Mele F, et al. Human IFN-gamma immunity to mycobacteria is governed by both IL-12 and IL-23. *Sci Immunol.* (2018) 3:aau6759. doi: 10.1126/sciimmunol.aau6759
35. Okada S, Markle JG, Deenick EK, Mele F, Averbuch D, Lagos M, et al. IMMUNODEFICIENCIES. Impairment of immunity to Candida and Mycobacterium in humans with bi-allelic RORC mutations. *Science.* (2015) 349:606–13. doi: 10.1126/science.aaa4282
36. Bhattad S, Dinakar C, Pinnamaraju H, Ganapathy A, Mannan A. Chronic mucocutaneous candidiasis in an adolescent boy due to a novel mutation in TRAF3IP2. *J Clin Immunol.* (2019) 39:596–9. doi: 10.1007/s10875-019-00664-x
37. Boisson B, Wang C, Pedergnana V, Wu L, Cypowyj S, Rybojad M, et al. An ACT1 mutation selectively abolishes interleukin-17 responses in humans with chronic mucocutaneous candidiasis. *Immunity.* (2013) 39:676–86. doi: 10.1016/j.immuni.2013.09.002
38. Li J, Ritelli M, Ma CS, Rao G, Habib T, Corvilain E, et al. Chronic mucocutaneous candidiasis and connective tissue disorder in humans with impaired JNK1-dependent responses to IL-17A/F and TGF-beta. *Sci Immunol.* (2019) 4:aax7965. doi: 10.1126/sciimmunol.aax7965
39. Glocker EO, Hennigs A, Nabavi M, Schaffer AA, Woellner C, Salzer U, et al. A homozygous CARD9 mutation in a family with susceptibility to fungal infections. *N Engl J Med.* (2009) 361:1727–35. doi: 10.1056/NEJMoa0810719
40. Du B, Shen N, Hu J, Tao Y, Mo X, Cao Q. Complete clinical remission of invasive Candida infection with CARD9 deficiency after G-CSF treatment. *Comp Immunol Microbiol Infect Dis.* (2020) 70:101417. doi: 10.1016/j.cimid.2020.101417
41. Wang X, Wang A, Li R, Yu J. Cutaneous mucormycosis caused by mucor irregularis in a patient with CARD9 deficiency. *Br J Dermatol.* (2019) 180:213–214. doi: 10.1111/bjd.17144
42. Perez L, Messina F, Negroni R, Arechavala A, Bustamante J, Oleastro M, et al. Inherited CARD9 deficiency in a patient with both exophiala spinifera and aspergillus nomius severe infections. *J Clin Immunol.* (2020) 40:359–66. doi: 10.1007/s10875-019-00740-2
43. Corvilain E, Casanova JL, Puel A. Inherited CARD9 deficiency: invasive disease caused by ascomycete fungi in previously healthy children and adults. *J Clin Immunol.* (2018) 38:656–93. doi: 10.1007/s10875-018-0539-2
44. Quan C, Li X, Shi RF, Zhao XQ, Xu H, Wang B, et al. Recurrent fungal infections in a Chinese patient with CARD9 deficiency and a review of 48 cases. *Br J Dermatol.* (2019) 180:1221–5. doi: 10.1111/bjd.17092
45. Queiroz-Telles F, Mercier T, Maertens J, Sola CBS, Bonfim C, Lortholary O, et al. Successful allogenic stem cell transplantation in patients with inherited card9 deficiency. *J Clin Immunol.* (2019) 39:462–9. doi: 10.1007/s10875-019-00662-z
46. Gavino C, Cotter A, Lichtenstein D, Lejtenyi D, Fortin C, Legault C, et al. CARD9 deficiency and spontaneous central nervous system candidiasis: complete clinical remission with GM-CSF therapy. *Clin Infect Dis.* (2014) 59:81–4. doi: 10.1093/cid/ciu215
47. Ferwerda B, Ferwerda G, Plantinga TS, Willment JA, van Spriel AB, Venselaar H, et al. Human dectin-1 deficiency and mucocutaneous fungal infections. *N Engl J Med.* (2009) 361:1760–7. doi: 10.1056/NEJMoa0901053
48. Drewniak A, Gazendam RP, Tool AT, van Houdt M, Jansen MH, van Hamme JL, et al.. Invasive fungal infection and impaired neutrophil killing in human CARD9 deficiency. *Blood.* (2013) 121:2385–92. doi: 10.1182/blood-2012-08-450551
49. Rosler B, Wang X, Keating ST, Joosten LAB, Netea MG, van de Veerdonk LF. HDAC inhibitors modulate innate immune responses to micro-organisms relevant to chronic mucocutaneous candidiasis. *Clin Exp Immunol.* (2018) 194:205–19. doi: 10.1111/cei.13192
50. Kiykim A, Charbonnier LM, Akcay A, Karakoc-Aydiner E, Ozen A, Ozturk G, et al. Hematopoietic stem cell transplantation in patients with heterozygous stat1 gain-of-function mutation. *J Clin Immunol.* (2019) 39:37–44. doi: 10.1007/s10875-018-0575-y
51. Leiding JW, Okada S, Hagin D, Abinun M, Shcherbina A, Balashov DN, et al. Hematopoietic stem cell transplantation in patients with gain-of-function signal transducer and activator of transcription. 1 mutations. *J Allergy Clin Immunol.* (2018):141:704–17.e5. doi: 10.1016/j.jaci.2017.03.049
52. Weinacht KG, Charbonnier LM, Alroqi F, Plant A, Qiao Q, Wu H, et al. Ruxolitinib reverses dysregulated T helper cell responses and controls autoimmunity caused by a novel signal transducer and activator of transcription 1 (STAT1) gain-of-function mutation. *J Allergy Clin Immunol.* (2017) 139:1629–40.e2. doi: 10.1016/j.jaci.2016.11.022
53. Vargas-Hernandez A, Mace EM, Zimmerman O, Zerbe CS, Freeman AF, Rosenzweig S, et al. Ruxolitinib partially reverses functional natural killer cell deficiency in patients with signal transducer and activator of transcription 1 (STAT1) gain-of-function mutations. *J Allergy Clin Immunol.* (2018) 141:2142–55.e5. doi: 10.1101/157271
54. Al Shehri T, Gilmour K, Gothe F, Loughlin S, Bibi S, Rowan AD, et al. Novel gain-of-function mutation in stat1 sumoylation site leads to

CMC/CID phenotype responsive to ruxolitinib. *J Clin Immunol.* (2019) 39:776–85. doi: 10.1007/s10875-019-00687-4

55. Mossner R, Diering N, Bader O, Forkel S, Overbeck T, Gross U, et al. Ruxolitinib induces interleukin 17 and ameliorates chronic mucocutaneous candidiasis caused by STAT1 gain-of-function mutation. *Clin Infect Dis.* (2016) 62:951–3. doi: 10.1093/cid/ciw020
56. Moriya K, Suzuki T, Uchida N, Nakano T, Katayama S, Irie M, et al. Ruxolitinib treatment of a patient with steroid-dependent severe autoimmunity due to STAT1 gain-of-function mutation. *Int J Hematol.* (2020) 112:258–62. doi: 10.1007/s12185-020-02860-7

Conflict of Interest: The authors declare that the research was conducted in the absence of any commercial or financial relationships that could be construed as a potential conflict of interest.

frontiers in Immunology

ORIGINAL RESEARCH
published: 21 January 2021
doi: 10.3389/fimmu.2020.563473

Lymphocyte-Specific Biomarkers Associated With Preterm Birth and Bronchopulmonary Dysplasia

Soumyaroop Bhattacharya[1], Jared A. Mereness[1], Andrea M. Baran[2], Ravi S. Misra[1], Derick R. Peterson[2], Rita M. Ryan[3,4], Anne Marie Reynolds[3], Gloria S. Pryhuber[1] and Thomas J. Mariani[1]**

[1] Division of Neonatology, Department of Pediatrics, University of Rochester, Rochester, NY, United States, [2] Department of Biostatistics and Computational Biology, University of Rochester, Rochester, NY, United States, [3] Department of Pediatrics, University at Buffalo, Buffalo, NY, United States, [4] Department of Pediatrics, Case Western Reserve University, Cleveland, OH, United States

OPEN ACCESS

Edited by:
Lisa G. Rider,
National Institute of Environmental Health Sciences (NIEHS), United States

Reviewed by:
Li-Tung Huang,
Kaohsiung Chang Gung Memorial Hospital, Taiwan
Mikko Hallman,
University of Oulu, Finland

***Correspondence:**
Gloria S. Pryhuber
gloria_pryhuber@urmc.rochester.edu
Thomas J. Mariani
Tom_Mariani@urmc.rochester.edu

Specialty section:
This article was submitted to Autoimmune and Autoinflammatory Disorders, a section of the journal Frontiers in Immunology

Received: 18 May 2020
Accepted: 07 December 2020
Published: 21 January 2021

Citation:
Bhattacharya S, Mereness JA, Baran AM, Misra RS, Peterson DR, Ryan RM, Reynolds AM, Pryhuber GS and Mariani TJ (2021) Lymphocyte-Specific Biomarkers Associated With Preterm Birth and Bronchopulmonary Dysplasia. Front. Immunol. 11:563473. doi: 10.3389/fimmu.2020.563473

Many premature babies who are born with neonatal respiratory distress syndrome (RDS) go on to develop Bronchopulmonary Dysplasia (BPD) and later Post-Prematurity Respiratory Disease (PRD) at one year corrected age, characterized by persistent or recurrent lower respiratory tract symptoms frequently related to inflammation and viral infection. Transcriptomic profiles were generated from sorted peripheral blood CD8+ T cells of preterm and full-term infants enrolled with consent in the NHLBI Prematurity and Respiratory Outcomes Program (PROP) at the University of Rochester and the University at Buffalo. We identified outcome-related gene expression patterns following standard methods to identify markers for oxygen utilization and BPD as outcomes in extremely premature infants. We further identified predictor gene sets for BPD based on transcriptomic data adjusted for gestational age at birth (GAB). RNA-Seq analysis was completed for CD8+ T cells from 145 subjects. Among the subjects with highest risk for BPD (born at <29 weeks gestational age (GA); n=72), 501 genes were associated with oxygen utilization. In the same set of subjects, 571 genes were differentially expressed in subjects with a diagnosis of BPD and 105 genes were different in BPD subjects as defined by physiologic challenge. A set of 92 genes could predict BPD with a moderately high degree of accuracy. We consistently observed dysregulation of *TGFB, NRF2, HIPPO*, and *CD40*-associated pathways in BPD. Using gene expression data from both premature and full-term subjects (n=116), we identified a 28 gene set that predicted the PRD status with a moderately high level of accuracy, which also were involved in *TGFB* signaling. Transcriptomic data from sort-purified peripheral blood CD8+ T cells from 145 preterm and full-term infants identified sets of molecular markers of inflammation associated with independent development of BPD in extremely premature infants at high risk for the disease and of PRD among the preterm and full-term subjects.

Keywords: prematurity and respiratory outcomes program, bronchopulmonary dysplasia, RNA-sequencing, Pathway, Newborn Lung, Peripheral Blood Mononucleated cells, CD8+ lymphocytes

INTRODUCTION

Acute and chronic respiratory morbidities are common in extremely premature infants (1). Increased survival of very premature infants is leading to increasing numbers of children with chronic lung disease. Since the end of the last millennium, the rate of premature births <34 weeks of gestation have consistently increased in the United States, and in 2008 it was 12.3% (2). Among the extremely preterm infants, 20%–35% die before their discharge to home (1, 3). Prematurity-related deaths accounted for 35% of all infant deaths in 2010, more than any other single cause. Preterm birth cost the U.S. health care system more than $26 billion in 2005 (4). Among NICU survivors, approximately 40% develop Bronchopulmonary Dysplasia (BPD), a chronic lung disease of the newborn. BPD has both genetic and environmental risk factors. It is characterized by varying degrees of lung injury potentially due to required supplemental oxygen, exposure to inflammatory conditions *in utero*, and mechanical ventilation and is often associated with infection (5, 6). BPD results from abnormal repair and impaired lung development after acute lung injury. Airway function may even deteriorate during the first year of life in infants with BPD (7). A key component of BPD is persistent inflammation of the lung (8, 9). Infants with BPD are more likely to die than those without chronic lung disease, even if they survive the initial hospitalization. However, improved medical treatment plans have been developed that have led to a lower hospital mortality rate, however, the respiratory sequelae into childhood remain poorly defined (10). By developing a better understanding of the inflammatory process of infants with BPD, we could potentially identify biomarkers that relate to respiratory sequelae. Using such information, certain pathways could be targeted for drug development to improve the health of infants with BPD (11).

The NIH NHLBI Prematurity and Respiratory Outcomes Program (PROP) enrolled 835 extremely premature infants across the US and collected multiple biospecimens over time and extensive data including BPD and respiratory morbidity outcomes over the 1st year of life. PROP investigated the molecular mechanisms contributing to the risk of respiratory disease in premature neonates over the first year of life. A set of clinical and non-invasive respiratory assessments were performed, based on the respiratory status of the infant at the time of testing, and was used to predict the severity of respiratory outcomes in the first year of life. The primary goal of the PROP studies was to identify biomarkers (biochemical, physiological, and genetic) that are associated with, and thus potentially predictive of, respiratory morbidity in preterm infants up to 1-year corrected age. A validated, objective measure of pulmonary outcome at 1 year does not currently exist. In addition to the identification of markers of BPD, one of the primary outcomes in the PROP study was defined as presence or absence of Post-Prematurity Respiratory Disease (PRD) (12). In order to be classified as having PRD, infants were required to have a positive response in at least one of the four morbidity domains [(1) hospitalization for respiratory indication, (2) home respiratory support, (3) respiratory medication administration, and/or (4) respiratory symptoms without a cold] during at least two separate parental interviews conducted at 3-, 6-, 9-, and 12-months corrected age (13).

High throughput sequencing for genome-wide transcriptomic analysis, by RNA-Seq or microarrays, is an unbiased approach applied to identify biomarkers that may provide predictive value. These approaches have been proven to be powerful tools capable of biomarker discovery for various disease states including BPD. We have previously presented an analysis of lung tissue gene expression in subjects with BPD (14). Application of blood-based gene expression profiling can potentially provide novel biomarkers for diagnosis and therapeutic management of BPD. Previous studies have used whole blood–derived peripheral blood mononuclear cells (PBMC) as a means of mining for novel markers for BPD (15). PBMCs are relatively easy to obtain from whole blood and can be sorted into leukocytes, including B cells, T cells, monocytes, and natural killer cells (16). The use of peripheral blood has identified changes in CD4+ T cell populations in subjects with diagnosed with BPD (17, 18). Additional studies have identified that patterns of proinflammatory cytokines in blood from subjects with BPD were associated with the phenotype of BPD (19). Our study was funded to complete transcriptomics analyses of the CD8+ T cell population.

Emerging data suggest an important role for T lymphocytes in the pathogenesis of chronic lung disease in babies born prematurely. CD8+ T cells, TNF-α, TNF receptors, and NK cells provide protection from viral infection but also contribute to the immunopathology, by contact-dependent effector functions (perforin and FasL). IFN-γ and particularly TNF-α are thought to be primary perpetrators of T-cell-mediated lung injury (20). Furthermore, one study shows that CD8+ T cells isolated from blood of infants with BPD exhibited lower levels of surface CD62L, which is consistent with an activated phenotype (21). CD8+ T cells have shown adaptive immune insufficiency in newborn mice infected with influenza A within 1 week of birth (22). RSV infected neonatal mice recruited CD8+ T cells defective in IFN-γ production in association with mild symptoms. Re-infection as adults however resulted in limited viral replication but enhanced inflammation and T cell recruitment, including Th2 cells and eosinophils (23, 24). Depletion of CD8+ T cells (but not CD4) cells during the primary neonatal infection was protective against the adult challenge. We have previously shown that CD8+ T cells appear to play a pathogenic role in subjects with BPD, and may be associated with overall risk for lung morbidity (25). In related studies, we have observed that CD8+ T cells are increased in both mouse and human lungs exposed as neonates to hyperoxia, and have a hyper-responsive, fibrotic and destructive response to subsequent viral infection (14, 26). Further, these cells have a predominant role in direct cytotoxicity in the lung, *via* interactions with epithelial cells and as regulators of macrophage responses, as well as in general human resistance to viral infection. In a separate population of premature infants, enrolled in the PROP study, phenotyped T cells at birth, at 36 weeks of adjusted gestational age, and at 12-months corrected age, were associated with a PROP-defined respiratory morbidity at 12 months (27). The goal for the current study was to demonstrate that transcriptional profiling of

CD8+ T cells, obtained from premature infants at discharge, can identify disease-related gene expression patterns informative for pathogenesis and capable of predicting risk of future respiratory distress. We hypothesized that transcriptomic analysis of sorted lymphocyte sub-populations could identify predictive markers and pathways associated with respiratory outcomes. We followed a cohort of 157 infants, ranging from 23 to 41 weeks of gestation at birth, enrolled in the Prematurity and Respiratory Outcomes Program (PROP) at the University of Rochester Medical Center and Children's Hospital of Buffalo (12).

Here, we present a novel gene expression RNA-seq data set generated from CD8+ T cells from 145 subjects with varying levels of premature birth and report the identification of disease biomarkers for BPD and PRD. In subjects who were diagnosed with BPD, we identified pathways associated with TGFB signaling (Regulation of Epithelial-Mesenchymal Transition Pathway) and T cell activation and polarization (e.g., IL-2, IL-17, IL-4, and iCOS signaling). In subjects who developed PRD at one year of life, we also identified the TGFB pathway as being important as well as the Cell2Cell pathway (which includes genes important for CD8+ T cell activation). Given that TGFB has been identified as an important factor for controlling CD8+ T cell mediated inflammation (28–32), we provide new makers in CD8+ T cells that are associated with the BPD and PRD. Such information will be of interest to researchers who are trying to develop a better understanding of factors associated with inflammatory pediatric lung disease.

METHODS

This study aimed at generating transcriptomic profiles of CD8+ T cells from newborn human blood. This study was approved by the Institutional Review Board of University of Rochester with a Memorandum of Understanding executed with the University of Buffalo IRB. Subjects were enrolled within gestational age at birth (GAB) epochs, in order to characterize the relationship among prematurity, disease risk, and gene expression. The steps involved in the process, starting from sample collection to isolation of total RNA have been described in detail in our previous publication (16). Additional steps relevant to this study are shown in **Supplemental Figure 1**.

Oxygen Exposure, BPD Diagnosis, and PRD

The traditional categorical approach of classifying BPD as absent or present is likely an oversimplification. Tooley (33) recommended that oxygen use at 28 days of age would identify preterm infants with BPD. Almost a decade later, Shennan and colleagues proposed that the best predictor of abnormal pulmonary outcomes among very low birth weight premature infants was the clinical use of oxygen at 36 weeks postmenstrual age (PMA) (34). A workshop convened by the National Institutes of Health (NIH) proposed severity-based diagnostic criteria for BPD (35) that included the use of oxygen for at least 28 days (not necessarily consecutive) and an assessment of respiratory support at 36 weeks PMA, recognizing that some infants breathing room air at 36 weeks PMA may have residual lung disease. The majority of infants with birth weights less than 1 kg will have a diagnosis of at least mild BPD by the Consensus Conference definition based on 28 days in oxygen (35). Given clinical variations in oxygen administration, a structured trial of room air test was developed by the NICHD Neonatal Research Network (36), the frequency of BPD among the subjects was determined using two previously published definitions: the Shennan definition (34), which defines BPD as supplemental oxygen requirement at 36 weeks PMA in infants born with birth weight (BW) less than 1,500 grams, and a physiologic definition with a room-air challenge (RAC) which defines BPD as requirement of oxygen support (>21% O_2) for at least 28 days and a subsequent assessment at 36 weeks PMA or discharge, whichever comes first (13, 36).

NICU oxygen exposure was calculated, as previously reported, from the FIO2 recorded in the medical record once each noon for the first 14 days of life. FIO2 was corrected to Effective FiO2 for low nasal cannula flow using established tables (37). Oxygen utilization or $Oxygen_{AUC}$ was calculated by the formula defined in Benaron and Benitz (37) using information recorded in the daily respiratory flowsheet data (FIO2, respiratory support mode, and applied airway pressure or cannula flow) through the first 28 days of life. We chose to look at $Oxygen_{AUC}$ at 14 days of postnatal age ($Oxygen_{AUC14}$) to include the second postnatal week to capture pulmonary deterioration as presented in BPD (38).

The infants enrolled in the study were followed up periodically for up to 12 months of age, corrected by gestational age (CGA) at birth. At the 12-month CGA follow-up visit they were assessed for persistent respiratory distress based on the frequency of hospitalization due to any kind of respiratory distress. Persistent Respiratory Distress (PRD) was diagnosed if there were positive responses in at least one of the following domains: (1) hospitalization for respiratory indication, (2) respiratory support at home, (3) respiratory medication administration, and/or (4) cough or wheeze without a cold, reported on at least two caregiver post-discharge surveys completed at 3, 6, 9, and 12 months CGA, as previously reported (13). The definitions and criteria for the different diagnoses have been listed in **Supplemental Table 1**.

Sample Collection and RNA Isolation

An average of 2.5 ml of venous blood was collected into sodium heparin glass vacutainers from premature infants enrolled with consent in the Prematurity and Respiratory Outcomes Program (PROP), at the time of hospital discharge at the University of Rochester and the University at Buffalo and shipped to a central laboratory in Rochester. Freshly purified PBMCs were isolated by Ficoll gradient (Amersham Pharmacia Biotech # 17-1440-03) centrifugation, from the whole blood diluted 1:2 with 1x dPBS, and counted according to previously established protocols (39). In subjects with at least 8 million cells, 5 million cells were stained with antibodies to individual lymphocyte markers, and

sorted on a FACSAriaII sorter at the Flow Cytometry Core facility of the University of Rochester as previously reported (16). CD3+CD8+, CD3+CD4+, CD3-CD56+ (NK), or CD3-CD19+ (B) cells were collected separately. Non-marker positive and dead cells were discarded. Sorted cells were spun into pellets, which were further lysed and frozen. The steps from collection to lysis of each sample were completed within a 24-h period in order to preserve RNA quality and integrity. Frozen lysates were thawed and RNA was extracted using Agilent Absolute RNA Microprep kit (catalog #400805), with an on-column DNase digestion, as per manufacturer recommended protocol.

RNA-Seq and Data Generation

For the current study, RNA isolated from the sorted CD8+ T cells from 145 pre-term and full-term subjects, was used for transcriptomic profiling by RNA-seq. cDNA libraries were generated with 1 ng RNA, using the SMARter Ultra Low Amplification kit (Clonetech, Mountain, CA). cDNA quantity was determined with the Qubit Flourometer (Life Technologies, Grand Island, NY) and quality was assessed using the Agilent Bioanalyzer 2100 (Santa Clara, CA). Libraries were sequenced (single endreads) on the Illumina HiSeq2500 (Illumina, San Diego, CA) to generate 20 million reads/sample. Reads generated from the sequencer were aligned using the TopHat algorithm (40) and expression values were summarized using HTSeq (41). The data from this study has been provided in dbGAP. The dbGaP accession assigned to this study is phs001297.v1.p1.

Normalization and Filtering

Samples were excluded based on poor read count/mapped read numbers, or if they were extreme outliers in hierarchical clustering and Principal Components Analysis (PCA). Genes were excluded if they were not consistently identified as expressed (a count of zero in over 1/3 of subjects). Subjects with high prevalence (>75%) of zero/low reads (raw count value ≤5) were excluded. Genes with high prevalence (>75%) of low counts (normalized count value ≤3) across subjects were excluded.

The subject-specific conditional upper quartile (UQ, 75^{th} percentile) among non-zero reads was computed. The subject-specific normalization factor was calculated by dividing the UQ for a given subject by the mean UQ across all subjects. The normalized gene values for a given subject were calculated by dividing the raw count values by the normalization factor for that subject. After adding 1 to all values to account for zeros, the normalized counts were $\log_2$ transformed.

Selection of Univariately Differentially Expressed Genes

Differences in gene expression between subject groups was assessed by SAM-Seq (42) and Likelihood Ratio Test (LRT). SAM-Seq was used to identify genes with expression patterns significantly (FDR<0.05) associated with BPD, RAC. LRT for log (normalized RNA-Seq), adjusted for GAB *via* logistic regression, was used to identify genes with expression patterns significantly (FDR<0.05) associated with BPD in subjects born at less than 29 weeks of age. For quantitative analysis, the correlations between normalized counts and oxygen utilization at 14 days were estimated. Expression changes of the genes, identified as significantly different in BPD by the tests, were assessed in transcriptomic profiles of PBMCs obtained from infants with BPD, and age matched controls generated from an independent cohort (15), using the data available on Gene Expression Omnibus (GSE32472).

Prediction of Bronchopulmonary Dysplasia (BPD) *via* Screened Principal Components

The following method is our minor variant of *Screened Principal Components Analysis (sPCA)* (43), where the genes were univariately screened, and those with a nominal Wilcoxon $p < 0.10$ were used for further analysis. The first principal component (PC1) of the genes was derived, and genes with loadings close to 0 were removed. Genes most strongly univariately associated with BPD (with or without adjusting for gestational age) were selected using a screening threshold chosen by cross-validation (CV). The first Principal Component (PC1) of the genes passing the univariate screen was constructed and a logistic regression model was fit to predict BPD as a function of PC1 (and optionally gestational age). Receiver Operating Characteristic (ROC) curves depicting sensitivity and specificity along with associated AUC were estimated without (naïve AUC) and with an outer loop of nested CV (CV-AUC).

Prediction of Post-Prematurity Respiratory Disease (PRD) *via* Canonical Pathways

We have used canonical pathway analysis where we grouped our 13,434 genes into 1,330 biologically-relevant pathway-based gene sets of molecular signature database (mSigDB) (44), where each gene belongs to 0, 1, or more pathways. We then reduced the constituent genes in each pathway to their PC1. Genes belonging to 0 pathways were thus excluded from consideration, while CV screened logistic forward selection (or LASSO) was applied to the 1,330 pathway-based PC's. Bivariate CV was used to simultaneously select both the threshold for univariate logistic likelihood ratio test screening of pathways (with or without adjusting for gestational age) and the final number of pathways chosen by forward selection (or the LASSO penalty). The entire procedure was then nested within an outer loop of nested CV in order to estimate performance *via* the Receiver Operating Characteristic (ROC) curve and its associated Area Under the ROC Curve (CV-AUC). This method has been described in details in our previous publication (45).

Functional Classification

Genes identified as differentially expressed in individual comparisons were used for independent functional classification through canonical pathway analysis, and upstream regulators identification using Ingenuity Pathway Analysis (IPA; Qiagen, Carlsbad, CA). Pathways and upstream regulators were identified as significantly associated with the diagnoses by Fisher's exact test ($p < 0.05$ or -log(p-value) > 1.3) as calculated by IPA.

Quantitative Reverse Transcriptase–Polymerase Chain Reaction (qPCR)

cDNA was synthesized from 100 ng RNA using iScript cDNA synthesis kit (Biorad, HerculesCA) and quantitative reverse transcriptase–polymerase chain reaction (qPCR) was performed with a Viia7 (Applied Biosytems, Carlsbad, CA) using SYBR green chemistry as previously described (14) using noncommercial (http://pga.mgh.harvard.edu/primerbank) assays. Gene expression levels were calculated relative to GAPDH as an internal, endogenous control, according to the ddCT method.

RESULTS

Subject Demographics

Peripheral blood was collected at the time of first hospital discharge, from 145 preterm and full-term infants enrolled in the NHLBI Prematurity and Respiratory Outcomes Program (PROP) at the University of Rochester and the University at Buffalo. Of the 145 subjects, 72 were extremely premature having been born at less 29 weeks of gestation. There was insufficient evidence that the distribution of race (p=0.64) or sex (p=1) differed between BPD and non-BPD subjects, while as expected gestational age at birth was lower for those with BPD (p=0.03). Similarly, among all subjects (n=130) there was insufficient evidence of any difference in race (p=0.70) or sex (p=1) by PRD status, while as expected gestational age at birth was lower for those with PRD (p=0.01; **Table 1**). The age (in days) at the time of sample collection varied by subject, and it ranged from four days to 6 months after birth, depending on the gestational age at birth. However, age was consistent in terms of corrected gestational age, which ranged between 39 to 41 weeks. Detailed diagnostic and demographic information for the individual subjects in provided in **Supplemental Table 2**.

Transcriptomic profiles were generated from sorted and purified CD8+ T cells obtained from the blood collected at discharge. The analytical data set includes values from 13,455 genes for 130 samples, post filtering. As reported previously, the average number of sequence reads in the samples were high (9.93 ± 3.69 million sequence reads). Overall, approximately 60% of possible genes showed detectable transcript as expected for a subset of differentiated cell type (16) as shown in **Supplemental Figure 2**.

Molecular Markers for BPD

Gene expression patterns associated with cumulative oxygen exposure (over the first 14 days of life) in subjects at greatest risk for BPD (born at GAB<29 weeks; n=72) was assessed. Rank correlation analysis identified 501 genes to be significantly associated (at pFDR<0.1) with oxygen exposure, of which 403 were upregulated in BPD, while 98 genes were downregulated in BPD. The magnitude of change, however, was not large, with only 1 gene (*GPCPD1*) induced by 2.3 fold, while all other changes were less than 2-fold, irrespective of the directionality. Twelve of these genes (*RETN, EPHX2, CD27, NOSIP, APOA1BP, TMCO6, KLHL3, B3GALNT1, SLC9A4, PRKCD, ZNF791, and B3GNT2*) were also identified as differentially expressed in BPD in an independent study studying BPD markers in PBMCs (15). The 501 genes, when further assessed for functional classification by Ingenuity Pathway Analysis (IPA), were found to be associated with 104 pathways and 300 upstream regulators (**Figure 1**). The pathways associated with oxygen utilization included TGFB signaling (epithelial-mesenchymal transition), and multiple immune signaling pathways, while tubule formation associated and immunologic molecules were present among the upstream regulators.

Data from 72 subjects born at <29 weeks CGA was used to identify gene expression associated with BPD as defined by physiologic challenge (RAC) or by Shennan criteria. Using SAM-Seq (at mFDR<0.1), 571 genes were differentially expressed in subjects receiving a diagnosis of BPD (Shennan). While all of the 571 genes were upregulated in BPD, only five genes (*GPCPD1, TMEM2, USP2, TSPYL2, and ELL2*) showed a magnitude of induction of greater than 2.0 fold. Fourteen of these genes (*RNF125, FEM1C, FAM54A, ZNF791, AXIN2, B3GNT2, ZNF565, SPON1, TIPARP, ZBTB3, FAM115C, PELO, MXD1, and PFKFB3*) were also identified as differentially expressed, and over expressed in BPD in an independent study looking at BPD markers in PBMCs (15). These 571 genes, when further assessed for functional classification by IPA, identified 113 canonical pathways and 409 upstream regulators to be associated with BPD. In addition, 105 genes were differentially expressed (SAM-

TABLE 1 | Subject demographics.

Subjects with GAB < 29 Weeks (n=72)	**BPD N=34**	**Non BPD N=38**	**P value***	
GAB in Weeks, mean ± SD	26.1 ± 1.4	26.9 ± 1.5	0.03	
Male Sex, No. (%)	17 (50)	18 (47)	1.00	
White Race No. (%)	20 (59)	20 (53)	0.64	
Demographics All Subjects (n=130)	**PRD YES N=70**	**PRD NO N=46**	**PRD NA# N=14**	**P value***
GAB in Weeks, mean ± SD	28.5 ± 3.3	31.1 ± 5.2	32.2 ± 4.1	0.01
Male Sex, No. (%)	34 (48)	23 (50)	10 (71)	1.00
White Race, No. (%)	43 (61)	30 (65)	9 (64)	0.7

**Fisher's Exact or t-test P-value.*
GAB, gestational age at birth; PRD NA#, PRD Status Not Available.

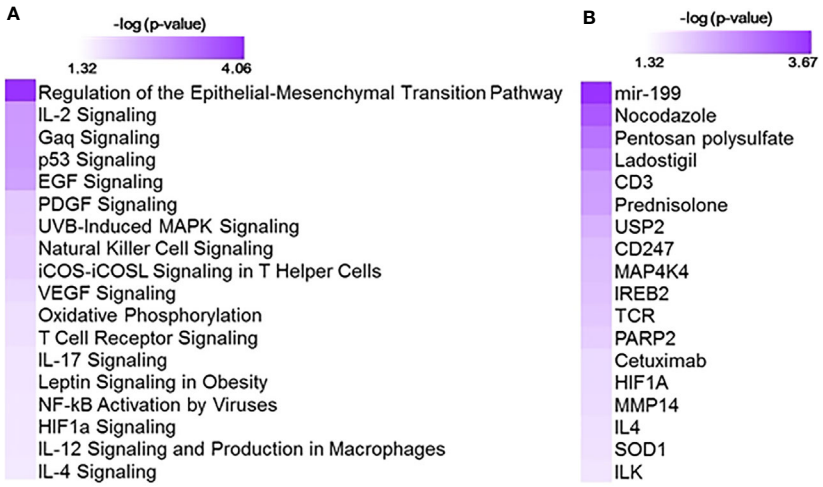

FIGURE 1 | Functional analysis using 501 genes associated with oxygen utilization at day 14 ($Oxygen_{AUC14}$) identified with 104 pathways and 300 upstream regulators. Shown here are selected significant canonical pathways **(A)** and upstream regulators **(B)**, along with their significance level (-logP) as generated by Ingenuity Pathway Analysis (IPA).

Seq at mFDR<0.1) in subjects who failed a room air challenge. While all of the 105 genes were upregulated in BPD, only two genes (*GPCPD1 and TSPYL2*) showed a magnitude of induction of greater than 2.0 fold. These 105 genes when analyzed by IPA, identified 18 canonical pathways and 415 upstream regulators (**Figure 2**). Among the pathways associated with BPD, *PEDF, CD40, PI3K/AKT, VEGF* and *NF-kB* signaling were predicted to be activated, while p53 signaling was inhibited in BPD. Among the BPD associated upstream regulators, *CD23, CD28, PTEN*, and *TCR*, are inhibited, while *NFκB* inhibitor, *camptothecin*, and *dexamethasone* were activated in BPD.

When adjusted for gestational age at birth, 75 genes were associated with the diagnosis of BPD (Shennan) as identified by the Likelihood Ratio Test (LRT at FDR<0.1), and were upregulated in BPD. On further analysis by IPA, the genes provided 113 canonical pathways and 409 upstream regulators (**Figure 3**), of which neuroinflammation pathway appeared to be inhibited, while upstream regulators, *CD23, CD28*, and *TCR*, are

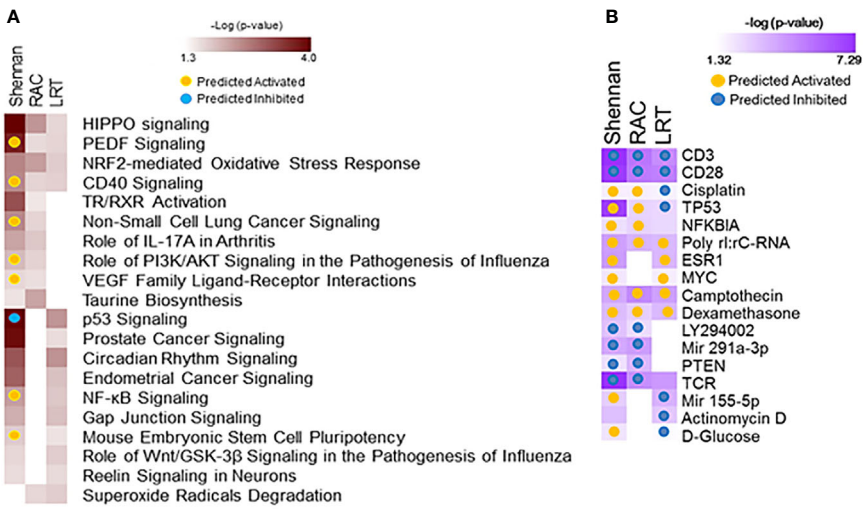

FIGURE 2 | Functional analysis of genes associated with bronchopulmonary dysplasia (BPD). Separate analyses were performed for gene sets identified from analysis of 571 genes associated with BPD (Shennan) and 101 genes associated with room-air challenge (RAC) as identified by SAM-Seq, and 92 genes identified by Screened Principal Components Analysis (sPCA) [adjusted for gestational age at birth (GAB)] to be associated with BPD (Shennan). Selected canonical pathways **(A)** and upstream regulators **(B)** identified are listed for each analysis (columns), with significance (-logP) and directionality (activated/inhibited) as generated by Ingenuity Pathway Analysis (IPA).

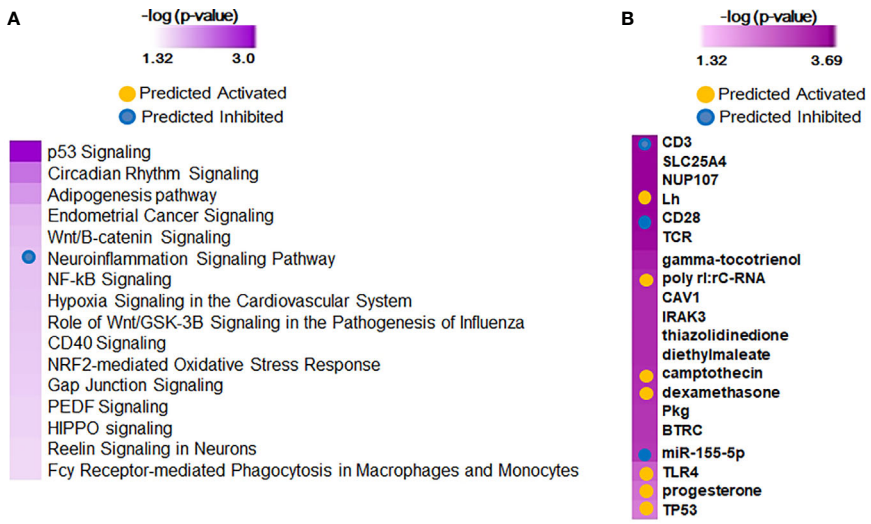

FIGURE 3 | Functional analysis of 75 predictor genes for bronchopulmonary dysplasia (BPD) defined by Likelihood Ratio Test (LRT), identified 113 canonical pathways and 409 upstream regulators. Selected significant canonical pathways **(A)** and upstream regulators **(B)** identified are shown, along with their significance level (-logP) as generated by Ingenuity Pathway Analysis (IPA).

inhibited, and *camptothecin*, and *dexamethasone* were activated in BPD. Screened Principal Components Analysis (sPCA), with screening adjusted for GAB, outperformed both screened LASSO and forward selection and identified a classifier gene set consisting of 92 genes (naïve AUC=0.86; CV-AUC=0.71) associated with BPD (Shennan), representing 21 canonical pathways and 253 upstream regulators (**Supplemental Figure 3**). All of the 92 genes were upregulated in BPD, however, none of the genes except *GPCPD1* had a magnitude of induction of greater than two-fold. These 92 genes were also inclusive of all the 75 genes identified by LRT. We subsequently assessed gene expression changes in BPD based on multiple physiologic and clinical definitions and were successful in identifying nine genes (*GPCPD1, MTSS1L, USP15, DDX24, KLF9, CLK1, ZC3H7A, ITCH*, and *PIK3R1*) that were consistently different, and upregulated in BPD, irrespective of definitions, or analytical approaches (**Supplemental Figure 4**).

Classifiers for PRD Status

Gene expression data from all subjects with PRD status (n=116), was used to identify a set of marker genes, based on our novel *canonical pathway analysis* (45), in order to classify the subjects by PRD status (PRD: n=70 and No PRD: n=46). Screened logistic forward selection outperformed both screened LASSO and sPCA, and gestational age was excluded since it did not improve performance. This process identified a set of 28 genes, derived from four canonical pathways (**Table 2**), which predicted PRD status with a moderately high degree of accuracy (naïve AUC=0.85; CV-AUC=0.70) (**Figure 4**). Interestingly, gene predictors of PRD were associated with pathways involving *TGFB* signaling, and organic ion transport. Several genes identified are also involved in T cell skewing and activation (e.g., *PRKCZ* and *FKBP1A*).

qPCR Validation

Molecular validation of the BPD-associated transcriptomic changes, was attempted on a set of eleven genes selected based on their magnitude of difference or biological relevance, by quantitative reverse transcriptase-polymerase chain reaction (qPCR) (**Table 3**). For each gene, the UQ normalized RNA-seq counts were correlated with the gene expression levels determined by qPCR of the CD8+ T cell cDNA as defined by the dCt. *GAPDH* was used as the endogenous control or housekeeping gene, whose Ct was subtracted from gene Ct to determine the dCT values for each of the genes tested. Spearman's rank correlation coefficient was estimated along with an associated p-value for each gene. We observed validation of the sequence data for nine of the 11 genes, as defined by a significant Spearman rank correlation ($p<0.05$) in expression between sequence-based and qPCR-based expression levels. Three genes (*KLF9, DLG5, and ZNF44*) differed in expression between BPD and non-BPD subjects ($p<0.05$), while one additional gene (*PSME4*) had borderline yet insufficient evidence of a difference ($0.05<p<0.10$).

DISCUSSION

Premature birth is defined as birth taking place prior to 37 weeks of GAB. Prematurity associated lung diseases have been reported to affect not only children as newborns but to also predispose to prolonged respiratory morbidity later in life. Unfortunately, not much is known about the pathophysiology of the prematurity associated lung diseases, such as BPD, and other chronic and prolonged childhood respiratory diseases. BPD is a complex disorder involving genetic–environmental interactions, with each preterm subject having a range (e.g., 1%–99%) of both hereditary

TABLE 2 | Canonical pathway based analysis selected four pathways including a total of 28 genes using cross-validated screened logistic forward selection for prediction of Post-Prematurity Respiratory Disease (PRD) status.

Source: Pathway	Pathway Coefficient (logOR)	Gene	Gene OR
Reactome: Recycling Of Bile Acids And Salts	-1.49	SLC10A1	0.61
		SLC27A5	0.66
		SLCO1A2	0.71
Reactome: Transport Of Organic Anions	1.71	SLCO1A2	0.71
		SLCO3A1	1.27
		SLCO4A1	1.58
		SLCO4C1	1.45
Reactome: TGF-Beta Receptor Signaling In Epithelial To Mesenchyme Transition	-0.49	ARHGEF18	0.93
		CGN	0.84
		F11R	0.77
		FKBP1A	0.72
		PARD3	0.58
		PARD6A	0.88
		PRKCZ	0.69
		RHOA	0.76
		RPS27A	0.85
		SMURF1	0.91
		TGFB1	1.07
		TGFBR1	0.81
		TGFBR2	1.09
		UBA52	0.87
Biocarta: Cell2Cell Pathway	-0.46	ACTN1	0.5
		CSK	0.86
		CTNNA1	0.87
		CTNNB1	1.01
		PECAM1	0.65
		PTK2	0.76
		PXN	0.76
		VCL	0.82

Pathway logOR are log of odds ratios per standard deviation (SD) of the 1st PC of the screened genes (Wilcoxon p<0.1) within the pathway. * Gene OR = exp (Gene Loading * log (Screened Pathway OR)/SDPathway) = (Pathway OR)(Gene Loading/(SD of Pathway)). Shown are pathway and gene names, estimated pathway coefficients (logOR), and constrained gene odds ratios (OR) factoring in the PCA loadings for each gene within a pathway.*

and environmental risks (46). We have previously published data on hereditary components to BPD risk by genetic analysis in the PROP cohort, including some of the subjects described in the current manuscript (47, 48). Transcriptomic assessment using gene-expression microarrays has previously been used to identify markers for normal lung development as well as BPD (14, 49, 50). As an alternative to lung tissues, gene expression analyses using peripheral blood have been used in lung diseases to study pathogenesis, severity, and recently as a diagnostic tool (45, 51). In this study, we have used high-throughput sequencing to explore peripheral gene-expression changes associated with prematurity and helps to add to the literature base on potential defects in the immune system of infants with BPD (11). Our analysis identified 571 genes differentially expressed in subjects with diagnosed instances of BPD when compared to extremely low birth weight (ELBW) controls born at less than 29 weeks of GAB by SAM-Seq. An independent study also that examined BPD marker genes from bulk PBMCs identified 12 genes (*RETN, EPHX2, CD27, NOSIP, APOA1BP, TMCO6, KLHL3, B3GALNT1, SLC9A4, PRKCD, ZNF791*, and *B3GNT2*) that were differentially expressed in BPD (15). Thus, our results are consistent with published literature.

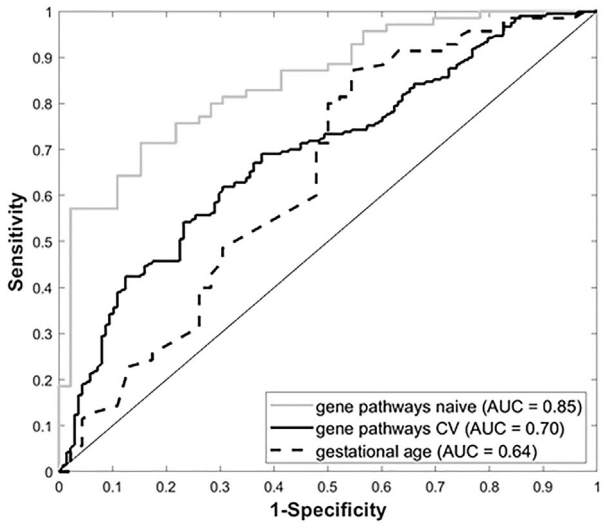

FIGURE 4 | Receiver Operating Characteristic (ROC) curves for gestational age and our four-pathway 28-gene model, with associated Area Under the ROC Curve (AUC).

TABLE 3 | Validation of bronchopulmonary dysplasia (BPD) markers.

Gene	Rank Correlation (r, GAPDH)	P-Value
USP15	0.49	<0.01
SOD2	0.35	<0.01
ITCH	0.13	0.27
AHR	0.28	0.02
*PSME4***	0.34	<0.1
STAT1	0.60	<0.01
GFI1	0.18	0.14
*KLF9**	0.29	0.02
*DLG5**	0.27	0.02
*ZNF44**	0.25	0.04
NEAT1	0.42	<0.01

**KLF9, DLG5, and ZNF44 differed in expression between BPD and non-BPD subjects (p<0.05),*
***PSME4 had borderline yet insufficient evidence of a difference between BPD and non-BPD (0.05<p<0.10).*

Our gene list is further restricted to 92, when we adjust for gestational age at birth (sPCA) as shown in **Supplemental Figure 4**. In addition, we have identified markers, pathways and upstream regulators putatively associated with cumulative oxygen utilization. The pathway most closely associated with oxygen utilization involves several *TGFB* signaling genes (epithelial-mesenchymal transition pathway), which is important for helping to diminish CD8+ T cell activation (28–32). Additional pathways involved with T cell activation (e.g., T cell receptor signaling) and differentiation (e.g., IL-12 signaling). Thus, we have identified pathways that could be useful for identifying new therapeutic targets to treat the postnatal inflammation of preterm infants and to improve the health of children with BPD (52).

Among the differentially expressed genes associated with BPD, the *PFKFB3* gene was not only consistently identified as

differentially expressed in BPD subjects irrespective of the approach used, but was also identified as a BPD marker in an independent transcriptomic analysis of PBMCs derived from BPD subjects (15). Through murine studies *PFKFB3* has been identified as potential therapeutic target for the treatment of Pulmonary Hypertension (PH) (53). Increased expression *PFKFB3* in BPD is consistent with PH associated with BPD which is characterized by abnormal vascular remodeling, and vascular growth arrest, which are well documented pathophysiology associated with BPD (54). *In vitro* studies have reported that *PFKFB3-kinase* activity attenuates the activation of T cells, and demonstrated the effectiveness of *PFKFB3* antagonists, even in small amounts, as T cell immunosuppressive agents (55). One of the differentially expressed genes, *KLF9*, has been previously identified as differentially expressed in T cells from patients with autoimmune rheumatoid arthritis (56), while another, *DLG5*, is involved in the *HIPPO* pathway and modulated *TGFB* signaling (57–59).

Pathway analyses indicate dysregulation of *NRF2, HIPPO and CD40* pathways to be consistently associated with BPD. Another marker, *PSME4*, has been associated with tuberculosis through *in vitro* and *in vivo* cultures, and is also related to *CD4, IFNβ1*, and *TGFBI* pathways (60). Interestingly, *NRF2* has been linked to the generation of reactive oxygen species that contributes to inflammation in a variety of diseases (61). The *HIPPO* has been shown to play a role in T cell receptor signaling and in Th17 differentiation (62, 63). Systemic administration of agonistic *CD40* antibody has been shown to increase CD8+ T cell responses in the lungs of non-human primates (64). While *IL2* signaling is expected, *Gnaq* is known to play a role in survival of immune cells (B and T-cells) (65, 66). In addition, *iCOS-iCOSL* are known to be involved in T-cell skewing, and reduced SOD expression is related to impaired CD8+ T cell responses in tumor infiltrating lymphocytes (67). Interestingly, regulators associated by anti-survival, dexamethasone and camptothecin, appear to be activated in BPD, while T cell co-receptors, *CD3* and *CD28*, appear to be inhibited in BPD. One study shows that T cells isolated from patients with chronic viral infection rely on topoisomerase activity to maintain DNA stability and inhibit apoptosis (68). It is well established that chronically activated T cells become hyporesponsive to T cell receptor mediated stimulation (69). These may indicate potential arrest in lung development as a consequence of BPD and indicate induced immune and stress response as a result of therapeutic responses to BPD, due to either oxidative stress, or surfactant treatment (70). Thus, we have identified significant differences in the expression of several genes and pathways in BPD subjects that are related to T cell signaling and effector function.

In addition to studying CD8+ T cell gene expression in relationship to BPD, we also explored multiple approaches to identify a set of genes whose expression may be useful for classification of markers associated with Post-Prematurity Respiratory Disease (PRD) respiratory morbidity. This included approaches to leverage biological priors as a means of identifying the most robust predictors since (1) expression changes at the individual gene level alone may not be sufficient to identify biologically meaningful data and (2) there exists substantial statistical advantages to dimension reduction strategies in the analysis of genome-wide data. We used a curated list of genes (71) to partition our transcriptomic data into 1,330 biologically-relevant gene sets. Using a novel data reduction approach, we identified a 28 gene set classifier that groups subjects according to their PRD status with a moderately high degree of accuracy. Similar to BPD, the *TGFB* pathway was also found to be associated with PRD status. Several genes identified control T cell function. For instance, *SMURF1* accumulation in cells infected with RNA viruses leads to the downregulation of Type I Interferons (72). *RhoA* is a *GTPase* plays an essential role in the migration and activation of T cells (73). *PRKCZ* is a protein kinase C family member that is highly expressed in Th2 CD4+ T cells (74). *PARD3* and *PARD6A* have been shown regulate the *RhoA* signaling pathway (75). *PARD3* also modulates *HIPPO* signaling pathways (75). *FKBP1A* is a signaling molecule in the *mTOR* pathway that regulates memory CD8+ T cell formation (76). Expression of *F11Rm* which encodes for the protein junctional adhesion molecule A, plays a role in T cell adhesion and migration that is upregulated in T cells of lupus patients (77). Their association with persistent respiratory disease indicates propensity to future immunological complications, which may result in chronic lung disorders. Even with the limited set of predictive markers, it does appear that gene expression changes, in peripheral blood at the time of initial discharge after birth, are indicative of future respiratory diseases later in childhood.

One of the limitations of this study is the use of CD8+ T-cells in identifying biomarkers of a lung disease. While peripheral markers have been widely used in identifying expression based markers, it needs to be acknowledged that these hematopoietic cells are from different cell lineage from the pulmonary system, which is the primary organ system affected in BPD and subsequently in PRD. However, even with only one cell type of a different lineage, we have been able to identify previously known, as well as novel molecular markers, and pathways, associated with pulmonary disease due to premature birth. In a longitudinal study involving a subset of subjects from the current cohort, we were able to identify differences in T cell development, post birth, which were able to predict respiratory outcome at 1 year of age (25). Another limitation of the study is the usage of multiple definitions of BPD in order to assess transcriptomic changes caused by it. Despite the various definitions and analytical approaches used, we were able to identify a set of nine marker genes that were observed to be increased in BPD, irrespective of the diagnostic definition and approach used. By using approaches similar to those presented here, researchers will be able to develop better correlations between clinical courses of preterm infants with alterations in the immune system. Previously published data indicate that the patterns of cytokines in the blood of BPD patients relates to the subtype of disease (19). Through the current study we have established proof-of-principle that gene expression provides value for predicting respiratory morbidity following pre-term birth.

In conclusion, we have successfully generated genome-wide transcriptomic data from sort-purified peripheral CD8+ T cells obtained from early pre-term, late preterm, and term infants. We have identified molecular markers, pathways and upstream regulators putatively associated with cumulative oxygen utilization, BPD diagnosis, and PRD prediction. Further studies are needed to determine if the findings are unique to the circulating T cells sampled in this study, or reflective of similar effects in other cells including lung parenchymal cells.

DATA AVAILABILITY STATEMENT

The datasets presented in this study can be found in dbGap (https://www.ncbi.nlm.nih.gov/gap/) with accession number phs001297.v1.p1.

ETHICS STATEMENT

The studies involving human participants were reviewed and approved by the (Institutional Review Boards of the University of Rochester (IRB# 00037933) and the Children's Hospital of Buffalo (IRB# 612707). Written informed consent to participate in this study was provided by the participants' legal guardian/next of kin.

AUTHOR CONTRIBUTIONS

SB, JM, AB, and DP analyzed the data. SB, RM, and DP wrote the paper. RR, AR, GP, and TM conceived and designed the study. RM, TM, and GP oversaw the project. All authors contributed to the article and approved the submitted version.

FUNDING

The Prematurity and Respiratory Outcomes Program (PROP) was supported by National Institutes of Health (NIH); National Heart, Lung, and Blood Institute (NHLBI); and *Eunice Kennedy Shriver* National Institute of Child Health and Human Development (U01 HL101794 [to University of Pennsylvania, B. Schmidt]; U01 HL101456 [to Vanderbilt University, J.L. Aschner]; U01 HL101798 [to University of California San Francisco, P.L. Ballard and R.L. Keller]; U01 HL101813 [to University of Rochester and University at Buffalo, G. Pryhuber, R. Ryan, and T. Mariani]; U01 HL101465 [to Washington University, A. Hamvas and T. Ferkol]; U01 HL101800 [to Cincinnati Children's Hospital Medical Center, A.H. Jobe and C.A. Chougnet]; and 5R01HL105702 [to Indiana University and Duke University, C.M. Cotton, S.D. Davis, and J.A. Voynow]). This research was conducted through cooperative agreements with NHLBI and in collaboration with the PROP Steering Committee. The project described in this publication was supported by the University of Rochester CTSA award UL1 TR002001 from the National Center for Advancing Translational Sciences of the National Institutes of Health. The content is solely the responsibility of the authors and does not necessarily represent the official views of the National Institutes of Health.

ACKNOWLEDGMENTS

University of Rochester: Chin-Yi Chu, Heidie Huyck, Shelley Secor-Socha, Ernest Wang, Elizabeth Werner-Carbonell, Tanya Scalise, Dee Moffatt, Valerie Lunger, Sara Misra, Ashley Lopez, Jason Emo, Clement Ren (now at Indiana University), Carl D'Angio, William Maniscalco, Timothy Stevens, Sally Quataert, Kristin Scheible, Jeanne Holden-Wiltse, Sanjukta Bandopadhyay, the UR BLIS Data Management Team, UR RedCAP Database Team, UR Flow Core, UR Data Entry Team, UR Genomics Research Center.

University at Buffalo: Jack Sharp, Shannon Castiglione, Mike Sacilowski, Aimee Horan, Karen Wynn, Patrick Conway, UB Data Entry Team.

PROP Investigators

Cincinnati Children's Hospital Medical Center:

Barbara Alexander, RN, Claire Chougnet, PhD, Tari Gratton, PA, James M. Greenberg, MD, Cathy Grisby, BSN, CCRC, William Hardie, MD, Alan H. Jobe MD, PhD, Beth Koch, BHS, RRT, RPFT, Karen McDowell, MD, Kelly Thornton BS

Washington University:

Pamela Bates, CRT, RPFT, RPSGT, Claudia Cleveland, RRT, Thomas Ferkol, MD, Aaron Hamvas, MD, Julie Hoffmann, RN, Mark R. Holland, PhD, James Kemp, MD, Philip T. Levy, MD, Laura Linneman, RN, Jayne Sicard-Su, RN, Gina Simpson, RRT, CPFT, Gautam K. Singh, MD, Barbara Warner, MD

University of California at San Francisco:

Investigators

Philip L. Ballard, MD, PhD[1], Roberta A. Ballard, MD[1], David J. Durand, MD[2], Eric C. Eichenwald, MD[4], Roberta L. Keller, MD[1], Amir M. Khan, MD[4], Leslie Lusk, MD[1], Jeffrey D. Merrill, MD[3], Dennis W. Nielson, MD, PhD[1], Elizabeth E. Rogers, MD[1]

Research Staff

Jeanette M. Asselin, MS, RRT-NPS[2], Samantha Balan1, Katrina Burson, RN, BSN[4], Cheryl Chapin[1], Erna Josiah-Davis, RN, NP[3], Carmen Garcia, RN, CCRP[4], Hart Horneman[1], Rick Hinojosa, BSRT, RRT, CPFT-NPS[4], Christopher Johnson, MBA, RRT[4], Susan Kelley, RRT[1], Karin L. Knowles[1], M. Layne Lillie, RN, BSN[4], Karen Martin, RN[4], Sarah Martin, RN, BSN[1], Julie Arldt-McAlister, RN, BSN4, Georgia E. McDavid, RN4, Lori Pacello, RCP2, Shawna Rodgers, RN, BSN[4], Daniel K. Sperry, RN4,[1]

[1]Department of Pediatrics, University of California San Francisco, San Francisco, CA; [2]Children's Hospital and Research Center Oakland, Oakland, CA

[3]Alta Bates Summit Medical Center, Berkeley, CA

[4]University of Texas Health Science Center- Houston, Houston, TX

Vanderbilt University:

Judy Aschner, MD, Amy B Beller BSN, Candice Fike, MD, Scott Guthrie, MD, Tina Hartert, MD, Nathalie Maitre, MD, Paul Moore, MD, Mark O' Hunt, Theresa J. Rogers, RN, Odessa L. Settles, RN, MSN, CM, Steven Steele, RN, Marshall Summar, MD, Sharon Wadley, BSN, RN, CLS

University of Rochester-University at Buffalo:

Investigators:

Carl D'Angio, MD, Vasanth Kumar, MD, Tom Mariani, PhD, Gloria Pryhuber, MD, Clement Ren, MD, Anne Marie Reynolds, MD, MPH, Rita M. Ryan, MD*, Kristin Scheible, MD, Timothy Stevens, MD, MPH

Technical Staff:

Heidie Huyck, BS, Valerie Lunger, MS

Study Staff:

Shannon Castiglione, RN, Aimee Horan, LPN, Deanna Maffet, RN, Jane O'Donnell, PNP, Michael Sacilowski, MAT, Tanya Scalise, RN, BSN, Elizabeth Werner, MPH, Jason Zayac, BS Respiratory Therapists and Nurses:

Kim Bordeaux, RRT, Pam Brown, RRT, Julia Epping, AAS, RT, Lisa Flattery-Walsh, RRT, Donna Germuga, RRT, CPFT, Nancy Jenks, RN, Mary Platt, RN, Eileen Popplewell, RRT, Sandra Prentice, CRT

*Present address, Case Western Reserve University, Cleveland, OH

Duke University:

Kim Ciccio, RN, C. Michael Cotten, M.D., Kim Fisher, Ph.D., Jack Sharp, M.D., Judith A. Voynow, M.D.*

*Present address, Virginia Commonwealth University

Indiana University:

Charles Clem, RRT, Stephanie Davis, M.D., Susan Gunn, NNP, CCRC, Lauren Jewett, RN, CCRC Brenda Poindexter, M.D., M.S.#

#Present address, University of Cincinnati

Steering Committee Chair:

Lynn M. Taussig, MD, University of Denver

NHLBI Program Officer:

Carol J. Blaisdell, MD

University of Pennsylvania Data Coordinating Center:

Scarlett Bellamy, ScD, Maria Blanco, BS, Denise Cifelli, MS, Sara DeMauro, MD,

Jonas Ellenberg, PhD, Rui Feng, PhD, Melissa Fernando, MPH, Howard Panitch, MD,

Barbara Schmidt, MD, MSc Pamela Shaw, PhD, Ann Tierney, BA, MS

SUPPLEMENTARY MATERIAL

The Supplementary Material for this article can be found online at: https://www.frontiersin.org/articles/10.3389/fimmu.2020.563473/full#supplementary-material

REFERENCES

1. Ehrenkranz RA, Walsh MC, Vohr BR, Jobe AH, Wright LL, Fanaroff AA, et al. Validation of the National Institutes of Health consensus definition of bronchopulmonary dysplasia. *Pediatrics* (2005) 116(6):1353–60. doi: 10.1542/peds.2005-0249
2. Mathews TJ, Minino AM, Osterman MJ, Strobino DM, Guyer B. Annual summary of vital statistics: 2008. *Pediatrics* (2011) 127(1):146–57. doi: 10.1542/peds.2010-3175
3. Schmidt B, Asztalos EV, Roberts RS, Robertson CM, Sauve RS, Whitfield MF, et al. Impact of bronchopulmonary dysplasia, brain injury, and severe retinopathy on the outcome of extremely low-birth-weight infants at 18 months: results from the trial of indomethacin prophylaxis in preterms. *JAMA J Am Med Assoc* (2003) 289(9):1124–9. doi: 10.1001/jama.289.9.1124
4. (CDC) C.f.D.C. Preterm Birth. 2014 12/23/2014 02/04/2015].
5. Villamor-Martinez E, Alvarez-Fuente M, Ghazi AMT, Degraeuwe P, Zimmermann LJI, Kramer BW, et al. Association of Chorioamnionitis With Bronchopulmonary Dysplasia Among Preterm Infants: A Systematic Review, Meta-analysis, and Metaregression. *JAMA Netw Open* (2019) 2(11): e1914611. doi: 10.1001/jamanetworkopen.2019.14611
6. Wang SH, Tsao PN. Phenotypes of Bronchopulmonary Dysplasia. *Int J Mol Sci* (2020) 21(17):1–21. doi: 10.3390/ijms21176112
7. Jacob SV, Coates AL, Lands LC, MacNeish CF, Riley SP, Hornby L, et al. Long-term pulmonary sequelae of severe bronchopulmonary dysplasia. *J Pediatr* (1998) 133(2):193–200. doi: 10.1016/S0022-3476(98)70220-3
8. Collins JJP, Tibboel D, de Kleer IM, Reiss IKM, Rottier RJ. The Future of Bronchopulmonary Dysplasia: Emerging Pathophysiological Concepts and Potential New Avenues of Treatment. *Front Med (Lausanne)* (2017) 4:61. doi: 10.3389/fmed.2017.00061
9. Balany J, Bhandari V. Understanding the Impact of Infection, Inflammation, and Their Persistence in the Pathogenesis of Bronchopulmonary Dysplasia. *Front Med (Lausanne)* (2015) 2:90. doi: 10.3389/fmed.2015.00090
10. Islam JY, Keller RL, Aschner JL, Hartert TV, Moore PE. Understanding the Short- and Long-Term Respiratory Outcomes of Prematurity and Bronchopulmonary Dysplasia. *Am J Respir Crit Care Med* (2015) 192(2):134–56. doi: 10.1164/rccm.201412-2142PP
11. Kolls JK. Commentary: Understanding the Impact of Infection, Inflammation and Their Persistence in the Pathogenesis of Bronchopulmonary Dysplasia. *Front Med (Lausanne)* (2017) 4:24. doi: 10.3389/fmed.2017.00024
12. Pryhuber GS, Maitre NL, Ballard RA, Cifelli D, Davis SD, Ellenberg JH, et al. Prematurity and respiratory outcomes program (PROP): study protocol of a prospective multicenter study of respiratory outcomes of preterm infants in the United States. *BMC Pediatr* (2015) 15:37. doi: 10.1186/s12887-015-0346-3
13. Dylag AM, Kopin HG, O'Reilly MA, Wang H, Davis SD, Ren CL, et al. Early Neonatal Oxygen Exposure Predicts Pulmonary Morbidity and Functional Deficits at 1 Year. *J Pediatr* (2020) 223:20–8.e2. doi: 10.1016/j.jpeds.2020.04.042
14. Bhattacharya S, Go D, Krenitsky DL, Huyck HL, Solleti SK, Lunger VA, et al. Genome-wide transcriptional profiling reveals connective tissue mast cell accumulation in bronchopulmonary dysplasia. *Am J Respir Crit Care Med* (2012) 186(4):349–58. doi: 10.1164/rccm.201203-0406OC
15. Pietrzyk JJ, Kwinta P, Wollen EJ, Bik-Multanowski M, Madetko-Talowska A, Gunther CC, et al. Gene expression profiling in preterm infants: new aspects of bronchopulmonary dysplasia development. *PloS One* (2013) 8(10):e78585. doi: 10.1371/journal.pone.0078585
16. Misra RS, Bhattacharya S, Huyck HL, Wang JC, Slaunwhite CG, Slaunwhite SL, et al. Flow-based sorting of neonatal lymphocyte populations for transcriptomics analysis. *J Immunol Methods* (2016) 437:13–20. doi: 10.1016/j.jim.2016.07.001
17. Wright CJ, Kirpalani H. Targeting inflammation to prevent bronchopulmonary dysplasia: can new insights be translated into therapies? *Pediatrics* (2011) 128(1):111–26. doi: 10.1542/peds.2010-3875
18. Pagel J, Twisselmann N, Rausch TK, Waschina S, Hartz A, Steinbeis M, et al. Increased Regulatory T Cells Precede the Development of Bronchopulmonary Dysplasia in Preterm Infants. *Front Immunol* (2020) 11:565257. doi: 10.3389/fimmu.2020.565257
19. D'Angio CT, Ambalavanan N, Carlo WA, McDonald SA, Skogstrand K, Hougaard DM, et al. Blood Cytokine Profiles Associated with Distinct Patterns of Bronchopulmonary Dysplasia among Extremely Low Birth

Weight Infants. *J Pediatr* (2016) 174:45–51.e5. doi: 10.1016/j.jpeds.2016.03.058
20. Bruder D, Srikiatkhachorn A, Enelow RI. Cellular immunity and lung injury in respiratory virus infection. *Viral Immunol* (2006) 19(2):147–55. doi: 10.1089/vim.2006.19.147
21. Turunen R, Vaarala O, Nupponen I, Kajantie E, Siitonen S, Lano A, et al. Activation of T cells in preterm infants with respiratory distress syndrome. *Neonatology* (2009) 96(4):248–58. doi: 10.1159/000220764
22. You D, Ripple M, Balakrishna S, Troxclair D, Sandquist D, Ding L, et al. Inchoate CD8+ T cell responses in neonatal mice permit influenza-induced persistent pulmonary dysfunction. *J Immunol* (2008) 181(5):3486–94. doi: 10.4049/jimmunol.181.5.3486
23. Tregoning JS, Yamaguchi Y, Harker J, Wang B, Openshaw PJ. The role of T cells in the enhancement of respiratory syncytial virus infection severity during adult reinfection of neonatally sensitized mice. *J Virol* (2008) 82(8):4115–24. doi: 10.1128/JVI.02313-07
24. Tasker L, Lindsay RW, Clarke BT, Cochrane DW, Hou S. Infection of mice with respiratory syncytial virus during neonatal life primes for enhanced antibody and T cell responses on secondary challenge. *Clin Exp Immunol* (2008) 153(2):277–88. doi: 10.1111/j.1365-2249.2008.03591.x
25. Scheible KM, Emo J, Laniewski N, Baran AM, Peterson DR, Holden-Wiltse J, et al. T cell developmental arrest in former premature infants increases risk of respiratory morbidity later in infancy. *JCI Insight* (2018) 3(4). doi: 10.1172/jci.insight.96724
26. Bhattacharya S, Zhou Z, Yee M, Chu CY, Lopez AM, Lunger VA, et al. The genome-wide transcriptional response to neonatal hyperoxia identifies Ahr as a key regulator. *Am J Physiol Lung Cell Mol Physiol* (2014) 307(7):L516–23. doi: 10.1152/ajplung.00200.2014
27. Keller RL, Feng R, DeMauro SB, Ferkol T, Hardie W, Rogers EE, et al. Bronchopulmonary Dysplasia and Perinatal Characteristics Predict 1-Year Respiratory Outcomes in Newborns Born at Extremely Low Gestational Age: A Prospective Cohort Study. *J Pediatr* (2017) 187:89–97 e3. doi: 10.1016/j.jpeds.2017.04.026
28. Mishra S, Liao W, Liu Y, Yang M, Ma C, Wu H, et al. TGF-beta and Eomes control the homeostasis of CD8+ regulatory T cells. *J Exp Med* (2021) 218(1):1–15. doi: 10.1084/jem.20200030
29. Zhuang H, Zhang C, Hou B. GTF2IRD1 overexpression promotes tumor progression and correlates with less CD8+ T cells infiltration in pancreatic cancer. *Biosci Rep* (2020) 40(9):1–12. doi: 10.1042/BSR20202150
30. Wang Y, Gao Z, Du X, Chen S, Zhang W, Wang J, et al. Co-inhibition of the TGF-beta pathway and the PD-L1 checkpoint by pH-responsive clustered nanoparticles for pancreatic cancer microenvironment regulation and anti-tumor immunotherapy. *Biomater Sci* (2020) 8(18):5121–32. doi: 10.1039/D0BM00916D
31. de Streel G, Bertrand C, Chalon N, Lienart S, Bricard O, Lecomte S, et al. Selective inhibition of TGF-beta1 produced by GARP-expressing Tregs overcomes resistance to PD-1/PD-L1 blockade in cancer. *Nat Commun* (2020) 11(1):4545. doi: 10.1038/s41467-020-17811-3
32. Bromley SK, Akbaba H, Mani V, Mora-Buch R, Chasse AY, Sama A, et al. CD49a Regulates Cutaneous Resident Memory CD8(+) T Cell Persistence and Response. *Cell Rep* (2020) 32(9):108085. doi: 10.1016/j.celrep.2020.108085
33. Tooley WH. Epidemiology of bronchopulmonary dysplasia. *J Pediatr* (1979) 95(5 Pt 2):851–8. doi: 10.1016/S0022-3476(79)80451-5
34. Shennan AT, Dunn MS, Ohlsson A, Lennox K, Hoskins EM. Abnormal pulmonary outcomes in premature infants: prediction from oxygen requirement in the neonatal period. *Pediatrics* (1988) 82(4):527–32.
35. Jobe AH, Bancalari E. Bronchopulmonary dysplasia. *Am J Respir Crit Care Med* (2001) 163(7):1723–9. doi: 10.1164/ajrccm.163.7.2011060
36. Walsh MC, Yao Q, Gettner P, Hale E, Collins M, Hensman A, et al. Impact of a physiologic definition on bronchopulmonary dysplasia rates. *Pediatrics* (2004) 114(5):1305–11. doi: 10.1542/peds.2004-0204
37. Benaron DA, Benitz WE. Maximizing the stability of oxygen delivered via nasal cannula. *Arch Pediatr Adolesc Med* (1994) 148(3):294–300. doi: 10.1001/archpedi.1994.02170030064015
38. Wai KC, Kohn MA, Ballard RA, Truog WE, Black DM, Asselin JM, et al. Early cumulative supplemental oxygen predicts bronchopulmonary dysplasia in high risk extremely low gestational age newborns. *J Pediatr* (2016) 177:97–102.e2. doi: 10.1016/j.jpeds.2016.06.079
39. Scheible K, Secor-Socha S, Wightman T, Wang H, Mariani TJ, Topham DJ, et al. Stability of T cell phenotype and functional assays following heparinized umbilical cord blood collection. *Cytometry A* (2012) 81p(11):937–49. doi: 10.1002/cyto.a.22203
40. Kim D, Pertea G, Trapnell C, Pimentel H, Kelley R, Salzberg SL. TopHat2: accurate alignment of transcriptomes in the presence of insertions, deletions and gene fusions. *Genome Biol* (2013) 14(4):R36. doi: 10.1186/gb-2013-14-4-r36
41. Anders S, Pyl PT, Huber W. HTSeq–a Python framework to work with high-throughput sequencing data. *Bioinformatics* (2015) 31(2):166–9. doi: 10.1093/bioinformatics/btu638
42. Li J, Tibshirani R. Finding consistent patterns: a nonparametric approach for identifying differential expression in RNA-Seq data. *Stat Methods Med Res* (2013) 22(5):519–36. doi: 10.1177/0962280211428386
43. Bair E, Hastie T, Paul D, Tibshirani R. Prediction by supervised principal components. *J Am Stat Assoc* (2006) 101(473):119–37. doi: 10.1198/016214505000000628
44. Liberzon A, Subramanian A, Pinchback R, Thorvaldsdottir H, Tamayo P, Mesirov JP, et al. Molecular signatures database (MSigDB) 3.0. *Bioinformatics* (2011) 27(12):1739–40. doi: 10.1093/bioinformatics/btr260
45. Bhattacharya S, Rosenberg AF, Peterson DR, Grzesik K, Baran AM, Ashton JM, et al. Transcriptomic Biomarkers to Discriminate Bacterial from Nonbacterial Infection in Adults Hospitalized with Respiratory Illness. *Sci Rep* (2017) 7(1):6548. doi: 10.1038/s41598-017-06738-3
46. Bhandari V, Lodha A. Is bronchopulmonary dysplasia decided before birth? *Pediatr Res* (2020) 87(5):809–10. doi: 10.1038/s41390-020-0819-4
47. Ambalavanan N, Cotten CM, Page GP, Carlo WA, Murray JC, Bhattacharya S, et al. Integrated genomic analyses in bronchopulmonary dysplasia. *J Pediatr* (2015) 166(3):531–7 e13. doi: 10.1016/j.jpeds.2014.09.052
48. Hamvas A, Feng R, Bi Y, Wang F, Bhattacharya S, Mereness J, et al. Exome sequencing identifies gene variants and networks associated with extreme respiratory outcomes following preterm birth. *BMC Genet* (2018) 19(1):94. doi: 10.1186/s12863-018-0679-7
49. Kho AT, Bhattacharya S, Mecham BH, Hong J, Kohane IS, Mariani TJ, et al. Expression profiles of the mouse lung identify a molecular signature of time-to-birth. *Am J Respir Cell Mol Biol* (2009) 40(1):47–57. doi: 10.1165/rcmb.2008-0048OC
50. Kho AT, Bhattacharya S, Tantisira KG, Carey VJ, Gaedigk R, Leeder JS, et al. Transcriptomic analysis of human lung development. *Am J Respir Crit Care Med* (2010) 181(1):54–63. doi: 10.1164/rccm.200907-1063OC
51. Bhattacharya S, Tyagi S, Srisuma S, Demeo DL, Shapiro SD, Bueno R, et al. Peripheral blood gene expression profiles in COPD subjects. *J Clin Bioinform* (2011) 1(1):12. doi: 10.1186/2043-9113-1-12
52. Davidson LM, Berkelhamer SK. Bronchopulmonary Dysplasia: Chronic Lung Disease of Infancy and Long-Term Pulmonary Outcomes. *J Clin Med* (2017) 6(1):1–20. doi: 10.3390/jcm6010004
53. Cao Y, Zhang X, Wang L, Yang Q, Ma Q, Xu J, et al. PFKFB3-mediated endothelial glycolysis promotes pulmonary hypertension. *Proc Natl Acad Sci U S A* (2019) 116(27):13394–403. doi: 10.1073/pnas.1821401116
54. Hansmann G, Sallmon H, Roehr CC, Kourembanas S, Austin ED, Koestenberger M, et al. Pulmonary hypertension in bronchopulmonary dysplasia. *Pediatr Res* (2020). doi: 10.1038/s41390-020-0993-4
55. Telang S, Clem BF, Klarer AC, Clem AL, Trent JO, Bucala R, et al. Small molecule inhibition of 6-phosphofructo-2-kinase suppresses t cell activation. *J Trans Med* (2012) 10(1):95. doi: 10.1186/1479-5876-10-95
56. Ye H, Zhang J, Wang J, Gao Y, Du Y, Li C, et al. CD4 T-cell transcriptome analysis reveals aberrant regulation of STAT3 and Wnt signaling pathways in rheumatoid arthritis: evidence from a case-control study. *Arthritis Res Ther* (2015) 17:76. doi: 10.1186/s13075-015-0590-9
57. Kwan J, Sczaniecka A, Heidary Arash E, Nguyen L, Chen CC, Ratkovic S, et al. DLG5 connects cell polarity and Hippo signaling protein networks by linking PAR-1 with MST1/2. *Genes Dev* (2016) 30(24):2696–709. doi: 10.1101/gad.284539.116
58. Venugopal P, Veyssiere H, Couderc JL, Richard G, Vachias C, Mirouse V, et al. Multiple functions of the scaffold protein Discs large 5 in the control of growth, cell polarity and cell adhesion in Drosophila melanogaster. *BMC Dev Biol* (2020) 20(1):10. doi: 10.1186/s12861-020-00218-0
59. Sezaki T, Tomiyama L, Kimura Y, Ueda K, Kioka N, et al. Dlg5 interacts with the TGF-beta receptor and promotes its degradation. *FEBS Lett* (2013) 587(11):1624–9. doi: 10.1016/j.febslet.2013.04.015

60. Kaewseekhao B, Naranbhai V, Roytrakul S, Namwat W, Paemanee A, Lulitanond V, et al. Comparative Proteomics of Activated THP-1 Cells Infected with Mycobacterium tuberculosis Identifies Putative Clearance Biomarkers for Tuberculosis Treatment. *PloS One* (2015) 10(7):e0134168. doi: 10.1371/journal.pone.0134168
61. Mohan S, Gupta D. Crosstalk of toll-like receptors signaling and Nrf2 pathway for regulation of inflammation. *BioMed Pharmacother* (2018) 108:1866–78. doi: 10.1016/j.biopha.2018.10.019
62. Stampouloglou E, Cheng N, Federico A, Slaby E, Monti S, Szeto GL, et al. Yap suppresses T-cell function and infiltration in the tumor microenvironment. *PloS Biol* (2020) 18(1):e3000591. doi: 10.1371/journal.pbio.3000591
63. Zhou J, Zhang N, Zhang W, Lu C, Xu F. The YAP/HIF-1α/miR-182/EGR2 Axis is Implicated in Asthma Severity by Control of Th17 Cell Differentiation. *Res Square* (2020) 1–28. doi: 10.21203/rs.3.rs-61653/v1
64. Thompson EA, Liang F, Lindgren G, Sandgren KJ, Quinn KM, Darrah PA, et al. Human Anti-CD40 Antibody and Poly IC:LC Adjuvant Combination Induces Potent T Cell Responses in the Lung of Nonhuman Primates. *J Immunol* (2015) 195(3):1015–24. doi: 10.4049/jimmunol.1500078
65. Misra RS, Shi G, Moreno-Garcia ME, Thankappan A, Tighe M, Mousseau B, et al. G alpha q-containing G proteins regulate B cell selection and survival and are required to prevent B cell-dependent autoimmunity. *J Exp Med* (2010) 207(8):1775–89. doi: 10.1084/jem.20092735
66. Sun Y, Wang Y, Chen S, Fan G, Zhang J, Dai F, et al. Expression of Galphaq Is Decreased in Lymphocytes from Primary Sjogren's Syndrome Patients and Related to Increased IL-17A Expression. *J Immunol Res* (2018) 2018:8212641. doi: 10.1155/2018/8212641
67. Siska PJ, Beckermann KE, Mason FM, Andrejeva G, Greenplate AR, Sendor AB, et al. Mitochondrial dysregulation and glycolytic insufficiency functionally impair CD8 T cells infiltrating human renal cell carcinoma. *JCI Insight* (2017) 2(12):1–14. doi: 10.1172/jci.insight.93411
68. Ji Y, Dang X, Nguyen LNT, Nguyen LN, Zhao J, Cao D, et al. Topological DNA damage, telomere attrition and T cell senescence during chronic viral infections. *Immun Ageing* (2019) 16:12. doi: 10.1186/s12979-019-0153-z
69. Saeidi A, Zandi K, Cheok YY, Saeidi H, Wong WF, Lee CYQ, et al. T-Cell Exhaustion in Chronic Infections: Reversing the State of Exhaustion and Reinvigorating Optimal Protective Immune Responses. *Front Immunol* (2018) 9:2569. doi: 10.3389/fimmu.2018.02569
70. Wang J, Dong W. Oxidative stress and bronchopulmonary dysplasia. *Gene* (2018) 678:177–83. doi: 10.1016/j.gene.2018.08.031
71. Subramanian A, Tamayo P, Mootha VK, Mukherjee S, Ebert BL, Gillette MA, et al. Gene set enrichment analysis: a knowledge-based approach for interpreting genome-wide expression profiles. *Proc Natl Acad Sci U.S.A.* (2005) 102(43):15545–50. doi: 10.1073/pnas.0506580102
72. Zhang L, Liu J, Qian L, Feng Q, Wang X, Yuan Y, et al. Induction of OTUD1 by RNA viruses potently inhibits innate immune responses by promoting degradation of the MAVS/TRAF3/TRAF6 signalosome. *PloS Pathog* (2018) 14 (5):e1007067. doi: 10.1371/journal.ppat.1007067
73. Bros M, Haas K, Moll L, Grabbe S. RhoA as a Key Regulator of Innate and Adaptive Immunity. *Cells* (2019) 8(7):1–30. doi: 10.3390/cells8070733
74. Wang Z, Yoo YJ, De La Torre R, Topham C, Hanifin J, Simpson E, et al. Inverse correlation of TRIM32 and PKCzeta in Th2 biased inflammation. *J Invest Dermatol* (2020). doi: 10.1016/j.jid.2020.09.021
75. Lv XB, Liu CY, Wang Z, Sun YP, Xiong Y, Lei QY, et al. PARD3 induces TAZ activation and cell growth by promoting LATS1 and PP1 interaction. *EMBO Rep* (2015) 16(8):975–85. doi: 10.15252/embr.201439951
76. Araki K, Turner AP, Shaffer VO, Gangappa S, Keller SA, Bachmann MF, et al. mTOR regulates memory CD8 T-cell differentiation. *Nature* (2009) 460 (7251):108–12. doi: 10.1038/nature08155
77. Tsou PS, Coit P, Kilian NC, Sawalha AH. EZH2 Modulates the DNA Methylome and Controls T Cell Adhesion Through Junctional Adhesion Molecule A in Lupus Patients. *Arthritis Rheumatol* (2018) 70(1):98–108. doi: 10.1002/art.40338

Conflict of Interest: The authors declare that the research was conducted in the absence of any commercial or financial relationships that could be construed as a potential conflict of interest.

frontiers in Immunology

MINI REVIEW
published: 09 February 2021
doi: 10.3389/fimmu.2020.611573

T Cell Repertoire During Ontogeny and Characteristics in Inflammatory Disorders in Adults and Childhood

Svenja Foth[1], *Sara Völkel*[1], *Daniel Bauersachs*[1], *Michael Zemlin*[2] *and Chrysanthi Skevaki*[1]*

[1] German Center for Lung Research (DZL), Institute of Laboratory Medicine, Universities of Giessen and Marburg Lung Center (UGMLC), Philipps University Marburg, Marburg, Germany, [2] Department of General Pediatrics and Neonatology, Saarland University Medical School, Homburg, Germany

Since the first day of life, a newborn has to deal with various pathogens from the environment. While passive immune protection is provided by diaplacental maternal antibodies, the development of cellular immunity is ongoing. A mature immune system should be able not only to defend against pathogens, but should also be able to differentiate between self- and non-self-antigens. Dysregulation in the development of cellular immunity can lead to severe disorders like immunodeficiency, autoimmunity and chronic inflammation. In this review, we explain the role of T cell immunity in antigen detection and summarize the characteristics of a mature TCR repertoire as well as the current state of knowledge about the development of the TCR repertoire in ontogenesis. In addition, methods of assessments are outlined, with a focus on the advantages and disadvantages of advanced methods such as next generation sequencing. Subsequently, we provide an overview of various disorders occuring in early childhood like immunodeficiencies, autoimmunity, allergic diseases and chronic infections and outline known changes in the TCR repertoire. Finally, we summarize the latest findings and discuss current research gaps as well as potential future developments.

Keywords: T cell immunity, diversity, clonality, ontogeny, autoimmune disorders, immune deficiencies, allergy, next generation sequencing

OPEN ACCESS

Edited by:
Antonio Serrano, Instituto de Investigación Hospital 12 de Octubre, Spain

Reviewed by:
Giuseppe Fiume, University of Catanzaro, Italy
Encarnita Mariotti-Ferrandiz, Université Pierre et Marie Curie, France

***Correspondence:**
Chrysanthi Skevaki
chrysanthi.skevaki@uk-gm.de

Specialty section:
This article was submitted to Autoimmune and Autoinflammatory Disorders, a section of the journal Frontiers in Immunology

Received: *29 September 2020*
Accepted: *22 December 2020*
Published: *09 February 2021*

Citation:
Foth S, Völkel S, Bauersachs D, Zemlin M and Skevaki C (2021) T Cell Repertoire During Ontogeny and Characteristics in Inflammatory Disorders in Adults and Childhood. Front. Immunol. 11:611573. doi: 10.3389/fimmu.2020.611573

INTRODUCTION: T CELL IMMUNITY

The Role of T Cell Receptor in Antigen Recognition

The cellular immune system is based on the interaction between T cells and antigen presenting cells. Short peptides, that are presented by MHC-I molecules on the cell surface of antigen-presenting cells, are detected by the T cell receptor (TCR) of T cells. The TCR is a heterodimeric receptor, composed of α- and β-chains or γ- and δ-chains. Each chain is composed of a constant region and a variable region, which is either composed of a V- and a J-region (α chain) or a V, a D and a J region (β chain). The variable domain contains the complementarity determining region (CDR3), which mediates antigen binding and is mainly responsible for TCR diversity and antigen specificity. While each T cell expresses its unique TCRs, a high degree of diversity of TCRs is necessary to detect a broad spectrum of foreign antigens. The TCR gene loci on Chromosome 7 for TRB and on

chromosome 14 for TRA comprises over 250 different genes encoding for the V, D, and J region and diversity is provided by somatic gene rearrangement. Additionally, single nucleotides are inserted and deleted randomly (1).

Despite a broad repertoire to defend pathogens, the discrimination between self and non-self is crucial for immunocompetence. The selection of T lymphocytes takes place in the thymus and is known as central tolerance. Premature T lymphocytes emerging from bone marrow immigrate to the thymus to undergo a differentiation process including positive and negative selection. First, in the thymic cortex, only T cells with sufficient ability to bind to MHC molecules are not sorted out by apoptosis, which is called positive selection. During subsequent negative selection, T cells with high affinity to self-antigens are eliminated and only T cells without significant self-reactivity leave the thymus and immigrate to peripheral lymphoid organs (2).

Thus, the organism of a newborn is armed with a highly efficient cellular immune system, capable to defend itself against infections as well as tolerate self-antigens. Every disturbance in this highly regulated process can lead to inflammatory and autoimmune disorders or severe immunodeficiencies (1, 3, 4). Recent advances have shown that viral infections play a role in the central tolerance process and can lead to an impaired self-tolerance. For example, thymus atrophy occurs in acute virus infections and direct infiltration of the thymus epithelial cells by virus antigens is observed (5, 6). Thus, viral infections can influence antigen presentation and increase susceptibility to autoimmune disorders (7).

Characteristics of the TCR Repertoire

Diversity and Clonality

In a healthy immune repertoire, T lymphocytes that underwent the selection process in the thymus show a highly diverse receptor repertoire (polyclonal) and are thereby capable to defend almost against every pathogen (see **Figure 1**). Theoretically, the number of possible TCRß-chains is nearly limitless, but model calculations assume a number of 10^{11} possible ß-chains (8). New methodological approaches estimated an individual repertoire of about 10^6 ß-chains (9). Once a suitable MHC-presented peptide is identified and binds to a TCR, the T cell changes to an effector cell and starts clonal expansion (see **Figure 1**). After a pathogen is eliminated, the count of clonal T cells declines and only a small amount of antigen specific T cells rest as memory cells in the circulating blood pool. These T cells can be reactivated in a second exposure to the same antigen with a higher and faster response. It is remarkable that the immune response shows significant

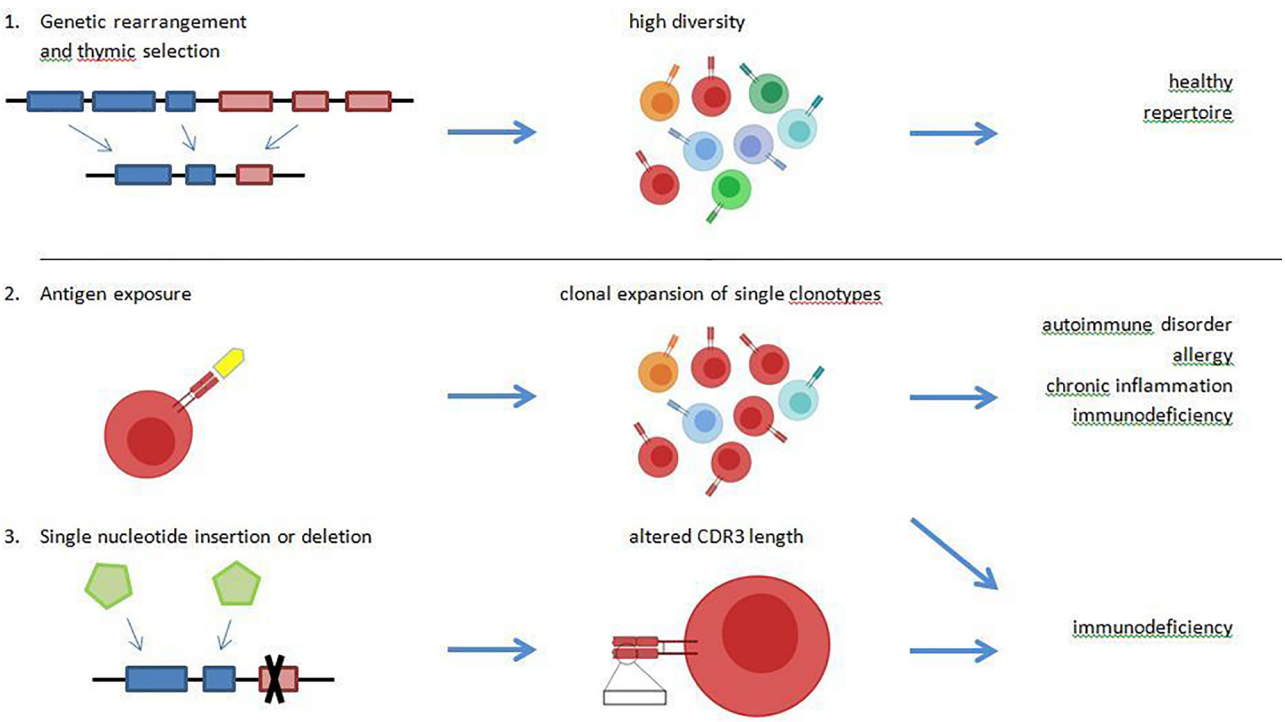

FIGURE 1 | A healthy T cell receptor (TCR) repertoire is characterized by a high diversity and the ability to detect foreign antigens as well as tolerate self-antigens. These properties are mediated by genetic rearrangement of the VDJ-region, and positive and negative selection in the thymus (1.). Driven by antigen exposure, some TCR undergo clonal expansion, which leads to a reduced diversity of the overall repertoire. A high abundance of single clonotypes with reduced repertoire diversity is observed in chronic virus infections like Epstein-Barr virus (EBV) and cytomegalovirus (CMV), in allergy, in chronic inflammation and possibly in immunodeficiencies (2.). Diversity of the TCR repertoire may be mediated by random nucleotide insertion and deletion. In specific immunodeficiency disorders, a reduced CDR3-length is observed due to nucleotidedeletion (3.).

differences between the primary and secondary antigen exposure. Bousso et al. could show that the selective expansion of specific T cells in the secondary response is independent from the relative frequency of memory T cell but may be associated to the epitope density (10). In chronic infections like EBV and CMV as well as in autoimmune diseases, a clonal expansion of T cells is observed and recent investigations showed that such TCR clones can serve as biomarkers (3, 11–13).

Private and Public TCR Clones

Considering the high diversity of an individual TCR repertoire, the statistical probability of finding the same clones in different individuals is rather low. Nevertheless, specific TCR clones are shared among individuals in a higher number than the statistical probability and are defined as "public". It has been demonstrated that the quantity of public clonotypes is around 1% and that these TCRs are less dependent on inherited factors like the HLA alleles but influenced by antigen-exposure (9). On the other hand, some TCR clones are highly individual and thus called "private". In some studies, public TCR clones are associated with autoimmune disorders. For example, a high amount of public TCR clones could be found in cerebrospinal fluid of patients with multiple sclerosis (14). In HIV-infected individuals, a high number of public TCRs is linked with a protective immune response (15, 16).

Use of Next Generation Sequencing (NGS) and Data Analysis

Due to the enormous diversity the characterization of the TCR repertoire is a challenging task. Over the past decades, various methods have been developed to investigate the TCR repertoire. Each method may decipher a smaller or larger part of the repertoire. Several reviews provide a broad overview of the available methods, their advantages and disadvantages (see **Table 1**) (1, 26, 28). The increasing use of next generation sequencing (NGS) techniques in this field has provided new and high-resolution insights into the TCR repertoire of healthy and diseased individuals. NGS offers several advantages for diagnostic applications. Compared to other methods the resolution of information is much higher using less input of biomaterial. However, several comparative studies have shown that the different approaches lead to significantly different results, even when using the same input material (27, 30). These studies indicate that there is still a need to standardize the analysis of TCR repertoires for clinical application. This is not only the requirement of a patient-specific TCR sequencing but also the customizable data analysis and evaluation. This point in particular is currently being addressed by many scientists. In addition to the development of different analysis tools for NGS data, different analytical approaches are compared in order to satisfy the great diversity of the TCR repertoire. Different approaches are summarized and compared by Miho and colleagues as well as by Bradley and Thomas (31, 32). In the following years, these further developments will increase the understanding of the diversity and evolution of the TCR repertoire and allow T cell receptors to become even more important in clinical diagnostics than they are today.

Development of TCR Repertoire

Although random events do play a significant role during the rearrangement of the genes of antigen receptors, the

TABLE 1 | Methods of assessment.

Methods	Biomaterial	Assessment	Advantages	Disadvantages	References
Flow cytometry	T cells	Detection of expressed TCRs by monoclonal antibodies	* rapid screening of CD4+ and CD8 + T cells * no purification of cell populations necessary	* limited availability of monoclonal antibodies * high amount of cells is necessary * low-frequency T cell clones are not detected	Faint et al. (17) Cossarizza et al. (18) Flores-Conzalez et al. (19)
CDR 3 spectratyping	T cell DNA or RNA	Electrophoresis of amplicons derived from the CDR3 region	* rapid analysis of T cell clones with different length * semi-quantitative	* blind for the underlying sequence * low-frequency T cell clones are not detected	Cochet et al. (20) Currier et al. (21) Fozza et al. (22)
Classical cloning combined with Sanger sequencing	T cell DNA or RNA	Sequencing of amplicons derived from the CDR3 region	* In comparison to classical spectratyping it additionally reveals the DNA sequence	* large workload * low-frequency T cell clones are not detected * massive data sets to analyse	Sanger et al. (23) Sant'Angelo et al. (24) Correia-Neves et al. (25)
NGS	T cell DNA or RNA	Amplification of the CDR3 region followed by sequencing	* low amount of starting material DNA * highly abundant * proportional to -the number of T cells RNA * only expressed TCRs are analysed * less biased by PCR artefacts and efficiencies	* in a bulk assay the pairing information of α and β chain is absent * massive data sets to analyse DNA * primer efficiency affects the results RNA * not proportional to the number of T cells	Woodworth et al. (1) Six et al. (26) Liu et al. (27) Rosati et al. (28) Simone et al. (29) Barennes et al. (30)

development of the BCR and TCR repertoires is strictly regulated during ontogeny and during the establishment of lymphocyte subpopulations (33, 34). In humans, fetal prothymocytes with rearranged TCR genes occur as early as 7 weeks of gestation in the yolk sac and liver. In the fetal blood, naïve $CD38^+CD45RA^+$ T cells predominate and the CD4/CD8 ratio is elevated in comparison to adults. Studies of human fetal tissues and cord blood revealed that the maturation of the T cell repertoire is mainly characterized by an expansion of clonality and by an increasing addition of N nucleotides within the hypervariable CDR3 region (35–37). Interestingly, the entire gene loci of the TCR alpha, beta, gamma and delta chains are accessible in the second trimester fetus, and the use of variable, diversity and joining gene elements appears to undergo fewer changes during ontogeny when compared to the immunoglobulin heavy chain genes (38). Overall, TCR repertoires are functionally more similar in cord blood but diverge during later life, paralleling the exposure to extrauterine antigens (37).

Schelonka et al. observed that TCR transcripts were clonally restricted in the second trimester fetus and were polyclonal later in life. The length of CDR3 regions increased during the fetal development in TCR transcripts regardless of their V region usage, due to an increasing addition of N nucleotides (35). γδ-T cells bearing a TCR with the Vγ9 and Vδ2 variable region (Vγ9Vδ2 T Cells) are typically reactive to phosphoantigens and predominate both among fetal and adult circulating T cells (36, 39). However, fetal Vγ9Vδ2 T cells express divergent CDR3 repertoires. Taken together with functional differences, this indicates that in contrast to murine γδ-T cells, the human adult Vγ9Vδ2 do not arise from the abundant fetal Vγ9Vδ2 T cell population but from the small number of Vγ9Vδ2 T cells generated in the postnatal thymus (39). Moreover, Ben Youssed et al. found that $V\alpha7.2^+$ CD161high mucosal-associated invariant T (MAIT) cells which are reactive to microbial riboflavin precursor derivatives, acquire a memory phenotype within a few weeks of life depending on their antigen specificity. Thus, during the antigen-driven T cell memory formation, fetal T cell populations with other reactivities are diluted out over a period of at least 6 years (40).

TCR REPERTOIRE IN INFLAMMATORY DISORDERS

Asthma and Allergy

Bronchial asthma is a chronic inflammatory disease and affects over 330 million people worldwide (41). It is one of the most common chronic disorders in childhood with up to 10% of children in Western Europe being afflicted (42). The pathogenesis of allergic asthma is characterized by activation of a TH2-immune response with the secretion of proinflammatory cytokines like IL-4 and IL-5, which in turn leads to an increase in IgE production as well as activation of mast cells and eosinophils (43). There is some evidence that allergic asthma is associated with a skewed TCR repertoire. In 1998, Hodges showed that the TRBV5-5/5-6 subset of the CD4+ T cell population was increased in asthmatics compared to healthy controls, albeit there was a high inter-individual difference in specific TCR frequency in both groups (44). Wahlström also demonstrated an altered TCBV usage in patients with allergic asthma with similar results for peripheral blood and bronchoalveolar lavage (45).

Likewise, in regard to atopy, Kircher et al. (46) found an increased frequency of certain Vß and Vα-chains in individuals with house dust mite allergy. Sade and colleagues (47) could show that the usage of Vß subsets is altered by specific immunotherapy (SIT). Recently, Cao et al. demonstrated a higher diversity and increased clonality in the TCR ß repertoire of allergic children compared to healthy controls using NGS methods (48). Such findings support the hypothesis, that antigen exposure in early life alters immune responses and leads to atopy and related disorders like bronchial asthma.

Autoimmune Disorders

Autoimmune disorders are a heterogenic group of diseases, characterized by an altered immune response of auto-antibodies and self-reactive T cells that leads to inflammation and tissue damage in different organ systems. Studies based on methods like flow-cytometry and CDR3 spectratyping as well as recent research in NGS techniques demonstrate a decreased diversity of the TCR repertoire, as well as an increased number of public T cell clones in autoimmune disorders like systemic lupus erythematosus (SLE), arthritis and Crohn's Disease (12, 49, 50), but these findings are not consistent For example, an animal model of autoimmune encephalomyelitis revealed that a reduced diversity of the TCRαβ repertoire is responsible for protection from autoimmunity (51). It is discussed that exposure to certain antigens leads to an increased susceptibility to autoreactivity. For example, in Myasthenia Gravis (MG) and in Typ1 diabetes, chronic viral infections with EBV and Coxsackievirus could be identified as a trigger for autoimmune responses (52–54). These findings of a skewed TCR repertoire with a clonal pattern in TCRß spectratyping could be confirmed by other authors with some evidence towards a more pronounced effect in systemic autoimmune disorders like SLE or juvenile polyarthritis compared to organ-specific disorders such as diabetes mellitus (49, 55).

So far, studies using high throughput sequencing methods in children are rare. Dokai et al. found a preferential use of Vß families in children with MG in the development and relapse phase, but not in the remission phase, supporting the hypothesis of antigen-driven selection of T cell clones (56). Eugster et al. used NGS in children with autoantibodies (e.g., pre-diabetes), revealing a highly diverse repertoire (57). This may be due to early investigation before the onset of disease and such findings should be reevaluated in other autoimmune disorders in children.

Immunodeficiency

Primary immunodeficiencies are a group of rare diseases that leads to severe infections and often to a shortened lifespan. Susceptibility to bacterial infections is mainly mediated by a decreased number of B-cell and thus reduced numbers or total absence of immunoglobulins. Moreover, various defects in the

cellular immune system such as lymphopenia and impaired T lymphocyte function are described. While the early onset of infections may lead to sepsis and is often a cause of death at a young age, the patient clinical characteristics include autoimmune manifestations such as granulomatosis, enteritis, dermatitis, and vitiligo (58, 59).

With regard to the TCR repertoire, an oligoclonal pattern of the TRBV chain was detected in children with DiGeorge-Syndrom and bone marrow failure (60, 61). In recent studies, oligoclonality could be confirmed using NGS in patients with Wiscott-Aldrich-Syndrom, common variable immune deficiency and X-linked agammaglobulinaemia (58, 59, 62). Additionally, results show a reduced junctional diversity with less nucleotide deletions and insertions in the CDR3 region and a reduced CDR3 length (62). Whether these changes are due to inherited defects or signs of reduced thymic output and subsequent peripheral expansion of T cells is still under research.

Chronic Infections

Human immunodeficiency virus (HIV), Epstein-Barr virus (EBV), and Cytomegalovirus (CMV) cause lifelong infections in the human host. Their replication is tightly controlled by virus-specific CD8+ T cells (63). In the US, the overall seroprevalence is 50.4% and 66.5% for CMV and EBV, respectively (64, 65). While the role of effector memory T (T_{EM}) cells in CMV- and EBV-infected children has recently been evaluated (66), studies on the TCR repertoire in early childhood are lacking. However, in adults, it is known that the CD8+ T cell repertoire in response to CMV infection is highly skewed, due to public TCR that are often dominant within an individual and germline (TCRα chain) or nearly germline-encoded (TCRβ chain) (67). Similar findings have been reported for EBV (11, 68, 69). Further, it has been shown that public recognition of immunodominant EBV epitopes is mainly driven by the TCRα chain (11).

It is already known that HIV-exposed uninfected children have a reduced $CD4^+/CD8^+$+ ratio, as well as CD4+ and CD8+ naïve T cell percentage, but an increased rate of activated CD8+ T cells, and that these abnormalities persist over time (70). Further, their thymic output is reduced, which, together with the lower number of CD4+ cells, is caused by decreased cloning efficiency of their progenitors (71). Newer investigations yielded that human immunodeficiency virus (HIV)-exposed uninfected infants (HEU) has a significantly reduced TCRβ diversity and identifiable clonotypes compared to HIV not-exposed (HU) children and that this reduced diversity is associated with greater numbers of high abundance clonotypes (15).

Other Chronic Inflammatory Disorders

Celiac disease (CeD) is a chronic inflammatory disease caused by an increase in gut intraepithelial γδT cells due to cereal gluten exposure. Compared to healthy individuals, CeD patients have a more extensive and more diverse γδTCR repertoire, a higher usage of TRGV1 and TRDV3, and different patterns of TCRγ and TCRδ- pairing. However, no CeD-specific γδCDR3 motifs could be detected (72).

Also, for inflammatory bowel disease (IBD), a persistent inflammatory response to gut bacteria, a significant increase in TCR in circulating lymphocytes of IL10/IL10R-deficient patients was observed. The authors found shorter CDR3β length and altered hydrophobicity in T cells but could not find specific TCR clones unique to each patient (73). Further, it has been shown that intestinal TCR repertoires show a lower clonotype diversity and a stronger clonal expansion than those in blood. This loss of diversity is caused by the selective bias of V and J gene usage (74).

For other chronic inflammatory disorders like bronchopulmonary dysplasia (BPD) or idiopathic pulmonary fibrosis (IPF), only little is known about the role of the TCR repertoire. For BPD, it has been shown that the TCR receptor pathway in infants suffering from BPD is significantly down-regulated in comparison to healthy individuals (75). Regarding IPF, it is known that T cells in IPF infants were relatively decreased, but the CD4+ memory T cells, the memory T cells relative to naïve T cells, as well as the CD4/CD8 ratio increased compared to the healthy control group (76).

DISCUSSION

The development of the human immune system starts within the first weeks of gestation. From about 7 weeks onwards, fetal prothymocytes with rearranged TCR genes occur in the yolk sac and liver. Besides random insertion and deletion of single nucleotides, the genetic rearrangement of the BCR and TCR repertoire is a highly regulated process. In the fetus, the TCR repertoire is limited by clonal restriction and by short CDR3-regions. During ontogeny, these restrictions are gradually released in a controlled manner under the influence of extrauterine antigens. Soon after birth, such changes in the repertoire show a rapid increase, probably dependent on one's individual microbiome. Ravens et al. could show an increase in γδ T cell subsets in European and African children and a high number of public clonotypes, independent on inherited factors. This increase was reinforced by acute infections but not by vaccination, leading to the hypothesis that only severe immunological challenges leads to a change in the repertoire (77).

In adults, recent research reveals a consistent pattern of oligo- or monoclonal TCR repertoire due to clonal expansion of single TCR clones and a skewed CDR3 length in autoimmune disorders and chronic viral infections. It could be demonstrated that investigations in the TCR repertoire can help to develop new biomarkers. Furthermore, new therapeutic options were established in cancer therapy using engineered T cell subsets (78, 79). Whether these advantages are suitable for clinical application and could be transferred to chronic infections and autoinflammatory diseases is still a topic of research (80).

Until now, there are only a few studies in children focussing on the TCR repertoire and the underlying causes of many chronic disorders in childhood remain unclear. However, chronic disorders in childhood are common and lead to a high burden of disease and often permanent injuries. Some studies in children showed similar findings to the research in the elderly, but findings are not consistent and studies using NGS are still rare. NGS techniques can provide

new and high-resolution insights into the TCR repertoire of healthy and diseased individuals. Studies in children using NGS techniques have the potential to unravel the relevance of antigen exposure and the subsequent changes in the TCR repertoire. Understanding the role of fetal/neonatal imprinting and the relevance of specific antigen exposure in early childhood can lead to new diagnostic approaches or even prevention strategies such as vaccination. New studies in infancy and childhood, regarding the age of onset, stage of disease and ongoing therapy are necessary for a better understanding of immune protection on the one hand and dysregulation of the immune response on the other hand.

AUTHOR CONTRIBUTIONS

CS and SF planned, structured, and edited the manuscript. SV described the methods and added **Table 1**. All authors searched the literature and integrated all contributions. All authors contributed to the article and approved the submitted version.

FUNDING

MZ is supported by Bundesministerium für Bildung und Forschung (BMBF), PRIMAL Consortium grant 01GL1746D. CS is supported by the Universities Giessen and Marburg Lung Center (UGMLC), the German Center for Lung Research (DZL), University Hospital Giessen and Marburg (UKGM) research funding according to article 2, section 3 cooperation agreement, and the Deutsche Forschungsgemeinschaft (DFG)-funded SFB 1021 (C04), KFO 309 (P10), and SK 317/1-1 (Project number 428518790) as well as by the Foundation for Pathobiochemistry and Molecular Diagnostics.

REFERENCES

1. Woodsworth DJ, Castellarin M, Holt RA. Sequence analysis of T-cell repertoires in health and disease. *Genome Med* (2013) 5:98. doi: 10.1186/gm502
2. Albano F, Vecchio E, Renna M, Iaccino E, Mimmi S, Caiazza C, et al. Insights into Thymus Development and Viral Thymic Infections. *Viruses* (2019) 11 (9):836. doi: 10.3390/v11090836
3. Attaf M, Huseby E, Sewell AK. αβ T cell receptors as predictors of health and disease. *Cell Mol Immunol* (2015) 12:391–9. doi: 10.1038/cmi.2014.134
4. Rechavi E, Somech R. Survival of the fetus: FEtal B and T cell receptor repertoire development. *Semin Immunopathol* (2017) 39:577–83. doi: 10.1007/s00281-017-0626-0
5. Liu B, Zhang X, Deng W, Liu J, Li H, Wen M, et al. Severe influenza A(H1N1) pdm09 infection induces thymic atrophy through activating innate CD8(+) CD44(hi) T cells by upregulating IFN-γ. *Cell Death Differ* (2014) 5:e1440. doi: 10.1038/cddis.2014.323
6. Vogel AB, Haasbach E, Reiling SJ, Droebner K, Klingel K, Planz O. Highly Pathogenic Influenza Virus Infection of the Thymus Interferes with T Lymphocyte Development. *J Immunol (Baltimore Md 1950)* (2010) 185:4824–34. doi: 10.4049/jimmunol.0903631
7. Michaux H, Martens H, Jaïdane H, Halouani A, Hober D, Geenen V. How Does Thymus Infection by Coxsackievirus Contribute to the Pathogenesis of Type 1 Diabetes? *Front Immunol* (2015) 6:338. doi: 10.3389/fimmu.2015.00338
8. Robins HS, Srivastava SK, Campregher PV, Turtle CJ, Andriesen J, Riddell SR, et al. Overlap and effective size of the human CD8+ T cell receptor repertoire. *Sci Trans Med* (2010) 2:47ra64. doi: 10.1126/scitranslmed.3001442
9. Warren RL, Freeman JD, Zeng T, Choe G, Munro S, Moore R, et al. Exhaustive T-cell repertoire sequencing of human peripheral blood samples reveals signatures of antigen selection and a directly measured repertoire size of at least 1 million clonotypes. *Genome Res* (2011) 21:790–7. doi: 10.1101/gr.115428.110
10. Bousso P, Lemaitre F, Bilsborough J, Kourilsky P. Facing two T cell epitopes: A degree of randomness in the primary response is lost upon secondary immunization. *J Immunol (Baltimore Md 1950)* (2000) 165:760–7. doi: 10.4049/jimmunol.165.2.760
11. Bousso P, Lemaitre F, Bilsborough J, Kourilsky P. Facing two T cell epitopes: a degree of randomness in the primary response is lost upon secondary immunization. *J Immunol* (2000) 165(2):760–7. doi: 10.4049/jimmunol.165.2.760
12. Thapa DR, Tonikian R, Sun C, Liu M, Dearth A, Petri M, et al. Longitudinal analysis of peripheral blood T cell receptor diversity in patients with systemic lupus erythematosus by next-generation sequencing. *Arthritis Res Ther* (2015) 17:132. doi: 10.1186/s13075-015-0655-9
13. Yao Y, Zia A, Neumann RS, Pavlovic M, Balaban G, Lundin KE, et al. T cell receptor repertoire as a potential diagnostic marker for celiac disease. *Clin Immunol (Orlando Fla.)* (2020) 222:108621. doi: 10.1016/j.clim.2020.108621
14. de Paula Alves Sousa A, Johnson KR, Nicholas R, Darko S, Price DA, Douek DC, et al. Intrathecal T-cell clonal expansions in patients with multiple sclerosis. *Ann Clin Trans Neurol* (2016) 3:422–33. doi: 10.1002/acn3.310
15. Chen H, Ndhlovu ZM, Liu D, Porter LC, Fang JW, Darko S, et al. TCR clonotypes modulate the protective effect of HLA class I molecules in HIV-1 infection. *Nat Immunol* (2012) 13:691–700. doi: 10.1038/ni.2342
16. Gabriel B, Medin C, Alves J, Nduati R, Bosire RK, Wamalwa D, et al. Analysis of the TCR Repertoire in HIV-Exposed but Uninfected Infants. *Sci Rep* (2019) 9:11954. doi: 10.1038/s41598-019-48434-4
17. Faint JM, Pilling D, Akbar AN, Kitas GD, Bacon PA, Salmon M. Quantitative flow cytometry for the analysis of T cell receptor Vbeta chain expression. *J Immunol Methods* (1999) 225:53–60. doi: 10.1016/s0022-1759(99)00027-7
18. Cossarizza A, Chang H-D, Radbruch A, Akdis M, Andrä I, Annunziato F, et al. Guidelines for the use of flow cytometry and cell sorting in immunological studies. *Eur J Immunol* (2017) 47:1584–797. doi: 10.1002/eji.201646632
19. Flores-Gonzalez J, Cancino-Diaz JC, Chavez-Galan L. Flow Cytometry: From Experimental Design to Its Application in the Diagnosis and Monitoring of Respiratory Diseases. *Int J Mol Sci* (2020) 21(22):8830. doi: 10.3390/ijms21228830
20. Cochet M, Pannetier C, Regnault A, Darche S, Leclerc C, Kourilsky P. Molecular detection and in vivo analysis of the specific T cell response to a protein antigen. *Eur J Immunol* (1992) 22:2639–47. doi: 10.1002/eji.1830221025
21. Currier JR, Robinson MA. Spectratype/immunoscope analysis of the expressed TCR repertoire. *Curr Protoc Immunol* (2001) 10:10.28. doi: 10.1002/0471142735.im1028s38. Chapter 10:Unit 10.28.
22. Fozza C, Barraqueddu F, Corda G, Contini S, Virdis P, Dore F, et al. Study of the T-cell receptor repertoire by CDR3 spectratyping. *J Immunol Methods* (2017) 440:1–11. doi: 10.1016/j.jim.2016.11.001
23. Sanger F, Air GM, Barrell BG, Brown NL, Coulson AR, Fiddes CA, et al. Nucleotide sequence of bacteriophage phi X174 DNA. *Nature* (1977) 265:687–95. doi: 10.1038/265687a0
24. Sant'Angelo DB, Waterbury PG, Cohen BE, Martin WD, van Kaer L, Hayday AC, et al. The imprint of intrathymic self-peptides on the mature T cell receptor repertoire. *Immunity* (1997) 7:517–24. doi: 10.1016/s1074-7613(00)80373-8
25. Correia-Neves M, Waltzinger C, Mathis D, Benoist C. The shaping of the T cell repertoire. *Immunity* (2001) 14:21–32. doi: 10.1016/s1074-7613(01)00086-3
26. Six A, Mariotti-Ferrandiz ME, Chaara W, Magadan S, Pham H-P, Lefranc M-P, et al. The past, present, and future of immune repertoire biology - the rise of next-generation repertoire analysis. *Front Immunol* (2013) 4:413. doi: 10.3389/fimmu.2013.00413
27. Liu X, Zhang W, Zeng X, Zhang R, Du Y, Hong X, et al. Systematic Comparative Evaluation of Methods for Investigating the TCRβ Repertoire. *PloS One* (2016) 11:e0152464. doi: 10.1371/journal.pone.0152464

28. Rosati E, Dowds CM, Liaskou E, Henriksen EK, Karlsen TH, Franke A. Overview of methodologies for T-cell receptor repertoire analysis. *BMC Biotechnol* (2017) 17:61. doi: 10.1186/s12896-017-0379-9
29. de Simone M, Rossetti G, Pagani M. Single Cell T Cell Receptor Sequencing: Techniques and Future Challenges. *Front Immunol* (2018) 9:1638. doi: 10.3389/fimmu.2018.01638
30. Barennes P, Quiniou V, Shugay M, Egorov ES, Davydov AN, Chudakov DM, et al. Benchmarking of T cell receptor repertoire profiling methods reveals large systematic biases. *Nat Biotechnol* (2020). doi: 10.1038/s41587-020-0656-3
31. Miho E, Yermanos A, Weber CR, Berger CT, Reddy ST, Greiff V. Computational Strategies for Dissecting the High-Dimensional Complexity of Adaptive Immune Repertoires. *Front Immunol* (2018) 9:224. doi: 10.3389/fimmu.2018.00224
32. Bradley P, Thomas PG. Using T Cell Receptor Repertoires to Understand the Principles of Adaptive Immune Recognition. *Annu Rev Immunol* (2019) 37:547–70. doi: 10.1146/annurev-immunol-042718-041757
33. Zemlin M, Schelonka RL, Bauer K, Schroeder HW, Regulation JR. and chance in the ontogeny of B and T cell antigen receptor repertoires. *Immunol Res* (2002) 26:265–78. doi: 10.1385/IR:26:1-3:265
34. Wang C, Sanders CM, Yang Q, Schroeder HW, JR,, Wang E, Babrzadeh F, et al. High throughput sequencing reveals a complex pattern of dynamic interrelationships among human T cell subsets. *Proc Natl Acad Sci United States America* (2010) 107:1518–23. doi: 10.1073/pnas.0913939107
35. Schelonka RL, Raaphorst FM, Infante D, Kraig E, Teale JM, Infante AJ. T cell receptor repertoire diversity and clonal expansion in human neonates. *Pediatr Res* (1998) 43:396–402. doi: 10.1203/00006450-199803000-00015
36. Dimova T, Brouwer M, Gosselin F, Tassignon J, Leo O, Donner C, et al. Effector Vγ9Vδ2 T cells dominate the human fetal γδ T-cell repertoire. *Proc Natl Acad Sci United States America* (2015) 112:E556–65. doi: 10.1073/pnas.1412058112
37. Britanova OV, Shugay M, Merzlyak EM, Staroverov DB, Putintseva EV, Turchaninova MA, et al. Dynamics of Individual T Cell Repertoires: From Cord Blood to Centenarians. *J Immunol (Baltimore Md 1950)* (2016) 196:5005–13. doi: 10.4049/jimmunol.1600005
38. Raaphorst FM, Kaijzel EL, van Tol MJ, Vossen JM, van den Elsen PJ. Non-random employment of V beta 6 and J beta gene elements and conserved amino acid usage profiles in CDR3 regions of human fetal and adult TCR beta chain rearrangements. *Int Immunol* (1994) 6:1–9. doi: 10.1093/intimm/6.1.1
39. Papadopoulou M, Tieppo P, McGovern N, Gosselin F, Chan JK, Goetgeluk G, et al. TCR Sequencing Reveals the Distinct Development of Fetal and Adult Human Vγ9Vδ2 T Cells. *J Immunol (Baltimore Md 1950)* (2019) 203:1468–79. doi: 10.4049/jimmunol.1900592
40. Ben Youssef G, Tourret M, Salou M, Ghazarian L, Houdouin V, Mondot S, et al. Ontogeny of human mucosal-associated invariant T cells and related T cell subsets. *J Exp Med* (2018) 215:459–79. doi: 10.1084/jem.20171739
41. Soriano JB, Abajobir AA, Abate KH, Abera SF, Agrawal A, Ahmed MB, et al. Global, regional, and national deaths, prevalence, disability-adjusted life years, and years lived with disability for chronic obstructive pulmonary disease and asthma, 1990-2015: A systematic analysis for the Global Burden of Disease Study 2015. *Lancet Respir Med* (2017) 5:691–706. doi: 10.1016/S2213-2600(17)30293-X
42. Lai CK, Beasley R, Crane J, Foliaki S, Shah J, Weiland S. Global variation in the prevalence and severity of asthma symptoms: Phase three of the International Study of Asthma and Allergies in Childhood (ISAAC). *Thorax* (2009) 64:476–83. doi: 10.1136/thx.2008.106609
43. Mims JW. Asthma: Definitions and pathophysiology. *Int Forum Allergy Rhinol* (2015) 5 Suppl 1:S2–6. doi: 10.1002/alr.21609
44. Hodges E, Dasmahapatra J, Smith JL, Quin CT, Lanham S, Krishna MT, et al. T cell receptor (TCR) Vbeta gene usage in bronchoalveolar lavage and peripheral blood T cells from asthmatic and normal subjects. *Clin Exp Immunol* (1998) 112:363–74. doi: 10.1046/j.1365-2249.1998.00611.x
45. Wahlström J, Gigliotti D, Roquet A, Wigzell H, Eklund A, Grunewald J. T cell receptor Vbeta expression in patients with allergic asthma before and after repeated low-dose allergen inhalation. *Clin Immunol (Orlando Fla.)* (2001) 100:31–9. doi: 10.1006/clim.2001.5045
46. Kircher MF, Haeusler T, Nickel R, Lamb JR, Renz H, Beyer K. Vbeta18.1(+) and V(alpha)2.3(+) T-cell subsets are associated with house dust mite allergy in human subjects. *J Allergy Clin Immunol* (2002) 109:517–23. doi: 10.1067/mai.2002.121945
47. Sade K, Kivity S, Levy A, Fireman E. The effect of specific immunotherapy on T-cell receptor repertoire in patients with allergy to house-dust mite. *Allergy* (2003) 58:430–4. doi: 10.1034/j.1398-9995.2003.00055.x
48. Cao K, Wu J, Li X, Xie H, Tang C, Zhao X, et al. T-cell receptor repertoire data provides new evidence for hygiene hypothesis of allergic diseases. *Allergy* (2020) 75:681–3. doi: 10.1111/all.14014
49. Amariglio N, Klein A, Dagan L, Lev A, Padeh S, Rechavi G, et al. T-cell compartment in synovial fluid of pediatric patients with JIA correlates with disease phenotype. *J Clin Immunol* (2011) 31:1021–8. doi: 10.1007/s10875-011-9580-0
50. Chapman CG, Yamaguchi R, Tamura K, Weidner J, Imoto S, Kwon J, et al. Characterization of T-cell Receptor Repertoire in Inflamed Tissues of Patients with Crohn's Disease Through Deep Sequencing. *Inflamm Bowel Dis* (2016) 22:1275–85. doi: 10.1097/MIB.0000000000000752
51. Fazilleau N, Delarasse C, Motta I, Fillatreau S, Gougeon M-L, Kourilsky P, et al. T cell repertoire diversity is required for relapses in myelin oligodendrocyte glycoprotein-induced experimental autoimmune encephalomyelitis. *J Immunol (Baltimore Md 1950)* (2007) 178:4865–75. doi: 10.4049/jimmunol.178.8.4865
52. Cavalcante P, Serafini B, Rosicarelli B, Maggi L, Barberis M, Antozzi C, et al. Epstein-Barr virus persistence and reactivation in myasthenia gravis thymus. *Ann Neurol* (2010) 67:726–38. doi: 10.1002/ana.21902
53. Gong L, Li Y, Li X, Tu Q, Mou X, Wang S, et al. Detection of human parvovirus B19 infection in the thymus of patients with thymic hyperplasia-associated myasthenia gravis. *Clin Microbiol Infect* (2019) 25:109.e7–109.e12. doi: 10.1016/j.cmi.2018.03.036
54. Laitinen OH, Honkanen H, Pakkanen O, Oikarinen S, Hankaniemi MM, Huhtala H, et al. Coxsackievirus B1 Is Associated With Induction of β-Cell Autoimmunity That Portends Type 1 Diabetes. *Diabetes* (2014) 63:446–55. doi: 10.2337/db13-0619
55. Tzifi F, Kanariou M, Tzanoudaki M, Mihas C, Paschali E, Chrousos G, et al. Flow cytometric analysis of the CD4+ TCR Vβ repertoire in the peripheral blood of children with type 1 diabetes mellitus, systemic lupus erythematosus and age-matched healthy controls. *BMC Immunol* (2013) 14:33. doi: 10.1186/1471-2172-14-33
56. Dokai H, Nomura Y, Fujikawa Y, Nihei K, Segawa M, Shinomiya N. A study of the factors inducing the development of childhood-onset myasthenia gravis using CDR3 spectratyping analysis of the TCR repertoire. *J Neuroimmunol* (2007) 187:192–200. doi: 10.1016/j.jneuroim.2007.04.021
57. Eugster A, Lindner A, Catani M, Heninger A-K, Dahl A, Klemroth S, et al. High diversity in the TCR repertoire of GAD65 autoantigen-specific human CD4+ T cells. *J Immunol (Baltimore Md 1950)* (2015) 194:2531–8. doi: 10.4049/jimmunol.1403031
58. Wu J, Liu D, Tu W, Song W. Zhao X. T-cell receptor diversity is selectively skewed in T-cell populations of patients with Wiskott-Aldrich syndrome. *J Allergy Clin Immunol* (2015) 135:209–16. doi: 10.1016/j.jaci.2014.06.025
59. Yu X, Almeida JR, Darko S, van der Burg M, DeRavin SS, Malech H, et al. Human syndromes of immunodeficiency and dysregulation are characterized by distinct defects in T-cell receptor repertoire development. *J Allergy Clin Immunol* (2014) 133:1109–15. doi: 10.1016/j.jaci.2013.11.018
60. McLean-Tooke A, Barge D, Spickett GP, Gennery AR. Flow cytometric analysis of TCR Vβ repertoire in patients with 22q11.2 deletion syndrome. *Scand J Immunol* (2011) 73:577–85. doi: 10.1111/j.1365-3083.2011.02527.x
61. de Vries AC, Langerak AW, Verhaaf B, Niemeyer CM, Stary J, Schmiegelow K, et al. T-cell receptor Vbeta CDR3 oligoclonality frequently occurs in childhood refractory cytopenia (MDS-RC) and severe aplastic anemia. *Leukemia* (2008) 22:1170–4. doi: 10.1038/leu.2008.23
62. Ramesh M, Hamm D, Simchoni N, Cunningham-Rundles C. Clonal and constricted T cell repertoire in Common Variable Immune Deficiency. *Clin Immunol (Orlando Fla.)* (2017) 178:1–9. doi: 10.1016/j.clim.2015.01.002
63. Appay V, Dunbar PR, Callan M, Klenerman P, Gillespie GM, Papagno L, et al. Memory CD8+ T cells vary in differentiation phenotype in different persistent virus infections. *Nat Med* (2002) 8:379–85. doi: 10.1038/nm0402-379
64. Bate SL, Dollard SC, Cannon MJ. Cytomegalovirus seroprevalence in the United States: The national health and nutrition examination surveys, 1988-2004. *Clin Infect Dis an Off Publ Infect Dis Soc America* (2010) 50:1439–47. doi: 10.1086/652438
65. Dowd JB, Palermo T, Brite J, McDade TW, Aiello A. Seroprevalence of Epstein-Barr virus infection in U.S. children ages 6-19, 2003-2010. *PloS One* (2013) 8:e64921. doi: 10.1371/journal.pone.0064921

66. van den Heuvel D, Jansen MA, Dik WA, Bouallouch-Charif H, Zhao D, van Kester KA, et al. Cytomegalovirus- and Epstein-Barr Virus-Induced T-Cell Expansions in Young Children Do Not Impair Naive T-cell Populations or Vaccination Responses: The Generation R Study. *J Infect Dis* (2016) 213:233–42. doi: 10.1093/infdis/jiv369
67. Attaf M, Malik A, Severinsen MC, Roider J, Ogongo P, Buus S, et al. Major TCR Repertoire Perturbation by Immunodominant HLA-B(*)44:03-Restricted CMV-Specific T Cells. *Front Immunol* (2018) 9:2539. doi: 10.3389/fimmu.2018.02539
68. Klarenbeek PL, Remmerswaal EB, ten Berge IJ, Doorenspleet ME, van Schaik BD, Esveldt RE, et al. Deep sequencing of antiviral T-cell responses to HCMV and EBV in humans reveals a stable repertoire that is maintained for many years. *PloS Pathog* (2012) 8:e1002889. doi: 10.1371/journal.ppat.1002889
69. Li H, Ye C, Ji G, Han J. Determinants of public T cell responses. *Cell Res* (2012) 22:33–42. doi: 10.1038/cr.2012.1
70. Clerici M, Saresella M, Colombo F, Fossati S, Sala N, Bricalli D, et al. T-lymphocyte maturation abnormalities in uninfected newborns and children with vertical exposure to HIV. *Blood* (2000) 96:3866–71. doi: 10.1182/blood.V96.12.3866
71. Nielsen SD, Jeppesen DL, Kolte L, Clark DR, Sørensen TU, Dreves AM, et al. Impaired progenitor cell function in HIV-negative infants of HIV-positive mothers results in decreased thymic output and low CD4 counts. *Blood* (2001) 98:398–404. doi: 10.1182/blood.v98.2.398
72. Eggesbø LM, Risnes LF, Neumann RS, Lundin KE, Christophersen A, Sollid LM. Single-cell TCR sequencing of gut intraepithelial γδ T cells reveals a vast and diverse repertoire in celiac disease. *Mucosal Immunol* (2020) 13:313–21. doi: 10.1038/s41385-019-0222-9
73. Werner L, Lee YN, Rechavi E, Lev A, Yerushalmi B, Ling G, et al. Alterations in T and B Cell Receptor Repertoires Patterns in Patients With IL10 Signaling Defects and History of Infantile-Onset IBD. *Front Immunol* (2020) 11:109. doi: 10.3389/fimmu.2020.00109
74. Saravanarajan K, Douglas AR, Ismail MS, Omorogbe J, Semenov S, Muphy G, et al. Genomic profiling of intestinal T-cell receptor repertoires in inflammatory bowel disease. *Genes Immun* (2020) 21:109–18. doi: 10.1038/s41435-020-0092-x
75. Pietrzyk JJ, Kwinta P, Wollen EJ, Bik-Multanowski M, Madetko-Talowska A, Günther C-C, et al. Gene expression profiling in preterm infants: New aspects of bronchopulmonary dysplasia development. *PloS One* (2013) 8:e78585. doi: 10.1371/journal.pone.0078585
76. Unterman A, Neumark N, Zhao A, Schupp JC, Adams T, Antin-Ozerkis DE, et al. Single Cell RNA Sequencing Reveals Altered T-Cell Repertoire and Gene Expression in the Peripheral Blood and Lungs of Patients with Idiopathic Pulmonary Fibrosis. In: *A95. NOVEL INSIGHT INTO IPF PATHOGENESIS*. American Thoracic Society; International Conference, May 15-20, 2020 - Philadelphia, PA (2020). p. A2516–6.
77. Ravens S, Fichtner AS, Willers M, Torkornoo D, Pirr S, Schöning J, et al. Microbial exposure drives polyclonal expansion of innate γδ T cells immediately after birth. *Proc Natl Acad Sci United States America* (2020) 117:18649–60. doi: 10.1073/pnas.1922588117
78. Healy K, Pasetto A, Sobkowiak MJ, Soon CF, Cornberg M, Aleman S, et al. Chronic Viral Liver Diseases: Approaching the Liver Using T Cell Receptor-Mediated Gene Technologies. *Cells* (2020) 9(6):1471. doi: 10.3390/cells9061471
79. Schober K, Müller TR, Busch DH. Orthotopic T-Cell Receptor Replacement-An "Enabler" for TCR-Based Therapies. *Cells* (2020) 9(6):1367. doi: 10.3390/cells9061367
80. Chen Y, Sun J, Liu H, Yin G, Xie Q. Immunotherapy Deriving from CAR-T Cell Treatment in Autoimmune Diseases. *J Immunol Res* (2019) 2019:5727516. doi: 10.1155/2019/5727516

Conflict of Interest: For CS: Consultancy and research funding, Hycor Biomedical and Thermo Fisher Scientific; Research Funding, Mead Johnson Nutrition (MJN); Consultancy, Bencard Allergie.

The remaining authors declare that the research was conducted in the absence of any commercial or financial relationships that could be construed as a potential conflict of interest.

frontiers in Immunology

CASE REPORT
published: 11 February 2021
doi: 10.3389/fimmu.2020.604759

Case Report: Severe Complement-Mediated Thrombotic Microangiopathy in IgG4-Related Disease Secondary to Anti-Factor H IgG4 Autoantibodies

OPEN ACCESS

Edited by:
Jennifer Konopa Mulligan,
Medical University of South Carolina,
United States

Reviewed by:
Eleni Gavriilaki,
G. Papanikolaou General Hospital, Greece
John Chapin,
Takeda, United States

***Correspondence:**
Gautier Breville
gautier.breville@hcuge.ch

†These authors have contributed equally to this work

Specialty section:
This article was submitted to Autoimmune and Autoinflammatory Disorders, a section of the journal Frontiers in Immunology

Received: 10 September 2020
Accepted: 14 December 2020
Published: 11 February 2021

Citation:
Breville G, Zamberg I, Sadallah S, Stephan C, Ponte B and Seebach JD (2021) Case Report: Severe Complement-Mediated Thrombotic Microangiopathy in IgG4-Related Disease Secondary to Anti-Factor H IgG4 Autoantibodies. Front. Immunol. 11:604759. doi: 10.3389/fimmu.2020.604759

Gautier Breville[1,2*†], *Ido Zamberg*[3,4†], *Salima Sadallah*[5], *Caroline Stephan*[6], *Belen Ponte*[7†] *and Jörg D. Seebach*[1†]

[1] Department of Medicine, Division of Immunology and Allergy, Geneva University Hospitals, Geneva, Switzerland, [2] Department of Clinical Neurosciences, Division of Neurology, Geneva University Hospitals, Geneva, Switzerland, [3] Department of Medicine, Division of General Internal Medicine, Geneva University Hospitals, Geneva, Switzerland, [4] Department of Anaesthesiology, Division of Anaesthesiology, Clinical Pharmacology, Intensive Care and Emergency Medicine, Geneva University Hospitals, Geneva, Switzerland, [5] Département de médecine de laboratoire et pathologie, Service d'immunologie et d'allergie, Centre Hospitalier Universitaire Vaudois, Lausanne, Switzerland, [6] Department of Medicine, Immuno-Hematology Unit, Geneva University Hospitals, Geneva, Switzerland, [7] Department of Medicine, Division of Nephrology, Geneva University Hospitals, Geneva, Switzerland

Objective: To first describe and estimate the potential pathogenic role of Ig4 autoantibodies in complement-mediated thrombotic microangiopathy (TMA) in a patient with IgG4-related disease (IgG4-RD).

Methods: This study is a case report presenting a retrospective review of the patient's medical chart. Plasma complement C3 and C4 levels, immunoglobulin isotypes and subclasses were determined by nephelometry, the complement pathways' activity (CH50, AP50, MBL) using WIESLAB® Complement System assays. Human complement factor H levels, anti-complement factor H auto-antibodies were analyzed by ELISA, using HRP-labeled secondary antibodies specific for human IgG, IgG4, and IgA, respectively. Genetic analyses were performed by exome sequencing of 14 gens implicated in complement disorders, as well as multiplex ligation-dependent probe amplification looking specifically for *CFH, CFHR1-2-3, and 5*.

Results: Our brief report presents the first case of IgG4-RD with complement-mediated TMA originating from both pathogenic *CFHR* 1 and *CFHR* 4 genes deletions, and inhibitory anti-complement factor H autoantibodies of the IgG4 subclass. Remission was achieved with plasmaphereses, corticosteroids, and cyclophosphamide. Following remission, the patient was diagnosed with lymphocytic meningitis and SARS-CoV-2 pneumonia with an uneventful recovery.

Conclusion: IgG4-RD can be associated with pathogenic IgG4 autoantibodies. Genetic predisposition such as *CFHR*1 and *CFHR*4 gene deletions enhance the susceptibility to the formation of inhibitory anti-Factor H IgG4 antibodies.

Keywords: thrombotic microangiopathy, atypical hemolytic uremic syndrome, IgG4-related disease, antibodies, complement factor H-related protein, complement factor H, anti-factor H auto-antibodies, SARS CoV2

INTRODUCTION

IgG4-related disease (IgG4-RD) is a protean fibro-inflammatory condition characterized by tumefactive and hyperplastic lesions with storiform fibrosis and dense lymphoplasmocytic infiltrates rich in IgG4-positive plasma cells (1). Depending on the referenced cut-off level, elevated serum IgG4 concentrations can be detected in up to 80% of the cases, but are not exclusive to IgG4-RD being also present in a broad spectrum of other autoimmune diseases, allergic conditions, neoplasia, and Castleman's disease (2). Histopathological analysis of biopsy specimens remains, therefore, the cornerstone of diagnosis of IgG4-RD. Current diagnostic criteria are based on organ involvement (dysfunction, localized, or diffuse swelling), serum IgG4 concentration (> 1.35 g/l), number of IgG4-positive plasma cells in tissue (>10 IgG4+ cells per high-power field) or the ratio of IgG4 to IgG (3). In comparison, IgG4 is the rarest of all four IgG subclasses, representing only 3–6% of total IgG; despite sharing more than 95% homology, differences in the amino-acid sequence in the second constant domain lead to weak or negligible binding to both C1q (classical complement pathway activation) and Fcγ receptors (4). Thus, IgG4 is believed to have mainly neutralizing and anti-inflammatory functions due to limited complement fixation and crosslinking, although this remains controversial (1).

Thrombotic microangiopathy (TMA), also known as atypical hemolytic uremic syndrome, is characterized by hemolytic anemia, thrombocytopenia, and organ failure (often renal) related to vascular damage provoking arteriolar and capillary thrombosis (5, 6). Complement-mediated TMA, an urgent life-threatening syndrome, results from uncontrolled activation of the alternative pathway of complement. In most cases, a hereditary origin can be identified, related to genetic abnormalities such as single nucleotide polymorphisms in the genes of complement factor H (CFH) and CD46, copy-number variations in the CFH-related 1 and 3 genes (CFHR), and fusion or deletion of genes in the CFHR region caused by non-allelic homologous recombination (5). In addition, mutations that can lead to lower activity levels of other complement inhibitor factors such as MCP and Factor I have been described. In contrast, 6-10% of complement-mediated TMA are acquired and linked to the presence of inhibitory autoantibodies directed against CFH (7).

Abbreviations: CH50, haemolytic complement 50%; AP50, alternative pathway 50%; CFH, complement factor H; CFHR, CFH-related protein; IgG4-RD, IgG4-related disease; MGUS, monoclonal gammopathy of undetermined significance; MBL, Mannose Binding Lectin.

CASE REPORT

A 45-year-old woman, born in Cameroon, presented in December 2019 at the Emergency Department (ED) with a three-day history of epigastric abdominal pain, nausea, vomiting, and macroscopic hematuria. The patient had a clinical history of IgG4-RD diagnosed in 2015 with elevated serum IgG4 (5.3 g/l), plasmablast counts (57,000/ml), and tubulointerstitial nephritis with more than 10/HPF IgG4+ plasma cells. She was treated with corticosteroids and rituximab but had multiple relapses, as summarized in **Figure 1**. Other comorbidities included IgA lambda monoclonal gammopathy of undetermined significance (MGUS), α-thalassemia minor and a pituitary microadenoma with hyperprolactinemia. Four months before ED consultation, the patient had complained of worsening fatigue associated with cervical and submaxillary swellings. Flow cytometry revealed increased peripheral blood plasmablast counts (3,010/ml, normal: < 900), while the serum IgG4 level was normal (1.1 g/l, **Figure 1**). A relapse of IgG4-RD was suspected and treatment with oral prednisone 20 mg/d initiated with partial clinical regression despite an incomplete adherence to the treatment. An infusion of rituximab (1,000 mg) was prescribed but had to be discontinued due to a grade III anaphylactic reaction.

On admission, blood tests revealed hemolytic anemia (hemoglobin 100 g/l) with undetectable haptoglobin, increased LDH levels at 992 U/l, 2% of schistocytes on the blood smear, thrombocytopenia (35 G/l), and acute kidney injury with creatinine measured at 369 µmol/l for a baseline value of 77 µmol/l (KDIGO stage 3). Leucocyturia, glomerular hematuria, and nephrotic range glomerular proteinuria (estimated over 6.6 g/day) were present. Blood albumin levels were 28 g/l. Specific coagulation parameters (TP, PTT, and fibrinogen) were in the normal range. ADAMTS13 (a disintegrin and metalloproteinase with a thrombospondin type 1 motif, member 13) activity was normal (78%), and antiphospholipid antibodies were absent. Antinuclear antibodies (ANA) titers were at 1/5,000 with homogenous and nucleolar pattern without anti-nucleoprotein or -nucleosome specificities. Total IgG and IgG4 levels were at normal range, 11.1 and 1.2 g/l, respectively. Plasma complement C3 was significantly decreased, 0.14 g/l (0.66–1.35), with normal plasma C4 levels 0.16 g/l (0.08–0.34); the results of the last control two years earlier were 1.19 and 0.21 g/l, respectively. Activity of all three complement pathways, classical, alternative and lectin, was decreased: CH50 25% (Normal: 70–140), AP50 0% (Normal > 71), MBL 27% (Normal > 49). Detectable complement factor H (CFH) levels were low at 49 µg/ml (400–800, **Figure 2**) with high levels of anti-CFH antibodies detected

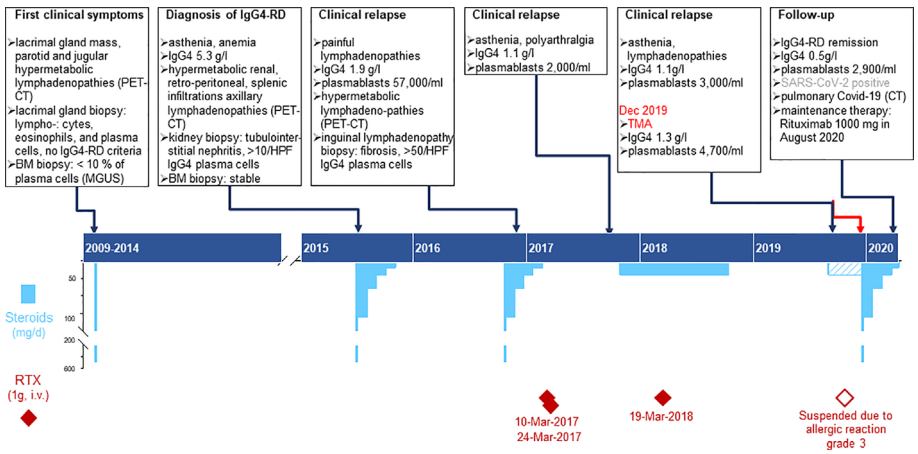

FIGURE 1 | Time course depicting the clinical presentation of IgG4RD, laboratory results and treatment plans from 2009 to 2020. Chronic phase of the patient's disease: the upper part summarizes the specific features of clinical findings, biopsy, imaging, and immunological laboratory results; the lower part shows the therapy, specifying dose, duration, and dates for Rituximab infusions (deep red diamonds) and steroids (sky blue bars). Pulse treatment with methyl-prednisone (500mg i.v.) is represented by the bottom scale blue bars and was usually followed by oral Prednisone (top scale blue bars); the dashed bar corresponds to the period when the patient did not adhere thoroughly to the prescribed therapy.

at 801 AU/ml (Normal < 30, **Figure 2**). Intriguingly, elevated levels of anti-CHF antibodies and decreased FH activity were already present in frozen stored samples from 4 months before the clinical manifestation of TMA (**Figure 2**), but not from 1 year earlier (data not shown). Plasma complement C3 and C4 were determined by nephelometry while the determination of the complement pathways activity (CH50, AP50, MBL) were done using WIESLAB® Complement System assay (SVAR life science AB.SE.) in the serum. Human Complement factor H levels were determined using ELISA-Hycult biotech. Com. in the plasma and anti-CFH antibodies were measured using ELISA-VIDITEST from VIDIA.CZ in the serum.

Both clinical and laboratory features were compatible with a diagnosis of complement-mediated TMA caused by inhibitory antibodies against CFH. While waiting for the results of CFH and anti-CFH antibodies levels, the patient was treated with daily

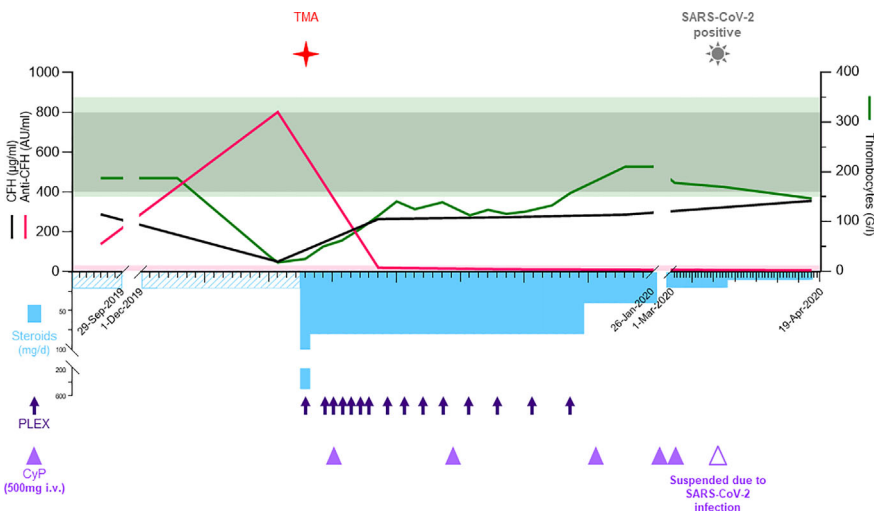

FIGURE 2 | In the acute phase, the upper part shows the laboratory values for CFH (black, µg/ml), anti-CFH (pink, AU/ml), left y-axis, and thrombocytes (green, G/l) at the right y-axis. The normal reference values are shown with shades matching the colors of the different parameters. The lower part depicts the therapy including methylprednisolone/prednisone (sky blue bars, mg/d), plasma exchanges (deep blue arrows), and cyclophosphamide (purple triangles, 500 mg i.v.). The time when TMA and COVID-19 were diagnosed are shown with symbols. AU, arbitrary units; BM, bone marrow; Covid-19; coronavirus disease 2019; CT, computed tomography; CTX, cyclophosphamide; HPF, high-power field; IgA, immunoglobulin A; IgG4-RD, immunoglobulin G4-related disease; i.v., intra venous; PET-CT, positron emission tomography-computed tomography; PLEX, plasma exchange; RTX, Rituximab; SARS-CoV-2 severe acute respiratory syndrome coronavirus 2; TMA, thrombotic microangiopathy.

plasma exchanges (PLEX, 13 cures in total) by fresh frozen plasma twice the plasma volume and corticosteroids (methylprednisolone 500 mg iv, followed by oral prednisone 1 mg/kg/day) with gradual tapering until May 2020 (**Figure 2**). Treatment with eculizumab was considered but not retained due to stabilization of laboratory parameters, including CFH and anti-CFH antibodies levels (263 µg/ml and 19 AU/ml, respectively). Withholding eculizumab was based on a joint decision between the medical staff and the patient after presenting the risks, benefits, and economic burden. However, the patient was vaccinated against meningococci and eculizumab was retained as a second line treatment option in case of non-response or premature relapse. To treat the underlying immunological condition iv cyclophosphamide was initiated one week later for a total of six infusions (500 mg each) over three months. Kidney function, proteinuria, hemolysis, thrombocytopenia, and complement activity progressively normalized. After five weeks of treatment, the patient achieved global clinical response and laboratory remission. In March 2020, the patient was diagnosed with lymphocytic meningitis and bilateral pneumonia due to SARS-CoV-2 infection with an uneventful recovery. Rituximab maintenance therapy (1,000 mg infusion) was administered in August 2020 using an induction of tolerance protocol and upon her last follow up in November 2020 the patient is free of symptoms with normal laboratory levels.

In the context of IgG4-RD we further elucidated whether the anti-factor H inhibitory antibody belonged to the IgG4 subclass. Results are presented in **Figure 3A** demonstrating a significant anti-CFH total IgG elevation mainly of IgG4 subclass. Of note, the total serum IgG4 level was 1.2 g/l at that time. In the light of the known MGUS of the patient with IgA lambda paraproteinemia (6.4 g/l) and a previously published case (9), specific anti-CFH IgA antibodies were measured. Results indicate an absence of specific anti-CFH IgA (**Figure 3B**). Finally, genetic analyses were performed by sequencing the exome of 14 gens implicated in complement disorders (Twist Human Core Exome+RefSer_V1 EF Multiplex, Illumina NextSeq500), as well as multiplex ligation-dependent probe amplification looking specifically for *CFH*, *CFHR1-2-3* and *5* (kit MRC Holland SALSA p236_A3 + kit custom by V Fremeaux-BAcchi, Paris). Deletions in the genes of CFHR 1 and *CFHR 4*, GRCh37/hg19 chr.1:g.(196789032_196794607)_(196887536_196913011)del, were identified that are known risk factors for complement-mediated TMA (10).

DISCUSSION

To our knowledge, we present here the first case of complement-mediated TMA secondary to deletions in the *CFHR 1* and *CFHR 4* genes associated with pathogenic IgG4-type anti-CFH antibodies in a patient suffering from IgG4-RD with major salivary gland enlargement, orbital disease, lymphadenopathy, and IgG4 nephritis.

IgG4-RD physiopathology is still not well elucidated. Nevertheless, effectors mechanisms may include B and T cell interactions, with a pathogenic role of CD4+ cytotoxic T lymphocytes (CTL) balanced by B-lymphocytes, as well as T helper lymphocytes (Th-2) and regulatory T cells (Treg) that also regulate B-cell differentiation and TGF-β-mediated tissue fibrosis. IgG4 overexpression and accumulation could be inflammatory leftovers of chronic inflammation that results from massive plasma cell production. IgG4 antibodies are supposed to be nonpathogenic in IgG4-RD (1). However, tissue IgG4 accumulation could modulate local inflammatory

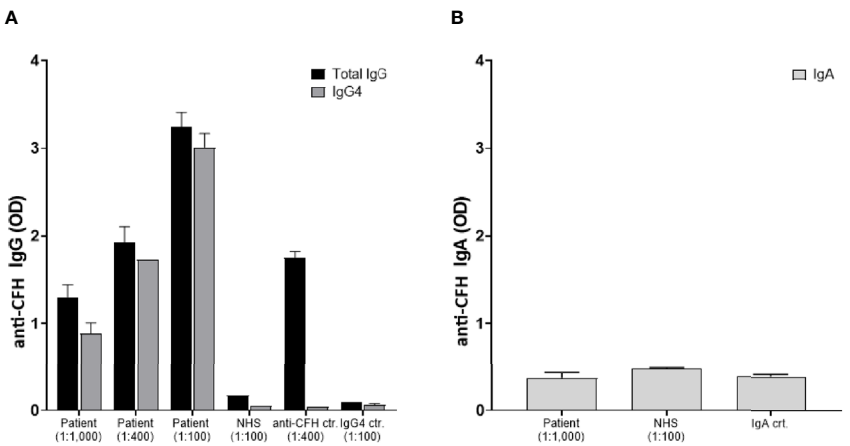

FIGURE 3 | Identification of IgG4 anti-factor H autoantibodies: Plasma samples were analyzed for anti-factor H antibodies by a previously reported specific ELISA which was developed using Horse Radish peroxidase (HRP)-labeled secondary antibodies specific for human IgG, IgG4, and IgA, respectively (8). Data are shown as optic density at 490 nm (OD). **(A)** The patient's serum was tested in duplicates at different dilutions 1:100, 1:400, and 1:1,000 for both IgG (black bars) and IgG4 (grey bars). Controls included a normal human serum (NHS), a serum with known elevated anti-CFH IgG levels, and a serum with elevated IgG4 but no anti-CFH activity. **(B)** Absence of IgA anti-factor H autoantibodies: Specific anti-CFH IgA antibodies were measured in the patient's serum (total IgA level of 6.4 g/l), NHS, and another serum with a high total IgA concentration of 12.4 g/l.

responses. Tissue fibrosis evolution may be the product of this accumulation in association with CD4+ CTL and Treg cytokines production (11).

On the other hand, pathogenic autoreactive IgG4 antibodies have been observed in other autoimmune diseases such as myasthenia gravis, directed against muscle-specific tyrosine kinase (MuSK) receptor subtype, pemphigus vulgaris, directed against desmoglein 1, and idiopathic membranous glomerulonephritis, directed against M-type phospholipase A2 receptor (1). Moreover, in patients with acquired thrombotic thrombocytopenic purpura (TTP) related to anti-ADAMTS13 autoantibodies, specific IgG subclasses have all been detected but with a clear predominance of IgG4 (12, 13). Interestingly, IgG4 pathogenic autoantibodies directed against ADAMTS13 were reported in a patient with IgG4-RD causing acquired TTP (14). Our observation illustrates the potential pathogenic role of IgG4 and adds complement-mediated TMA to the list of diseases possibly caused by autoreactive IgG4 antibodies. Finally, since IgG4 polyclonal proteins have been reported incorrectly as M-protein bands in electrophoretic analysis (15) and the patient had longstanding stable IgA lambda MGUS, it was important to clearly distinguish IgG4 from IgA in our analysis. To this end, the concurrent presence of IgA MGUS and elevated IgG4 levels was confirmed by specific nephelometry and ELISA assays.

Complement-mediated TMA results from uncontrolled activation of the alternative pathway, and CFH autoantibodies are found in approximately 10% of reported cases. CFH is a major complement regulatory factor that acts as a cofactor for complement factor I (serine protease) converting C3b to an inactive form, as a decay-accelerating factor *via* competing with complement factor B in binding to C3b, and dissociates the alternative C3 convertase with formation of C3b and Bb. CFH-related protein 1 (CFHR1) is likely to inhibit the formation of C5 convertase and may compete with CFH for binding to C3b. Deficiency of CFHR1 can arise from homozygote *CFHR1/4* gene deletions (10). The majority of patients with CFH autoantibodies exhibited complete deficiency of CFHR1 and CFHR3 secondary to homozygous genes deletion (10). Our case revealed both acquired anti-CFH IgG4 autoantibodies and a genetic predisposition with *CFHR 1* and *CFHR 4* gene deletions. The later are considered as risk factors for complement-mediated TMA (10), since they may lead to structural changes that increase the antigenicity of CFH, or decrease the basal levels of effective CFHR (both in quantity and in function). CFHR alterations could therefore lead to a lower threshold for complement-mediated TMA in the presence of inhibitory anti-CFH IgG4 antibodies. Uncontrolled activation of the complement cascade triggers endothelial dysregulation, inflammatory reactions with leucocyte recruitment, and platelet activation resulting in tissue damage and thrombus formation, especially in the kidney (16, 17).

Therapeutic strategies for complement-mediated TMA are evolving with the recent introduction of complement inhibitors in particular eculizumab, a monoclonal antibody that binds complement component C5 and prevents its cleavage by C5 convertases and formation of the membrane attack complex (MAC) (18). In our case, eculizumab was considered early in the treatment strategy but was not administered due to a rapid and satisfactory clinical and biological response to plasma exchanges and corticosteroids. Our intention was to treat the underlying disease, ie IgG4-RD, in order to efficiently suppress further production of inhibitory anti-CFH IgG4 autoantibodies by induction with cyclophosphamide followed by maintenance treatment using rituximab.

Severe infections such as HIV, influenza, and pneumococcus are known causes of TMA and related to relapse (19). In our patient, COVID-19 infection was uneventful without any signs of clinical or biological relapse during a six-week follow up. According to the recent finding that severe COVID-19 infection is associated to systemic endotheliitis (20), the fact that our patient was immunosuppressed might have been a protective factor. Nevertheless, this hypothesis requires more research on the mechanisms of severe COVID-19 and the role of immunosuppression.

In conclusion, we describe for the first time a pathogenic role of IgG4 autoantibodies directed against CFH causing complement-mediated TMA in a patient with IgG4-RD and a genetic predisposition with homozygote *CFHR1/4* gene deletion.

ETHICS STATEMENT

Ethical review and approval were not required for the study on human participants in accordance with the local legislation and institutional requirements. The patient provided their written informed consent to participate in this study.

AUTHOR CONTRIBUTIONS

Conceptualization and design of the study: GB, IZ, BP, and JS. Acquisition and analysis of data: GB, IZ, SS. Drafting of a significant portion of the manuscript or figures: GB, IZ. Correction of the manuscript: GB, IZ, CS, BP, JS. All authors contributed to the article and approved the submitted version.

ACKNOWLEDGMENTS

We thank Dr. A. Giacobino for genetic analysis, Dr. G. Puga Yung for superb assistance with graphic artwork, and Dr. Pascale Roux-Lombard for access to stored serum samples of the patient.

REFERENCES

1. Stone JH, Zen Y, Deshpande V. IgG4-related disease. *New Engl J Med* (2012) 366(6):539–51. doi: 10.1056/NEJMra1104650

2. Hao M, Liu M, Fan G, Yang X, Li J. Diagnostic Value of Serum IgG4 for IgG4-Related Disease: A PRISMA-compliant Systematic Review and Meta-analysis. *Med (Baltimore)* (2016) 95(21):e3785. doi: 10.1097/MD.0000000000003785

3. Pieringer H, Parzer I, Wöhrer A, Reis P, Oppl B, Zwerina J. IgG4- related disease: an orphan disease with many faces. *Orphanet J Rare Dis* (2014) 9:110. doi: 10.1186/s13023-014-0110-z
4. Tao MH, Smith RI, Morrison SL. Structural features of human immunoglobulin G that determine isotype-specific differences in complement activation. *J Exp Med* (1993) 178(2):661–7. doi: 10.1084/jem.178.2.661
5. George JN, Nester CM. Syndromes of thrombotic microangiopathy. *New Engl J Med* (2014) 371(7):654–66. doi: 10.1056/NEJMra1312353
6. Brocklebank V, Wood KM, Kavanagh D. Thrombotic Microangiopathy and the Kidney. *Clin J Am Soc Nephrol* (2018) 13(2):300–17. doi: 10.2215/CJN.00620117
7. Durey MA, Sinha A, Togarsimalemath SK, Bagga A. Anti-complement-factor H-associated glomerulopathies. *Nat Rev Nephrol* (2016) 12(9):563–78. doi: 10.1038/nrneph.2016.99
8. Guo WY, Song D, Liu XR, Chen Z, Xiao HJ, Ding J, et al. Immunological features and functional analysis of anti-CFH autoantibodies in patients with atypical hemolytic uremic syndrome. *Pediatr Nephrol* (2019) 34(2):269–81. doi: 10.1007/s00467-018-4074-4
9. Rigothier C, Delmas Y, Roumenina LT, Contin-Bordes C, Lepreux S, Bridoux F, et al. Distal Angiopathy and Atypical Hemolytic Uremic Syndrome: Clinical and Functional Properties of an Anti–Factor H IgAλ Antibody. *Am J Kidney Dis* (2015) 66(2):331–6. doi: 10.1053/j.ajkd.2015.03.039
10. Moore I, Strain L, Pappworth I, Kavanagh D, Barlow PN, Herbert AP, et al. Association of factor H autoantibodies with deletions of CFHR1, CFHR3, CFHR4, and with mutations in CFH, CFI, CD46, and C3 in patients with atypical hemolytic uremic syndrome. *Blood* (2010) 115(2):379–87. doi: 10.1182/blood-2009-05-221549
11. Bledsoe JR, Della-Torre E, Rovati L, Deshpande V. IgG4-related disease: review of the histopathologic features, differential diagnosis, and therapeutic approach. *Apmis* (2018) 126(6):459–76. doi: 10.1111/apm.12845
12. Ferrari S, Mudde GC, Rieger M, Veyradier A, Kremer Hovinga JA, Scheiflinger F. IgG subclass distribution of anti-ADAMTS13 antibodies in patients with acquired thrombotic thrombocytopenic purpura. *J Thromb Haemost* (2009) 7(10):1703–10. doi: 10.1111/j.1538-7836.2009.03568.x
13. Sinkovits G, Szilágyi Á, Farkas P, Inotai D, Szilvási A, Tordai A, et al. Concentration and Subclass Distribution of Anti-ADAMTS13 IgG Autoantibodies in Different Stages of Acquired Idiopathic Thrombotic Thrombocytopenic Purpura. *Front Immunol* (2018) 9:1646. doi: 10.3389/fimmu.2018.01646
14. Saeki T, Ito T, Youkou A, Ishiguro H, Sato N, Yamazaki H, et al. Thrombotic thrombocytopenic purpura in IgG4-related disease with severe deficiency of ADAMTS-13 activity and IgG4 autoantibody against ADAMTS-13. *Arthritis Care Res (Hoboken)* (2011) 63(8):1209–12. doi: 10.1002/acr.20484
15. Jacobs JFM, Van Der Molen RG, Keren DF. Relatively Restricted Migration of Polyclonal IgG4 May Mimic a Monoclonal Gammopathy in IgG4-Related Disease. *Am J Clin Pathol* (2014) 142(1):76–81. doi: 10.1309/AJCP41XCVBHEQCEL
16. Yoshida Y, Kato H, Ikeda Y, Nangaku M. Pathogenesis of Atypical Hemolytic Uremic Syndrome. *J Atheroscler Thromb* (2019) 26(2):99–110. doi: 10.5551/jat.RV17026
17. Noris M, Mescia F, Remuzzi G. STEC-HUS, atypical HUS and TTP are all diseases of complement activation. *Nat Rev Nephrol* (2012) 8(11):622–33. doi: 10.1038/nrneph.2012.195
18. Gavriilaki E, Anagnostopoulos A, Mastellos DC. Complement in Thrombotic Microangiopathies: Unraveling Ariadne's Thread Into the Labyrinth of Complement Therapeutics. *Front Immunol* (2019) 10:337. doi: 10.3389/fimmu.2019.00337
19. Fakhouri F, Zuber J, Frémeaux-Bacchi V, Loirat C. Haemolytic uraemic syndrome. *Lancet* (London, England) (2017) 390(10095):681–96.
20. Varga Z, Flammer AJ, Steiger P, Haberecker M, Andermatt R, Zinkernagel AS, et al. Endothelial cell infection and endotheliitis in COVID-19. *Lancet (London England)* (2020) 395(10234):1417–8. doi: 10.1016/S0140-6736(20)30937-5

Conflict of Interest: The authors declare that the research was conducted in the absence of any commercial or financial relationships that could be construed as a potential conflict of interest.

frontiers in Immunology

ORIGINAL RESEARCH
published: 29 March 2021
doi: 10.3389/fimmu.2021.605930

cGAS-STING Pathway Does Not Promote Autoimmunity in Murine Models of SLE

Mona Motwani[1], Jason McGowan[1], Jennifer Antonovitch[1], Kevin MingJie Gao[1], Zhaozhao Jiang[1], Shruti Sharma[1], Gretchen A. Baltus[2], Kevin M. Nickerson[3], Ann Marshak-Rothstein[4†] and Katherine A. Fitzgerald[1†]*

[1] Program in Innate Immunity, Division of Infectious Diseases and Immunology, Department of Medicine, University of Massachusetts Medical School, Worcester, MA, United States, [2] Merck & Co., Inc., Kenilworth, NJ, United States, [3] Department of Immunology, University of Pittsburgh, Pittsburgh, PA, United States, [4] Division of Rheumatology, Department of Medicine, University of Massachusetts Medical School, Worcester, MA, United States

OPEN ACCESS

Edited by:
Jennifer Konopa Mulligan, Medical University of South Carolina, United States

Reviewed by:
Onkar Prakash Kulkarni, Birla Institute of Technology and Science, India
Edith Janssen, Janssen Research and Development, United States

***Correspondence:**
Katherine A. Fitzgerald
kate.fitzgerald@umassmed.edu

[†] These authors have contributed equally to this work

Specialty section:
This article was submitted to Autoimmune and Autoinflammatory Disorders, a section of the journal Frontiers in Immunology

Received: 13 September 2020
Accepted: 22 February 2021
Published: 29 March 2021

Citation:
Motwani M, McGowan J, Antonovitch J, Gao KM, Jiang Z, Sharma S, Baltus GA, Nickerson KM, Marshak-Rothstein A and Fitzgerald KA (2021) cGAS-STING Pathway Does Not Promote Autoimmunity in Murine Models of SLE. Front. Immunol. 12:605930. doi: 10.3389/fimmu.2021.605930

Detection of DNA is an important determinant of host-defense but also a driver of autoinflammatory and autoimmune diseases. Failure to degrade self-DNA in DNaseII or III(TREX1)-deficient mice results in activation of the cGAS-STING pathway. Deficiency of cGAS or STING in these models ameliorates disease manifestations. However, the contribution of the cGAS-STING pathway, relative to endosomal TLRs, in systemic lupus erythematosus (SLE) is controversial. In fact, STING deficiency failed to rescue, and actually exacerbated, disease manifestations in Fas-deficient SLE-prone mice. We have now extended these observations to a chronic model of SLE induced by the i.p. injection of TMPD (pristane). We found that both cGAS- and STING-deficiency not only failed to rescue mice from TMPD-induced SLE, but resulted in increased autoantibody production and higher proteinuria levels compared to cGAS STING sufficient mice. Further, we generated $cGAS^{KO}Fas^{lpr}$ mice on a pure MRL/Fas^{lpr} background using Crispr/Cas9 and found slightly exacerbated, and not attenuated, disease. We hypothesized that the cGAS-STING pathway constrains TLR activation, and thereby limits autoimmune manifestations in these two models. Consistent with this premise, mice lacking cGAS and Unc93B1 or STING and Unc93B1 developed minimal systemic autoimmunity as compared to cGAS or STING single knock out animals. Nevertheless, TMPD-driven lupus in B6 mice was abrogated upon AAV-delivery of DNAse I, implicating a DNA trigger. Overall, this study demonstrated that the cGAS-STING pathway does not promote systemic autoimmunity in murine models of SLE. These data have important implications for cGAS-STING-directed therapies being developed for the treatment of systemic autoimmunity.

Keywords: cGAS/STING, SLE, pristane, DNaseI, TLRs

INTRODUCTION

Systemic lupus erythematosus (SLE) is a heterogeneous autoimmune disease with a number of clinical manifestations including systemic inflammation, development of pathogenic antibodies, deposition of immune complexes and finally end organ damage (1). Genetic predisposition, environmental factors as well as both innate and adaptive arms of the immune system play an

important role in initiation and amplification of this disease. Innate immune sensors present in endosomal compartments and in the cytosol, such as TLR9 and cGAS, respectively, can detect both microbial and host nucleic acids. It's been established in numerous murine models, that the endosomal TLRs, TLR7, and TLR9, play a critical role in SLE and related systemic autoimmune diseases (2, 3), while the role of STING in SLE is more controversial. Importantly, loss of function (LOF) mutations in the extracellular DNAse, DNAse1L3, originally identified in SLE patients (4–6), results in the accrual of DNA/RNA-associated microparticles in the blood (7–9). In mice, genetic deletion of DNAse1L3 promotes an SLE-like disease through a mechanism that is dependent on TLR7 and TLR9 and not STING (7, 9).

By contrast, LOF mutations of cytosolic DNAses such as DNAse II or DNAse III (Trex1) in patient populations are associated with systemic monogenic autoinflammatory diseases (10, 11). Genetic deletion of these cytosolic nucleases in mice, leads to embryonic lethality (DNAse II) (12) or myocarditis (TrexI) (13) through mechanisms dependent on the cGAS-STING pathway (14, 15). These data suggest that SLE is driven by extracellular DNA that is delivered to endosomal TLRs through receptors such as the BCR, LL37, or FcγRs while monogenic autoinflammatory diseases are driven by the aberrant accumulation of DNA in the cytosol that is detected by the cGAS/STING pathway. Autoantibody production has been detected in both Trex1 and DNAse II/IFNAR double deficient mice however, autoantibodies in DNAse II/IFNAR double defiicent mice have been shown to be Unc93B1 dependent (16). In addition, autoimmunity in DNAseIL3-deficient mice is dependent on endosomal MyD88 and endosomal TLRs (17).

Nevertheless, the cGAS/STING pathway has been postulated as a driver of lupus pathogenesis, although direct evidence for this is still limited. STING was recenlty implicated in the autoimmune phenotypes that develop in FcγR2-/- mice on a 129 background. However, since these mice were intercrossed with B6 STING^{gt} mice, the potential contribution of 129-associated risk alleles linked to the STING locus need to be considered (18). cGAMP, the cyclic dinucleotide generated by cGAS that activates STING, has been shown to be modestly elevated in the serum of a limited number of SLE patients (19). Most recently, UVB exposure which can drive lupus flares leads to an elevated type I IFN-I gene signature in the skin of mice which is dependent on the cGAS pathway and enhanced when cGAMP hydrolysis is blocked (20). Elevated STING activity has further been associated with increased expression of type I IFNs and ISGs (21, 22) and the degradation of damaged mitochondrial DNA by autophagy in patient populations (23). Moreover, while point mutations in human TREX1, that eliminate catalytic activity, cause the autoinflammatory disease Aicardi-Goutieres, point mutations in the N-terminus of TREX1, that retain DNAse activity, are associated with SLE and other unrelated conditions (24). The N-terminal mutations disrupt STING localization, and also disrupt the activity of the ER-resident enzyme oligosaccharyltransferase (OST) (25). In the absence of OST activity, immunogenic glycans accumulate in the ER and are the likely explanation for the association between the N-terminal mutations and SLE (24).

Murine models of C-terminal and N-terminal TREX1 mutations also develop distinct phenotypes. Patients heterozygous for a mutation that abrogates TREX1 catalytic activity, D18N, develop a skin disease that resembles familial chilblain lupus, while mice homozygous for this mutation develop myocarditis, multi-organ inflammation and autoantibody production, similar to TREX1$^{-/-}$ mice (26). By contrast, mice homozygous for C-terminal frameshift mutation, D272fs, previously associated with SLE (27), exhibit no clinical manifestations of disease but do develop high autoantibody titers primarily directed against non-nuclear antigens, and thus distinct from the autoantibody specificities associated with SLE (28). Therefore, the association between TREX1 mutations and murine lupus is weak.

We previously generated STING/Fas double deficient autoimmune prone mice and found that STING deficient mice developed more severe, not less severe, disease compared to Fas-deficient autoimmune prone controls (29). Mechanistically, we showed that STING-deficient macrophages expressed decreased levels of negative regulators of immune activation and therefore were hyper-responsive to TLR ligands (29). Together, our data indicated that the STING pathway does not promote, but rather constrains, TLR-driven lupus-like diseases. However, our prior work used STING-deficient autoimmune mice that were generated by intercrossing STING-deficient B6/129 and MRL/Fas^{lpr} mice; a limitation to these F2 studies was the potential contribution of risk alleles derived from the B6/129 background, that could be linked to the STING locus in the STING-deficient mice. Moreover, a critical question that remained unexplored was whether the regulatory effects of STING were dependent on the upstream DNA sensor cGAS. To address these issues, we have now further defined the role of STING and cGAS by directly targeting MRL/lpr mice using CRISPR/Cas9 genome editing. There has also been some concerns in the literature regarding the relevance of the MRL/lpr model to human disease. To address this concern, we have also expanded our analysis to the chronic model of TMPD-induced SLE in both cGAS- and STING-deficient B6 mice. We found that neither cGAS- nor STING- deficiency protected MRL/lpr mice. We also found that neither cGAS- nor STING-deficiency prevented TMPD-induced lupus. These studies further confirm our original observations and demonstrate that STING does not promote murine SLE in either genetically programmed or inducible models of SLE.

One caveat to the TMPD model is that it is thought to be driven predominantly by the RNA-sensing TLR, TLR7 (30, 31) bringing into question the actual role of DNA sensors in these mice. To evaluate the potential role of DNA sensors in the TMPD model, we overexpressed DNAseI using an AAV9 gene therapy approach by injecting an AAV9-DNAse I vector i.p., prior to the TMPD inoculation. The DNAseI expressing mice developed much less severe clinical manifestations than mice injected with the vector control. Thus, DNA contributes to systemic inflammation in TMPD injected mice, along with TLR7 ligands. Overall, our study shows that the cGAS-STING pathway is not a driver of disease in TLR-dependent models of SLE, but instead constrains disease activity, presumably by

limiting TLR activation. Nonetheless, DNA sensing still plays an important role in mediating autoimmune pathologies and depleting extracellular DNA can rescue TMPD-injected mice from SLE.

MATERIALS AND METHODS

Mice

Wild-type C57BL/6 mice were purchased from the Jackson Laboratory. STING^{KO} mice, fully backcrossed to the C57BL/6 background, were kindly provided by Dr. Daniel Stetson University of Washington, Seattle, WA (32). cGAS^{KO} mice on a B6 background were generated using cryopreserved embryos obtained from the European Conditional Mouse Mutagenesis Program (EUCOMM). cGAS^{KO} MRL/MpJ-*Fas*^{lpr} mice were generated via CRISPR/Cas9 genome editing at Merck & Co., Inc., Kenilworth, NJ using two gRNA sequences "*AGGACCAGAACACCTTGTAG*" and "*TGACCGCACGACTTACCCTG*" targeting exon 2. The deletion of exon 2, resulting in 581bp deletion, was confirmed using common forward primer 5′CCTAGCCTTGGCTATGTGGT3′ and reverse primer 5′AACAGTTCTAAATAACCGCTTTCG3′ for WT and 5′GAGCTGTAGATGCCCAAGTG3′ reverse primer for cGAS^{KO}. Unc93B1^{KO} mice were provided by Eicke Latz, University of Massachusetts Medical School, Worcester, MA (33). All mice were bred and maintained at the Department of Animal Medicine of the University of Massachusetts Medical School in accordance with the regulations of the American Association for the Accreditation of Laboratory Animal Care, and all protocols were approved by the Institutional Animal Care and Use Committee.

TMPD and AAV Injection

12–16-week-old mice received a single intraperitoneal injection of 500 ul of 2,6,10,14-Tetramethylpentadecane (TMPD, Sigma) and were analyzed 5–6 months after TMPD injection (34). In some experiments, C57BL/6 mice were injected with either AAV9-GFP or AAV9-DNAse1 10 weeks prior to TMPD injections (35). Each mouse received 10^{11} virus particles in 200 uL PBS delivered by intraperitoneal injection and AAV expression was measured by qPCR.

Flow Cytometry

Peritoneal exudate was collected in Hanks' Balanced Salt Solution (HBSS) media. Single cell suspensions obtained from the peritoneal cavity were stained with the following antibodies: anti-CD11b PercpCy5.5, anti-F4/80 PECy7, anti-Ly-6C APC, anti-Tim4 PE and anti-Ly-6G FITC. Flow cytometric analysis was carried out using a BD LSRII with Diva software (BD) and FlowJo Software (Tree Star). Live and single cells were gated to identify CD11b^{+} cells which were then gated to identify Ly6C^{hi} monocytes and Ly6G^{hi} granulocytes. Macrophages post TMPD injections were identified as live and single cells that were Ly6C^{-} Ly6G^{-} Tim4^{-} CD11b^{+} and F4/80^{hi} expressing cells. Splenocytes were stained with anti-CD11c pacific blue, SiglecH PE, anti-Bst2 APC, anti-CD3 PerCPCy5.5, anti-B220 Pacific blue, anti-CD4 PECy7 and anti-CD8 PE.

Generation of Bone Marrow Derived Macrophages

Bone marrow extracts were differentiated *in vitro* into bone marrow derived macrophages (BMDMs) in the presence of L929 supernatants for 7 days. The rested BMDMs were then transfected with ISD (interferon stimulatory DNA) (5 μM) overnight using Lipofectamine 2000 from Invitrogen.

Measurement of Serum Autoantibodies

HEp-2 human tissue culture substrate slides (MBL Code # ANK-120) were incubated with serum samples and bound antibodies were detected with DyLight 488-coupled detecting reagents as described in Christensen et al. (2). Anti–nucleosome concentrations were measured by ELISA with absorbance at 405/630 nm and compared with PL2-3 (in-house) as previously described (2). Autoantibodies reactive with dsDNA were measured by ELISA. Calf thymus DNA (Sigma) treated with S1 nuclease (ThermoFisher) was incubated for 1 h at room temperature on to poly-L-lysine treated ELISA plates. 1:50 diluted mouse sera was used and goat anti-mouse IgG H&L (HRP) (ab205719) was used as a secondary antibody. Anti-ds DNA antibody (ab27156) was used as standard.

Proteinuria and Cytokine Measurement

An anti-mouse albumin ELISA kit was used to measure urine protein as per manufacturer's protocol (Bethyl Laboratories). Serum cytokine levels were determined using ELISA kits as per manufacturer's protocol: anti-mIFNγ and anti-mIL-17 (BD Biosciences), anti-mIL-10 (eBioscience) and anti-mTNFa (R&Dsystems). The IFN-β level in media supernatant was determined as previously described (36).

Nanostring Analysis

Total RNA was isolated (Qiazol; Qiagen) and quantitated via a Nanodrop ND-1000 spectrophotometer (Thermo Scientific). Next, 50 ng of RNA was hybridized and quantified with a custom probe set using the NanoString nCounter analysis system (NanoString Technologies). Gene-expression data were normalized to housekeeping genes. All values were scaled by a log2(x – min(x) + 1) function and a heatmap generated using R-based software.

Western Blot

Cells were lysed in 50 μL of ice-cold Pierce RIPA lysis buffer (ThermoFisher Scientific) supplemented with 1× complete protease and phosphatase mixture inhibitor (Sigma). Protein concentration was measured using a protein DC assay kit. Whole-cell lysates were denatured for 5 min at 85 °C in presence of 1× Sample Buffer and reducing agent (Invitrogen). Fifty micrograms of samples were separated by SDS/PAGE on 10% gels. Each gel was run initially for 15 min at 80 V and then at 120 V. Transfer onto nitrocellulose membranes (Bio-Rad) was done using a Trans-Blot Turbo Transfer system for 10 min. Membranes were blocked for 1 h with 5% skim-milk (Sigma Aldrich) at room temperature in PBS supplemented with 0.05% Tween-20 (PBST). Membranes were probed overnight at 4°C with the following primary antibodies: anti-cGAS (31659;

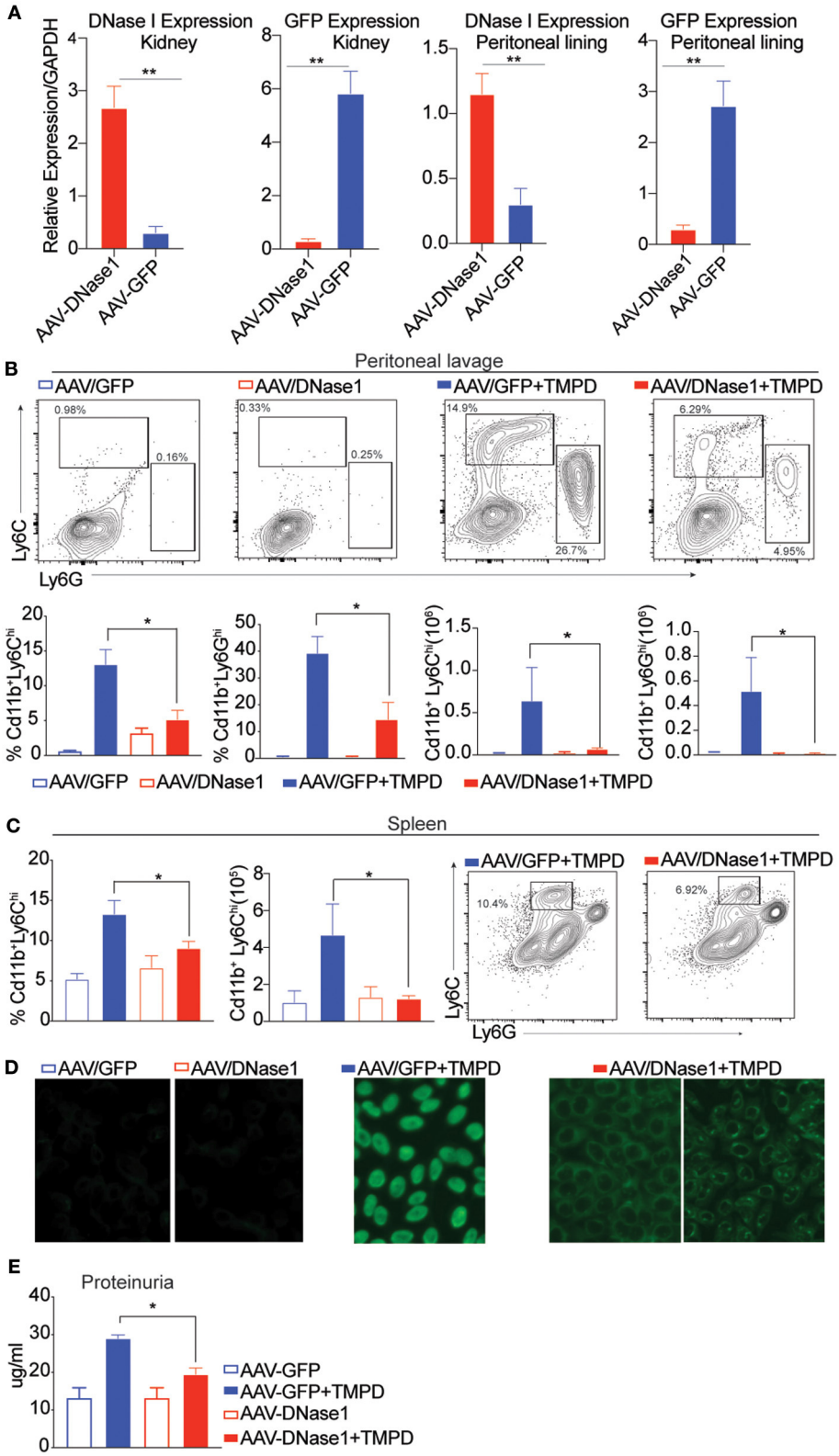

FIGURE 1 | Overexpression of DNAse I ameliorates inflammation in chronic TMPD mediated peritonitis. 8–10 weeks old female C57BL6/J WT mice were either injected i.p. with 10^{11} AAV/GFP or AAV/DNAsel particles in 200 uL PBS. 10 weeks later mice were either injected with 500 ul TMPD or un-injected and analyzed from

(Continued)

FIGURE 1 | two independent experiments 6 months after TMPD injection. All the experiments were performed using the following N's of mice- AAV/GFP (blue open bars) AAV/DNAseI (red open bars) are uninjected mice $n = 3$. AAV/GFP+TMPD (blue closed bars) $n = 4$ and AAV/DNAseI +TMPD (red closed bars) are injected mice $n = 8$. **(A)** qPCR was performed to measure DNAse1 and GFP gene expression in total tissue, peritoneal lining and kidney. AAV/DNAseI injected mice are indicated in red bars and AAV/GFP mice are indicated in blue. **(B)** $CD11b^+$ peritoneal exudate cells stained to identify $Ly6C^{hi}$ monocytes and $Ly6G^{hi}$ granulocytes. AAV/GFP (blue) and AAV/DNAse I (red) uninjected mice are indicated by open bars and TMPD injected mice are indicated as closed bars. The top panel shows representative flow plots and frequency/ numbers are graphed in the bottom panel. **(C)** $CD11b^+$ splenic cells stained to identify $Ly6C^{hi}$ monocytes. AAV/GFP (blue) and AAV/DNAseI (red) uninjected mice are indicated by open bars and TMPD injected mice are indicated as closed bars. The right panel shows representative flow plots and frequency/numbers are graphed in the left panel **(D)** Sera was collected 6 months after TMPD injection and ANA was measured using HEp2 substrate slides. Representative image from uninjected mice and AAV/GFP +TMPD injected mice is shown. Representative image is shown for two patterns observed in AAV DNAseI TMPD injected mice at 20X magnification. **(E)** Urine samples collected 6 months after TMPD injection were screened for proteinuria using an albumin ELISA assay. AAV/GFP (blue) and AAV/DNAseI (red) uninjected mice are indicated by open bars and TMPD injected mice are indicated as closed bars. Statistical significance is represented by $^*P < 0.05$, $^{**}P < 0.01$.

CST) and anti–beta-actin Peroxidase (A3854; Sigma-Aldrich). All membranes were washed with PBST and exposed using the SuperSignal West Pico PLUS chemiluminescent substrate (ThermoScientific) on ImageQuant LAS4000 mini Imager (GE Healthcare).

H & E Staining of Tissues

All tissues were fixed in 10% neutral buffered formalin for 24–48 h before being processed and paraffin-embedded. Five-micrometer-thin sections were stained by H&E in an automated stainer (Leica Autostainer XL). Histomorphology of each H&E slides was evaluated by Applied Pathology Systems at low and high-power field on Olympus BX40 microscope, and the images were captured with Olympus cellSens Entry software at indicated magnifications.

Statistical Analysis

All data were analyzed by non-parametric Mann-Whitney test using GraphPad Prism Software (GraphPad Software, San Diego, CA). Experiments are reported as mean +/– SEM. Differences are designated as one asterisk if $p < 0.05$, as two asterisks if $p < 0.01$ and three asterisks if $p < 0.001$.

RESULTS

Overexpression of DNAseI Enzyme Ameliorates Inflammation in Chronic TMPD Mediated Peritonitis

TMPD (2,6,10,14-Tetramethylpentadecane) or pristane is a naturally occurring hydrocarbon oil, which when introduced into the peritoneal cavity induces features of SLE in non-autoimmune prone mice (34). These include systemic inflammation, autoantibody production and glomerulonephritis. TMPD-driven lupus in B6 mice is highly dependent on TLR7 (30, 31), while the role of TLR9 is less straightforward. In general, TLR9 is required for the production of anti-dsDNA autoantibodies (2), but $TLR9^{-/-}$ SLE-prone mice invariably develop more severe autoimmunity, and $TLR9^{-/-}$ TMPD-injected BALB/c mice develop much more severe renal disease than their TLR9-sufficient littermates (37). Since TMPD induces cell death, DNA- and RNA-associated-cellular debris is likely to accumulate in the peritoneal cavity and other tissues throughout the body (34, 38). In addition, dysregulation of extracellular enzymes like DNAseI and DNAse1L3 that degrade DNA and DNA-associated complexes (microparticles) released from dying cells have also been implicated in SLE (9). DNAse1 is the most abundant secreted endonuclease, that is primarily expressed in the salivary glands, kidneys and gut. To explore the role of extracellular DNA in TMPD-induced lupus, we overexpressed DNase I using AAV9 that leads to widespread expression in order to test whether it could limit DNA uptake and thereby prevent or enhance clinical manifestations of SLE.

B6 mice were first inoculated with AAV-9 expressing either GFP or DNaseI, and then injected with TMPD 10 weeks later. 6 months post-TMPD injection, these mice were evaluated for both DNAseI expression and features of systemic autoimmunity. The levels of DNAseI were examined in multiple tissues and found to be expressed at high levels in both the kidney and peritoneal lining in mice that were injected with AAV-9 expressing DNaseI as compared to mice that received AAV-GFP. Similarly, high level of GFP expression was detected only in mice that received AAV-GFP and not in AAV-DNAseI injected mice (**Figure 1A**). TMPD leads to an inflammatory infiltrate in the peritoneal cavity that includes both $CD11b^+$ $Ly6C^{hi}$ monocytes and $CD11b^+$ $Ly6G^{hi}$ granulocytes. We found that the frequency and total number of both $CD11b^+$ $Ly6C^{hi}$ inflammatory monocytes and $CD11b^+$ $Ly6G^{hi}$ granulocytes in the peritoneal exudate was dramatically decreased in the AAV/DNAseI+TMPD mice compared to the AAV/GFP+TMPD mice (**Figure 1B**). We also evaluated the spleen of these mice and observed reduced frequency and number of $CD11b^+$ $Ly6C^{hi}$ inflammatory monocytes in AAVDNaseI treated mice that received TMPD (**Figure 1C**). We next evaluated the autoantibody profiles of TMPD treated mice and observed that the mice expressing AAV DNAseI showed very different ANA patterns when compared to the AAV GFP treated mice. Fifty percent of the AAV/GFP+TMPD sera gave a homogenous nuclear staining pattern, indicative of autoantibodies reactive with dsDNA, while the sera from the AAV/DNAseI+TMPD mice gave either a cytoplasmic and/or a speckled nuclear pattern (**Figure 1D**). Finally, the AAV/DNAseI+TMPD mice developed less severe renal disease as indicated by proteinuria levels (**Figure 1E**). These results highlight the importance of DNA sensing in TMPD mediated systemic autoimmunity.

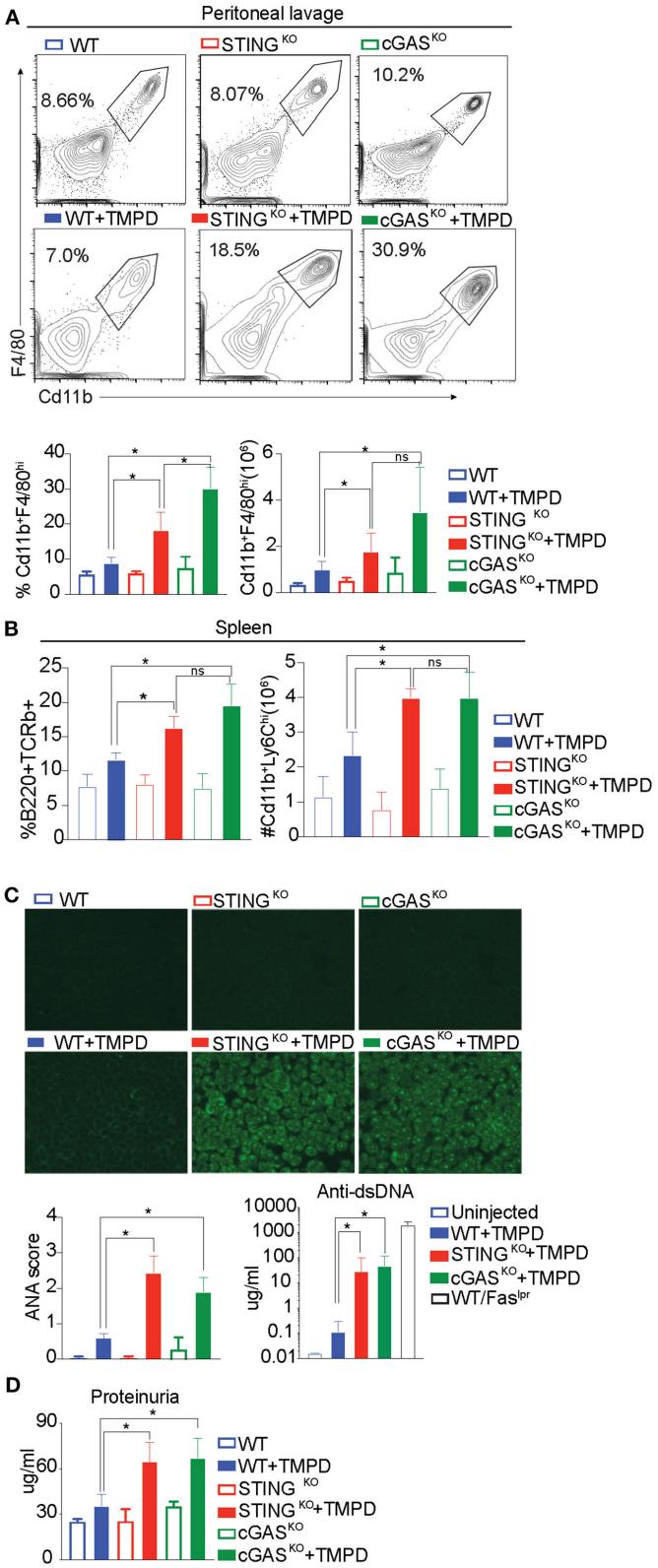

FIGURE 2 | STING and cGAS deficiency exacerbate disease in chronic model of TMPD induced autoimmunity. 12–16 week-old female WT, STING^{KO} or cGAS^{KO} mice were either uninjected (open bars, $n = 5$) or injected with 500 ul of TMPD (closed bars, $n = 15$) were analyzed from two independent experiments. **(A)** 6 months

(Continued)

FIGURE 2 | later, peritoneal exudate cells were evaluated by flow cytometry. Live and single Ly6C$^-$Ly6G$^-$ cells were gated for CD11b$^+$ and F4/80^{hi}. The top panel indicates representative flow plots from uninjected mice (WT = blue open bar, STING^{KO} = green open bar and cGAS^{KO} = red open bar). The middle panel shows representative flow plots from injected animals (closed bars) and the graphs for both frequency and numbers of CD11b$^+$ and F4/80^{hi} cells are shown in the bottom panel. **(B)** Flow cytometry was performed on splenocytes and double negative T cells (CD4$^-$ CD8$^-$) were identified as CD3$^+$ B220$^+$ and CD11b$^+$ and Ly6C^{hi} cells were identified as inflammatory monocytes. The frequency of double negatives and cell numbers for inflammatory monocytes are graphed. **(C)** Sera was collected 3 months after TMPD injection and ANAs were detected using HEp2 substrate slides at 1:50 serum dilution. The representative images from each genotype and condition are shown at 20X magnification in the top panel. The slides were scored for fluorescence intensity and the scores are graphed at the bottom. Anti-ds DNA antibodies were measured in the serum at 3 months after TMPD injection (closed bars, $n = 6$). Sera from a WT/Fas^{lpr} strain was used as a positive control. **(D)** Proteinuria was assessed in urine collected 6 months after TMPD injection by using an albumin ELISA assay. Statistical significance is represented by $^*P < 0.05$.

STING and cGAS Deficiency Exacerbate Disease in a Chronic Model of TMPD Induced Autoimmunity

The development of autoimmunity progresses over a 6-month time course following administration of TMPD. To evaluate the role of STING and/or cGAS in disease progression, we injected WT, STING^{KO} and cGAS^{KO} with TMPD and assessed them 6 months later for various features of autoimmune disease. While B6 mice do not develop kidney pathology, they do develop immune cell abnormalities and modest proteinurea. We evaluated several parameters of inflammation, focusing first on the inflammatory infiltrate in the peritoneal cavity. We found a comparable frequency and number of CD11b$^+$ Ly6C^{hi} monocytes and CD11b$^+$ Ly6G^{hi} granulocytes in the TMPD-injected STING and cGAS deficient animals as in the TMPD-injected WT mice (**Supplementary Figure S1A**). However, within the cells that were CD11b$^+$ Ly6C$^-$ Ly6G$^-$ we found a myeloid subset that was CD11b$^+$ and F4/80^{hi} (**Figure 2A**). This subset of cells was Tim4$^+$ in uninjected mice but Tim4$^-$ in all TMPD injected mice indicating that these are not resident macrophages (**Supplementary Figure S1B**). This CD11b$^+$F4/80^{hi} macrophage subset was increased in STING and cGAS deficient mice as compared to the WT mice both in frequency and number (**Figure 2A**). Several studies have reported distinct macrophage subsets to be pathological and major contributors of renal disease in both SLE prone patients and mice (39, 40). We also analyzed different immune cell subsets in the spleen and found that the numbers of Cd11b$^+$ Ly6C^{hi} monocytes was increased in the spleen of STING and cGAS deficient pristane injected mice as compared to the WT. Moreover, we observed an increased percentage of CD3$^+$ B220$^+$ (CD8 CD4 double negative) T cells in the STING and cGAS deficient pristane injected mice as compared to the WT pristane injected mice (**Figure 2B** and **Supplementary Figure S1C**). These double negative cells are expanded in SLE patient populations and contribute to kidney disease (41, 42). Overall, we found increased frequency and number of cellular subsets that contribute to disease pathology both in the peritoneal lavage and in the spleen of the STING and cGAS deficient mice.

To further evaluate TMPD-injected WT, STING^{KO} and cGAS ^{KO} mice we examined serum for autoantibody production by immunofluorescent staining of HEp2 cells. Both STING- and cGAS-deficient mice developed detectable autoantibody levels by 12 weeks post TMPD injection, while the WT mice did not, as quantified in the bottom panel (**Figure 2C** left). We also quantified the production of anti-ds DNA antibodies in the serum and observed that the STING^{KO} and cGAS^{KO} TMPD injected animals had increased anti-dsDNA antibody titers as compared to WT injected mice (**Figure 2C** right). We also measured the status of serum cytokines in these animals and found increased levels of IL10, IL17, IFNγ and TNFα in STING^{KO} and cGAS^{KO} TMPD injected animals compared to WT mice (**Supplementary Figure S1D**).

Renal function was evaluated by assaying albumin titers in urine samples and both STING^{KO} and cGAS^{KO} injected mice showed evidence of increased proteinuria as compared to the WT injected mice (**Figure 2D**). Taken together, our data suggests that STING- or cGAS-deficient mice were not protected from TMPD-induced SLE, and even exhibited features of autoimmunity that were severe than their wild type counterparts.

Exacerbation of TMPD-Induced SLE in cGAS or STING Deficient Mice Is Dependent on Endosomal TLRs

Our previous study showed that STING deficient macrophages when stimulated with TLR9 and TLR7 ligands CpGB and CL097, respectively, produced increased levels of the proinflammatory cytokines IL6 and TNFα as compared to STING sufficient cells (29). This hyper-responsiveness correlated with reduced expression of genes involved in negative regulation of TLR signaling such as A20, suppressor of cytokine signaling 1 (SOCS1) and 3 (SOCS3) (29). To determine whether the STING-exacerbated features of SLE were dependent on endosomal TLRs *in vivo*, we generated STING^{KO} Unc93B1^{KO} and cGAS^{KO} Unc93B1^{KO} double deficient lines. We then injected single Unc93B1^{KO}, the double deficient mice, and their Unc93B1-sufficient counterparts with TMPD, and evaluated them for features of systemic autoimmunity 5 months later. As above, the number of CD11b$^+$ F/480^{hi} macrophages in the peritoneal cavity was increased in STING^{KO} and cGAS^{KO} mice as compared to WT mice and significantly reduced in cGAS^{KO} UNC93B1^{KO} and STING^{KO} Unc93B1^{KO} double-deficient mice (**Figure 3A**). We also found that again both STING^{KO} and cGAS^{KO} mice developed higher levels of autoantibody than the WT mice, but failed to produce autoantibodies if they were Unc93B1-deficient (**Figure 3B**). Moreover, the proteinuria levels of STING and cGAS deficient mice were significantly higher than the WT mice, but STING/Unc93B1 and cGAS/Unc93B1double deficient mice failed to develop detectable proteinuria (**Figure 3C**). Collectively, these findings indicate that the elevated features of autoimmunity observed in cGAS or STING-deficient mice was abrogated when

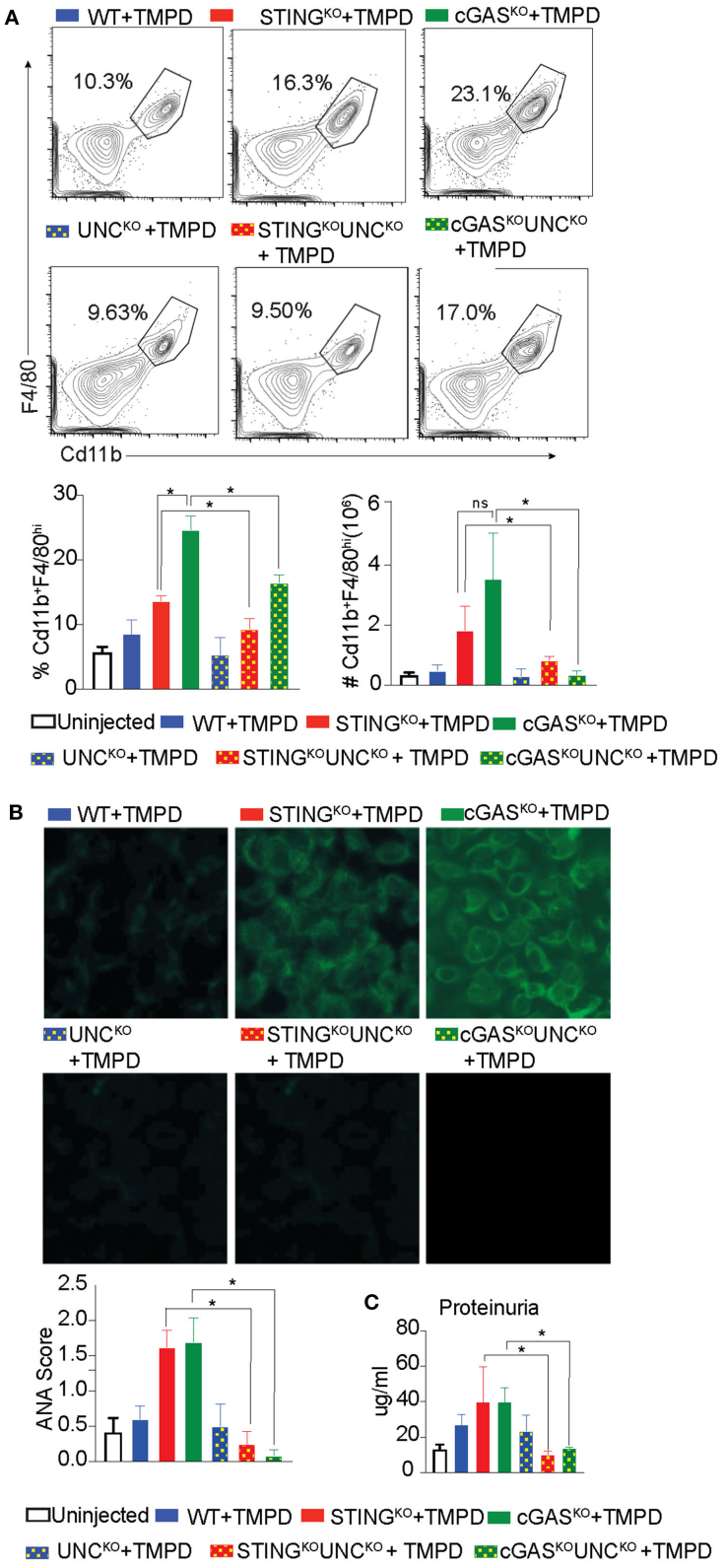

FIGURE 3 | Exacerbation of TMPD-induced SLE in cGAS or STING deficient mice is dependent on endosomal TLRs. 12–16 week old female WT (blue), STING^{KO} (red), cGAS^{KO} (green), UNC^{KO} (blue with dots), UNC^{KO} STING^{KO} (red with dots), and UNC^{KO}cGAS^{KO} (green with dots) mice were injected with 500 ul of TMPD

(Continued)

FIGURE 3 | ($n = 10$). Uninjected controls are indicated as open bars ($n = 4$ per genotype). The mice were analyzed 5 months post injection from two independent experiments. **(A)** Peritoneal exudate cells were evaluated by flow cytometry. Live and single $Ly6C^{-}Ly6G^{-}$ cells were gated for $CD11b^{+}$ and $F4/80^{hi}$. Representative flow plots for WT $STING^{KO}$, $cGAS^{KO}$ injected mice are shown in the top panel, the double deficient injected mice in the middle panel and the graphs for cell frequency and cell numbers are shown in bottom panel. **(B)** Sera was collected 3 months after TMPD injection and ANA were detected using HEp2 substrate slides at 1:50 serum dilution. The representative images from each genotype and condition are shown at 20X magnification in the top and middle panels and the scores for fluorescence intensity are graphed in the bottom. **(C)** Proteinuria was assessed in urine collected 5 months after TMPD injection by using an albumin ELISA assay. Statistical significance is represented by $^{*}P < 0.05$.

endosomal TLR signaling was abolished by deletion of Unc93B1 *in vivo*.

cGAS Deficiency Does Not Rescue SLE-Prone MRL/Fas^{lpr} Mice

We had previously reported exacerbation of autoimmune features in STING-deficient Fas^{lpr} mice generated by intercrossing B6/129 STING-deficient mice with MRL/Fas^{lpr} mice (29). To avoid any risk alleles that could be linked to the cGAS locus and modify disease outcome, we directly generated cGAS deficient MRL/Fas^{lpr} mice using a CRISPR/Cas9 genome editing strategy in MRL/lpr mice. We confirmed cGAS deficiency in the gene-edited strain by stimulating cGAS-deficient and control bone marrow derived macrophages (BMDMs) with ISD and measuring interferon production. $cGAS^{KO}$/ Fas ^{lpr} cells failed to produce Interferonβ (IFNβ) compared to WT/Fas^{lpr} cells in response to ISD, confirming that the CRISPR generated strain was functionally cGAS deficient (**Figure 4A** left). We also immunoblotted lysates obtained from WT/Fas^{lpr} and $cGAS^{KO}$/Fas ^{lpr} BMDMs. As expected, we found no detectable levels of cGAS protein in macrophages from $cGAS^{KO}$/Fas ^{lpr} mice whereas WT/Fas^{lpr} macrophages expressed cGAS protein (**Figure 4A** right). $cGAS^{KO}$/Fas^{lpr} and WT/Fas^{lpr} littermate controls were then evaluated for various SLE features and WT and cGAS deficient mice on a C57BL/6 background were used as negative controls since they do not develop autoimmunity spontaneously. Survival of the $cGAS^{KO}$/Fas^{lpr} mice was slightly compromised as compared to their WT/Fas^{lpr} littermates (**Figure 4B**). The $cGAS^{KO}$/Fas^{lpr} mice developed significantly higher levels anti-nucleosome antibodies in the serum as compared to WT/Fas^{lpr} littermate controls (**Figure 4C**). The $cGAS^{KO}$/Fas^{lpr} mice show increased proteinuria in the urine and increased cellular infiltrate in the kidneys as compared to the WT/Fas^{lpr} littermate controls (**Figure 4D**). However, splenomegaly or lymphadenopathy showed only trending increases in $cGAS^{KO}$/Fas^{lpr} as compared to littermate controls (**Figure 4E**). Similarly, the percentage of $CD3^{+}$ $B220^{+}$ (CD8 CD4 double negative) T cells or pDC were only modestly increased in the $cGAS^{KO}$/Fas^{lpr} mice compared to WT/Fas^{lpr} (**Figure 4F**). In addition, we also performed gene expression analysis in the total splenocytes obtained from these mice and we did not see any significant diffrences between the $cGAS^{KO}$/Fas^{lpr} mice compared to WT/Fas^{lpr} (**Supplementary Figure S2A**). Importantly, our data indicates that neither STING nor cGAS deficiency rescue MRL/lpr mice from SLE and are therefore unlikely to sense the extracellular DNA that accumulates in this model. Thus, the importance of the cGAS/STING pathway in the promotion of autoinflammation does not necessarily translate to the promotion of SLE.

DISCUSSION

Engagement of cGAS and the endosomal DNA sensor TLR9, can lead to the production of type I IFNs and proinflammatory cytokines. Stressed, damaged, or dying cells can provide sources of endogenous ligands that can activate both pathways. The importance of TLRs in SLE disease pathogenesis has been demonstrated by both loss-of-function and gain-of-function mutations in multiple animal models of SLE (3, 43–45), whereas DNA sensing mediated by the cGAS-STING pathway has been implicated in several human monogenic autoinflammatory diseases (46–48), as well as in mouse models of type I interferonopathies (49–51). In contrast to autoinflammatory diseases, where STING activation amplifies inflammation, our initial study showed that the STING pathway can attenuate clinical manifestations of SLE (29). We have now extended our initial observation to a chronic inducible model of SLE (TMPD induced SLE) as well as gene-targeted MRL/lpr SLE-prone mice, where we can monitor the progression of the disease without the caveat of additional risk alleles due to mixed genetic backgrounds. Our findings show that STING or cGAS deficiency does not cure lupus in either case. Rather, consistent with our earlier work (29), STING or cGAS deficiency leads to an earlier onset of SLE as measured by autoantibody levels in the serum and proteinuria in the urine. These data provide a cautionary note for the use of cGAS-STING targeted therapies for the treatment of SLE.

We have now also shown that neither Unc93B1/STING nor Unc93B1/cGAS mice develop TMPD induced SLE. These data further demonstrate that even in mice that fail to express STING, SLE is still dependent on endosomal TLRs. To determine whether DNA plays a role as an instigator of TMPD-induced lupus, we generated mice with increased levels of extracellular DNAse I using a one-time i.p. injection of AAV encoding DNAse I. We initially set out to test the premise that the protective role of STING (and TLR9) was DNA-dependent, and if this were the case, depletion of DNA should have resulted in an amplified TLR7 signal and led to a more severe clinical outcome. Instead, DNAseI-AAV-treated mice did not make autoantibodies against dsDNA, as indicated by the ANA staining pattern, and did not even develop other clinical manifestations of SLE. These data point to a critical role for a DNA sensor, possibly TLR9, in promoting the development of TMPD-induced SLE, and suggest that there may be a bimodal interplay between TLR7 and TLR9 in disease initiation and then disease progression. Alternatively, a DNA sensor other than cGAS or TLR9 may be involved. DNAseI-treated mice injected with TMPD show an overall reduction in inflammation and proteinuria but a very different autoantibody profile which could be more RNA driven,

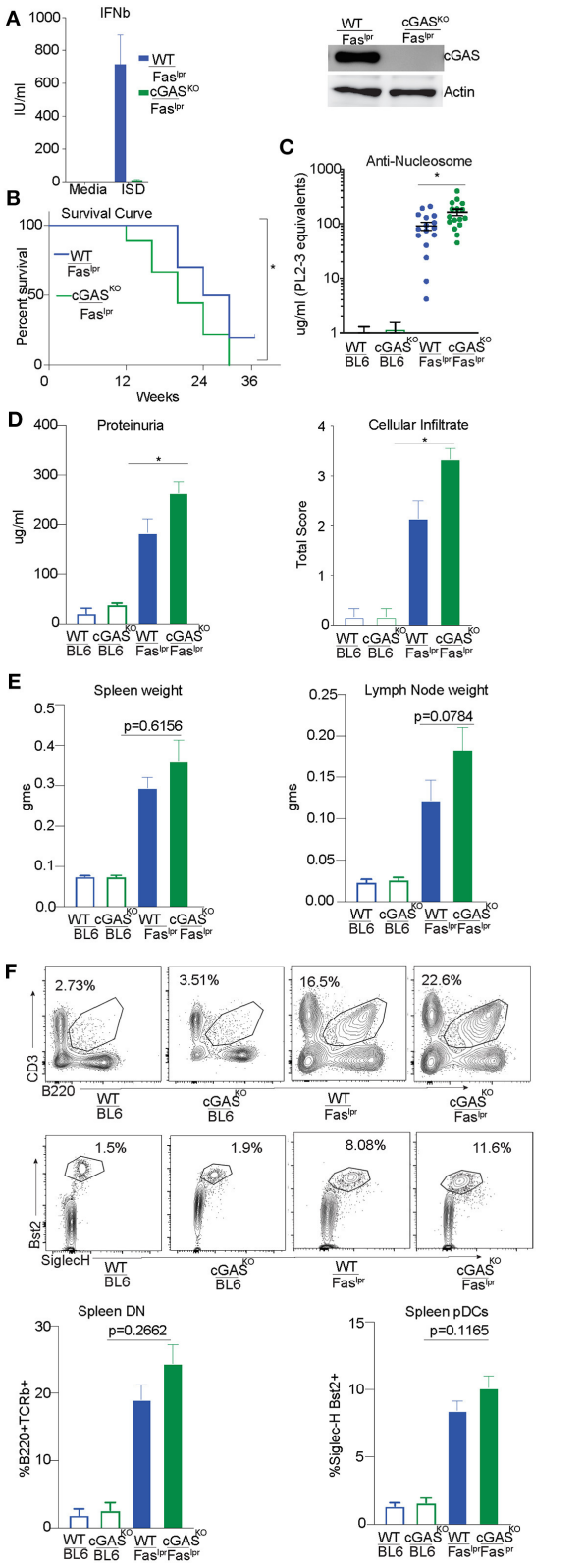

FIGURE 4 | cGAS deficiency does not rescue SLE-prone MRL/Fas^{lpr} mice. **(A)** BMDMs were isolated from WT/ Fas^{lpr} and cGAS ^{KO}/ Fas^{lpr} mice. These

(Continued)

FIGURE 4 | cells were either transfected or un-transfected with ISD 5 uM and interferon β ELISA was performed after overnight treatments. **(B)** BMDM cell lysates were prepared and western blot was performed to detect cGAS levels. Actin was blotted as loading control. **(B)** WT/Fas^{lpr} ($n = 10$) and cGAS^{KO}/Fas^{lpr} ($n = 18$) mice were observed until the time of death and Kaplan Meier survival analysis was performed. **(C)** Anti-nucleosome ELISA was performed for 12–16 week old mice B6 WT and B6 cGAS^{KO} mice (open bars), WT/Fas^{lpr} littermates (blue bar, $n = 16$), cGAS^{KO}/Fas^{lpr} mice (green bar, $n = 16$). **(D)** Urine samples from 16 week old B6 WT and B6 cGAS^{KO} mice (open bars), WT/Fas^{lpr} littermates (blue bar, $n = 16$), cGAS^{KO}/Fas^{lpr} mice (green bar, $n = 18$) were screened for proteinuria using an albumin ELISA assay. H&E staining was performed to analyze cellular infiltrate WT/Fas^{lpr} littermates (blue bar, $n = 7$), cGAS^{KO}/Fas^{lpr} mice (green bar, $n = 7$). **(E)** Spleen and lymph nodes weights were determined at 12 weeks of age ($n = 16$ mice each for WT/Fas^{lpr} and cGAS^{KO}/Fas^{lpr}). **(F)** Flow cytometry was performed on splenocytes and double negative T cells (CD4$^-$ CD8$^-$) were identified as CD3$^+$ B220$^+$. To enumerate pDCs, B220$^-$ CD3$^-$ CD11c$^+$ splenocytes were gated for SiglecH$^+$ and Bst2$^+$ cells. Representative flow plot is shown for each cell type and corresponding genotype in the top/middle panels and the frequency of cells is graphed in the bottom. All the flow analysis was performed on 12 week old female mice, ($n = 16$ mice each for WT/Fas^{lpr} and cGAS^{KO}/Fas^{lpr}). Statistical significance is represented by $^*P < 0.05$.

a phenomenon similar to the impact of TLR9-deficiency. TLR9- and TLR7-deficient SLE prone mice fail to make autoantibodies reactive with DNA and RNA, respectively, while TLR7-deficient and TLR7/TLR9 double deficient mice develop much less severe clinical phenotypes and exhibit markedly prolonged survival (2). It is also important to mention, that although DNAse1 is the most abundant secreted endonuclease expressed in some tissues including the kidneys, the AAV gene delivery approach here could have led to a more widespread expression of DNAseI than that seen under physiological conditions.

Although the mechanisms remain unresolved, this study reinforces the importance of investigating both proinflammatory and anti-inflammatory activities of nucleic acid-sensors. Both the TLR9 and STING pathways promote the IFN- and NFκB-driven expression of proinflammatory cytokines and chemokines, but at the same time induce negative regulators of these pathways. Thus, the outcome of nucleic acid sensor engagement will depend on the balance between positive and negative regulators of inflammation and transcriptional regulation of the relevant genes which is likely to reflect activation status of the receptor expressing cells. The dual functionality for cytosolic pathways is not surprising since a published study showed that the cytosolic RNA sensor, RIG-I also dampens TLR responses in myeloid cells by suppressing TLR driven interleukin 12 (IL-12b) gene transcription (52). The evidence of increased autoantibody production due to STING deficiency is also seen in a DNAse1L3-deficient mouse model used to evaluate SLE, where DNAse1L3 another extracellular DNAse clears microvesicle-associated DNA. The DNAse1L3 knockout mice were crossed with STING-deficient mice and serum titers of anti-dsDNA IgG as determined by ELISA, were higher in DNAse1L3/ STING double knockout mice than in single DNAse1L3 knockout mice (7).

More recently, several groups have described a role for the STING pathway in the clearance of DNA by autophagy (53, 54), suggesting that STING deficiency could lead to reduced

clearance of DNA. The ensuing accumulation of DNA in endosomal compartments of these cells could then enhance TLR dependent cytokine production through a cell intrinsic mechanism. DNAse II-deficient mice provide another example of excessive DNA accrual leading to the activation of multiple nucleic acid sensing pathways since the cGAS-STING, AIM2, and endosomal TLRs all have been shown to contribute to the development of autoimmunity or autoinflammation in this model (16, 55, 56). It is also possible that different DNA sensors may function in tissue specific manner for instance cGAS STING pathway can still contribute to certain aspects of disease such as the cutaneous lupus features as suggested by Skopelja-Gardner et al. (20). A better understanding of the interplay between cells responding to endogenous nucleic acid ligands will provide important insights for preventing the onset and progression of both autoinflammatory and autoimmune diseases in patients suffering from these conditions.

DATA AVAILABILITY STATEMENT

The original contributions generated for this study are included in the article/**Supplementary Material** and submitted to NCBI GEO (Gene Expression Omnibus) with accession number GSE169655 and linked to https://www.ncbi.nlm.nih.gov/geo/query/acc.cgi?acc=GSE169655. Further inquiries can be directed to the corresponding author/s.

ETHICS STATEMENT

All mice were bred and maintained at the Department of Animal Medicine of the University of Massachusetts Medical School in accordance with the regulations of the American Association for the Accreditation of Laboratory Animal Care and all protocols were approved by the Institutional Animal Care and Use Committee.

AUTHOR CONTRIBUTIONS

SS, AM-R, and KAF designed research. SS, MM, JM, JA, KMG, and ZJ performed research. GAB and KMN contributed new reagents and analytic tools. MM, AM-R, and KAF wrote the paper. All authors contributed to the article and approved the submitted version.

FUNDING

This work was supported by NIH grant AI128358 and AI132152. The funder was not involved in the study design, collection, analysis, interpretation of data, the writing of this article or the decision to submit it for publication.

ACKNOWLEDGMENTS

We would like to thank Sreya Ghosh for technical help and Dr. Mark Shlomchik, MD, PhD for his feedback on this study.

SUPPLEMENTARY MATERIAL

The Supplementary Material for this article can be found online at: https://www.frontiersin.org/articles/10.3389/fimmu.2021.605930/full#supplementary-material

REFERENCES

1. Pascual V, Farkas L, Banchereau J. Systemic lupus erythematosus: all roads lead to type I interferons. *Curr Opin Immunol.* (2006) 18:676–82. doi: 10.1016/j.coi.2006.09.014
2. Christensen SR, Shupe J, Nickerson K, Kashgarian M, Flavell RA, Shlomchik MJ. Toll-like receptor 7 and TLR9 dictate autoantibody specificity and have opposing inflammatory and regulatory roles in a murine model of lupus. *Immunity.* (2006) 25:417–28. doi: 10.1016/j.immuni.2006.07.013
3. Santiago-Raber ML, Baudino L, Izui S. Emerging roles of TLR7 and TLR9 in murine SLE. *J Autoimmun.* (2009) 33:231–8. doi: 10.1016/j.jaut.2009.10.001
4. Ueki M, Takeshita H, Fujihara J, Iida R, Yuasa I, Kato H, et al. Caucasian-specific allele in non-synonymous single nucleotide polymorphisms of the gene encoding deoxyribonuclease I-like 3, potentially relevant to autoimmunity, produces an inactive enzyme. *Clin Chim Acta.* (2009) 407:20–4. doi: 10.1016/j.cca.2009.06.022
5. Al-Mayouf SM, Sunker A, Abdwani R, Abrawi SA, Almurshedi F, Alhashmi N, et al. Loss-of-function variant in DNASE1L3 causes a familial form of systemic lupus erythematosus. *Nat Genet.* (2011) 43:1186–8. doi: 10.1038/ng.975
6. Carbonella A, Mancano G, Gremese E, Alkuraya FS, Patel N, Gurrieri F, et al. An autosomal recessive DNASE1L3-related autoimmune disease with unusual clinical presentation mimicking systemic lupus erythematosus. *Lupus.* (2017) 26:768–72. doi: 10.1177/0961203316676382
7. Sisirak V, Sally B, D'Agati V, Martinez-Ortiz W, Ozcakar ZB, David J, et al. Digestion of chromatin in apoptotic cell microparticles prevents autoimmunity. *Cell.* (2016) 166:88–101. doi: 10.1016/j.cell.2016.05.034
8. Mobarrez F, Fuzzi E, Gunnarsson I, Larsson A, Eketjall S, Pisetsky DS, et al. Microparticles in the blood of patients with SLE: size, content of mitochondria and role in circulating immune complexes. *J Autoimmun.* (2019) 102:142–9. doi: 10.1016/j.jaut.2019.05.003
9. Soni C, Reizis B. Self-DNA at the epicenter of SLE: immunogenic forms, regulation, and effects. *Front Immunol.* (2019) 10:1601. doi: 10.3389/fimmu.2019.01601
10. Crow YJ, Hayward BE, Parmar R, Robins P, Leitch A, Ali M, et al. Mutations in the gene encoding the 3′-5′ DNA exonuclease TREX1 cause Aicardi-Goutieres syndrome at the AGS1 locus. *Nat Genet.* (2006) 38:917–20. doi: 10.1038/ng1845
11. Rodero MP, Tesser A, Bartok E, Rice GI, Della Mina E, Depp M, et al. Type I interferon-mediated autoinflammation due to DNase II deficiency. *Nat Commun.* (2017) 8:2176. doi: 10.1038/s41467-017-01932-3
12. Yoshida H, Okabe Y, Kawane K, Fukuyama H, Nagata S. Lethal anemia caused by interferon-beta produced in mouse embryos carrying undigested DNA. *Nat Immunol.* (2005) 6:49–56. doi: 10.1038/ni1146
13. Stetson DB, Ko JS, Heidmann T, Medzhitov R. Trex1 prevents cell-intrinsic initiation of autoimmunity. *Cell.* (2008) 134:587–98. doi: 10.1016/j.cell.2008.06.032
14. Ahn J, Gutman D, Saijo S, Barber GN. STING manifests self DNA-dependent inflammatory disease. *Proc Natl Acad Sci U S A.* (2012) 109:19386–91. doi: 10.1073/pnas.1215006109
15. Gall A, Treuting P, Elkon KB, Loo YM, Gale M Jr., Barber GN, et al. Autoimmunity initiates in nonhematopoietic cells and progresses via lymphocytes in an interferon-dependent autoimmune disease. *Immunity.* (2012) 36:120–31. doi: 10.1016/j.immuni.2011.11.018

16. Baum R, Sharma S, Carpenter S, Li QZ, Busto P, Fitzgerald KA, et al. Cutting edge: AIM2 and endosomal TLRs differentially regulate arthritis and autoantibody production in DNase II-deficient mice. *J Immunol.* (2015) 194:873–7. doi: 10.4049/jimmunol.1402573
17. Serpas L, Chan RWY, Jiang P, Ni M, Sun K, Rashidfarrokhi A, et al. Dnase1l3 deletion causes aberrations in length and end-motif frequencies in plasma DNA. *Proc Natl Acad Sci U S A.* (2019) 116:641–9. doi: 10.1073/pnas.1815031116
18. Thim-Uam A, Prabakaran T, Tansakul M, Makjaroen J, Wongkongkathep P, Chantaravisoot N, et al. STING mediates lupus via the activation of conventional dendritic cell maturation and plasmacytoid dendritic cell differentiation. *iScience.* (2020) 23:101530. doi: 10.1016/j.isci.2020.101530
19. An J, Durcan L, Karr RM, Briggs TA, Rice GI, Teal TH, et al. Expression of cyclic GMP-AMP synthase in patients with systemic lupus erythematosus. *Arthritis Rheumatol.* (2017) 69:800–7. doi: 10.1002/art.40002
20. Skopelja-Gardner S, An J, Tai J, Tanaka L, Sun X, Hermanson P, et al. The early local and systemic Type I interferon responses to ultraviolet B light exposure are cGAS dependent. *Sci Rep.* (2020) 10:7908. doi: 10.1038/s41598-020-64865-w
21. Wang J, Dai M, Cui Y, Hou G, Deng J, Gao X, et al. Association of abnormal elevations in IFIT3 with overactive cyclic GMP-AMP synthase/stimulator of interferon genes signaling in human systemic lupus erythematosus monocytes. *Arthritis Rheumatol.* (2018) 70:2036–45. doi: 10.1002/art.40576
22. Murayama G, Chiba A, Kuga T, Makiyama A, Yamaji K, Tamura N, et al. Inhibition of mTOR suppresses IFNalpha production and the STING pathway in monocytes from systemic lupus erythematosus patients. *Rheumatology (Oxford).* (2020) 59:2992–3002. doi: 10.1093/rheumatology/keaa060
23. Gkirtzimanaki K, Kabrani E, Nikoleri D, Polyzos A, Blanas A, Sidiropoulos P, et al. IFNalpha impairs autophagic degradation of mtDNA promoting autoreactivity of SLE monocytes in a STING-dependent fashion. *Cell Rep.* (2018) 25:921–33 e925. doi: 10.1016/j.celrep.2018.09.001
24. Hasan M, Fermaintt CS, Gao N, Sakai T, Miyazaki T, Jiang S, et al. Cytosolic nuclease TREX1 regulates oligosaccharyltransferase activity independent of nuclease activity to suppress immune activation. *Immunity.* (2015) 43:463–74. doi: 10.1016/j.immuni.2015.07.022
25. Yan N. Immune diseases associated with TREX1 and STING dysfunction. *J Interferon Cytokine Res.* (2017) 37:198–206. doi: 10.1089/jir.2016.0086
26. Grieves JL, Fye JM, Harvey S, Grayson JM, Hollis T, Perrino FW. Exonuclease TREX1 degrades double-stranded DNA to prevent spontaneous lupus-like inflammatory disease. *Proc Natl Acad Sci U S A.* (2015) 112:5117–22. doi: 10.1073/pnas.1423804112
27. Lee-Kirsch MA, Gong M, Chowdhury D, Senenko L, Engel K, Lee YA, et al. Mutations in the gene encoding the 3′-5′ DNA exonuclease TREX1 are associated with systemic lupus erythematosus. *Nat Genet.* (2007) 39:1065–7. doi: 10.1038/ng2091
28. Sakai T, Miyazaki T, Shin DM, Kim YS, Qi CF, Fariss R, et al. DNase-active TREX1 frame-shift mutants induce serologic autoimmunity in mice. *J Autoimmun.* (2017) 81:13–23. doi: 10.1016/j.jaut.2017.03.001
29. Sharma S, Campbell AM, Chan J, Schattgen SA, Orlowski GM, Nayar R, et al. Suppression of systemic autoimmunity by the innate immune adaptor STING. *Proc Natl Acad Sci U S A.* (2015) 112:E710–7. doi: 10.1073/pnas.1420217112
30. Lee PY, Kumagai Y, Li Y, Takeuchi O, Yoshida H, Weinstein J, et al. TLR7-dependent and FcgammaR-independent production of type I interferon in experimental mouse lupus. *J Exp Med.* (2008) 205:2995–3006. doi: 10.1084/jem.20080462
31. Savarese E, Steinberg C, Pawar RD, Reindl W, Akira S, Anders HJ, et al. Requirement of Toll-like receptor 7 for pristane-induced production of autoantibodies and development of murine lupus nephritis. *Arthritis Rheum.* (2008) 58:1107–15. doi: 10.1002/art.23407
32. Ishikawa H, Barber GN. STING is an endoplasmic reticulum adaptor that facilitates innate immune signalling. *Nature.* (2008) 455:674–8. doi: 10.1038/nature07317
33. Pelka K, Bertheloot D, Reimer E, Phulphagar K, Schmidt SV, Christ A, et al. The Chaperone UNC93B1 regulates toll-like receptor stability independently of endosomal TLR transport. *Immunity.* (2018) 48:911–22.e917. doi: 10.1016/j.immuni.2018.04.011
34. Reeves WH, Lee PY, Weinstein JS, Satoh M, Lu L. Induction of autoimmunity by pristane and other naturally occurring hydrocarbons. *Trends Immunol.* (2009) 30:455–64. doi: 10.1016/j.it.2009.06.003
35. Schattgen SA, Gao G, Kurt-Jones EA, Fitzgerald KA. Cutting edge: DNA in the lung microenvironment during influenza virus infection tempers inflammation by engaging the DNA sensor AIM2. *J Immunol.* (2016) 196:29–33. doi: 10.4049/jimmunol.1501048
36. Roberts ZJ, Goutagny N, Perera PY, Kato H, Kumar H, Kawai T, et al. The chemotherapeutic agent DMXAA potently and specifically activates the TBK1-IRF-3 signaling axis. *J Exp Med.* (2007) 204:1559–69. doi: 10.1084/jem.20061845
37. Bossaller L, Christ A, Pelka K, Nundel K, Chiang PI, Pang C, et al. TLR9 deficiency leads to accelerated renal disease and myeloid lineage abnormalities in pristane-induced murine lupus. *J Immunol.* (2016) 197:1044–53. doi: 10.4049/jimmunol.1501943
38. Calvani N, Caricchio R, Tucci M, Sobel ES, Silvestris F, Tartaglia P, et al. Induction of apoptosis by the hydrocarbon oil pristane: implications for pristane-induced lupus. *J Immunol.* (2005) 175:4777–82. doi: 10.4049/jimmunol.175.7.4777
39. Chalmers SA, Chitu V, Herlitz LC, Sahu R, Stanley ER, Putterman C. Macrophage depletion ameliorates nephritis induced by pathogenic antibodies. *J Autoimmun.* (2015) 57:42–52. doi: 10.1016/j.jaut.2014.11.007
40. Ma WT, Gao F, Gu K, Chen DK. The role of monocytes and macrophages in autoimmune diseases: a comprehensive review. *Front Immunol.* (2019) 10:1140. doi: 10.3389/fimmu.2019.01140
41. Sieling PA, Porcelli SA, Duong BT, Spada F, Bloom BR, Diamond B, et al. Human double-negative T cells in systemic lupus erythematosus provide help for IgG and are restricted by CD1c. *J Immunol.* (2000) 165:5338–44. doi: 10.4049/jimmunol.165.9.5338
42. Crispin JC, Oukka M, Bayliss G, Cohen RA, Van Beek CA, Stillman IE, et al. Expanded double negative T cells in patients with systemic lupus erythematosus produce IL-17 and infiltrate the kidneys. *J Immunol.* (2008) 181:8761–6. doi: 10.4049/jimmunol.181.12.8761
43. Marshak-Rothstein A. Toll-like receptors in systemic autoimmune disease. *Nat Rev Immunol.* (2006) 6:823–35. doi: 10.1038/nri1957
44. Fairhurst AM, Hwang SH, Wang A, Tian XH, Boudreaux C, Zhou XJ, et al. Yaa autoimmune phenotypes are conferred by overexpression of TLR7. *Eur J Immunol.* (2008) 38:1971–8. doi: 10.1002/eji.200838138
45. Jackson SW, Scharping NE, Kolhatkar NS, Khim S, Schwartz MA, Li QZ, et al. Opposing impact of B cell-intrinsic TLR7 and TLR9 signals on autoantibody repertoire and systemic inflammation. *J Immunol.* (2014) 192:4525–32. doi: 10.4049/jimmunol.1400098
46. Liu Y, Jesus AA, Marrero B, Yang D, Ramsey SE, Sanchez GAM, et al. Activated STING in a vascular and pulmonary syndrome. *N Engl J Med.* (2014) 371:507–18. doi: 10.1056/NEJMoa1312625
47. Rodero MP, Crow YJ. Type I interferon-mediated monogenic autoinflammation: The type I interferonopathies, a conceptual overview. *J Exp Med.* (2016) 213:2527–38. doi: 10.1084/jem.20161596
48. Motwani M, Pesiridis S, Fitzgerald KA. DNA sensing by the cGAS-STING pathway in health and disease. *Nat Rev Genet.* (2019) 20:657–74. doi: 10.1038/s41576-019-0151-1
49. Gao D, Li T, Li XD, Chen X, Li QZ, Wight-Carter M, et al. Activation of cyclic GMP-AMP synthase by self-DNA causes autoimmune diseases. *Proc Natl Acad Sci U S A.* (2015) 112:E5699–705. doi: 10.1073/pnas.1516465112
50. Motwani M, Pawaria S, Bernier J, Moses S, Henry K, Fang T, et al. Hierarchy of clinical manifestations in SAVI N153S and V154M mouse models. *Proc Natl Acad Sci U S A.* (2019) 116:7941–50. doi: 10.1073/pnas.1818281116
51. Xiao N, Wei J, Xu S, Du H, Huang M, Zhang S, et al. cGAS activation causes lupus-like autoimmune disorders in a TREX1 mutant mouse model. *J Autoimmun.* (2019) 100:84–94. doi: 10.1016/j.jaut.2019.03.001
52. Negishi H, Yanai H, Nakajima A, Koshiba R, Atarashi K, Matsuda A, et al. Cross-interference of RLR and TLR signaling pathways modulates antibacterial T cell responses. *Nat Immunol.* (2012) 13:659–66. doi: 10.1038/ni.2307
53. Gui X, Yang H, Li T, Tan X, Shi P, Li M, et al. Autophagy induction via STING trafficking is a primordial function of the cGAS pathway. *Nature.* (2019) 567:262–6. doi: 10.1038/s41586-019-1006-9
54. Yang J, Tang X, Nandakumar KS, Cheng K. Autophagy induced by STING, an unnoticed and primordial function of cGAS. *Cell Mol Immunol.* (2019) 16:683–4. doi: 10.1038/s41423-019-0240-2

55. Pawaria S, Sharma S, Baum R, Nundel K, Busto P, Gravallese EM, et al. Taking the STING out of TLR-driven autoimmune diseases: good, bad, or indifferent? *J Leukoc Biol.* (2017) 101:121–6. doi: 10.1189/jlb.3MR0316-115R
56. Pawaria S, Nundel K, Gao KM, Moses S, Busto P, Holt K, et al. The role of IFNgamma-producing Th1 cells in a type I IFN-independent murine model of autoinflammation resulting from DNase II-deficiency. *Arthritis Rheumatol.* (2019) 72:359–70. doi: 10.1002/art.41090

Conflict of Interest: GAB is employed by the company Merck and Co., Inc., Kenilworth, NJ, United States. The authors declare that this study received funding from sponsored research agreement from GSK (100251747). The funder had the following involvement with the study: decision to submit it for publication.

The remaining authors declare that the research was conducted in the absence of any commercial or financial relationships that could be construed as a potential conflict of interest.

Advantages of publishing in Frontiers

OPEN ACCESS
Articles are free to read for greatest visibility and readership

FAST PUBLICATION
Around 90 days from submission to decision

HIGH QUALITY PEER-REVIEW
Rigorous, collaborative, and constructive peer-review

TRANSPARENT PEER-REVIEW
Editors and reviewers acknowledged by name on published articles

Frontiers
Avenue du Tribunal-Fédéral 34
1005 Lausanne | Switzerland

Visit us: www.frontiersin.org
Contact us: frontiersin.org/about/contact

REPRODUCIBILITY OF RESEARCH
Support open data and methods to enhance research reproducibility

DIGITAL PUBLISHING
Articles designed for optimal readership across devices

FOLLOW US
@frontiersin

IMPACT METRICS
Advanced article metrics track visibility across digital media

EXTENSIVE PROMOTION
Marketing and promotion of impactful research

LOOP RESEARCH NETWORK
Our network increases your article's readership